

TECHNICAL REPORT GL-86-14

# PERFORMANCE PREDICTION OF LOW VOLUME AIRFIELD PAVEMENTS

by

Albert J. Bush III

Geotechnical Laboratory

DEPARTMENT OF THE ARMY
Waterways Experiment Station, Corps of Engineers
PO Box 631, Vicksburg, Mississippi 39180-0631

September 1986
Final Report



Prepared for DEPARTMENT OF THE ARMY
Assistant Secretary of the Army (R&D)
Washington, DC 20314-1000

Under Project No. 4A161101A91D, Task 02
Work Unit 151

GEOTECHNICAL LABORATORY

## REPORT DOCUMENTATION PAGE

Form Approved
OMB No. 0704-0188
Exp. Date: Jun 30, 1986

1a REPORT SECURITY CLASSIFICATION
Unclassified

1b RESTRICTIVE MARKINGS

2a SECURITY CLASSIFICATION AUTHORITY

2b DECLASSIFICATION / DOWNGRADING SCHEDULE

3 DISTRIBUTION / AVAILABILITY OF REPORT
Approved for public release;
distribution unlimited

4 PERFORMING ORGANIZATION REPORT NUMBER(S)
Technical Report GL-86-14

5 MONITORING ORGANIZATION REPORT NUMBER(S)

6a NAME OF PERFORMING ORGANIZATION
USAEWES
Geotechnical Laboratory

6b OFFICE SYMBOL (*If applicable*)
WESGP-IP

7a NAME OF MONITORING ORGANIZATION
DEPARTMENT OF THE ARMY
Assistant Secretary of the Army (R&D)

6c ADDRESS (*City, State, and ZIP Code*)
PO Box 631
Vicksburg, MS 39180-0631

7b ADDRESS (*City, State, and ZIP Code*)
Washington, DC 20314-1000

8a NAME OF FUNDING / SPONSORING ORGANIZATION
US Army Corps of Engineers

8b OFFICE SYMBOL (*If applicable*)
DAEN-ECE-G

9 PROCUREMENT INSTRUMENT IDENTIFICATION NUMBER

8c ADDRESS (*City, State, and ZIP Code*)
Washington, DC 20314-1000

10 SOURCE OF FUNDING NUMBERS

| PROGRAM ELEMENT NO. | PROJECT NO. | TASK NO. | WORK UNIT ACCESSION NO. |
|---|---|---|---|
| 61101A | See Reverse | 02 | 151 |

11 TITLE (*Include Security Classification*)
Performance Prediction of Low Volume Airfield Pavements

12 PERSONAL AUTHOR(S)
Bush, Albert J., III

| 13a TYPE OF REPORT | 13b TIME COVERED | 14 DATE OF REPORT (*Year, Month, Day*) | 15 PAGE COUNT |
|---|---|---|---|
| Final report | FROM 1984 TO 1985 | September 1986 | 202 |

16 SUPPLEMENTARY NOTATION
Available from National Technical Information Service, 5285 Port Royal Road, Springfield, VA 22161.

| 17 COSATI CODES | | |
|---|---|---|
| FIELD | GROUP | SUB-GROUP |
| | | |
| | | |

18 SUBJECT TERMS (*Continue on reverse if necessary and identify by block number*)
Airfields
Nondestructive testing
Pavements
Pavement evaluation

19 ABSTRACT (*Continue on reverse if necessary and identify by block number*)

A pavement evaluation procedure is presented for evaluating conventional flexible airfield pavements that will fail in fewer than 100 coverages. The procedure utilizes deflection data obtained from a Falling Weight Deflectometer and the age of the pavement to predict the coverages of an F-4 aircraft to failure. Procedures for correcting temperature of the asphalt pavement layer and for predicting performance of other aircraft are presented.

20 DISTRIBUTION / AVAILABILITY OF ABSTRACT
☒ UNCLASSIFIED/UNLIMITED ☐ SAME AS RPT ☐ DTIC USERS

21 ABSTRACT SECURITY CLASSIFICATION
Unclassified

22a NAME OF RESPONSIBLE INDIVIDUAL

22b TELEPHONE (*Include Area Code*)

22c OFFICE SYMBOL

DD FORM 1473, 84 MAR

83 APR edition may be used until exhausted
All other editions are obsolete.

10. SOURCE OF FUNDING NUMBERS

Project No. 4A161101A91D

# PREFACE

This study was conducted by the Geotechnical Laboratory (GL), US Army Engineer Waterways Experiment Station (WES), during the period February 1984 through September 1985. The investigation was sponsored by the Department of the Army under the In-House Laboratory Independent Research (ILIR) program as Project No. 4A161101A91D, "Performance Prediction of Low Volume Airfield Pavements," Task Area 02, Work Unit 151.

The study was conducted under the general supervision of Dr. W. F. Marcuson III, Chief, GL; Mr. H. H. Ulery, Jr., Chief, Pavement Systems Division (PSD), GL; Mr. J. W. Hall, Jr., Chief, Engineering Investigations, Testing and Validation Group, PSD, GL; and Mr. R. W. Grau, Chief, Prototype Testing and Evaluation Unit, PSD, GL. The study was conducted by Mr. A. J. Bush III, Mr. S. J. Alford, and Mr. P. S. McCaffrey, Jr., PSD, GL. This report was written by Mr. Bush.

COL Allen F. Grum, USA, was the previous Director of WES. COL Dwayne G. Lee, CE, is the present Commander and Director. Dr. Robert W. Whalin is Technical Director.

PERFORMANCE PREDICTION OF LOW VOLUME AIRFIELD PAVEMENTS

LIST OF FIGURES

LIST OF FIGURES
(Continued)

LIST OF FIGURES
(Continued)

LIST OF FIGURES
(Continued)

LIST OF FIGURES
(Continued)

LIST OF TABLES

# SECTION I

# INTRODUCTION

## A. BACKGROUND

The US Air Force has a need to construct and maintain pavements to support a limited number of aircraft operations in the European theater. With the development of hardened shelters for the protection of aircraft and support equipment during conventional air attacks, the weapon system vulnerability to conventional bombing shifts toward the mission-essential runway. To counteract this threat, the US Air Force outlined a 9-year research program to provide the capability to launch and recover aircraft after an attack directed at runways and taxiways. One option is to construct and maintain Alternate Launch and Recovery Surfaces (ALRS). ALRS are large areas of relatively low quality pavement. ALRS can be constructed away from the main runway to effectively reduce the probability that all landing and takeoff areas would be destroyed in a given attack. The ALRS must (1) be relatively inexpensive in comparison to permanent pavements, (2) support the imposed loads, (3) be easily maintained, and (4) provide an adequate surface for a limited number of sorties of the design aircraft.

Research on ALRS has been reported by several investigators (References 1-11). These research efforts were directed toward the design of the pavements for structural support requirements and to minimize the effects of environmental deterioration. Two pavement systems were selected on the basis of costs and performance requirements from these efforts: (1) a conventional asphalt/crushed stone pavement with a minimum thickness of asphaltic concrete (AC) and (2) a pavement constructed with stabilized-material layers.

ALRS pavements will be located in areas where there are 300-325 freezing degree-days, 25-30 inches of rainfall and 14-36 inches of snowfall per year (Reference 5). These environmental conditions will cause structural deterioration of the pavement layers through thermal cracking, and freeze-thaw cyclic conditions. Freeze-thaw will saturate the subgrade and other frost susceptible layers, and cracking will allow water infiltration through cracks.

ALRS pavements will be designed to support 150 passes of a fighter aircraft such as the F-4 which has a single main gear with a maximum load of 27000 lbs and a 100 sq. in. contact area.

Normally, pavements are subjected to periodic traffic. If the pavement is not structurally adequate, distresses such as rutting or cracking appear indicating a need for strengthening. Distresses may be localized where corrections can be accomplished with patching, or they may cover the entire pavement feature where the loads exceed the design aircraft load or material properties have changed due to environmental effects. ALRS pavements will not be subjected to traffic except in contingency situations. If there is a change in the pavement conditions, there will be no indicator and failure could occur when the feature is critically needed. Therefore, ALRS pavements will require periodic monitoring life to insure that structural integrity is maintained.

The use of nondestructive testing devices for evaluating the load-carrying capability of both airport and highway pavements has been widely accepted throughout the pavements field (References 12-18). The procedures for determining the allowable load or allowable passes have been derived by:

1. Correlating the NDT measurement to the allowable load determined by sampling the pavement structure and using a conventional design procedure (Reference 13).

2. Back-calculating the pavement layer moduli and using a layered elastic model to calculate limiting stresses or strains (References 12, 14, 15, 17 and 18).

Both methods have been "calibrated" and apparently produce reasonable results though they have not been verified by actual performance data. In general, the methods have been verified only by laboratory or insitu materials tests.

Two research studies have been completed at the Waterways Experiment Station on the design of ALRS (References 6, and 10). Eleven pavement test sections were trafficked to failure with an F-4 load cart. Nondestructive Falling Weight Deflectometer (FWD) data were collected on these sections before, during, and after traffic. These data provide an excellent source for use in establishing failure mode, and pattern and predicting the performance of low volume traffic pavements.

## B. PURPOSE

The purpose of this study is to develop an FWD based evaluation procedure to predict the allowable F-4 aircraft load and the allowable aircraft passes for marginal asphalt pavements. Structural models for describing the pavement system response will be evaluated and the model that produces responses that most accurately correlate to pavement performance will be selected. The method developed will be applicable to pavements for which very little information is known.

## C. SCOPE

The nondestructive evaluation procedure developed in this study will be for flexible pavements with an asphaltic concrete surface and an unbound granular layer. The allowable load/passes will be predicted for aircraft with a tricycle gear having a single wheel main gear. The procedure will be developed based on data obtained from using a load cart simulating an F-4 aircraft having a 27000 pound single wheel load and a tire contact area of 100 square inches. Data collected during the aforementioned studies will be used to predict the expected life in terms of number of passes to produce failure as determined by rutting. The method will use only nondestructive data when thickness and type of the pavement layers are known. When thickness and types of layers are not known coring will be required to determine these parameters.

## D. THESIS FORMAT

Section II contains a description of the failure mechanisms for flexible pavements with thin asphaltic concrete surfaces and granular bases. Methods for evaluating the performance of flexible pavements are presented with the method selected for evaluating the data presented herein.

A description of the traffic tests is presented in Section III. Pavement properties and performance evaluation measurements are described.

An analysis of nondestructive data collected with the FWD and factors which influence FWD data is contained in Section IV.

Traffic test section data is analyzed in Section V. The performance of each traffic test section is compared to estimates of performance using the CBR design/evaluation procedure and layered elastic procedures.

Section VI contains the models developed to predict performance. The best estimator of performance is presented. A procedure for evaluating traffic volume pavements is outlined.

Section VII presents conclusions and recommendations for evaluation of low traffic volume pavements and future research for flexible pavements containing granular base courses.

## SECTION II

## PERFORMANCE PREDICTION

A structural model must be selected to predict pavement responses such as stress or strain. The model should be capable of utilizing the properties of the pavement layers such as modulus and strength. Responses derived from material properties can be used to relate to pavement performance. For ALRS evaluations, the model should not require the use of a main frame computer for analysis since in the cases of an evaluation of an airfield in an underdeveloped country an answer is required immediately.

The pavement evaluation methods that were considered are the California Bearing Ratio (CBR) design procedure, multilayer linear elastic model, multilayer nonlinear elastic models, and rut depth prediction. Each system will be described in the following sections.

### A. PAVEMENT PROPERTIES AFFECTING PERFORMANCE

#### 1. Distresses

An ALRS pavement structure will contain a thin AC layer (3 inches or less), an unbound granular layer, and a subgrade. Distress in pavements of this type and of interest to the pavement user are cracking of the AC layer and permanent deformation (rutting).

Cracking may be the initial distress particularly for older pavements when the AC surface course has oxidized and lost its flexibility. Cracking of the AC surface influences rut depth accumulation. A cracked surface course does not provide the confining for the base course which leads to loss of strength. Shear stress is increased below a cracked layer. Both decrease confining and increased shear stress enhance rutting accumulation.

Aircraft operations on ALRS will occur in a short time interval (probably less than 24 hours). Cracking is a primary pavement distress because it allows water to infiltrate into the base and subgrade which leads to weakening of those layers and eventually rutting. Severe cracking can lead to foreign object damage (FOD) to the aircraft engines. Due to the short time use (less than 24 hours) of ALRS pavements, water infiltration will not present a problem. FOD damage could be a problem for ALRS users, but most likely will not, since operations will be occurring during battle. Also, although cracking may occur, 100 to 200 aircraft passes probably will not break the surface into particles small enough to be dislodged.

Therefore, the primary load associated distress in ALRS pavements of concern is permanent deformation in the form of rutting. Permanent or plastic deformation can occur in the AC layer, the granular layer, and the subgrade. Deformations within the AC layer will be small in comparison to those in the base and subgrade since the surface AC layer is relatively thin (3 inches or less). Therefore, rutting distress will be associated with the granular and subgrade layers for low traffic volume ALRS pavements.

2. Granular Layers

Permanent strain in granular materials has been described (Reference 19) with the general form equation:

$$\epsilon_p = a + b \log N \qquad (1)$$

where

$\epsilon_p$ = Permanent strain

N = Number of load repititions

a,b = Experimentally derived factors from repeated load testing

Factors that affect the rate of permanent strain accumulation, the b term of the above equation, include the compacted density.

Barksdale reported in a detailed laboratory analysis of rutting in base course materials (Reference 20), the type and amount of fines increased the permanent strain. He further stated for crushed stone bases, only enough fines should be used to permit proper compaction if the amount of rutting in the base is to be minimized. Increase in the deviator stress ratio significantly increases the permanent axial strain. The deviator stress ratio is given as:

$$\frac{\sigma_1 - \sigma_3}{\sigma_3} \tag{2}$$

The degree of saturation also was found to significantly increase the tendancy to rut in the base (Reference 20).

A hyperbolic plastic stress-strain relationship has been proposed by Kondner (Reference 21), and used extensively by Duncan (Reference 22) for description of axial plastic strain as follows:

$$\epsilon_a = \frac{(\sigma_1 - \sigma_3)/(k\sigma_3^n)}{1 - \frac{(\sigma_1 - \sigma_3) R_f (1 - \sin\phi)}{2c\cos\phi + \sigma_3 \sin\phi}} \tag{3}$$

where

$\epsilon_a$ = axial strain

$k\sigma_3^n$ = relationship defining the initial tangent modulus as a function of confining pressure, (K and n are constants)

c = cohesion

$\phi$ = angle of internal friction

$R_f$ = a constant relating compressive strength to an asymptotic stress difference.

Barksdale (Reference 20) found that the above equation can fit the plastic stress-strain curves obtained from repeated load triaxial test results for 100,000 load repititions. For practical estimate of rut depth with pavement performance, an extensive testing program would be needed to calculate constants in the equations for various numbers of load repititions.

3. Subgrades

For fine grained soils, permanent strain is generally described by the following general equation.

$$\epsilon_p = A\, N^b \qquad (4)$$

where

$\epsilon_p$ = Permanent strain

N = Number of load repititions

A,b = Experimentally derived factors from repeated load testing data

Factors that influence the permanent deformation characteristics of fine grained soils include the applied stress, the moisture content, and the degree of compaction (Reference 19). An increase in moisture content or a decrease in the compactive effort both lead to decreased shear strength which contibutes to rutting.

Brabston reported in a study of deformation characteristics of subgrade soils (Reference 23) that the permanent axial strain response increases exponentially with load repititions to a point and then increases linearly thereafter at a much reduced rate. The rate of strain increase in both regions is a function of soil water content, density, and resistance to compaction as manifested by the slope of a plot of maximum density

versus compaction energy and the ratio of repetitive axial stress to failure deviator stress.

## B. DESTRUCTIVE EVALUATION METHODS

### 1. California Bearing Ratio (CBR)

The CBR flexible pavement design/evaluation procedure is used by the Department of Defense (Army, Navy, and Air Force)(Reference 24) and the Federal Aviation Administration (Reference 25). It has also been selected as the basis of determining the flexible pavement Aircraft Classification Number/Pavement Classification Number (ACN/PCN) by the International Civil Aviation Organization (ICAO) (Reference 26). The CBR system is the most universally used design/evaluation procedure for flexible airport pavements.

CBR is defined as the bearing ratio of soil determined by comparing the resistance to penetration of a 3 sq. in piston of the soil to that of a standard material (Reference 27). The method covers evaluation of the relative quality of subgrade soils but is applicable to subbase and some base course materials.

The CBR design method has been calibrated over the years with actual performance data and covers a wide range of pavement designs for most of the aircraft that are presently using airfields.

To evaluate a pavement using the CBR procedure, a test pit must be opened in the runway. The facility may be closed for a period of 1 to 3 days. CBR is measured on each pavement layer in the pit, and bulk samples are collected for laboratory testing. It is important to note that usually only one or two pits are constructed in a given runway or taxiway. Data from these pits are used to represent the characteristics for up to 10,000 lineal feet of pavement. ALRS pavements will vary in strength over these

distances. Since traffic will not locate "weak areas," additional data is necessary in order to locate the potential problem areas.

2. Rut Depth Prediction

Barber, et. al. (Reference 28) developed the following model for rut depth prediction for 2 layer flexible pavement systems with an AC surface course over a granular base:

$$RD = 1.9431 \left\{ \frac{P_K^{1.3127} \; t_p^{0.0499} \; R^{.3249}}{\left[\log (1.25Tac + Tbase)\right]^{3.4202} \; C_1^{1.6877} \; C_2^{0.1156}} \right\} \quad (5)$$

Standard Error = 0.411

r = 0.8779

where

RD = Rut depth, in.

$P_k$ = Equivalent single-wheel load (ESWL), kips

$t_p$ = Tire pressure, psi

Tac = Thickness of AC, in

Tbase = Thickness of Base, in

$C_1$ = CBR on top of Base

$C_2$ = CBR on top of Subgrade

R = Repetitions of load or passes

Destructive testing is required for this model to predict performance. Therefore, as with the CBR procedure, weak areas probably will not be located. However, this model will be used to evaluate the data generated in this study.

Barker (Reference 29) presented the following rut depth prediction model based on the relationship between resilient strain and permanent strain in the subgrade:

$$\frac{\epsilon_p}{\epsilon_R} = 0.14 \left(\frac{70800}{M_R}\right)^R \quad (6)$$

where

$R = 0.4\ (\text{Stress Repetitions})^{0.12}$

$M_R = \frac{\sigma_d}{\epsilon_R}$, ksi

$\sigma_d$ = Repeated deviation stress in laboratory triaxial test, ksi

$\epsilon_R$ = measured resilient strain in laboratory triaxial test, in/in.

$\epsilon_p$ = measured permanent deformation in laboratory triaxial test, in/in.

This model is applicable to permanent airfield pavements and assumes that most of the permanent deformation will occur in the subgrade. For ALRS pavements with a thin asphalt surface layer, rutting may also occur in the granular layer.

## C. NONDESTRUCTIVE EVALUATION METHODS

Nondestructive testing offers many advantages over conventional pavement evaluation testing. The major advantage is the ability to collect data at many locations on a runway or taxiway in a very short time. At least 20 tests can be conducted in one hour as compared to the day or more required for the construction and repair of one test pit.

Over the past 20 years several types of NDT equipment have been developed and used in the evaluation of roads and airfields. Most equipment applies either a vibratory or an impulse load to the pavement, and measures the resulting pavement surface deflection. Deflection is obtained with most devices by integrating the surface velocity measured with velocity

transducers. The force generators for the vibratory devices are either counterrotating masses or electrohydraulic systems that produce a sinusoidal loading. The impulse load devices utilize a falling weight dropped on a set of cushions to dampen the impulse to produce a loading time to simulate a moving wheel. The magnitude of the load is measured on some devices and calculated on others.

1. DSM Procedure

A nondestructive pavement evaluation procedure for airfield pavements was developed at the Waterways Experiment Station utilizing data collected with the WES 16-kip vibrator (Reference 13) for use with the CBR design method. The WES 16-kip vibrator is an electro-hydraulic actuated device that applies a sinusoidal loading of up to 30,000 lbs (peak-to-peak). The load is applied through an 18 in. diameter plate. The system is contained in a tractor-trailer unit.

Dynamic Stiffness Modulus (DSM) is defined as the slope of the upper third portion of the load/deflection relationship that is obtained when the sinusoidal dynamic loading is swept from 0 to 30,000 lbs (peak to peak). DSM from the WES 16-kip vibrator was correlated with the allowable single wheel load (ASWL) for 24,000 total departures of a single wheel aircraft as determined from destructive evaluation methods. Once the ASWL is determined, and layer thickness data is obtained, the CBR of the subgrade can be back-calculated. Using the CBR procedure with the derived subgrade CBR, allowable load for any aircraft can be determined.

Because it is an empirical correlation, the DSM procedure is valid only for the WES 16-kip vibrator. This device can not be air transported,

except on the C5A, and therefore would not be suitable for world wide testing.

2. Wave Propagation Methods

Techniques for determining the modulus of pavement layers through the analysis of surface waves traveling through the pavement system have been proposed by University of New Mexico and University of Texas researchers (References 30 and 31).

Both methods use an impact load from a falling weight device. Wave velocities are monitored with accelometers or velocity transducers located on the pavement surface. By describing the wave signals with Fourier series to give the amplitude and phase angle of each frequency, the signals between two accelometers are analyzed to estimate the difference in phase angle. Differences in phase angle are used to calculate the wave velocity for each frequency. The wave length of each frequency is estimated by multiplying the velocity by the frequency.

The wave velocity varies with the stiffness of the layers within the pavement system. A plot of velocity against wave length is called a dispersion curve. The University of New Mexico procedure, developed for the U. S. Air Force, relates the wave length to a depth within the pavement structure. The University of Texas procedure uses an inversion process to determine the propagation velocities at different depths. The wave velocity is then converted to shear modulus for each of the pavement layers.

These methods have not been developed for production testing on a large scale as would be required for ALRS type pavements. Analysis of the dispersion curve is difficult for untrained personnel.

3. Deflection Basin Methods

The deflection basin from an applied load offers a method to evaluate the stability of the layers within a pavement structure. Optimally each layer modulus can be quantified if the thickness is known.

Several methods have been applied to airfield pavement structures and are summarized in several reports (References 15, 16, and 18). Most methods match surface deflections to deflections from layered elastic (linear and nonlinear) or finite element (linear and nonlinear) models.

a. Surface/Base Curvature Index Methods

Peterson (Reference 32) presented a method using the deflection basin data obtained from the Dynaflect device. Problem areas of the pavement structure were identified as shown in Figure II-1

where:

Surface Curvature Index (SCI) = The difference between the deflections (mils) measured by the first and second sensors (DO - D12).

Base Curvature Index (BCI) = The difference between the deflections (mils) measured by the fourth and fifth sensor located 36 in and 48 in from the center of the loaded area, respectively (D36 - D48).

Spreadibility (SPR) = Determined from the equation:

$$SPR = \frac{DO + D12 + D24 + D36 + D48}{5(DO)} \quad (7)$$

This method of analyzing the deflection basin is applicable to the rapid field evaluation of ALRS pavements. To use the values given in Figure II-1, deflections must be converted to equivalent Dynaflect deflections or new criteria developed for the selected NDT device.

b. Area/DO Concepts.

Hoffman and Thompson (Reference 12) presented a pavement evaluation method that used the Falling Weight Deflectometer deflection at the center of the load (DO) normalized to 9000 lbs. and the normalized cross-sectional area (AREA) of the deflection basin out to the sensor at a 36 in. distance from the center of the applied load (Figure II-2). Algorithms and nomographs were developed to determine the modulus of the subgrade ($E_{RI}$) (See Figure II-3) from the ILLIPAVE finite element model (Reference 33).

c. Backcalculation methods

Lytton (Reference 18) summarized nine methods for matching deflection basins. Typically methods have been developed to calculate moduli for up to five layers. Most methods do not handle non-linear stress-strain effects, and most can be operated on either a microcomputer or main frame.

A nondestructive evaluation procedure using a layered elastic method of analysis has been developed by WES for light aircraft pavements (Reference 14). In this method, a computer program, CHEVDEF, was developed to backcalculate the modulus of the pavement layers from the measured deflection basin. In CHEVDEF, the Chevron layered elastic program is used to calculate the deflections.

The Chevron program was replaced with BISAR (Reference 34) to allow for varying interface conditions between the pavement layers. The revised version, BISDEF, reported in References 15 and 17, is described in Appendix B.

## D. METHODS SELECTED

### 1. Field Procedure

The Falling Weight Deflectometer (FWD) was selected as the testing apparatus for this study. The FWD offers distinct advantages over vibratory equipment for testing airport pavements all over the world. With an FWD, a force output in the range of loading expected for the design aircraft can be developed with a relatively light test apparatus. The FWD weighs about 1800 pounds and can be transported on most cargo aircraft. A maximum force output of approximately 25000 pounds can be generated. In comparison, the WES 16-kip vibrator places a 30000 pound peak-to-peak loading and weights 70,000 pounds. A Road Rater Model 2008 weights approximately 8000 pounds and outputs a 7000 pound peak-to peak load.

### 2. Mechanistic Analysis.

A layered elastic model was selected for analysis of the traffic test section data. The assumptions of linear elastic, homogeneous isotropic material properties are invalid particularly after traffic is initiated. Due to the high stress state in the granular base layer and the subgrade, permanent deformation is likely to occur during initial traffic. Material responses when significant permanent deformations occur are nonlinear. However, this model was selected since it has been used previously for airfield pavements (Reference 35). The CHEVRON program was used to develop the limiting vertical strain criteria (Figure II-4). BISAR will be used to calculate the stresses and strains for the pavements under the F-4 loading. BISAR is also the base program for BISDEF for calculation of layer moduli.

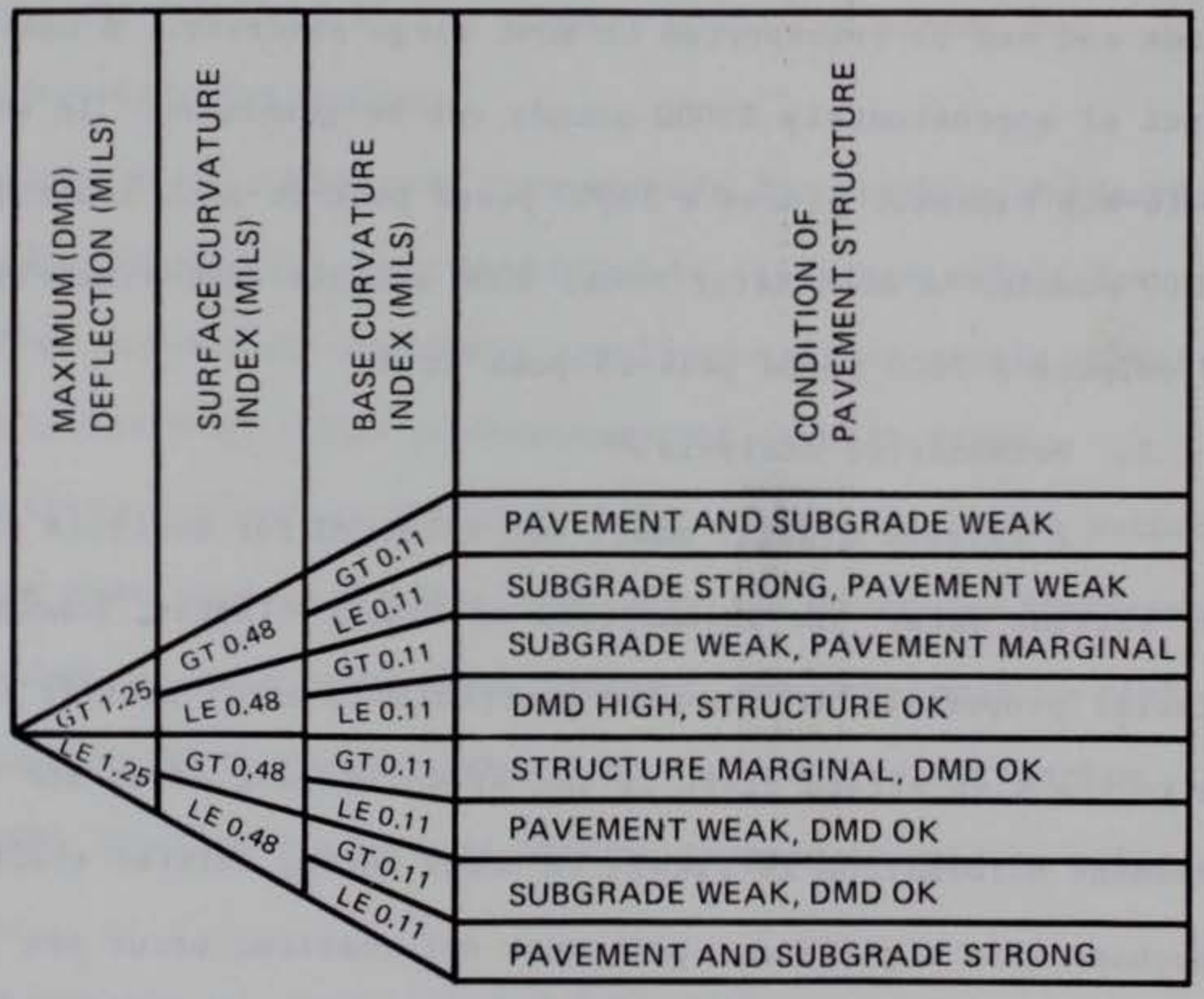


Figure II-1. Use of Deflection Basin Parameters to Analyze Pavement Structural Layers (Reference 32).

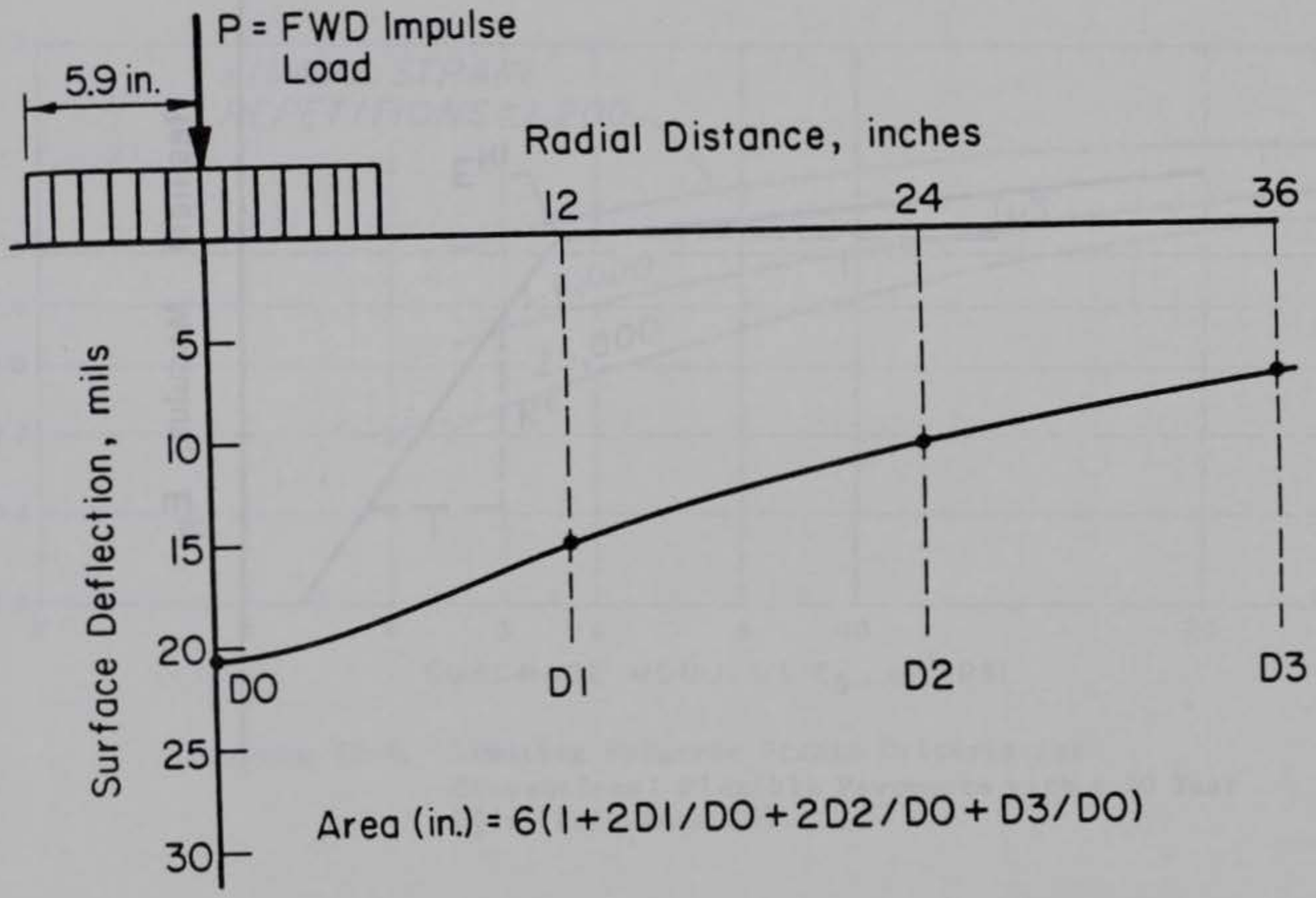


Figure II-2. Area of Deflection Basin (Reference 12).

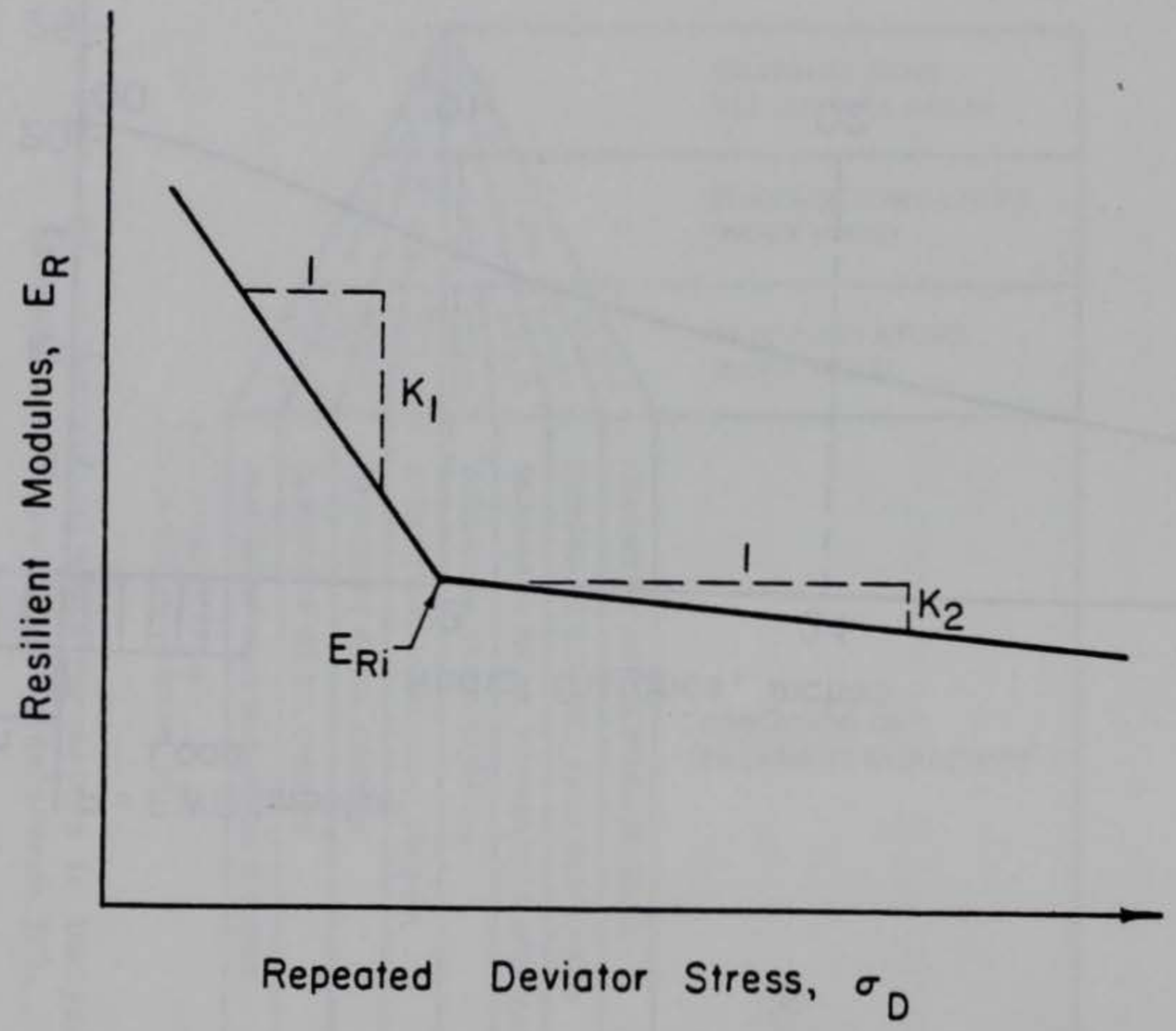


Figure II-3. Typical Resilient Modulus - Repeated Deviator Stress Relation (Reference 12).

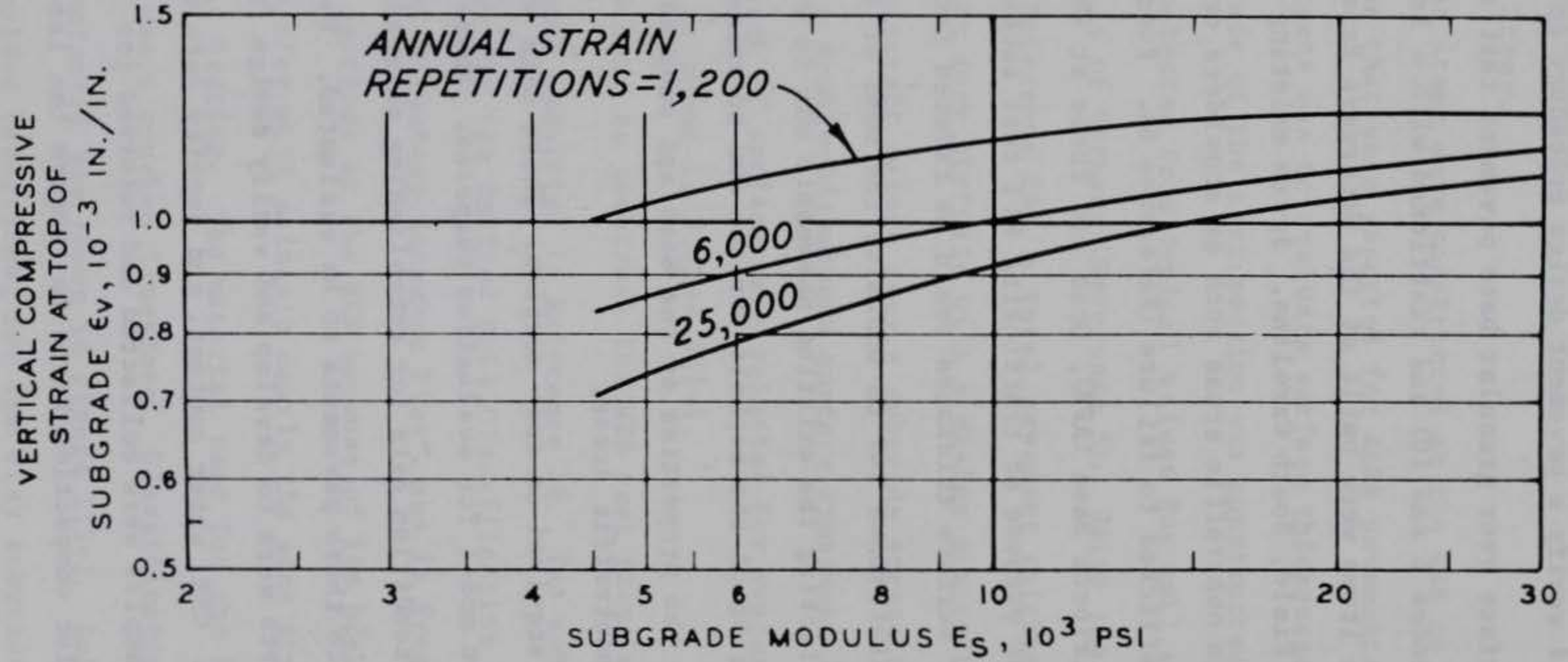


Figure II-4. Limiting Subgrade Strain Criteria for Conventional Flexible Pavements with a 20 Year Life (Reference 35).

# SECTION III

# FIELD TESTS

## A. INTRODUCTION

To develop and verify a pavement design procedure for ALRS pavements, four bituminous surface over granular base pavement test sections were constructed (References 6 and 10) and trafficked with a load cart simulating F-4 loading. Three items were built at the Waterways Experiment Station and one was built at North Field, South Carolina. Seven existing pavement sections, located in nontraffic areas such as shoulders or over-runs, were also trafficked to failure (Reference 6). Four were at Wright-Patterson Airforce Base (AFB), Ohio and three at Whiteman AFB, Missouri. The major purpose of trafficking all test sections was to evaluate whether the asphalt surface thickness could be reduced from the current required 3 inches (Reference 24) to minimize the cost of the ALRS pavements. The purpose of trafficking the existing pavements was to evaluate the effect of environmental aging of the asphalt surface due to oxidation and the effects of aging on the properties of the base and subgrade layers when the pavements were in nontraffic areas.

FWD data were acquired on each section. These data will be used to develop a prediction model for evaluation purposes. These pavements provide a range of age and condition data for establishing an evaluation procedure that is comparable to those pavements to be evaluated. The objectives of these research efforts were to develop and verify design for low volume airfield pavements. CBR, water content, and density data were collected on these pavements. Samples were collected and returned for labortory classi-fication tests and for compaction tests to compare the laboratory density to

that density obtained in the field. Funding was not available for resilient modulus testing.

## B. PAVEMENT CHARACTERISTICS

### 1. WES Test Items.

Three test items were constructed at the WES to simulate the strength conditions that were expected for ALRS pavements. The primary purpose of these tests was to evaluate surface thicknesses of less than 3 inches. The subgrade of the test section was constructed for a 6 CBR $\pm$ 1. The strength was selected from typical values for soil at U. S. airbases in the Federal Republic of Germany (Reference 5). Using the flexible pavement design procedure (Reference 24), a total pavement thickness of 12 inches is required for a light duty airfield with a design aircraft of gross weight of 60 kips, and 150 aircraft passes over a subgrade strength of 5 CBR. Three wearing surfaces, a double-bituminous surface treatment (DBST), a 1-inch AC surface, and a 2-inch AC surface were selected for evaluation. The layout of the test items is shown in Figure III-1.

The materials used to construct the WES test items were selected to meet the requirements specified in Reference 24. The subgrade soil was a CH material, according the the Unified Soil Classification System (USCS). It is commonly called "Vicksburg Buckshot Clay". and is frequently used in constructing test sections at the WES because of its high plasticity and low permability. This clay will maintain nearly the same strength over the duration of traffic testing. The material used for the base course of the ALRS test section was a crushed limestone. Classification data for the limestone and CH material are shown in Figure III-2. Laboratory compaction and CBR data, as-molded conditions, for the clay subgrade and base course

are shown in Figures III-3 and III-4. The crushed limestone base course showed very little strength loss with increased water content (Figure III-4).

The double-bituminous surface treatment (DBST) was constructed using a CRS-2 emulsified asphalt as the binder. The AC surface mix was designed in accordance with the 75-blow Marshall mix design method given in MIL-STD-620. Aggregates selected were a crushed limestone of coarse and fine gradations, and a local concrete sand. For identification, the items will be designated as WES1 for 2-inch AC, WES2 for 1-inch AC and WES3 for the DBST.

A summary of pre-traffic and post-traffic CBR, density and water contents of the WES test section is shown in Table III-1. In place density of the granular base material was determined using a nuclear density gage (Reference 36) and the water balloon method (Reference 37). Densities of the clay subgrade were obtained using the drive cylinder method (Reference 38). The density of the base course increased with traffic, but there was no significant change in the subgrade properties. As-built thickness data for the WES test items are shown in Table III-2. These data were determined from rod and level cross sections taken after each layer was completed. Therefore, the averages are from a large number of readings. These average thicknesses will be used for analysis.

2. Wright-Patterson and Whiteman Test Items.

The design freezing index was used as the basis for selection of continential United States test pavements that had been enviromentally aged under conditions similar to those in Germany and Korea, where ALRS pavements are to be built. Wright-Patterson AFB, Ohio and Whiteman AFB, Missouri were

selected, based on the design freezing index and because more pavement areas were available in fewer locations minimizing transportation costs. The design freezing index for Wright-Patterson and Whiteman AFB's were 892 and 686 freezing degree-days, respectively.

The areas selected for traffic test at both Wright-Patterson and Whiteman AFB's, were taxiway and apron shoulder pavement, runway overrun and a parking pad for fire equipment. All of the traffic test features, except one, were constructed with an AC surface course. One feature was constructed with a DBST surface. An airfield pavement layout and the location of the test features are shown in Figures III-5 and III-6. From each feature a section 10 feet by 30 feet was selected for traffic testing. A list of pertinent data including construction and maintenance dates are shown in Table III-3. The pavements ranged in age from 9 to 30 years at the time of testing. The surface thickness varied from 1-inch for the DBST to 3-inches. The base course thickness varied from 6 to 47-inches. The pavement structure with measured CBR values within the structure are shown in Figure III-7. Designations for these pavements are also shown and will be used herein.

Gradations for base and subgrade materials are shown in Figures III-8 and III-9. The dashed lines are limits for base course materials as specified by the Department of Defense in Reference 24. The base courses are relatively close to those limits but are one to two percent higher on the fines passing the number 200 sieve. Laboratory CE-55 compaction and CBR test results for the Wright-Patterson AFB and Whiteman AFB base courses are shown in Figures III-10 through III-16. These results are presented to show the effect of higher water contents on the CBR of the material. The field

measured CBR's, densities, and water contents are presented in Table III-4. Densities of granular bases were obtained with a nuclear gage (Reference 36). Densities of subgrade material were obrtained using the Drive Cylinder method (Reference 38). The base course densities met specifications at the top of the layer, but were significantly low from 6 to 10 inches into the layer. The subgrade layer was not reached on items WP-2 and W-1. The water table was reached at a significant depth into the pavement structure as indicated in Figure III-7. The sides of the pit became unstable and excavation was stopped.

3. North Field Test Section.

To verifiy design thicknesses determined from the WES test sections and the environmentally aged pavements at Wright-Patterson and Whiteman AFB's, a test section was constructed at North Field, South Carolina and subjected to F-4 aircraft traffic operating at maximum load. After aircraft trafficking was completed, the test section was trafficked to failure with load carts simulating maximum loaded F-4 and F-15 aircraft. A layout of the airfield with the location of the test area is shown in Figure III-17. The pavement structure at North Field was designed to support 150 passes of the F-4 aircraft. The subgrade soil at North Field was a sand, with a strength of more than 20 CBR measured before construction. The total thickness of granular base and AC above this subgrade was less than the minimum required base thickness as specified in the Tri-Service Manual (Reference 24). Therefore, the pavement was constructed with 2 inches of AC over 6 inches of crushed granite base, the minimum requirement for base thickness and the recommended thickness of surfacing for ALRS pavements.

The base course material used in the North Field test section was well graded crushed granite with the gradation shown in Figure III-18. Compaction test results for the base are shown in Figure III-19. The gradation for the subgrade material is shown in Figure III-18. Compaction tests were conducted at two efforts for the subgade. Results are presented in Figure III-20. The before and after traffic soils data are presented in Table III-5. Density data were obtained using a nuclear gage on the granular base material (Reference 36) and the drive cylinder method on the sand subgrade (Reference 38).

## C. TEST CONDITIONS AND PROCEDURES

### 1. Instrumentation.

The North Field test item was instrumented with linear variable differential transformer (LVDT) displacement transducers to measure vertical surface deflections. The LVDT produced DC output voltages directly proportional to the movement of the sensing unit. The transducer consisted of a main body, which housed the sensing coil and its associated electronics, and a movable core through the center of the sensing coil to transfer the mechanical movement of the core to a change in an electrical signal in the coil. The LVDT transducers were mounted on reference rods that extended to reference flanges located approximately 6 feet below the bottom of the test bed. The reference rods were cased with 2 inch PVC pipe attached to the gage housing with flexible hose. The construction and details of the deflection gage are given in References 6, 10, and 39.

Pressure gages were also installed in the North Field test item. Construction of the WES soil pressure cells is described in several publications (References 40-42). WES soil pressure cells are designed to average

vertical stress components applied across a 6-in-diameter faceplate. The soil stress acts on the faceplate which reacts on an internal mercury chamber. Pressure in the mercury chamber is an accurate analog of the average stress applied to the faceplate. The mercury chamber pressure is measured by a strain-gaged diaphragm which completes the transduction mechanism. The cells were calibrated to either 50 or 100 psi. Two sets of gages were placed in the item so that they would be under the main gears of the F-4 aircraft when the aircraft was centered on the test item. A set of gages consisted of one deflection gage mounted at the surface, one 100 psi pressure gage mounted at the subgrade surface and a 50 psi gage mounted 12 inches from the top of the subgrade. A layout of the instrumentation at North Field is shown in Figure III-21.

2. Nondestructive Testing.

A falling weight deflectometer (FWD) was used to determine the pavement deflections before, during, and after traffic tests on each of the test items. Two models of an FWD manufactured by Dynatest Consulting were used in this study. The model used on the WES test items and the environmently aged pavements at Wright-Patterson and Whiteman AFB's had a 440-pound drop weight which applied a dynamic force of up to 15,000 pounds through an 11.8 inch diameter plate on the pavement surface. The applied force and pavement deflections were measured with load cells and velocity transducers. On subgrades, a 17.7-inch plate was used to reduced the magnitude of the deflection to within the range of the velocity transducers (0.080 inches maximum). The data acquisition equipment displays the resulting pressure in kilopascals and the maximum peak displacement in micrometers. Only three displacement transducers are provided with this model. Therefore, to obtain five

deflections to describe the deflection basin, tests were conducted with the sensors at 0, 12, and 36 inches from the center of the load. Two sensors were repositioned to 24 and 48 inches from the center of the load and testing was repeated.

The model used for the North Field testing operated with the same configuration as described above but was controlled by a microcomputer. A total of seven deflections were recorded with each drop. The force output can range from 1,500 to 24,000 pounds by varying the mass level from 110 to 660 pounds and the drop height from 0.8 to 15.0 inches.

Nondestructive tests were conducted with the FWD at quarter points of the WES test items and at one third points on the Wright-Patterson, Whiteman, and North Field items. Testing was conducted before, during, and after traffic. Tests were conducted at force levels of approximately 9000 and 15000 pounds. Deflections in many tests at the 15000 pound force level exceeded the 80 mil limit of the velocity transducers.

3. F-4 Load Cart.

Traffic tests were performed on each test item using a specially constructed load cart to simulate a fully loaded F-4 aircraft. The cart was loaded to 27000 pounds and used a 30 x 11.5-14.5, 24-ply rated tire inflated to 265 psi. A tire contact area of 102 square inches was measured by placing the loaded tire on a plank of landing mat and painting the outline with spray paint. The outline was traced on a sheet of paper. The area was then measured with a plainimeter.

4. Traffic Pattern.

Each of the test items was trafficked with a distributed pattern simulating the expected wander width (70 inches) of the F-4 aircraft on

runway ends and taxiways. The traffic distribution pattern is shown in Figure III-22. To apply the traffic, the test cart was driven backward and forward along the same path, then shifted laterally the distance to one tire width (10 inches) and the process repeated. The interior 40 inches received 100 percent of the maximum number of passes in any wheel path and the exterior portions of the lane received 67 and 33 percent.

Traffic will be described in terms of coverages. For flexible pavements, a coverage at a point occurs, when that point on the pavement surface receives one application of the tire print. Based on traffic distribution sutdies the number of passes required to produce one coverage is computed for the distribution of traffic over the width of the pavement area (Runway, Taxiway, or Apron). for a single wheel aircraft such as the F4, the distribution is computed for one main gear. The F-4 aircraft pass to coverage ratio is 8.58. The pass to coverage ratio for the distribution pattern used in this study was 7.33. Therefore, predictions will be presented in term of coverages herein.

5. Failure Criteria.

The failure criteria proposed by the Air Force Engineering and Services Center for the ALRS pavements were as follows:

a. Base course aggregate exposure sufficient to pose a foreign object damage (FOD) potential;

b. AC disintegration sufficient to present FOD potential;

c. A rut depth in excess of 3 inches;

d. Other conditions, as determined by the project engineer, that cause the pavement to be nonserviceable.

Whenever one of these failure criteria was reached on a given item under testing, the traffic was discontinued and final data were recorded.

The CBR design procedure failure criteria (Reference 27) for flexible pavements designed as permanent structures based on accelerated traffic test data are:

a. Surface upheaval of the pavement adjacent to the traffic lane of 1 in. or more.

b. Surface cracking to the point that the pavement was no longer waterproof.

This criteria distinguishes between settlement due to traffic compaction and distortion due to shear deformation. Settlement, which is the result of densification of the base and subbase under accelerated traffic is expected because of problems of obtaining density in thin pavement layers on a weak subgrade.

For the purpose of this investigation both the ALRS criteria and the permanent pavement criteria will be evaluated. Rut depth was measured using a 10-foot staightedge. A 10-foot beam was placed across the traffic lane and the depth of rut was measured vertically to the lowest point within the traffic lane.

6. Other Data.

Rod and level cross section data were collected at quarter points on the WES items and at one third points on the remainder of the items. Data were collected prior to, during and after traffic. The amount of cracking of the AC surface was monitored throughout the traffic testing. The area was measured and recorded as a percent of the total area of the traffic test section.

TABLE III-1. SUMMARY OF CBR, DENSITY, AND WATER CONTENT DATA FOR SUBGRADE AND BASE ON WES TEST ITEMS

| Item | Pre-Traffic | | | | After Traffic | | | |
|---|---|---|---|---|---|---|---|---|
| | Depth in. | Water Content, % Dry Weight | Density pcf | CBR | Depth in. | Water Content, % Dry Weight | Density pcf | CBR |
| | | | | BASE COURSE | | | | |
| 1 | 2 | 2.2 | 144.9 | 91 | 2 | 1.9 | 148.0 | 110 |
| 2 | 1 | 2.7 | 144.4 | 85 | 1 | 2.2 | 148.8 | 107 |
| 3 | 1 | 2.3 | 144.1 | 96 | 1 | 2.1 | 145.3 | 103 |
| | | | | SUBGRADE | | | | |
| 1 | 12 | 26.2 | 93.4 | 6.3 | 12 | 26.5 | 92.8 | 7.0 |
| | 18 | 27.9 | 89.7 | 5.5 | 18 | 26.3 | 93.0 | 8.0 |
| | 24 | 26.6 | 92.9 | 6.9 | 24 | 25.9 | 93.3 | 6.0 |
| | Avg | 26.9 | 92.0 | 6.2 | Avg | 26.2 | 93.0 | 7.0 |
| 2 | 12 | 26.9 | 92.6 | 5.6 | 12 | 27.2 | 92.6 | 6.0 |
| | 18 | 27.7 | 91.2 | 7.0 | 18 | 27.5 | 91.9 | 6.7 |
| | 24 | 27.7 | 90.3 | 6.7 | 24 | 27.2 | 91.7 | 6.3 |
| | Avg | 27.4 | 90.4 | 6.4 | Avg | 27.3 | 91.1 | 6.3 |
| 3 | 12 | 26.8 | 92.1 | 6.7 | 12 | 26.7 | 91.9 | 7.3 |
| | 18 | 28.2 | 90.1 | 5.3 | 18 | 26.7 | 90.2 | 6.0 |
| | 24 | 27.7 | 91.0 | 5.6 | 24 | 28.7 | 90.5 | 5.0 |
| | Avg | 27.6 | 91.1 | 5.9 | Avg | 27.4 | 90.9 | 6.1 |

TABLE III-2. AS BUILT LAYER THICKNESS FOR WES TEST ITEMS

| Item Number | Layer | Average Thickness Inch | Standard Deviation Inch |
|---|---|---|---|
| 1 | Asphalt | 1.7 | 0.6 |
| 1 | Base | 8.2 | 0.6 |
| 2 | Asphalt | 1.4 | 0.3 |
| 2 | Base | 9.0 | 0.4 |
| 3 | DBST | 0.5 | 0.2 |
| 3 | Base | 9.4 | 0.5 |

TABLE III-3. PAVEMENT CONSTRUCTION HISTORY

| Feature | Location | Pavement | Base | | | Subgrade | | Constr. | Maintenance |
|---|---|---|---|---|---|---|---|---|---|
| | | | Type | Thickness | In-place CBR | Type | In-place CBR | Date | |
| | | | | Wright-Patterson AFB, Ohio | | | | | |
| WP-1 | Fire Equip. Parking Pad | 3 in. AC | Gravel (GW) | 6 in. | 12 | --- | --- | 1961 | --- |
| WP-2 | Shoulder Pavement T/W-17 | 1 in. AC over 2 in. AC | Clayey Gravel (GP-GC) | 47 in. | 33 | --- | --- | 1959 | Overlay, 1971 Rejuvenator, 1979 |
| WP-3 | Apron D | 2 in. AC | Gravel (GP) | 12 in. | 33 | Clayey Sand (SC) | 7 | 1974 | Excavated 2-in. base MC-30 prime coat 2 in. AC, 1974 |
| WP-4 | Shoulder Pavement T/W-5 | 2 in. AC | Silty Gravel (GW-GM) | 12 in. | 72 | Clayey Sand (SC) | 8 | 1962 | Rejuvenator, 1974 |
| | | | | Whiteman AFB, Missouri | | | | | |
| W-1 | North Overrun R/W-01-09 | 1 in. DBST | Sandy Clayey Gravel (GC) | 29 in. | 33 | --- | --- | 1961 | Seal coat, 1979 |
| W-2 | Shoulder Pavement T/W-9B | 2.5 in. AC | (GC) | 12 in. | 102 | Clay (CH) | 4.2 | 1953 | Slurry Seal, 1966 |
| W-3 | Blast Pavement Alert Apron | 2.5 in. AC | (GC) | 16 in. | 37 | Clay (CL) | 4.2 | 1959 | Slurry Seal, 1966 |

TABLE III-4. BASE COURSE AND SUBGRADE PROPERTIES FOR WRIGHT-PATTERSON AND WHITEMAN AFB ITEMS

| Test Feature | Depth Inches | Material | CBR | Water Content | Dry Density - PCF In-Place (A) | Dry Density - PCF CE-55* (B) | Dry Density - PCF Water Content | Percent CE-55 Density |
|---|---|---|---|---|---|---|---|---|
| WP-1 | 3.0 | Base (GW) | 12 | 4.3 | 143.3 | 141.3 | 5.5 | 101 |
| | 9.0 | Base (GW) | 13 | 11.8 | 119.0 | --- | --- | --- |
| WP-2 | 3.0 | Base (GP-GC) | 33 | 5.4 | 145.3 | 143.1 | 5.2 | 102 |
| | 16.0 | Base (GP-GC) | 35 | 15.3 | 117.0 | --- | --- | --- |
| WP-3 | 2.0 | Base (GP) | 33 | 5.3 | 135.3 | 140.1 | 5.4 | 97 |
| | 14.0 | Subg. (SC) | 7 | 11.7 | 112.3 | 129.2 | 8.3 | 87 |
| WP-4 | 2.0 | Base (GW-GM) | 72 | 3.6 | 138.7 | 143.3 | 5.7 | 97 |
| | 14.0 | Subg. | 8 | 20.6 | 100.8 | --- | --- | --- |
| W-1 | 1.0 | Base (GC) | 33 | 5.6 | 132.1 | 137.2 | 7.0 | 96 |
| W-2 | 2.5 | Base (GC) | 102 | 4.5 | 140.3 | 137.5 | 6.3 | 102 |
| | 15.0 | Subg. (CH) | 4.2 | 24.1 | 97.4 | 120.1 | 12.8 | 81 |
| W-3 | 2.5 | Base (GC) | 37 | 4.7 | 135.1 | 139.8 | 6.3 | 97 |
| | 19.0 | Subg. (CL) | 4.2 | 25.2 | 94.3 | 113.5 | 15.0 | 83 |

* Laboratory densities shown in this column are the CE-55 maximum densities at optimum water content.

Table III-5. SUMMARY OF CBR, DENSITY, AND WATER CONTENT FOR NORTH FIELD TEST ITEM

| Station | Material | Depth in. | CBR | Modulus of Subgrade Reaction, k pci | Water Content percent | Dry Density pcf | Percent of CE-55 Density |
|---|---|---|---|---|---|---|---|
| | | | | BEFORE TRAFFIC | | | |
| 25 | Subgrade | 0 | 16 | | 6.4 | 111.3 | 92 |
| | | 6 | 44 | | 4.8 | 115.2 | 95 |
| | | 12 | 45 | | 5.0 | 114.1 | 94 |
| 50 | | | | 444 | | | |
| 75 | | 0 | 27 | | 5.2 | 115.4 | 95 |
| | | 6 | 26 | | 5.2 | 115.6 | 96 |
| | | 12 | 25 | | 6.7 | 116.2 | 96 |
| 25 | Base | 0 | 52 | | 5.2 | 143.2 | 106 |
| 40 | | 0 | 96 | | 5.2 | 143.2 | 106 |
| 50 | | | | 526 | | | |
| 75 | | 0 | 69 | | 5.2 | 143.2 | 106 |
| | | | | AFTER TRAFFIC | | | |
| 35 | Subgrade | 0 | 63 | | 3.8 | 112.7 | 93 |
| | | 6 | 79 | | 3.5 | 111.5 | 92 |
| | | 12 | 53 | | 3.4 | 110.0 | 91 |
| 35 | Base | 0 | 100+ | | 4.1 | 147.2 | 109 |

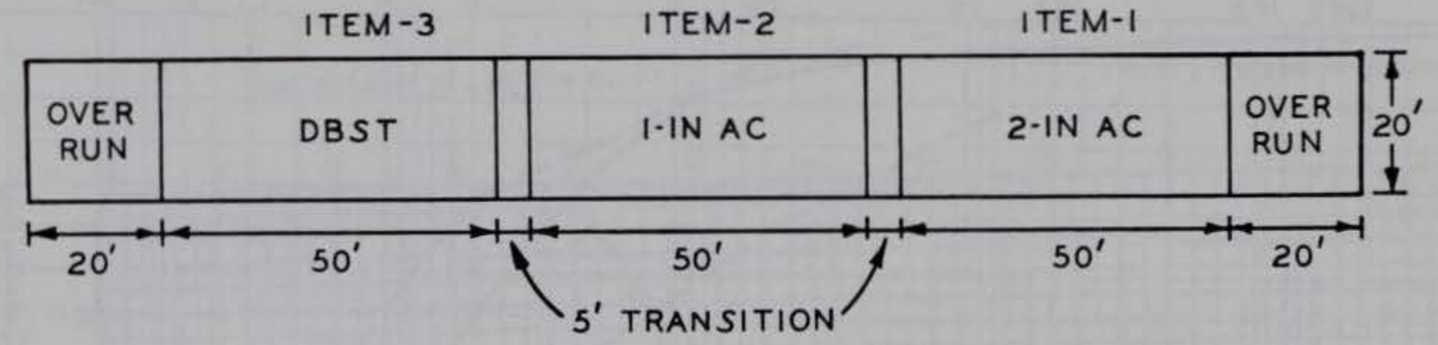


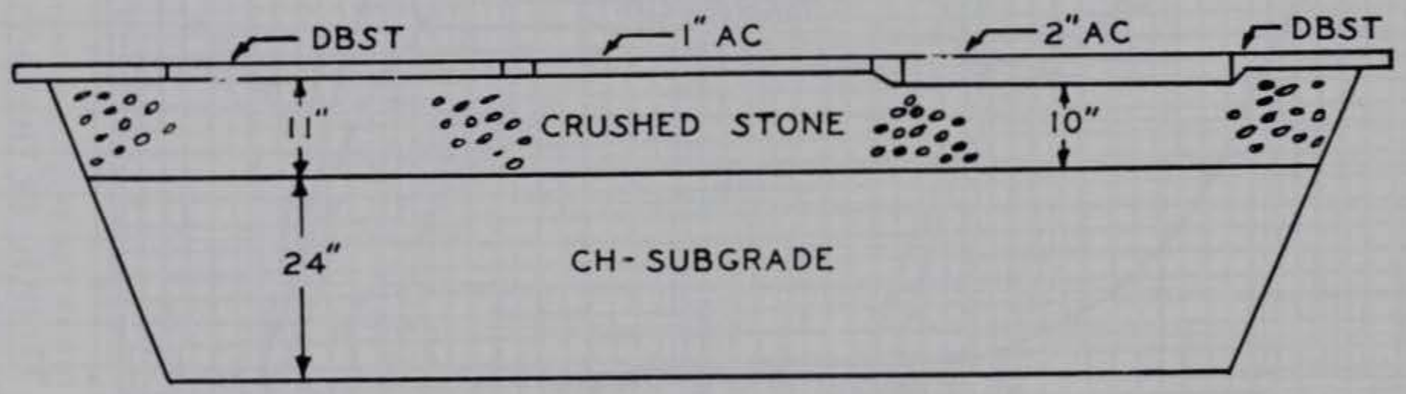


Figure III-1. Layout of WES Test Item.


| SAMPLE NO | ELEV OR DEPTH | CLASSIFICATION | NAT W% | LL | PL | PI |
|---|---|---|---|---|---|---|
| 1 | | HEAVY CLAY (CH) | | 66 | 18 | 48 |
| 2 | | CRUSHED LINESTONE | | NP | | |
| | | | | | | |
| | | | | | | |
| | | | | | | |

GRADATION CURVES

PROJECT ALRS TEST SECTION

AREA

BORING NO

DATE

ENG FORM 2087
1 MAY 63

REPLACES WES FORM NO. 1241, SEP 1962, WHICH IS OBSOLETE.

U.S. GOVERNMENT PRINTING OFFICE 1963 OF—709-128

Figure III-2. Grain Size Distributions for Subgrade and Base for WES Test Item.

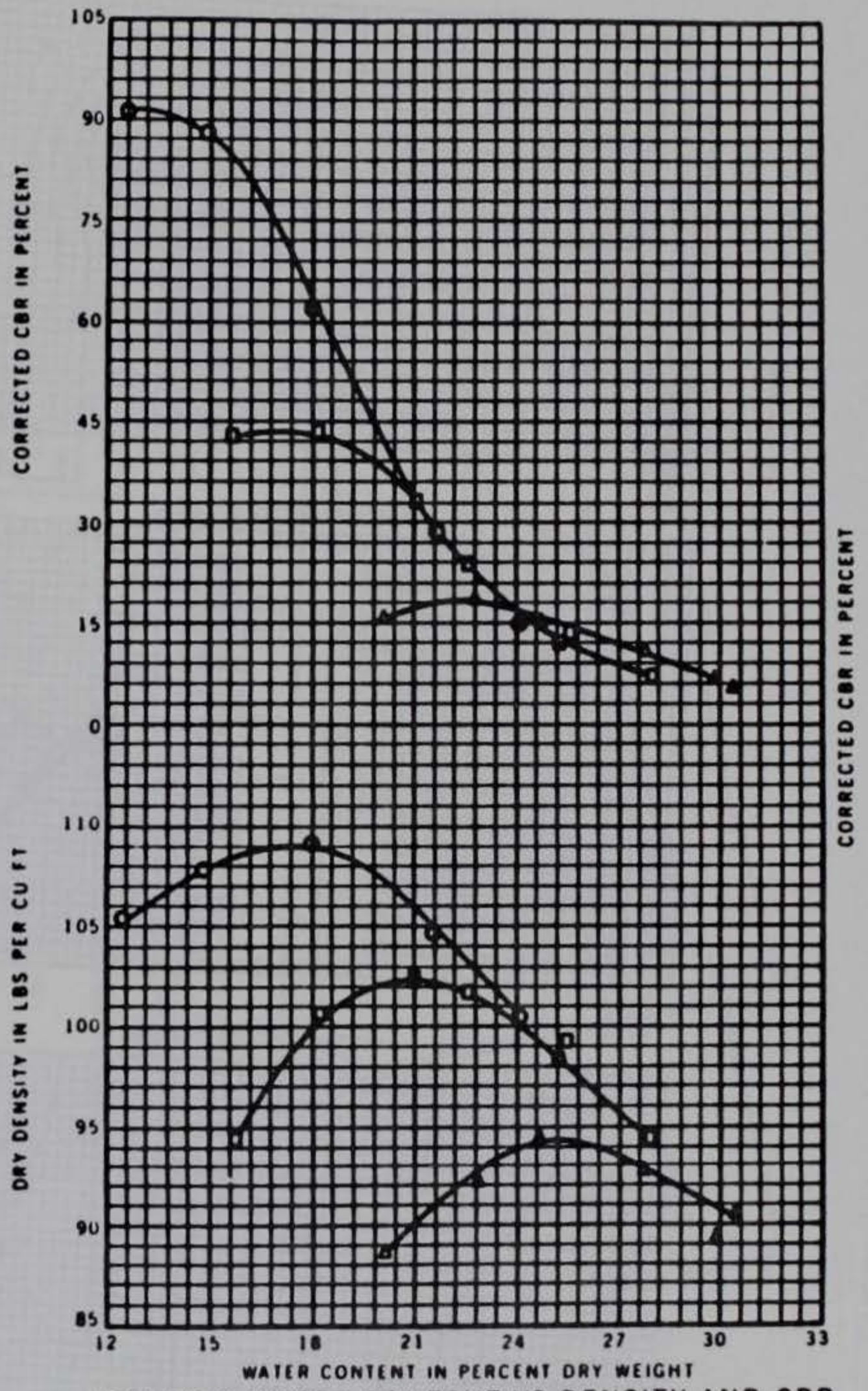


MOLDING WATER CONTENT VS DENSITY AND CBR

LEGEND

| SYMBOL | NO OF BLOWS/LAYER | COMPACTION EFFORT |
|---|---|---|
| △ | 12 | CE 12 |
| □ | 26 | CE 26 |
| ○ | 55 | CE 55 |

Figure III-3. Laboratory Compaction and CBR's for WES Test Item Subgrade.

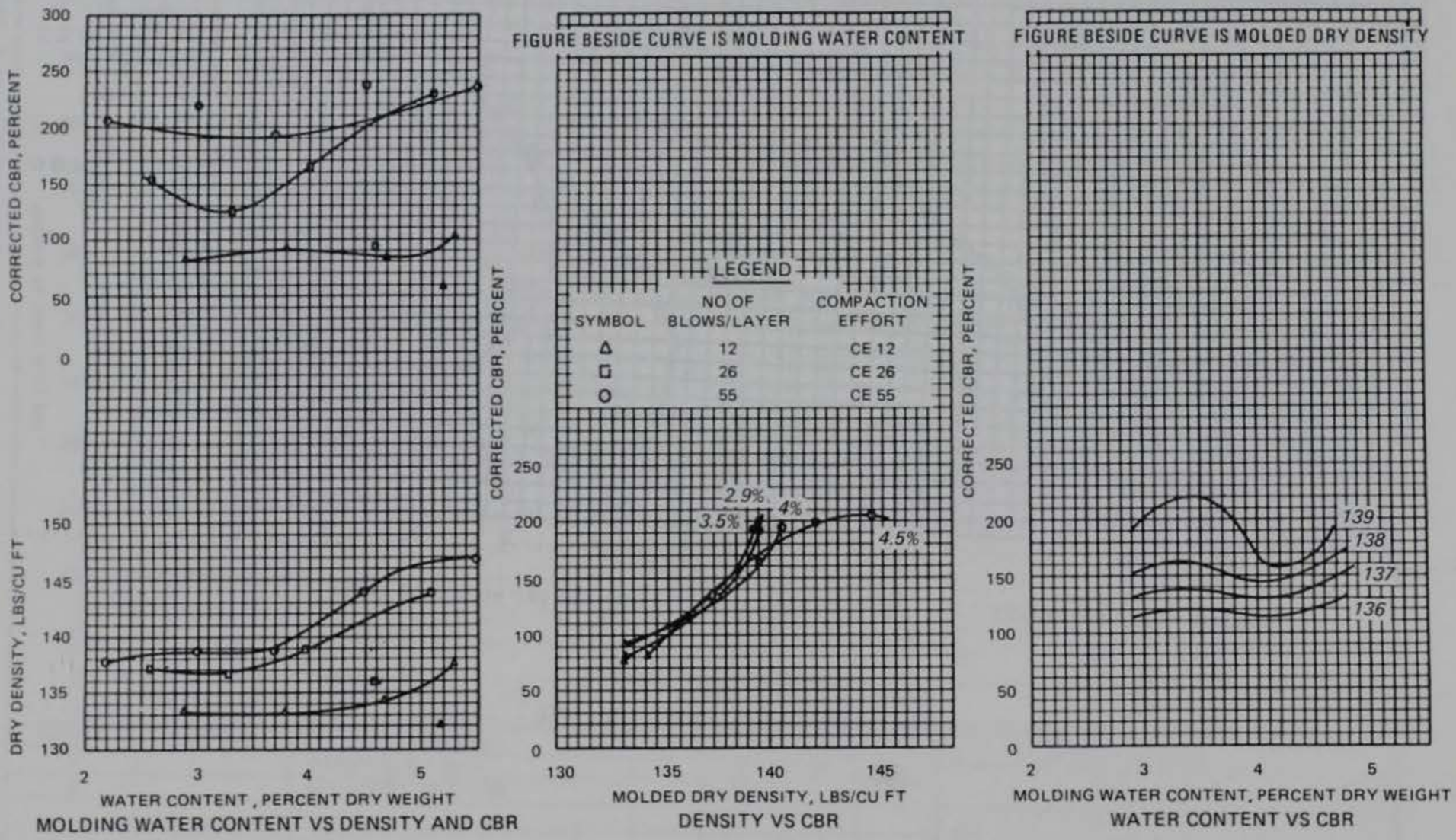


Figure III-4. Laboratory Compaction and CBR's for WES Test Item Base Course.

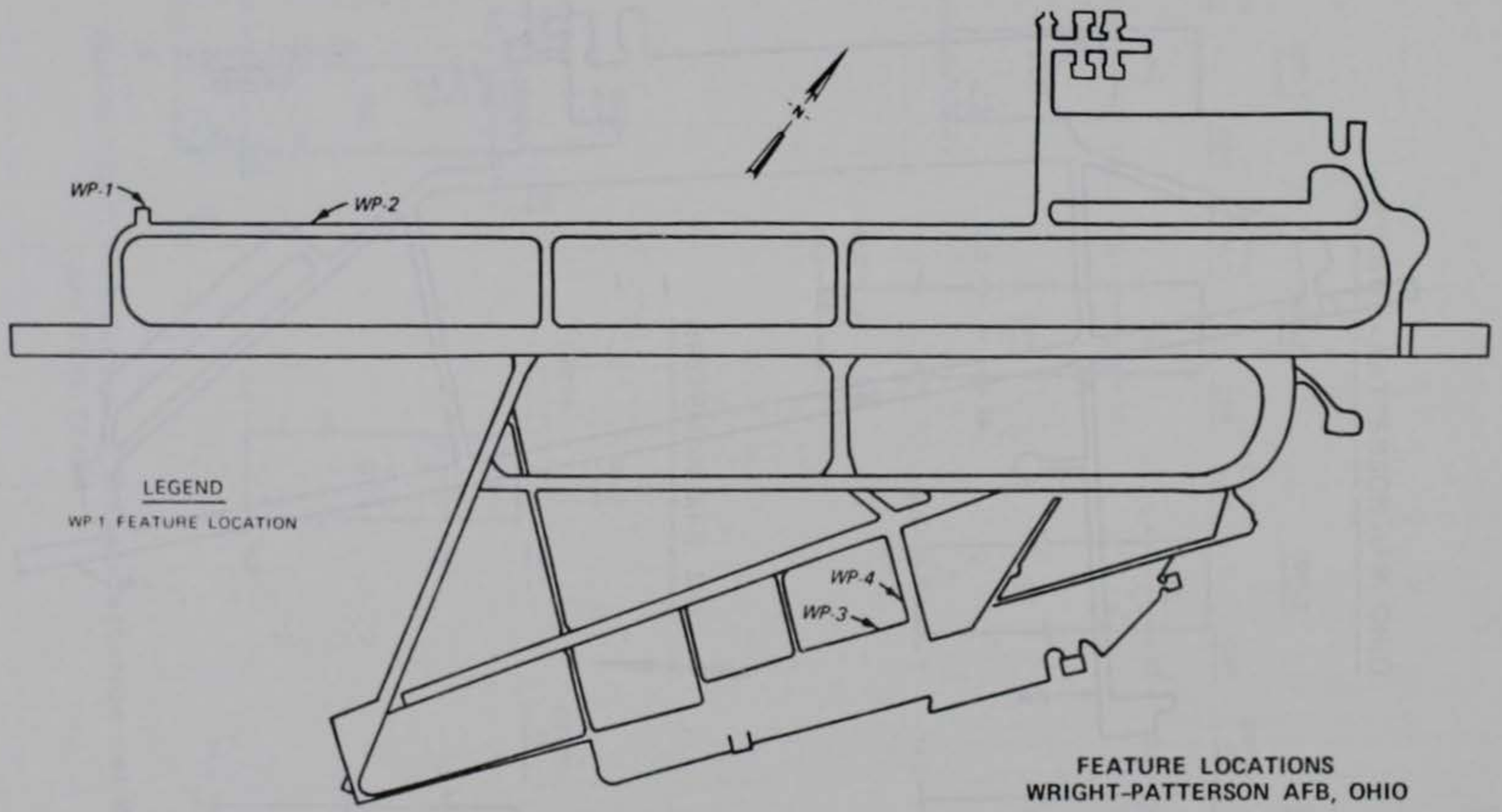


Figure III-5. Layout of Airfield Pavements Showing Location of Test Items, Wright-Patterson AFB, Ohio.

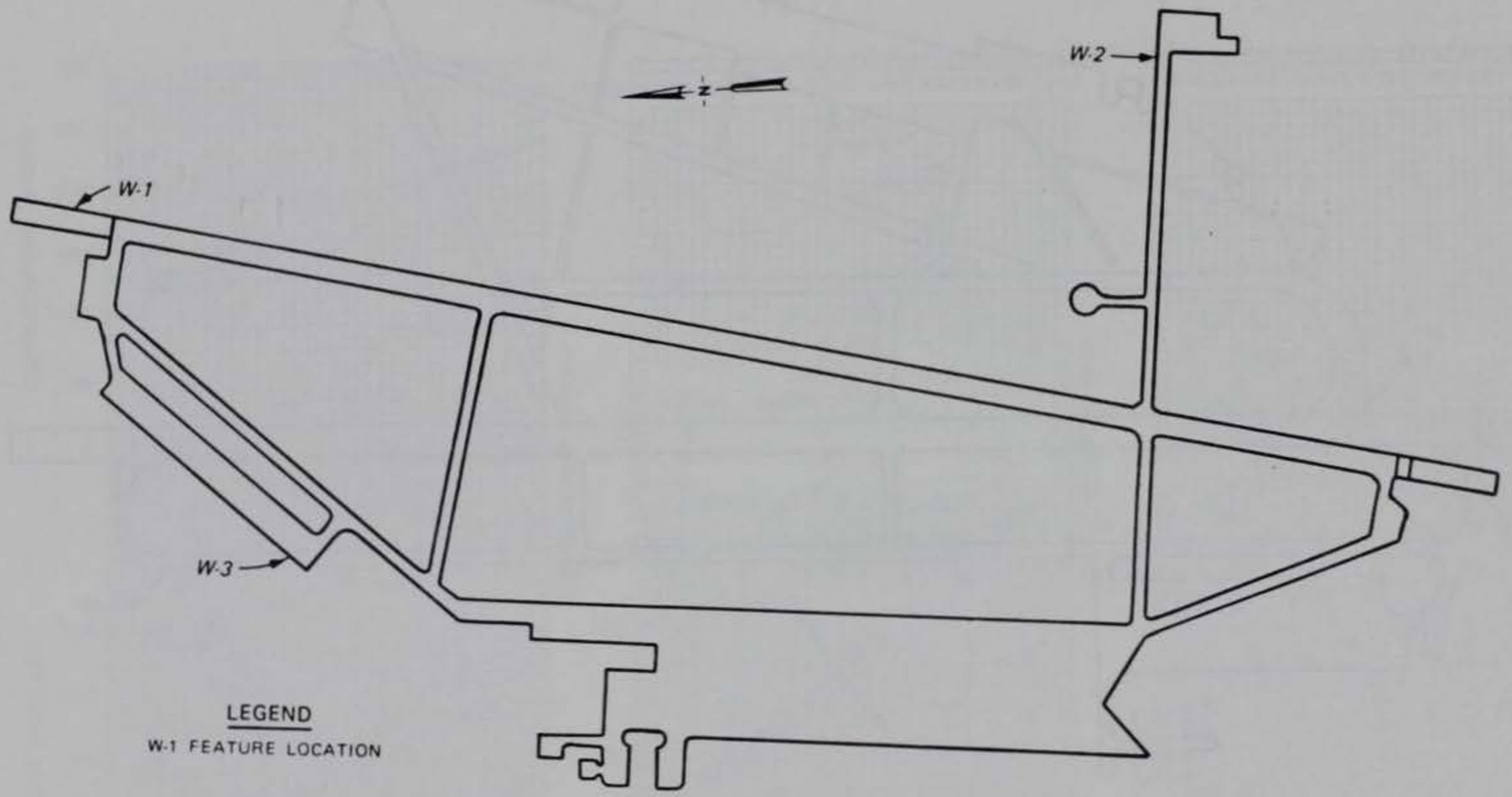


Figure III-6. Layout of Airfield Pavements Showing Location of Test Items, Whiteman AFB, Missouri.

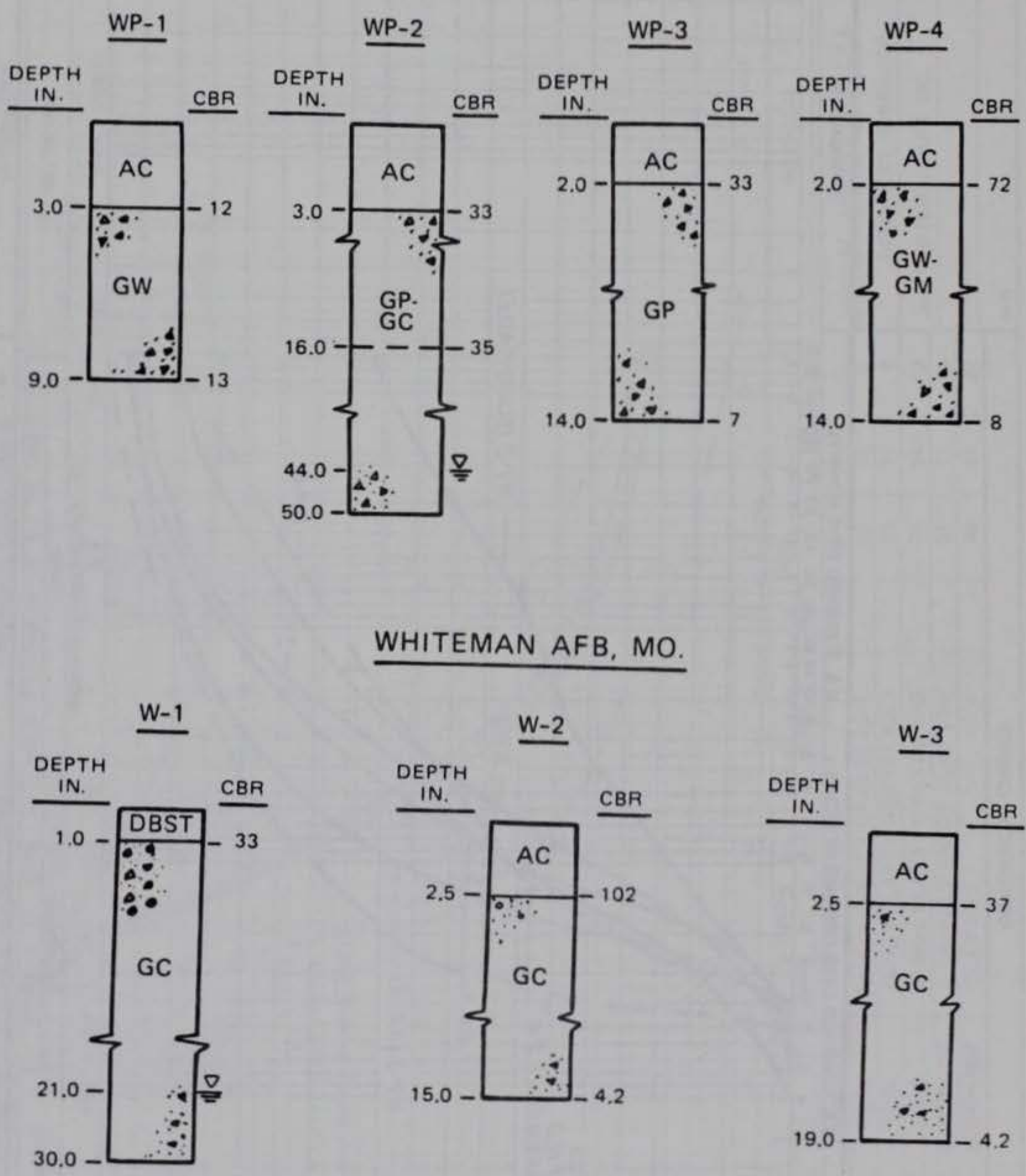


Figure III-7. Structure of Wright-Patterson and Whiteman AFB Test Items.

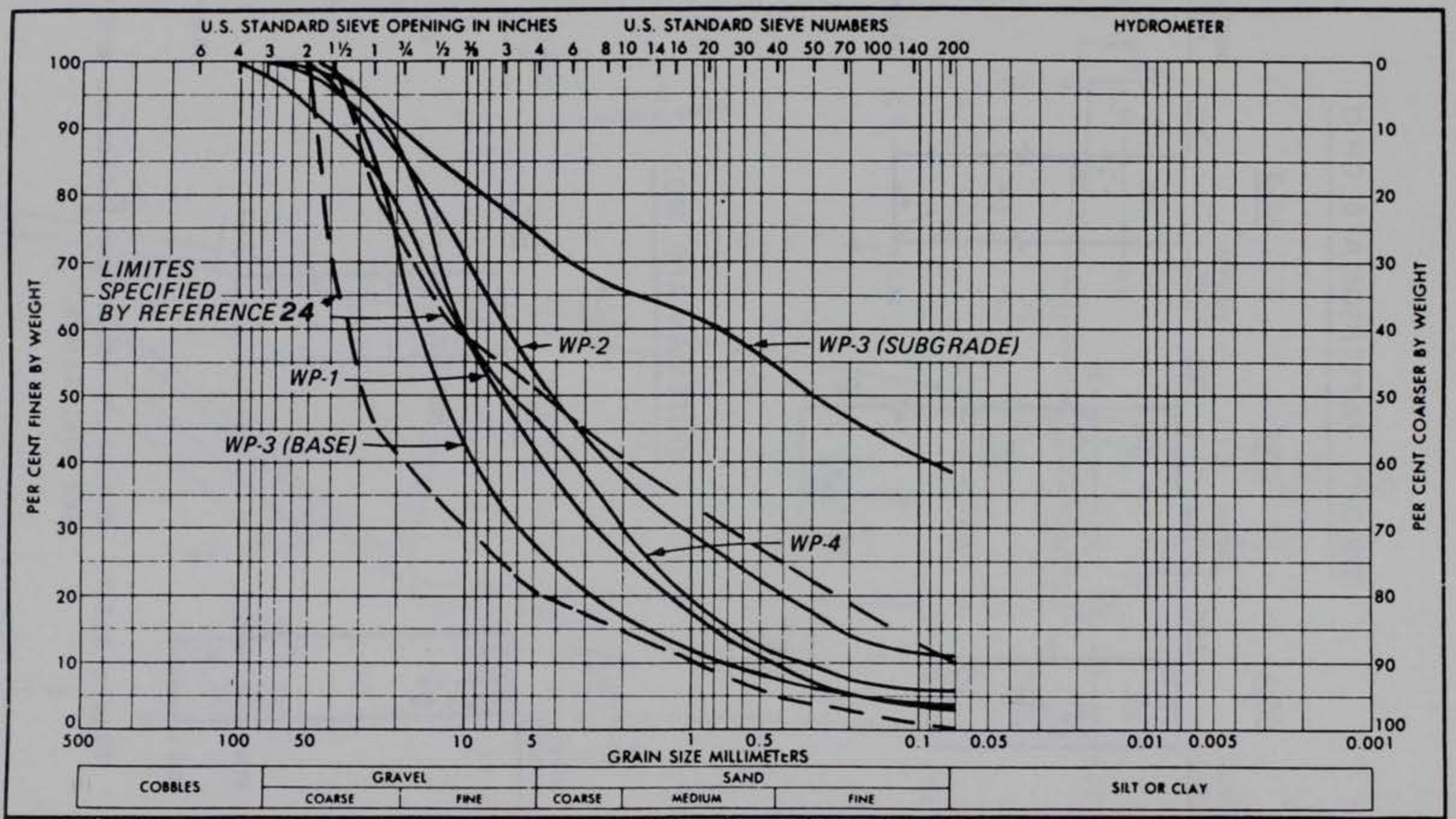


| SAMPLE NO | ELEV OR DEPTH | CLASSIFICATION | NAT W% | LL | PL | PI |
|---|---|---|---|---|---|---|
| WP-1 | BASE | GRAVEL (GW) BROWN | | 16 | 12 | 4 |
| WP-2 | BASE | CLAYEY GRAVEL (GP-GC) BROWN | | 20 | 14 | 6 |
| WP-3 | BASE | GRAVEL (GP) BROWN | | 17 | 13 | 4 |
| WP-3 | SUBGRADE | GRAVELLY CLAYEY SAND (SC) | | 31 | 15 | 16 |
| WP-4 | BASE | SILTY GRAVEL (GW-GM) | | 14 | 12 | 2 |

**GRADATION CURVES**

PROJECT ALTERNATE LAUNCH & RECOVERY SURFACES
AREA WRIGHT - PATTERSON AFB, OHIO
BORING NO
DATE

ENG FORM 2087
1 MAY 63

REPLACES WES FORM NO 1241, SEP 1962, WHICH IS OBSOLETE

U S GOVERNMENT PRINTING OFFICE 1963 OF—709-126

Figure III-8. Gradation Curves for Wright-Patterson AFB Materials.

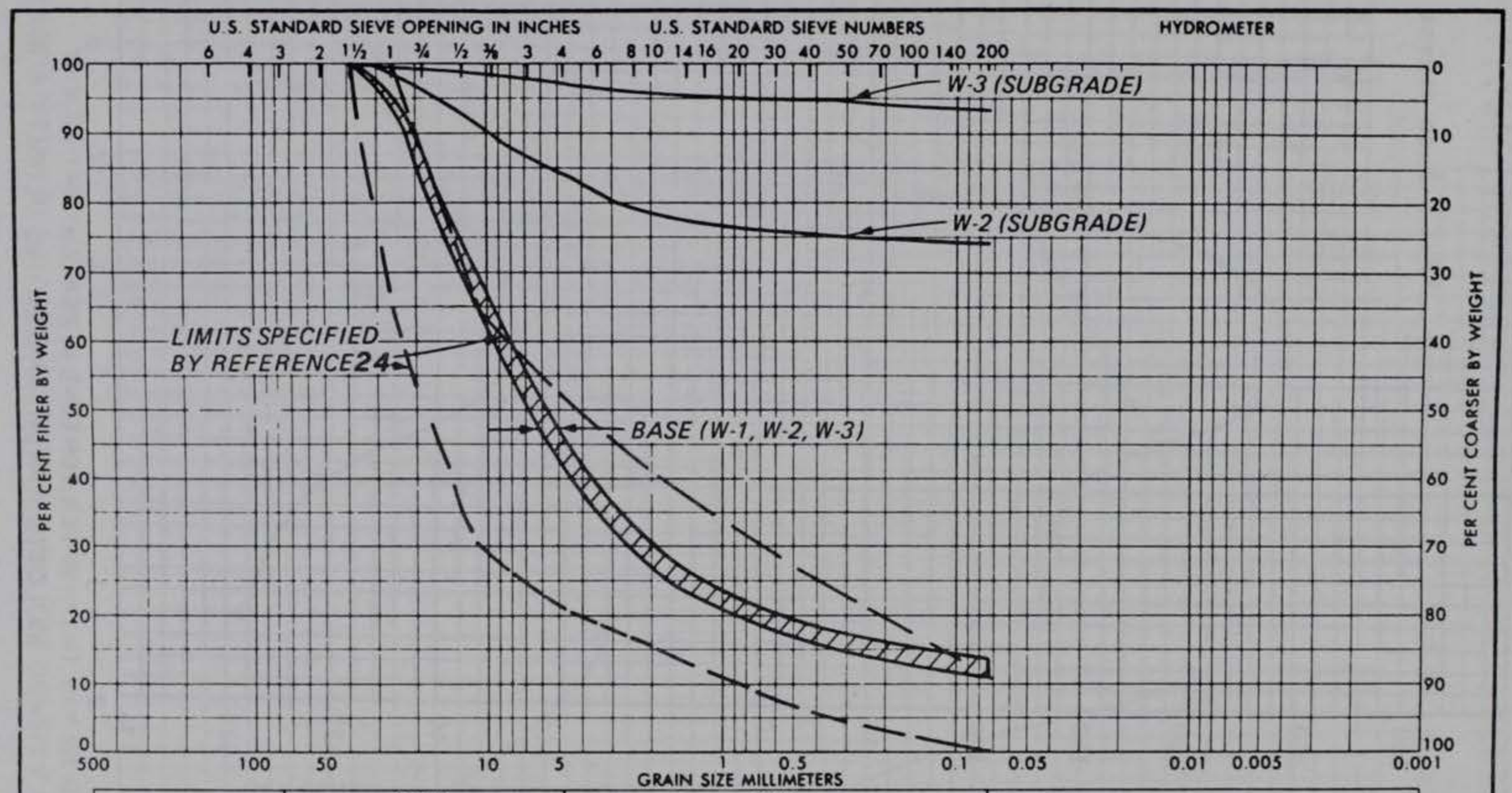


| SAMPLE NO | ELEV OR DEPTH | CLASSIFICATION | NAT W% | LL | PL | PI |
|---|---|---|---|---|---|---|
| W-1 | BASE | SANDY CLAYEY GRAVEL (GC) | | 23 | 15 | 8 |
| W-2 | BASE | SANDY CLAYEY GRAVEL (GC) | | 23 | 14 | 9 |
| W-3 | BASE | SANDY CLAYEY GRAVEL (GC) | | 24 | 14 | 10 |
| W-2 | SUBGRADE | GRAVELLY SANDY CLAY (CH) | | 51 | 17 | 34 |
| W-3 | SUBGRADE | CLAY (CL) | | 49 | 17 | 32 |

**GRADATION CURVES**

PROJECT ALTERNATE LAUNCH & RECOVERY SURFACES
AREA WHITEMAN AFB, MO.
BORING NO
DATE

ENG FORM 2087
1 MAY 63
REPLACES WES FORM NO 1241, SEP 1962, WHICH IS OBSOLETE

U S GOVERNMENT PRINTING OFFICE 1963 OF—709-126

Figure III-9. Gradation Curves for Whiteman AFB Materials.

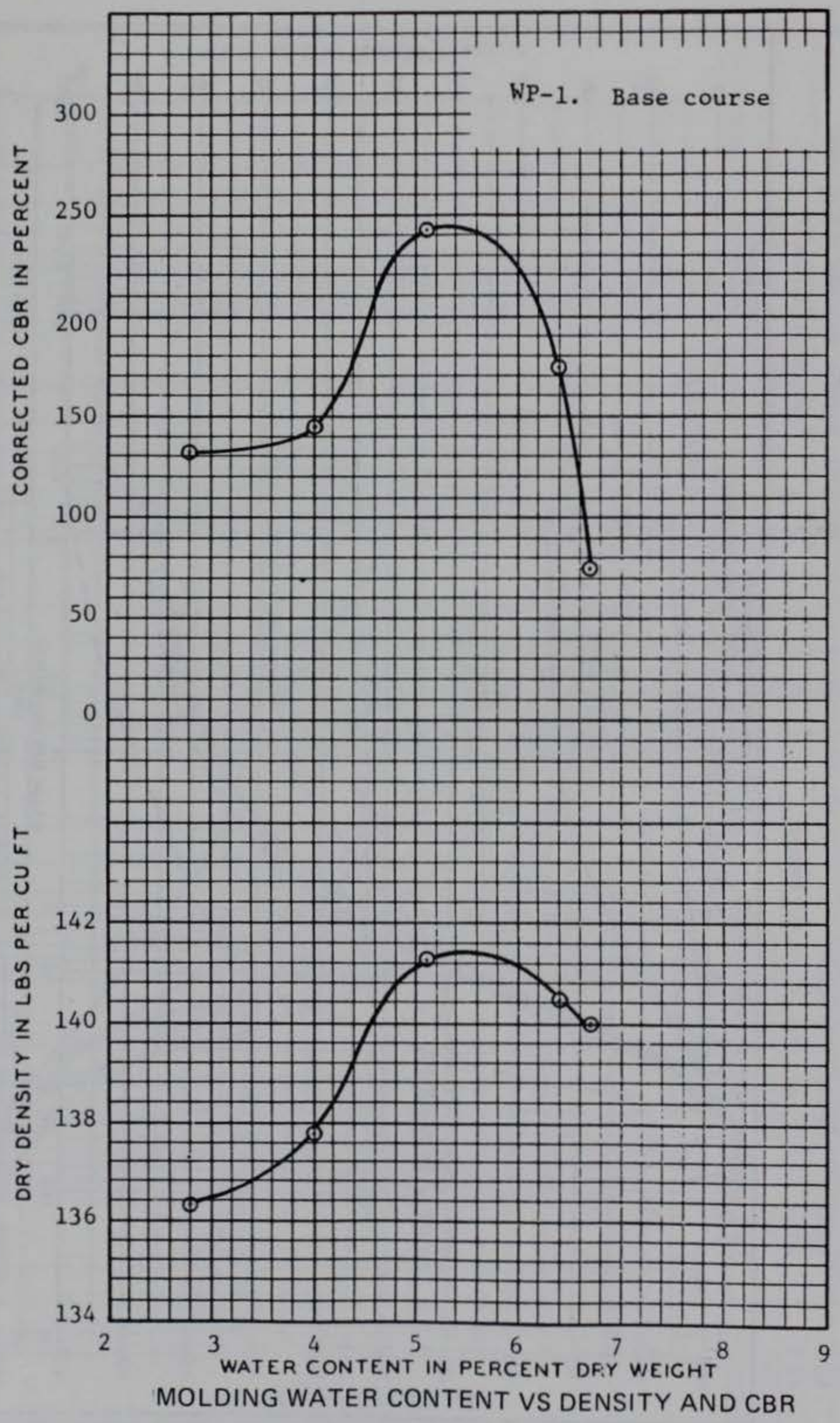


Figure III-10. Laboratory CE55 Compaction and Unsoaked CBR's for WP-1 Base Course.

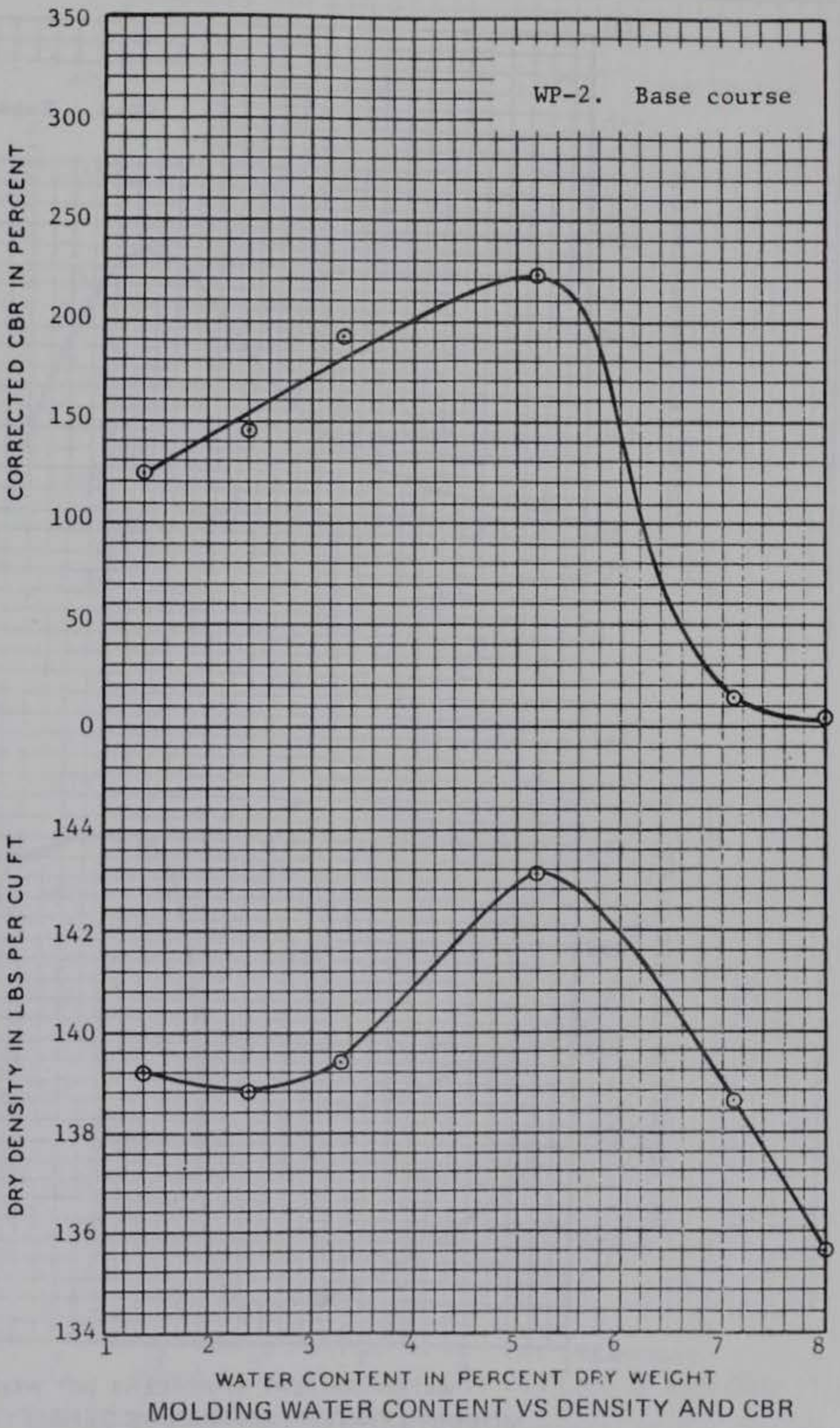


**Figure III-11.** Laboratory CE55 Compaction and Unsoaked CBR's for WP-2 Base Course.

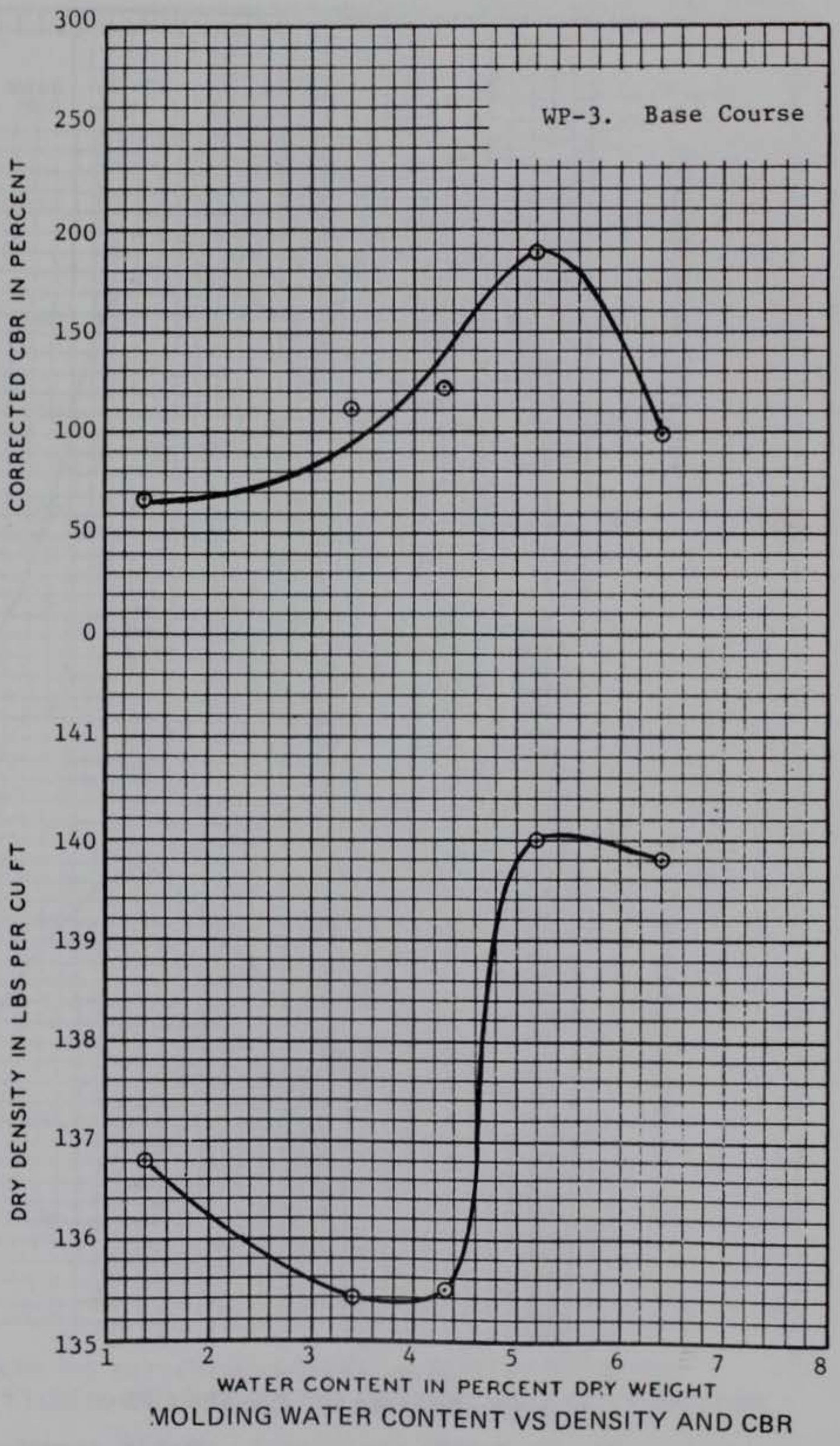


Figure III-12. Laboratory CE55 Compaction and Unsoaked CBR's for WP-3 Base Course.

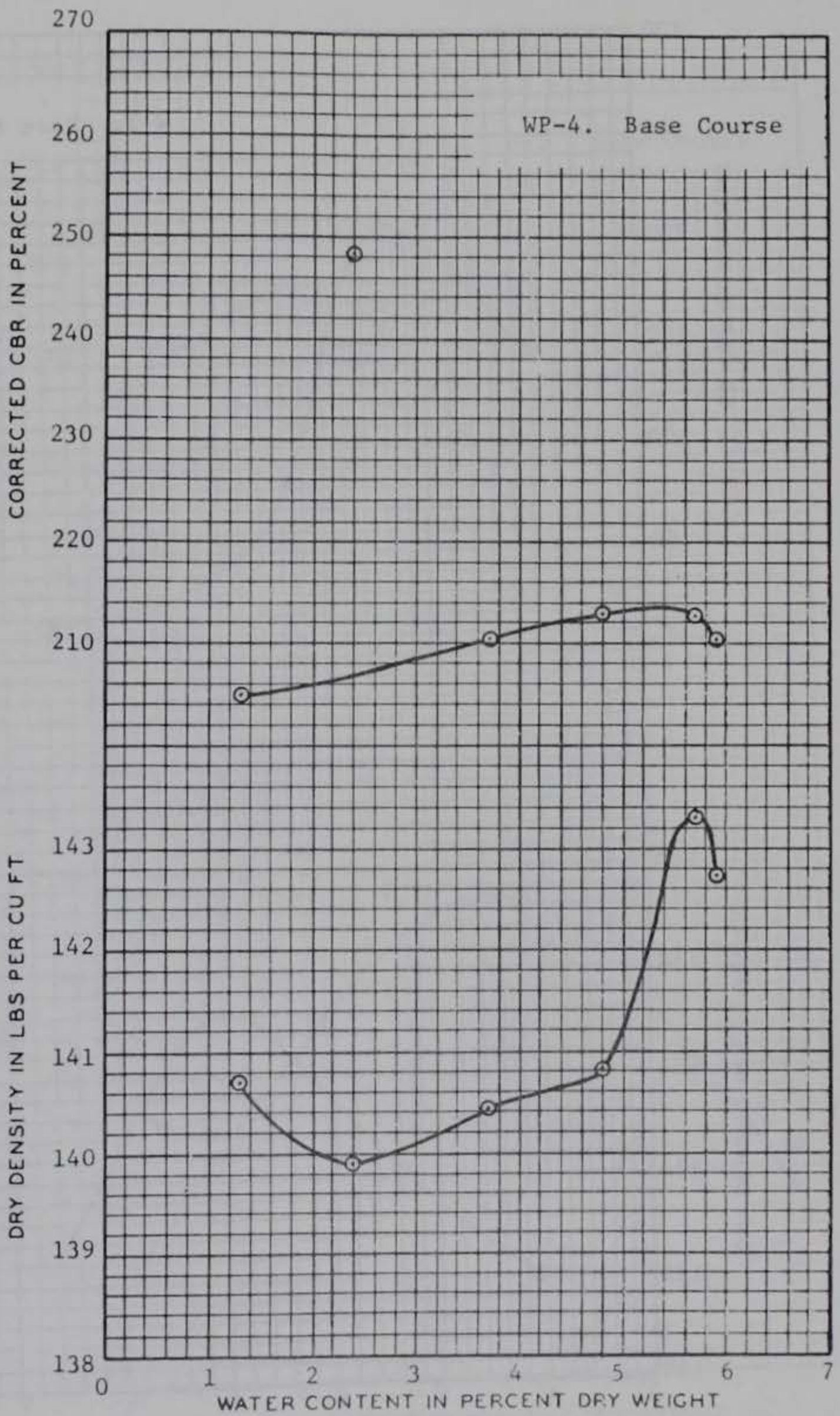


**Figure III-13.** Laboratory CE55 Compaction and Unsoaked CBR's for WP-4 Base Course.

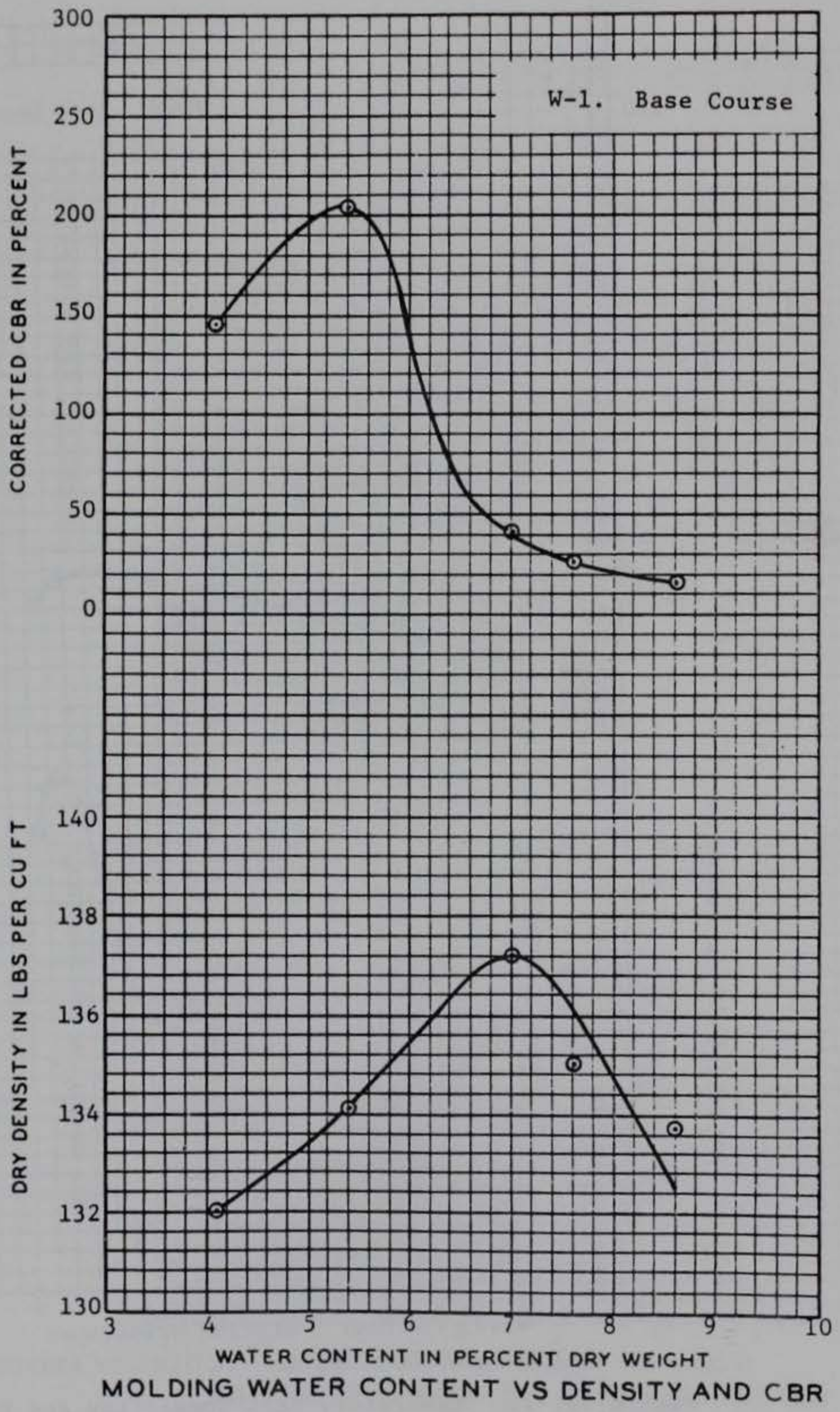


MOLDING WATER CONTENT VS DENSITY AND CBR

Figure III-14. Laboratory CE55 Compaction and Unsoaked CBR's for W-1 Base Course.

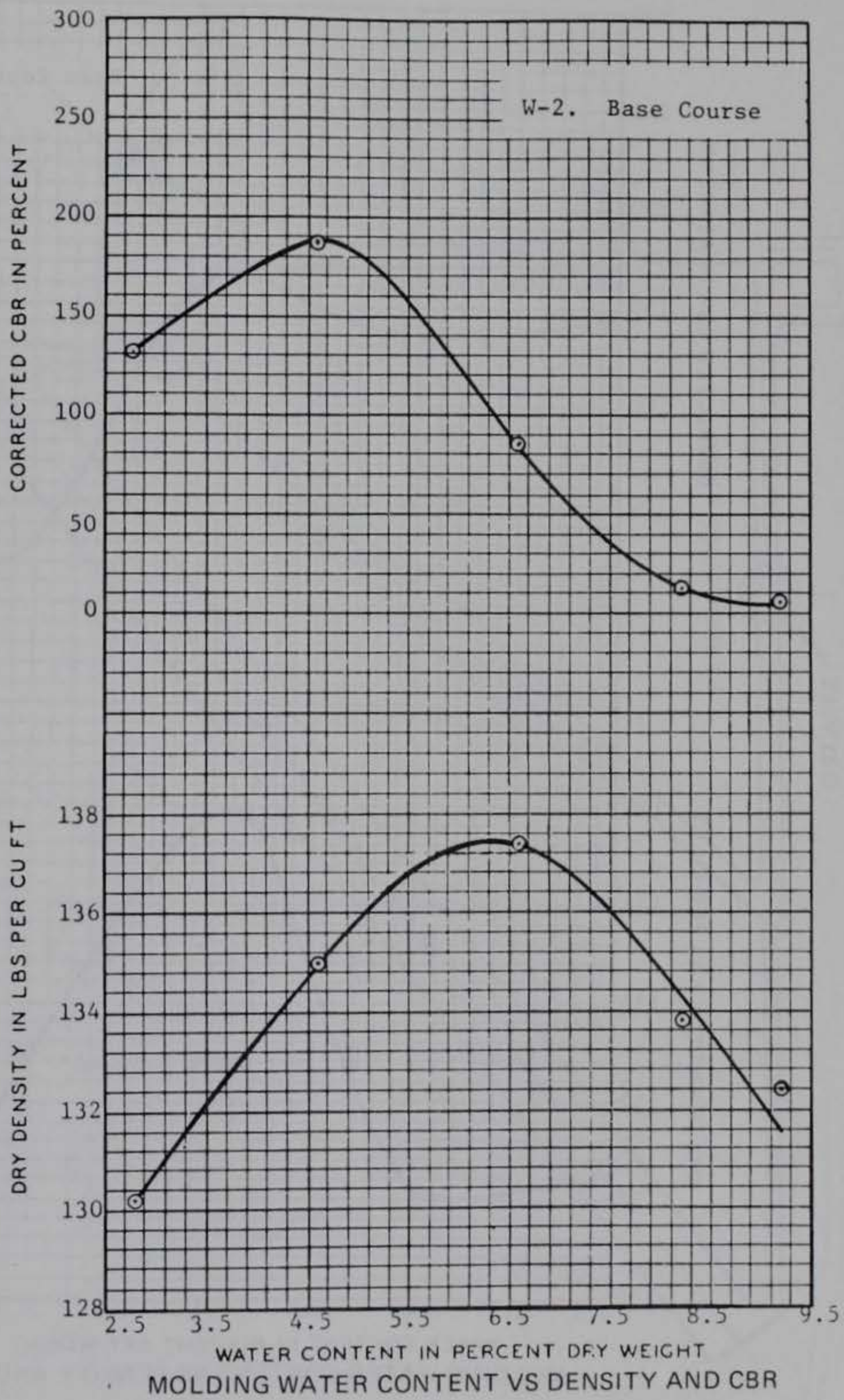


**Figure III-15. Laboratory CE55 Compaction and Unsoaked CBR's for W-2 Base Course.**

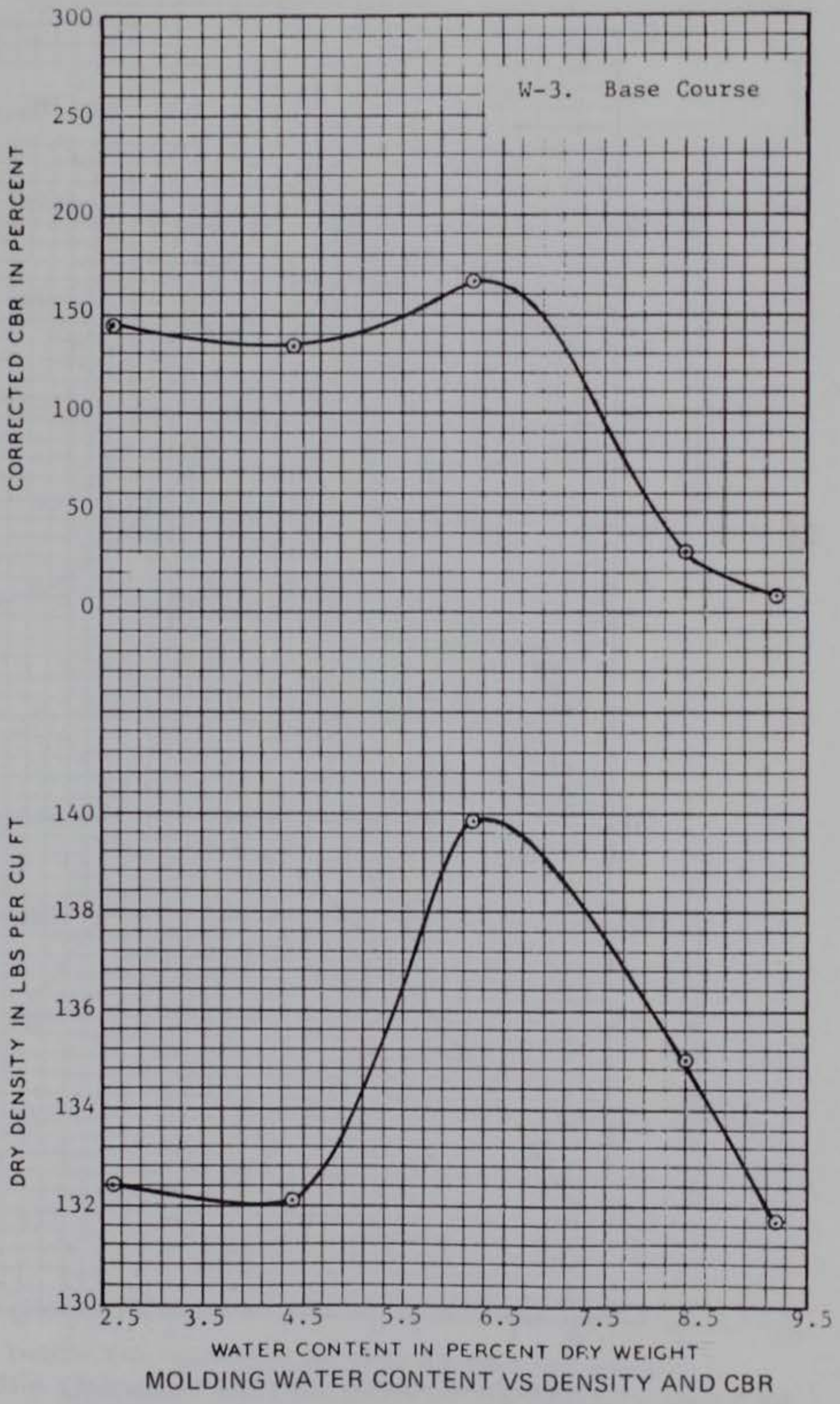


**Figure III-16. Laboratory CE55 Compaction and Unsoaked CBR's for W-3 Base Course.**

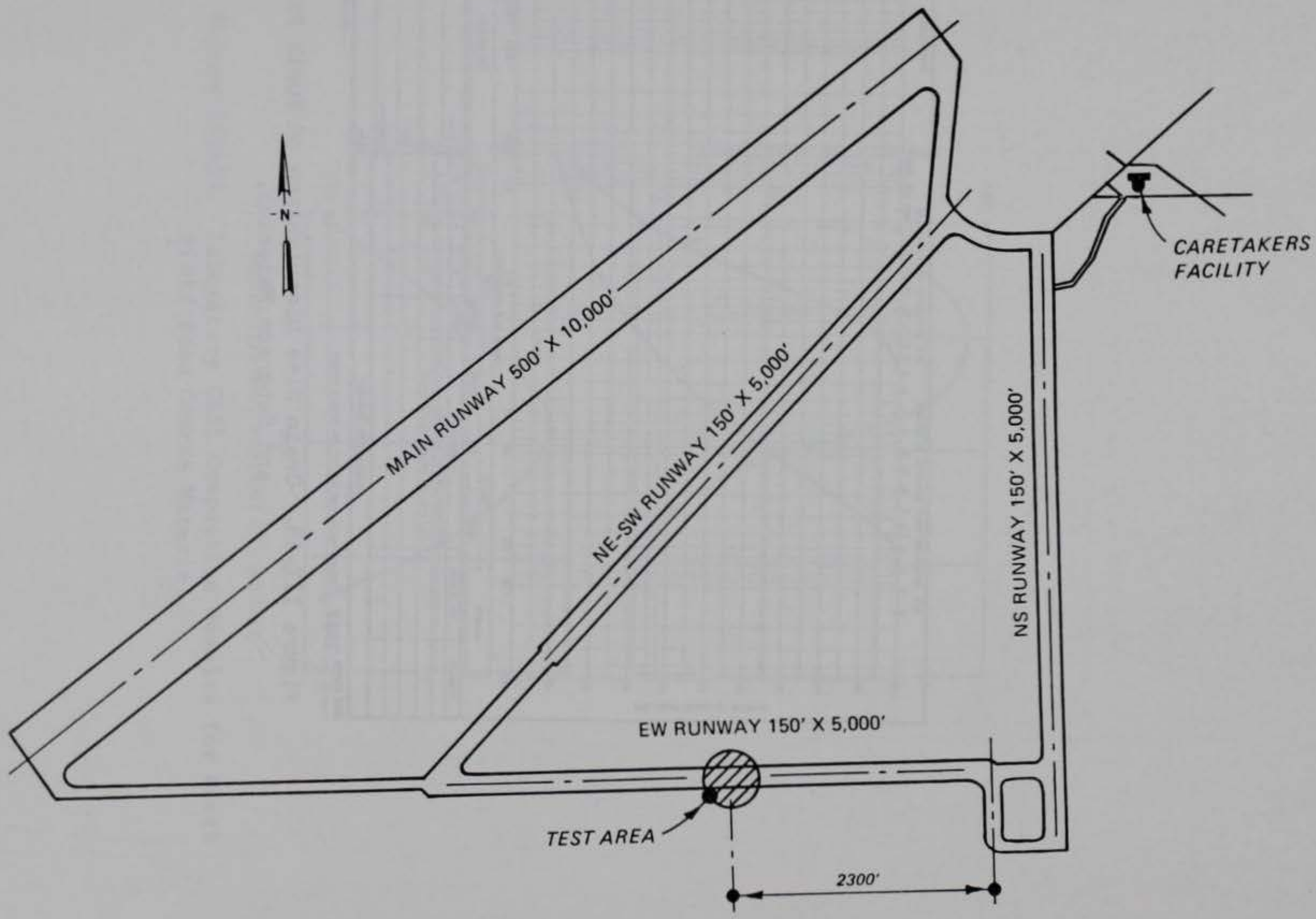


Figure III-17. Layout of North Field.

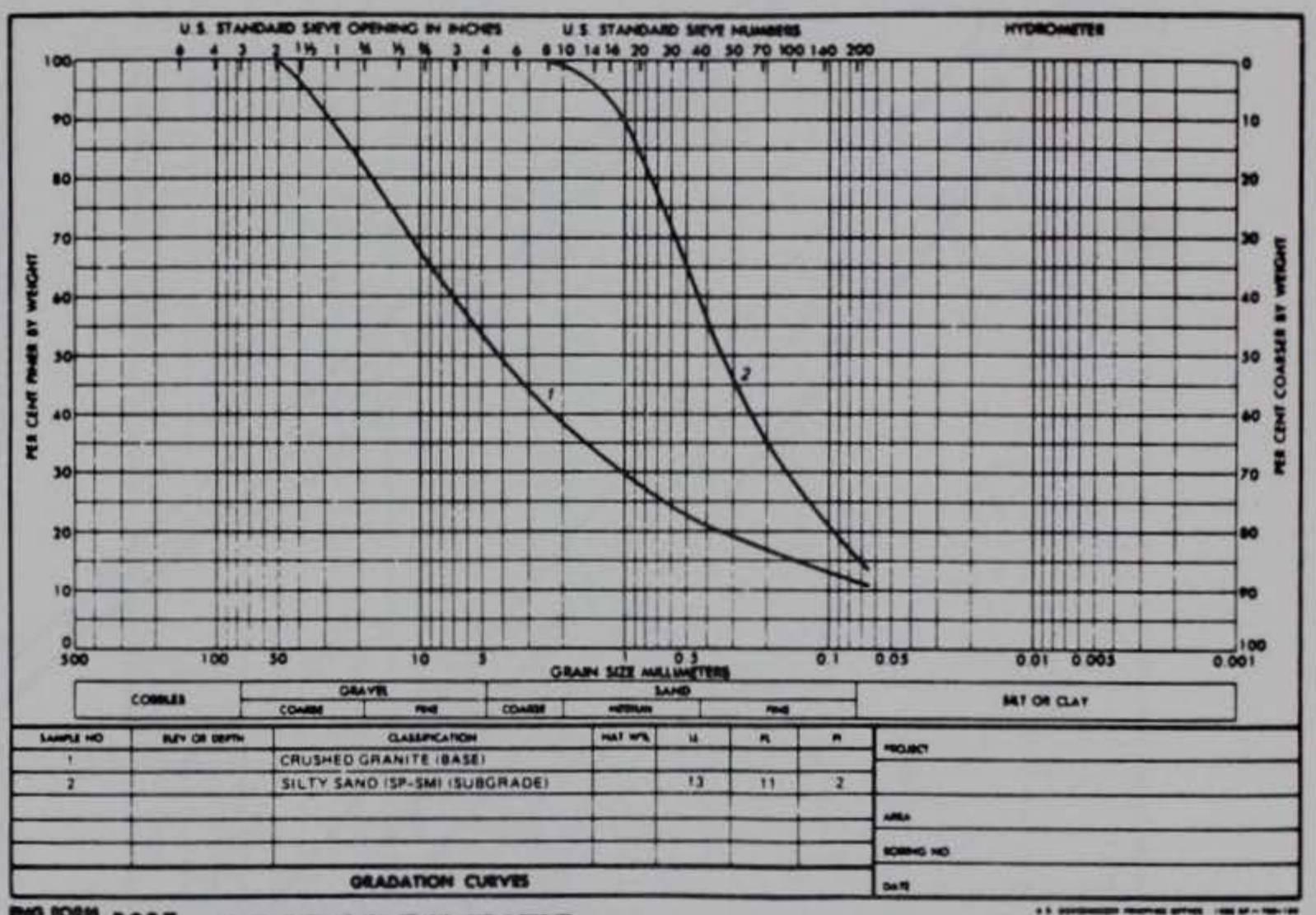


| SAMPLE NO | ELEV OR DEPTH | CLASSIFICATION | NAT WC% | LL | PL | PI |
|---|---|---|---|---|---|---|
| 1 | | CRUSHED GRANITE (BASE) | | | | |
| 2 | | SILTY SAND (SP-SM) (SUBGRADE) | | 13 | 11 | 2 |
| | | | | | | |
| | | | | | | |
| | | | | | | |

PROJECT

AREA

BORING NO

DATE

GRADATION CURVES

ENG FORM 2087

Figure III-18. Grain Size Distribution of North Field Base and Subgrade Material.

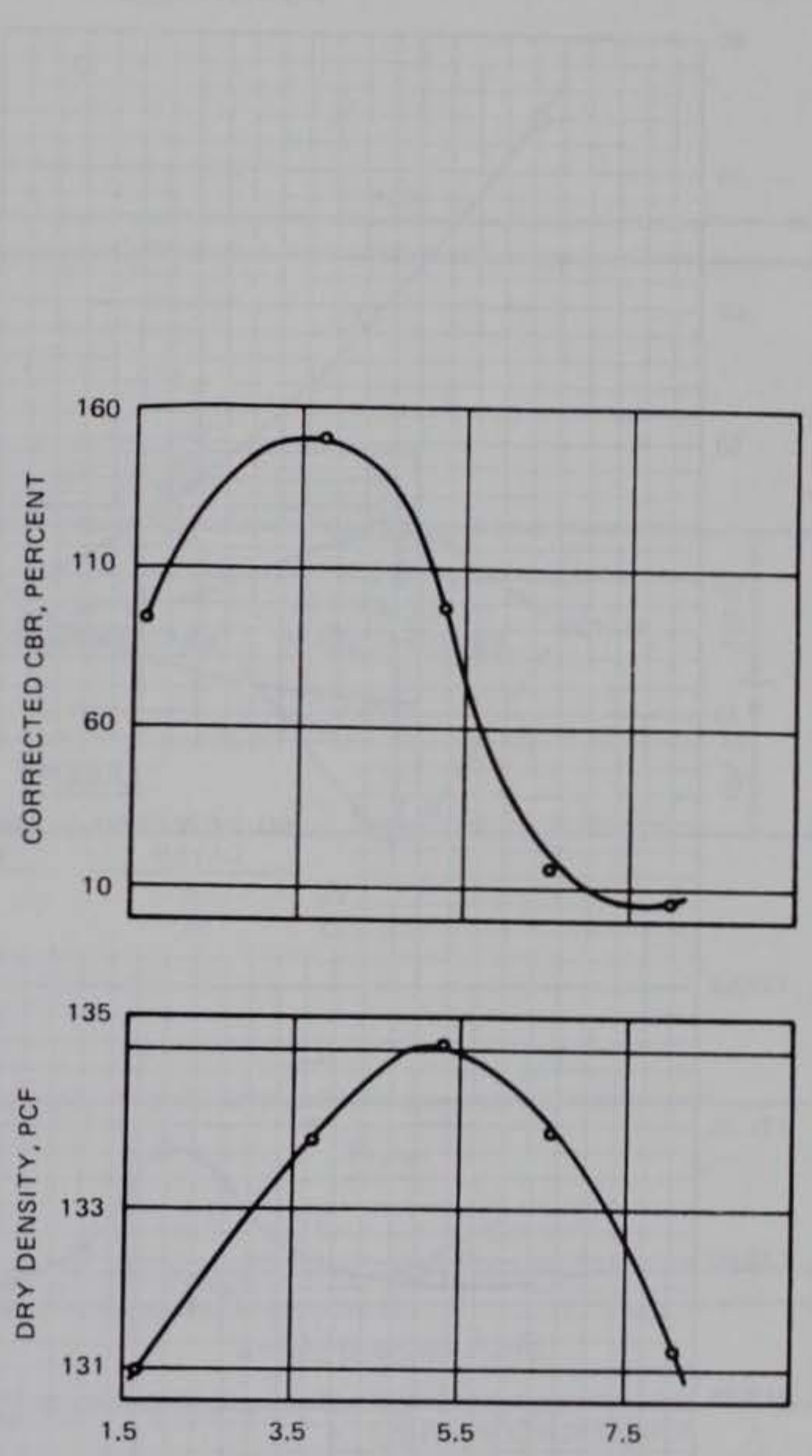


**Figure III-19. Laboratory CE55 Compaction Results for North Field Base Course Material.**

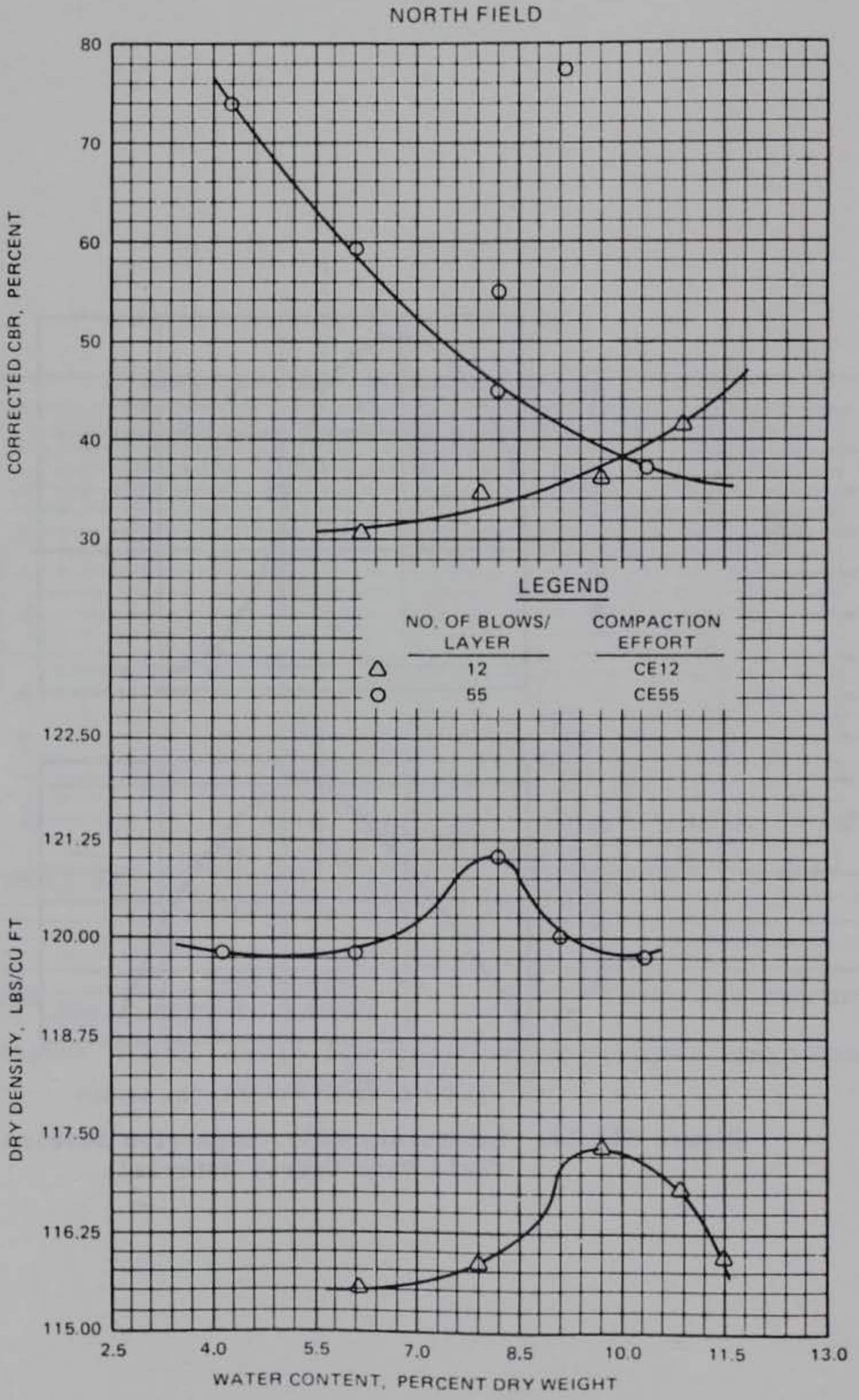


Figure III-20. Laboratory Compaction Results for North Field Subgrade.

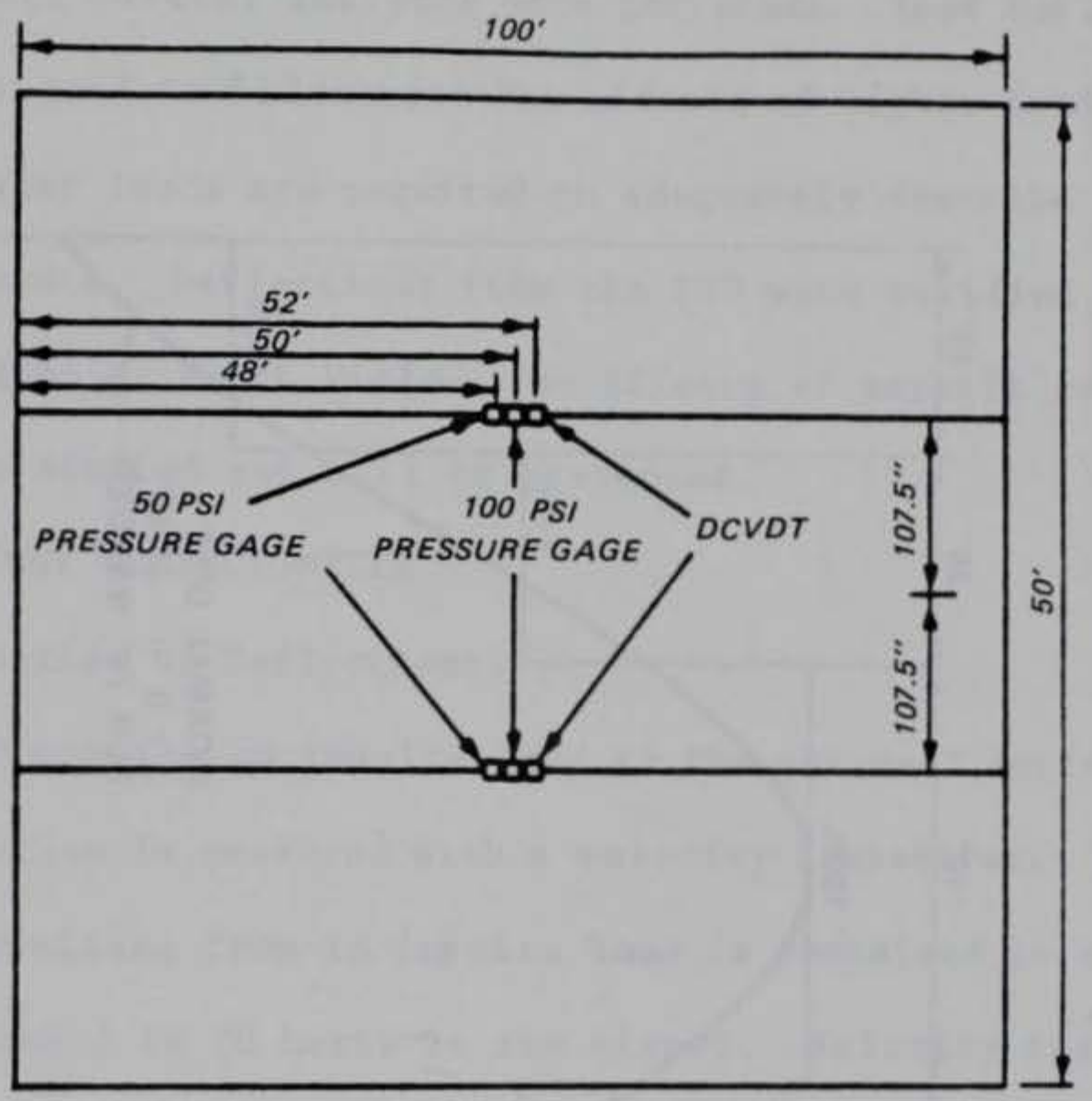


PLAN

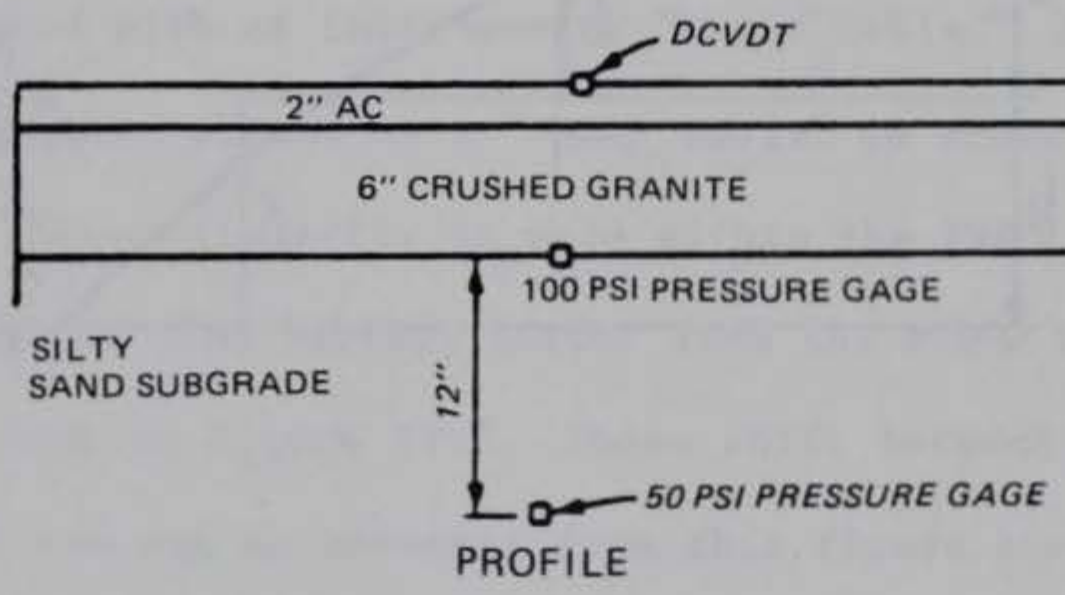


PROFILE

Figure III-21. North Field Instrumentation Layout.

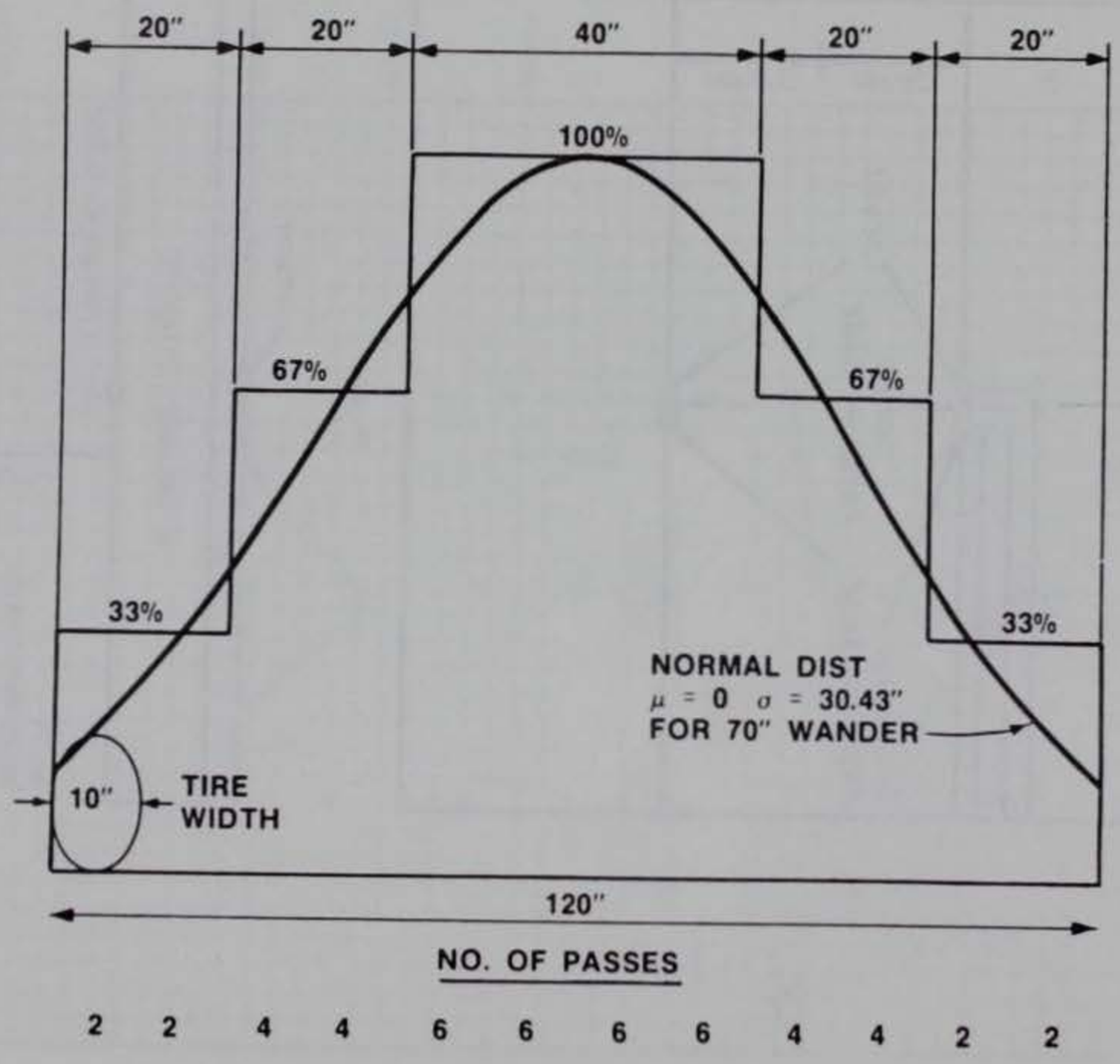


Figure III-22. Traffic Distrubution Pattern.

# SECTION IV

# ANALYSIS OF DATA

To extract as much information as possible from the Falling Weight Deflectometer data several analyses were performed. Load deflection response was analyzed to illustrate the effects of higher load levels and ascertain if higher loads are required to adequately describe the pavement response/performance. Deflections from the FWD were verified in the instrumented test section at North Field. The effects of asphalt concrete temperature were studied and will be presented.

## A. FALLING WEIGHT DEFLECTOMETER

### 1. Verification of Deflections.

The FWD applies an impulse load to the pavement surface. The resulting deflection is measured with a velocity transducer. The velocity time response resulting from an impulse load is contained in a frequency spectrum from about 1 to 70 hertz in the signal. Velocity tranducers used on the FWD are nonlinear below about 5 hertz. Therefore, calibration can not be accomplished with an instrumented "shake table." A typical response from an FWD transducer placed on a "shake table" is shown if Figure IV-1. A correction for the nonlinearity is made within the FWD's registration equipment. A typical time history output from the FWD's load and velocity transducers is shown in Figure IV-2. Phase shift between the force signal and the velocity can not be measured from this figure since the output from the velocity transducers contain a phase shift caused by the difference between the time the surface wave arrives at the transducer and when the signal is transmitted. Since there is a nonlinear response from the

velocity transducer, the deflections were verified by comparing the deflections to those of the deflections gages at North Field as described in Section IIIC. The FWD load plate was placed directly over the gages. The resulting outputs are shown below.

| FWD load lbs | FWD Deflection mils | LVDT deflection mils | Difference Percent |
|---|---|---|---|
| 9064 | 37.9 | 38.0 | -0.2 |
| 14232 | 55.9 | 57.5 | -3.0 |
| 13874 | 65.2 | 64.0 | 2.0 |

The differences are considered reasonable considering the accuracy of both measuring systems. Therefore, based on the above measurments the FWD deflections are assumed to be valid over a range from 1 to 80 mils (0.001 to 0.080 inches). The maximum displacement for the FWD deflection transducers is 80 mils. Readings greater than 80 mils should be discarded. Results from FWD tests on the eleven test items exceeded this 80 mil limit at load levels above 9000 lbs in most cases after traffic was initiated.

2. Effects of Force Level.

To evaluate the effects of different loads on ALRS type pavements, a test was conducted with the FWD 25,000 lb model over the full range of loads. Tests were conducted on a road section at the WES with a structure of 2 inches of AC over 6 inches of granular base over a CL subgrade. All loading weights were installed on the device and a test was conducted at the maximum drop height, two intermediate drop heights and the lowest drop height. Two weights were then removed and the process repeated. At each successive weight configuration, the manufacturers recommended configuration of rubber cushions was adopted. The process was repeated until all weights were removed and only the loading frame was dropped. The results of this test are presented in Figure IV-3. A minimum force of 2000 pounds was

obtained with all weights removed and the apparatus dropped at a minimum drop height. The results are nonlinear below 6000 pounds force and nearly linear above 6000 pounds force. Slight variations that occur at similar loads are the result of one test being at a intermediate or lower drop height, and greater weight configuration compared to a high drop, lower weight configuration test. Variations could be due to different load pulse widths or slight variation in deflection or load accuracy.

The force output from the FWD varies with temperature and the amount of deflection (stiffness) of the pavement when any particular load configuration and drop height are used. Foxworthy (Reference 43) reported a variation from 23532 pounds at 61 degrees F. to 28318 at 36 degrees F. measured at the center of a 21 inch thick Portland Cement Concrete slab. Alexander, et al,(Reference 11) reported the following results on asphalt pavements.

| Thickness,in. AC Surface | Granular Base | Pavement Temperature Degrees, F. | Force Lbs | Deflection, D0 mils |
|---|---|---|---|---|
| 3.5 | 20.5 | 55 | 24560 | 68.9 |
| | | 83 | 22960 | 72.2 |
| 3.0 | 10(PCC) | 38 | 28304 | 17.1 |
| | | 75 | 23608 | 23.3 |
| | | 66 | 24624 | 22.6 |

From the above results the following differences in force output of the FWD for the same drop height were observed.

1) 5,344 pounds or 23 percent on two different pavement sections.

2) 4,696 pounds or 20 percent on the same pavement section.

These results emphasize the need for a load cell to record the load from an impulse loading device.

To illustrate the effects of different FWD force levels on ALRS pavements, the Impulse Stiffness Modulus (ISM) was calculated for the

different tests on each of the test items. The Impulse Stiffness Modulus (ISM) (secant modulus) is defined as:

$$ISM = \frac{\text{FWD FORCE}}{\text{FWD DEFLECTION}} , \frac{\text{kips}}{\text{in.}} \quad (8)$$

ISM was selected over deflection because the FWD load varies as a function of the magnitude of deflection and ambient temperature.

Results for the three WES test items and the North Field test item are shown in Figure IV-4. Generally, the ISM value is constant for the range of loadings from 5000 to 14000 pounds. Results from the Wright-Patterson and Whiteman AFB items are shown in Figure IV-5. There is an increase in ISM for items WP2 and W1. These pavements had large granular base course thicknesses (47 and 29 inches, respectively). The granular base material stiffened with increase load and consequently increased confining stress and the sum of principal stresses ($\theta$).

To examine the effects of stress dependant materials on FWD reponse, tests were conducted on the subgrade, base, and pavement during the construction of the WES and North Field test items. The load deflection response on the CH subgrade material used in the WES test items is shown in Figure IV-6. The deflection at the center of the plate exceeded the 80 mil limit for the FWD, therefore the deflection at 12 inches is shown. The material exhibits a stress softening effect as would be expected for the clay material. Figure IV-7 show the reponse at the same location after the base course has been placed and compacted. The stress softening effect is somewhat reduced from that shown by the clay as would be expected. The load deflection response at the same location on item WES1 on the pavement surface is shown in Figure IV-8. The response is very linear on the surface

as shown in Figures IV-3 and IV-4. Figure IV-9 show the results on the subgrade, base and pavement and the decrease in nonlinearity.

Results from similar tests at North field are shown in Figure IV-10. The subgrade exhibts a nonlinearity, whereas the pavement and base are nearly linear.

3. Effects of Temperature.

The stiffness of pavements containing asphaltic concrete (AC) layers is related to the temperature of the asphalt layer. During the development of the dynamic stiffness modulus (DSM) evaluation procedure (Reference 13), it was realized that the stiffness of a pavement must be corrected in order to obtain a consistent evaluation of AC pavements tested at varying temperatures. A temperature test section was constructed, and tests were conducted at different temperatures. From these results a set of correction curves was developed.

These curves were later modified (Reference 44) using a mechanistic analysis. The pavements were modeled using the BISAR program to calculate deflections. A nominal load of 7000 lbs on a 9-in. radius circular area was used. The modulus-temperature relationship developed by Kingham and Kallas (Reference 45) was selected (Figure IV-11). Results of this analysis were selected for the DSM temperature correction procedure.

For ALRS pavements, the effect of temperature on the measured deflections must be considered. Since the FWD has a 11.8 inch diameter plate and the WES 16-kip vibrator has an 18 inch plate, the correction procedure was not applicable. A similar study was conducted with the FWD. Nine pavements were selected on the Waterways Experiment Station for testing over a range of temperatures. Thicknesses and structure of the nine sites

are shown in Figure IV-12. Testing was conducted with the FWD between January and June 1986 to cover a wide range of pavement temperatures.

The mean pavement temperature was selected as the temperature to use for calculations. During this study the method of measuring the pavement surface temperature with an Infared gun was evaluated. At each test site a one inch diameter core was drilled into the pavement to a depth greater than half the thickness of the AC layer. The hole was filled with oil and a thermistor was placed at a depth of one half the thickness of the AC layer. The temperature was allowed to stabilize. The temperature measured with this gage was assumed to be the mean pavement temperature.

The surface temperature was measured with an infared gun and with a thermistor taped to the pavement surface. For calculation of the mean pavement temperature, the method developed by H. F. Southgate, Kentucky Department of Highways and presented in Reference 46 was selected. The method correlated the pavement surface temperature added to the previous five day mean air temperature to the temperature measured at a depth in an ashpalt surfacing.

A comparison of measured to predicted center pavement temperature determined by measuring the surface temperature with both the infared gun and a thermistor and using the Kentucky procedure with the previous 5 day mean air temperature is shown in Figure IV-13. The infared gun measurements produce as good or better results than the thermistor. This may be due to the fact that the gun measures an average over an area from 2 to 6 square inches whereas the thermistor is only a point measurement.

The ISM values obtained on the nine sites are shown in Figures IV-14 through IV-22. For the pavements with 3 inches or more AC surface

thickness there is a definite decrease in stiffness with an increase in mean pavement temperature (Sites 1, 6, 7, 8, and 9). Other variables such as moisture conditions and accuracy of the FWD appear to have a greater influence on deflections in pavements with less than 3 inches of AC than temperature. Therefore, a temperatue correction factor will not be applied to the results obtained from those pavements.

To develop correction factors for pavements with 3 inches or more of AC, the procedure described above using modulus values from Figure IV-11 and the FWD loading configuration was selected. These relationships are presented in Figure IV-23.

For sites 1, 6, 7, and 8, the ISM value at a mean pavement temperature of 70°F was selected from polynomial regression of the ISM values. This value was divided by the ISM at all other temperatures for normalization. These values are shown in Figure IV-24 through IV-27. Also shown are the curves from Figure IV-23 for the corresponding thickness.

Since the measured data fits the curves, the relationships shown in Figure IV-23 are selected for application of correction factors for ISM. For a mean pavement temperature, the factor is multiplied by ISM to give a corrected ISM to 70°F. These factors can also be applied to the deflection measured at the center of the applied load by dividing the measured ISM by the correction factor. The relationships do not apply to deflections measured away from the load.

4. Effects of Traffic on ISM and Deflection Basin Descriptors.

The WES1 and NFF4 items were the only items where the FWD data was collected through traffic without overranging the velocity transducers. For those items, relationships of ISM, BCI, SCI, Area, and Spreadability will be

presented. WES1 was constructed over a clay subgrade whereas NFF4 had a sand subgrade. ISM relationships are presented in Figures IV-28 and IV-29. ISM for the WES1 item dropped rapidly and remained relatively constant throughout remainder of traffic testing. The stiffness of the NFF4 items decreased throughout traffic.

The normalized deflection basin area is shown in Figures IV-30 and IV-31. The change in area with traffic is different for the two items. NFF4 is constant for the first 20 coverages then decreases with traffic. The area for WES1 drops rapidly then increases. The magnitude of the change in area is small.

The Surface Curvature Index (SCI) relationships are shown in Figures IV-32 and IV-33. The contrast between SCI change for the two items is similar to ISM but inverted. There is a large change in magnitude for SCI values with traffic.

Base Curvature Index (BCI) change for the two items is shown in Figures IV-34 and IV-35. Except for Station 50, the BCI for NFF4 changed very little, whereas WES1 increased with traffic.

Spreadability for each item is shown in Figures IV-36 and IV-37. Spreadibility change for the items follows the change in ISM almost exactly. The magnitude of the change is very small.

B. USE OF DEFLECTION BASIN DESCRIPTORS

1. Surface/Base Curvature.

In an effort to identify future locations within each pavement from the FWD data, using the procedure shown in Figure II-1, the FWD deflections were converted to Dynaflect deflections using the following (from Reference 18):

Dynaflect Deflection = (FWD Deflection @ 9000 lbs. load

+ 7.24472)/29.6906 (9)

The SCI, BCI, and DO values were compared to the relationships in Figure II-1. From these results all pavements except WP2 and NFF4 were classified as subgrade strong, pavement weak. The NFF4 and WP2 gave a condition of the pavement structure as pavement weak and DMD ok.

2. Nonlinear Subgrade Modulus.

The value $E_{RI}$ (Figure II-3) values for each test item were calculated using the ILLIPAVE algorithm

$$E_{RI} = 24.06 - 5.08(D36) + 0.28(D36)^2 \quad (10)$$

$E_{RI}$ values and the modulus values from BISDEF are presented in Figure IV-38. As expected the $E_{RI}$ values are slightly lower but follow the same pattern as the BISDEF subgrade modulus values.

$E_{RI}$ was calculated for the WES1 item from FWD deflection data collected before, during, and after traffic. Results are presented in Figures IV-39. The change in $E_{RI}$ with traffic is very similar to the change in subgrade modulus from BISDEF as shown in Figure IV-43.

C. RESULTS FROM BACKCALCULATION PROCEDURE.

Results from FWD tests on all pavement items during construction, before, during and after traffic are given in Appendix A. For determination of layer moduli values, the BISDEF program was used. A description of BISDEF is given in Appendix B. Each pavement was treated as a three layer system with an AC surface, base, and subgrade. A stiff layer (E=1000000 psi) was placed at a depth of 20 feet from the pavement surface. For most pavements the base course and subgrade layers were allowed to vary in the program. The modulus of the AC surface course was estimated from surface

temperatures at the time of testing. Layer modulus values for all items backcalculated from the before traffic FWD data are given in Table IV-1. Moduli values for the base course were lower than subgrade moduli values for all Wright-Patterson pavements.

1. Verification of Modulus Values and Resulting Stress Calculations.

Laboratory tests were conducted on the North Field subgrade material to determine the resilient modulus properties of the sand at different confining pressures and normal stresses. Results of these tests are presented in Figure IV-40. The BISAR computer program was used to calculate the bulk stress ($\sigma_1 + \sigma_2 + \sigma_3$ or $\sigma_1 + 2\sigma_3$)at the top of the subgrade for the modulus values for Station 25 of NFF4 given in Table IV-1. For a 9000-lb FWD load, the bulk stress at the top of the subgrade was 131 psi. From Figure IV-40, the modulus would be approximately 35000 psi. This correspondes to the subgrade values for NFF4 given in Table IV-1.

The use a layered elastic model offers a method to compare stresses measured with pressure gages under a F-4 loading. A comparison of calculated stresses and measured pressures are shown in Figure IV-41. Measured and computed stresses are closer when the Boussinesq stress distribution was assumed.

Stresses and strains were calculated using modulus values from Table IV-1 for the F-4 loading at points in each pavement structure as shown in Figure IV-42. Values are shown in Table IV-2. These values will be used to predict performance.

2. Effects of Traffic on Modulus Values.

As in the comparison of basin parameters, items WES1 and NFF4 are the only test items with data within the range of the FWD transducers over

the all traffic applications. Change in subgrade modulus with traffic, as backcalculated from BISDEF, change for items WES1 and NFF4 are shown in Figures IV-43 and IV-44. After the initial 10 coverages on each item, both plastic and elastic deformation probably occurred under the FWD loading. The FWD does not measure the plastic or permanent deformation. The elastic layer model is not applicable when plastic deformation occurs.

Base course modulus change for the two items is shown in Figures IV-45 and IV-46. The change in base course modulus is significant and mirrors the change in ISM with coverages.

Table IV-1. LAYER MODULUS VALUES BACKCALCULATED FROM FWD 9 KIP DATA USING BISDEF

| ITEM | STATION FT | BACKCALCULATED MODULUS, PSI | | | AVG % DIFF. FROM MEASURED DEFLECTIONS |
|---|---|---|---|---|---|
| | | SURFACE | BASE | SUBGRADE | |
| WES1 | 10 | 300000 | 17666 | 11047 | 6.8 |
| | 20 | 300000 | 17000 | 9228 | 8.6 |
| | 30 | 300000 | 21170 | 10120 | 7.0 |
| | 40 | 100000 | 22116 | 8849 | 11.4 |
| WES2 | 10 | 300000 | 12164 | 7447 | 11.8 |
| | 20 | 300000 | 13598 | 7467 | 11.6 |
| | 30 | 300000 | 12308 | 7103 | 16.8 |
| | 40 | 100000 | 20959 | 7927 | 12.0 |
| WES3 | 10 | 300000 | 12970 | 6469 | 11.6 |
| | 20 | 300000 | 14003 | 5791 | 14.8 |
| | 30 | 300000 | 16188 | 6175 | 9.0 |
| | 40 | 300000 | 15199 | 7973 | 5.0 |
| WP1 | 5 | 500000 | 770 | 29334 | 25.8 |
| | 15 | 500000 | 1284 | 26617 | 14.4 |
| | 25 | 500000 | 974 | 25152 | 18.2 |
| WP2 | 5 | 424269 | 22653 | 32000 | 11.6 |
| | 15 | 363214 | 17166 | 30000 | 11.6 |
| | 25 | 381722 | 18213 | 30000 | 6.8 |
| WP3 | 5 | 300000 | 9739 | 14221 | 17.4 |
| | 15 | 300000 | 9385 | 16979 | 16.0 |
| | 25 | 300000 | 9000 | 13871 | 26.6 |
| WP4 | 5 | 300000 | 14131 | 18554 | 33.2 |
| | 15 | 300000 | 16958 | 23044 | 22.0 |
| | 25 | 300000 | 16652 | 23008 | 9.6 |
| W1 | 5 | 300000 | 20082 | 16471 | 12.6 |
| | 15 | 300000 | 16930 | 16972 | 13.6 |
| | 25 | 300000 | 22035 | 17536 | 19.4 |
| W2 | 5 | 300000 | 10135 | 8213 | 6.4 |
| | 15 | 300000 | 12012 | 8125 | 7.4 |
| | 25 | 300000 | 10710 | 9177 | 6.8 |
| W3 | 5 | 100673 | 12467 | 11556 | 3.4 |
| | 15 | 300000 | 10963 | 11375 | 3.2 |
| | 25 | 288293 | 10742 | 12527 | 0.4 |
| NFF4 | 25 | 125898 | 18177 | 35548 | 3.0 |
| | 50 | 142322 | 17283 | 30126 | 4.4 |
| | 75 | 190633 | 18189 | 33612 | 4.0 |

Table IV-2. STRESSES AND STRAINS FOR F-4 LOADING

| ITEM | STATION FT | ASPHALT STRAIN 10E-06 IN | BASE COURSE VERT STRESS PSI | BASE COURSE VERT STRAIN 10E-06 IN | BASE COURSE SHEAR STRESS PSI | BASE COURSE TENSILE STRESS 10E-06 IN/IN | SUBGRADE VERT STRESS PSI | SUBGRADE VERT STRAIN 10E-06 IN/IN |
|---|---|---|---|---|---|---|---|---|
| WES1 | 10 | 1860 | 223 | 9860 | 58.2 | 26.9 | 63.9 | 5710 |
| | 20 | 1940 | 220 | 10200 | 58.9 | 34.8 | 60.2 | 6480 |
| | 30 | 1580 | 228 | 8420 | 63.6 | 43.5 | 58.7 | 5780 |
| | 40 | 1120 | 254 | 8370 | 80.0 | 59.3 | 61.2 | 6840 |
| WES2 | 10 | 2390 | 234 | 14600 | 57.8 | 27.2 | 59.6 | 7970 |
| | 20 | 2150 | 238 | 13200 | 60.4 | 33.5 | 57.8 | 7730 |
| | 30 | 2370 | 235 | 14400 | 58.4 | 30.5 | 58.4 | 8190 |
| | 40 | 7260 | 263 | 8610 | 82.2 | 60.1 | 56.3 | 7050 |
| WES3 | 10 | 126 | 271 | 12900 | 80.9 | 45.3 | 65.4 | 10100 |
| | 20 | 244 | 270 | 11800 | 83.2 | 57.9 | 60.7 | 10500 |
| | 30 | 354 | 270 | 9990 | 85.1 | 63.6 | 59.0 | 9560 |
| | 40 | 207 | 270 | 10800 | 81.9 | 41.9 | 67.2 | 8390 |
| WP1 | 5 | 2810 | 39 | 27500 | 0.3 | 22.9 | 34.6 | 719 |
| | 15 | 2550 | 48 | 21000 | 0.9 | 27.0 | 41.2 | 1000 |
| | 25 | 2700 | 43 | 24200 | 0.6 | 24.6 | 37.3 | 932 |
| WP2 | 5 | 1290 | 135 | 5100 | 32.8 | 0.5 | 4.9 | 154 |
| | 15 | 1610 | 129 | 6410 | 30.8 | 1.0 | 5.2 | 170 |
| | 25 | 1520 | 129 | 6070 | 31.0 | 1.0 | 5.1 | 169 |
| WP3 | 5 | 2880 | 173 | 14200 | 37.5 | 6.8 | 45.8 | 3090 |
| | 15 | 2940 | 172 | 14600 | 36.3 | 11.1 | 47.9 | 2670 |
| | 25 | 3020 | 169 | 15000 | 36.0 | 7.9 | 45.9 | 3160 |
| WP4 | 5 | 2230 | 192 | 10900 | 44.1 | 4.5 | 46.7 | 2440 |
| | 15 | 1950 | 201 | 9480 | 47.0 | 5.4 | 48.1 | 2020 |
| | 25 | 1980 | 200 | 9620 | 46.6 | 5.8 | 48.2 | 2030 |

Table IV-2.STRESSES AND STRAINS FOR F-4 LOADING (CONCLUDED)

| ITEM | STATION FT | ASPHALT STRAIN 10E-06 IN | BASE COURSE VERT STRESS PSI | BASE COURSE VERT STRAIN 10E-06 IN | BASE COURSE SHEAR STRESS PSI | BASE COURSE TENSILE STRESS 10E-06 IN/IN | SUBGRADE VERT STRESS PSI | SUBGRADE VERT STRAIN 10E-06 IN/IN |
|---|---|---|---|---|---|---|---|---|
| W1 | 5 | 870 | 272 | 9370 | 68.5 | 2.7 | 11.7 | 720 |
| | 15 | 1120 | 271 | 11200 | 66.4 | 1.1 | 12.4 | 737 |
| | 25 | 755 | 272 | 8510 | 69.7 | 3.0 | 11.6 | 672 |
| W2 | 5 | 2620 | 138 | 11300 | 32.4 | 6.6 | 32.3 | 3890 |
| | 15 | 2380 | 146 | 10200 | 35.7 | 11.5 | 31.1 | 3820 |
| | 25 | 2530 | 141 | 10900 | 33.1 | 5.4 | 33.2 | 3570 |
| W3 | 5 | 3120 | 203 | 13500 | 53.7 | 3.5 | 27.3 | 2360 |
| | 15 | 2480 | 143 | 10800 | 33.0 | 1.1 | 25.0 | 2180 |
| | 25 | 2550 | 144 | 11100 | 33.1 | -0.6 | 25.9 | 2040 |
| NFF4 | 25 | 2010 | 237 | 10300 | 54.6 | -33.6 | 115.0 | 3160 |
| | 50 | 2090 | 231 | 10600 | 52.9 | -29.5 | 111.0 | 3510 |
| | 75 | 1930 | 222 | 9690 | 48.8 | -31.1 | 109.0 | 3080 |

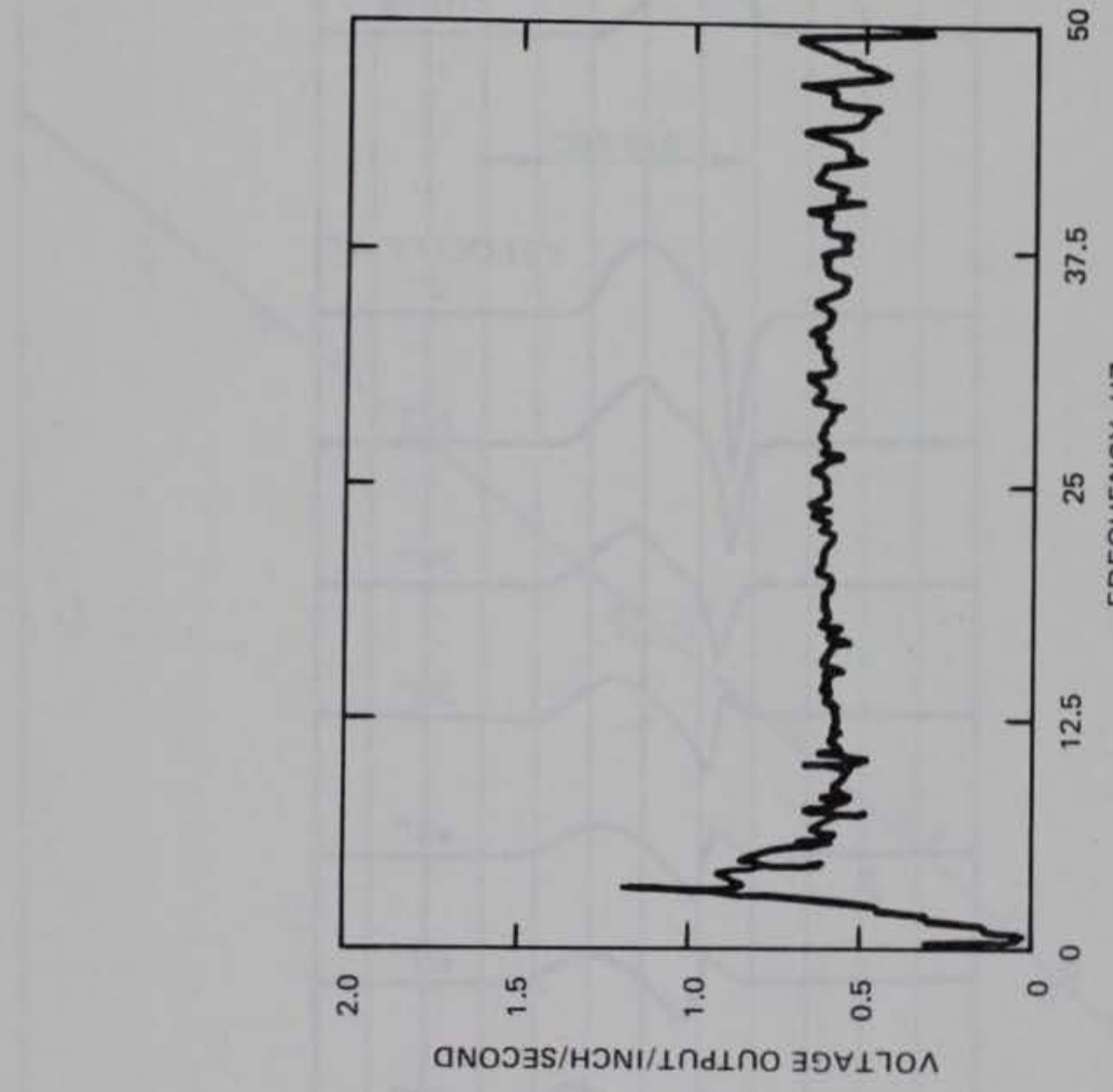


Figure IV-1. FWD Velocity Transducer Response

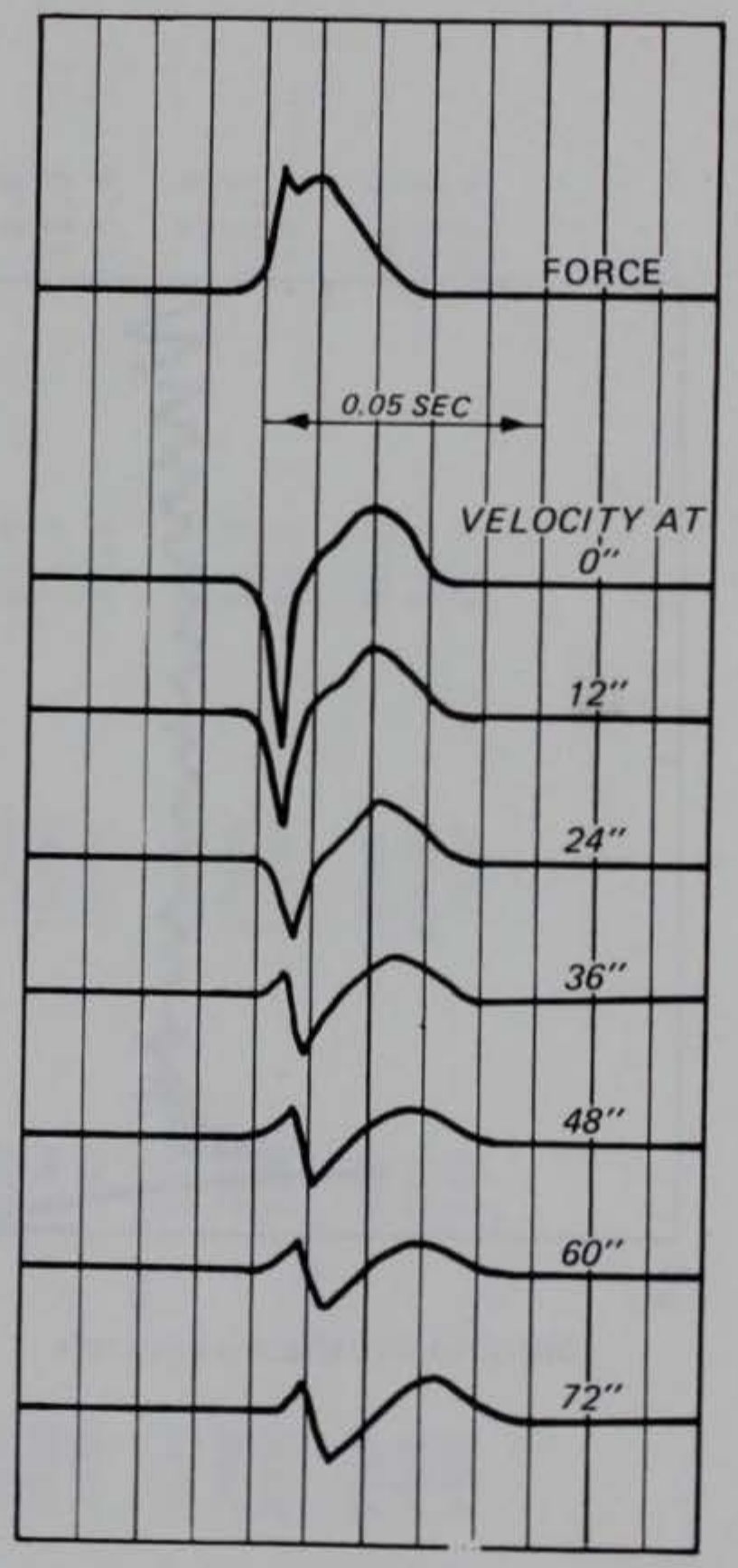


Figure IV-2. Time History Output from FWD Load Cell and Velocity Transducers.

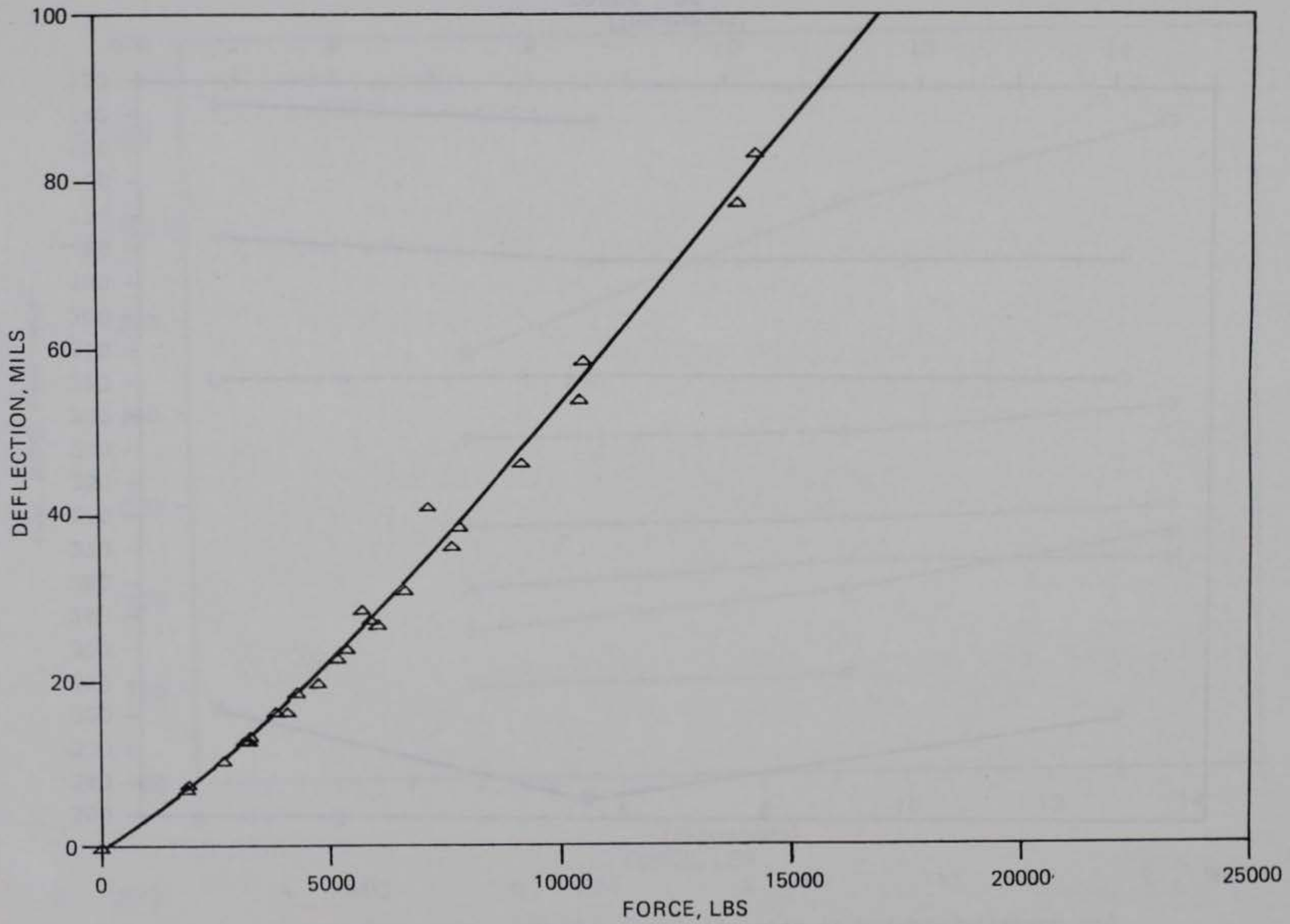


Figure IV-3. Load-Deflection Response of FWD Over Full Range of Deflections.

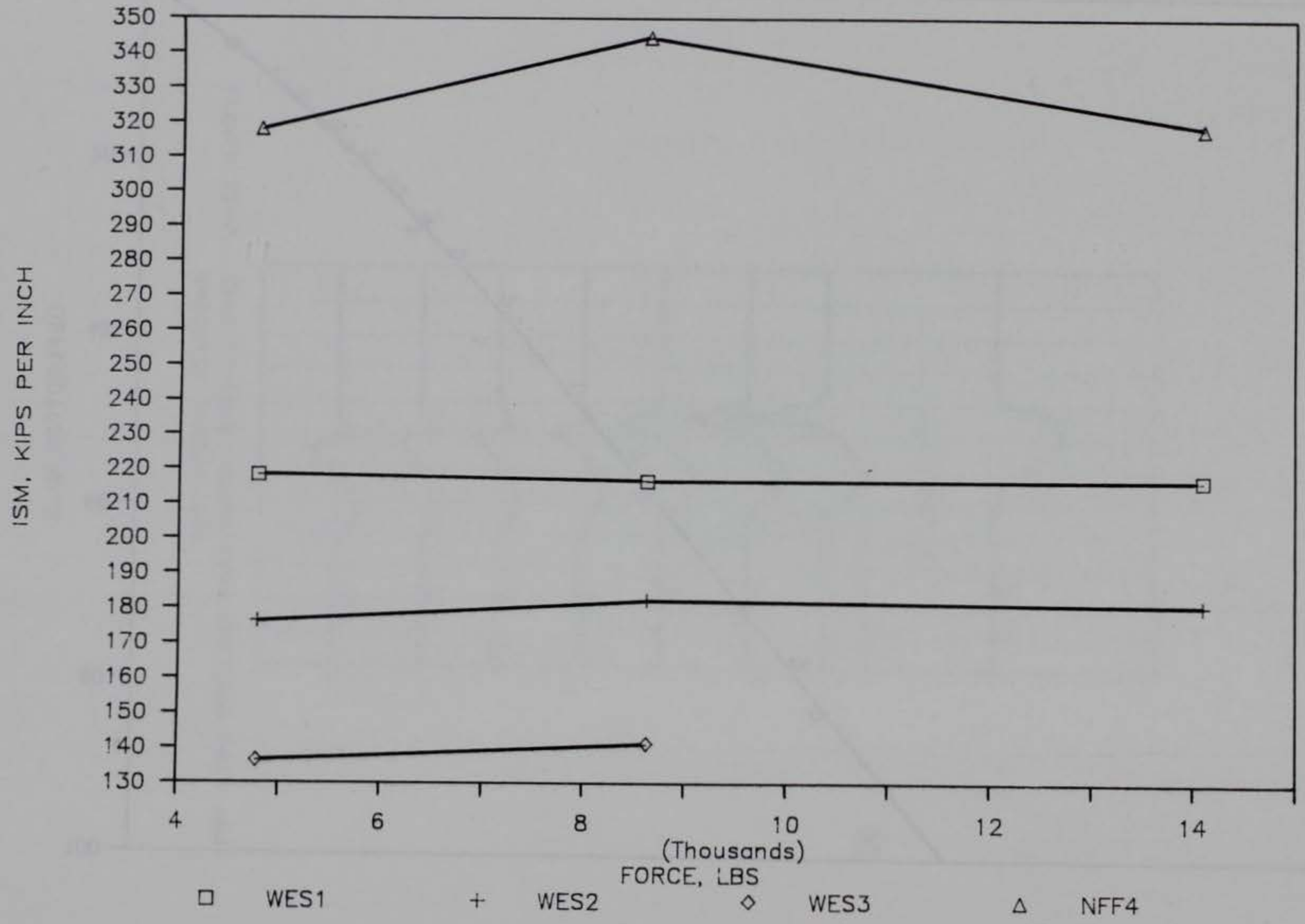


**Figure IV-4. ISM/Force Relationship on WES and NFF4 Items.**

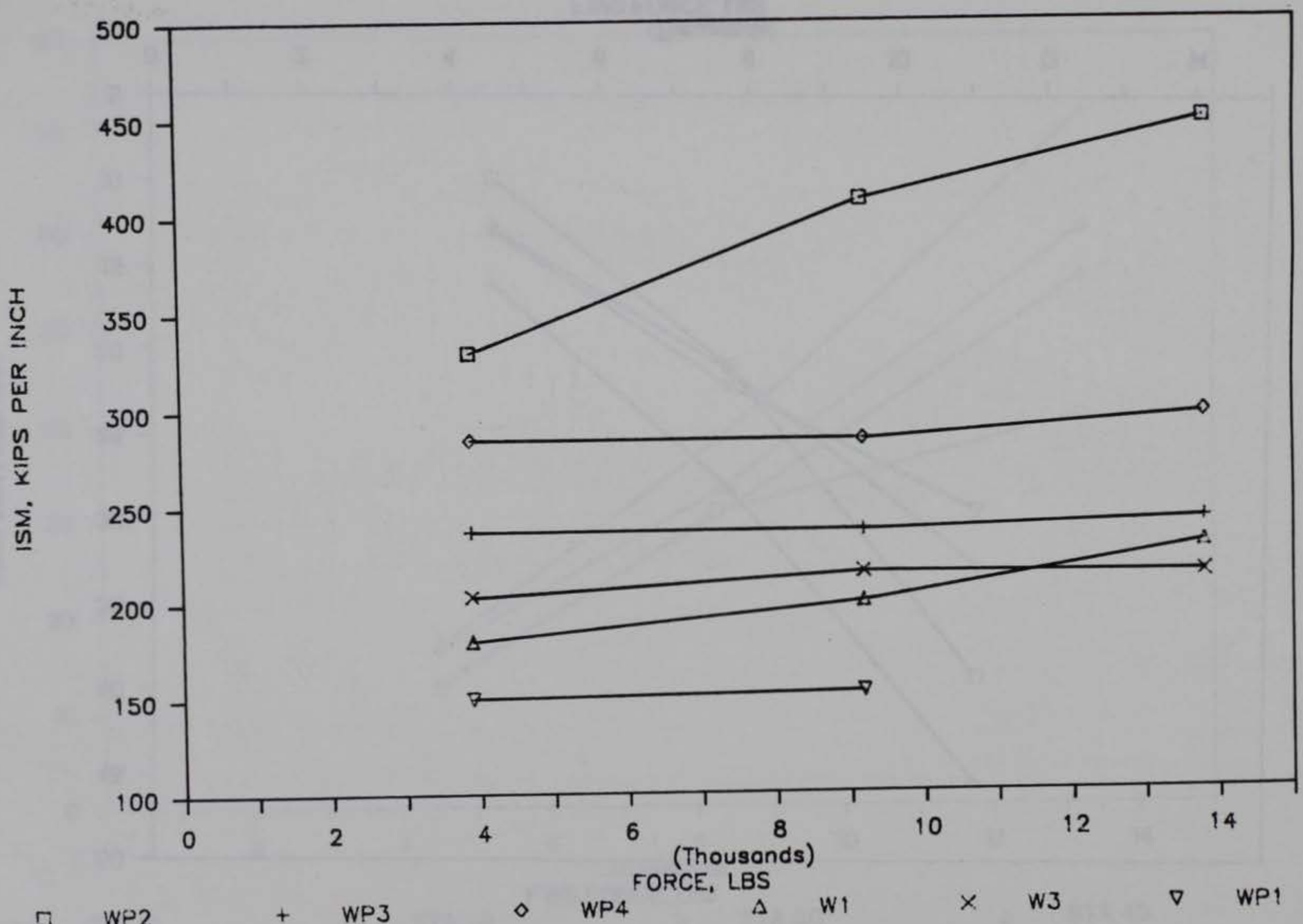


Figure IV-5. ISM/Force Relationship on Wright-Patterson and Whiteman AFB Items.

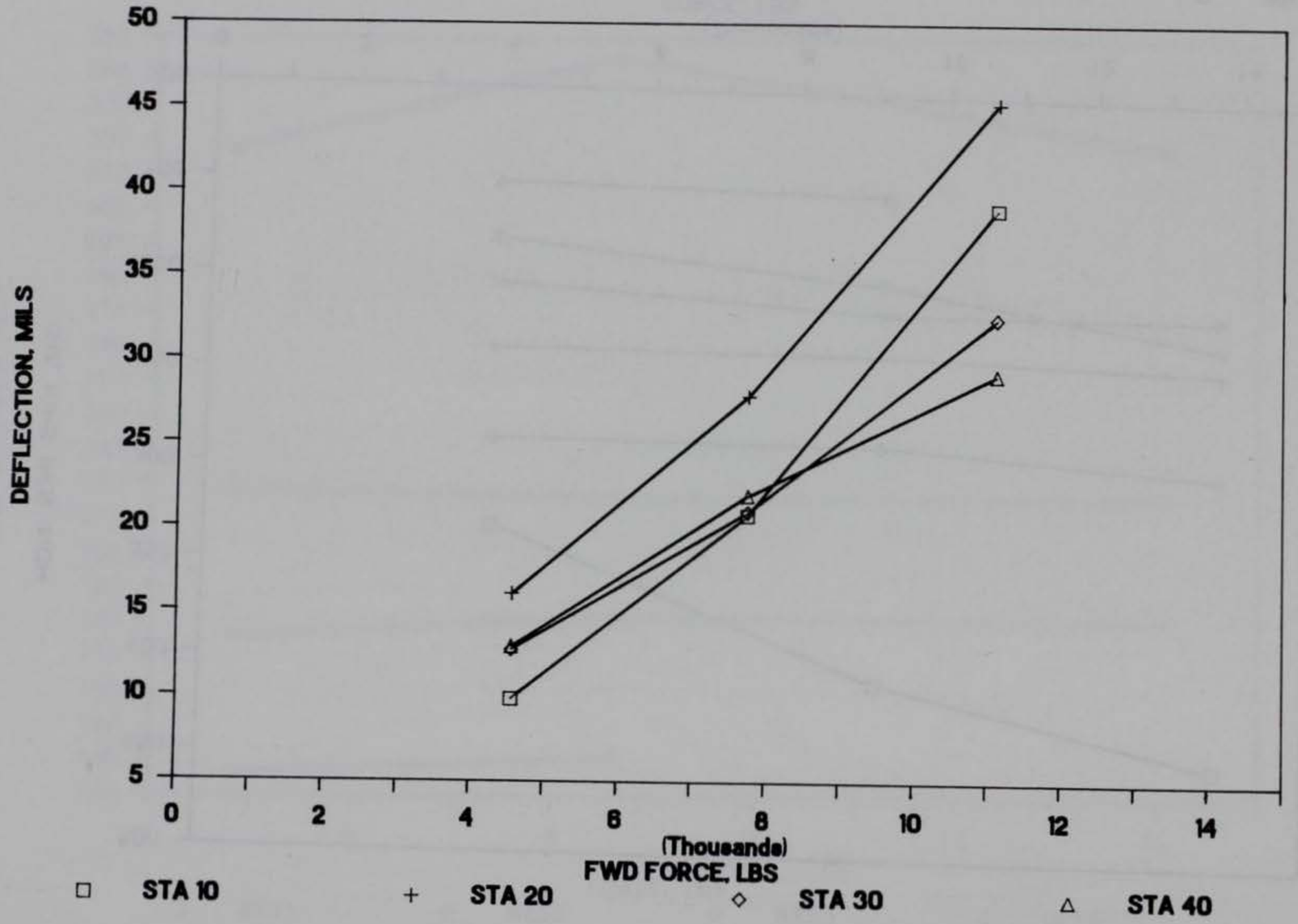


Figure IV-6. Load/Deflection Response on WES Test Item Clay Subgrade.

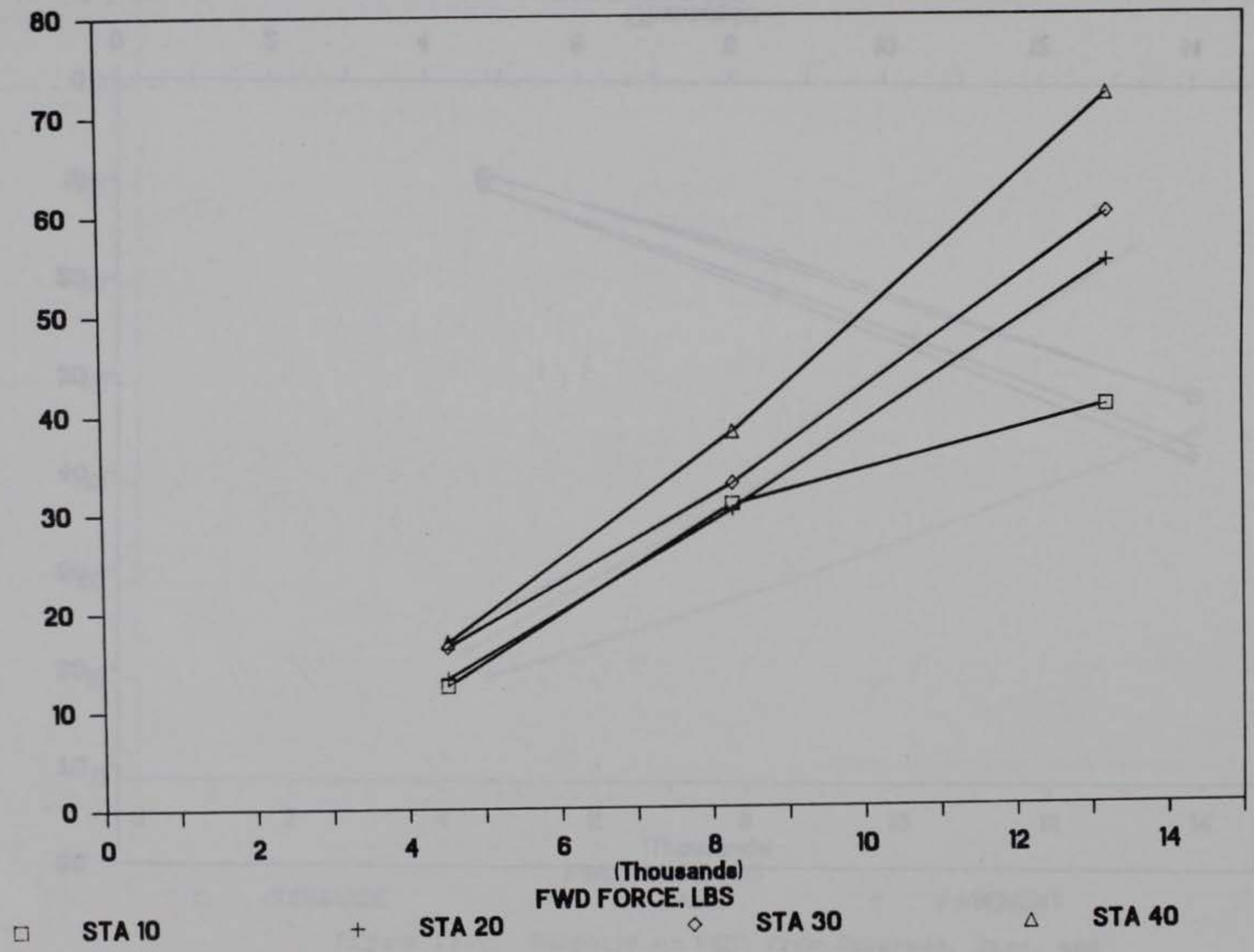


Figure IV-7. Load/Deflection Response on WES Test Item Base Course.

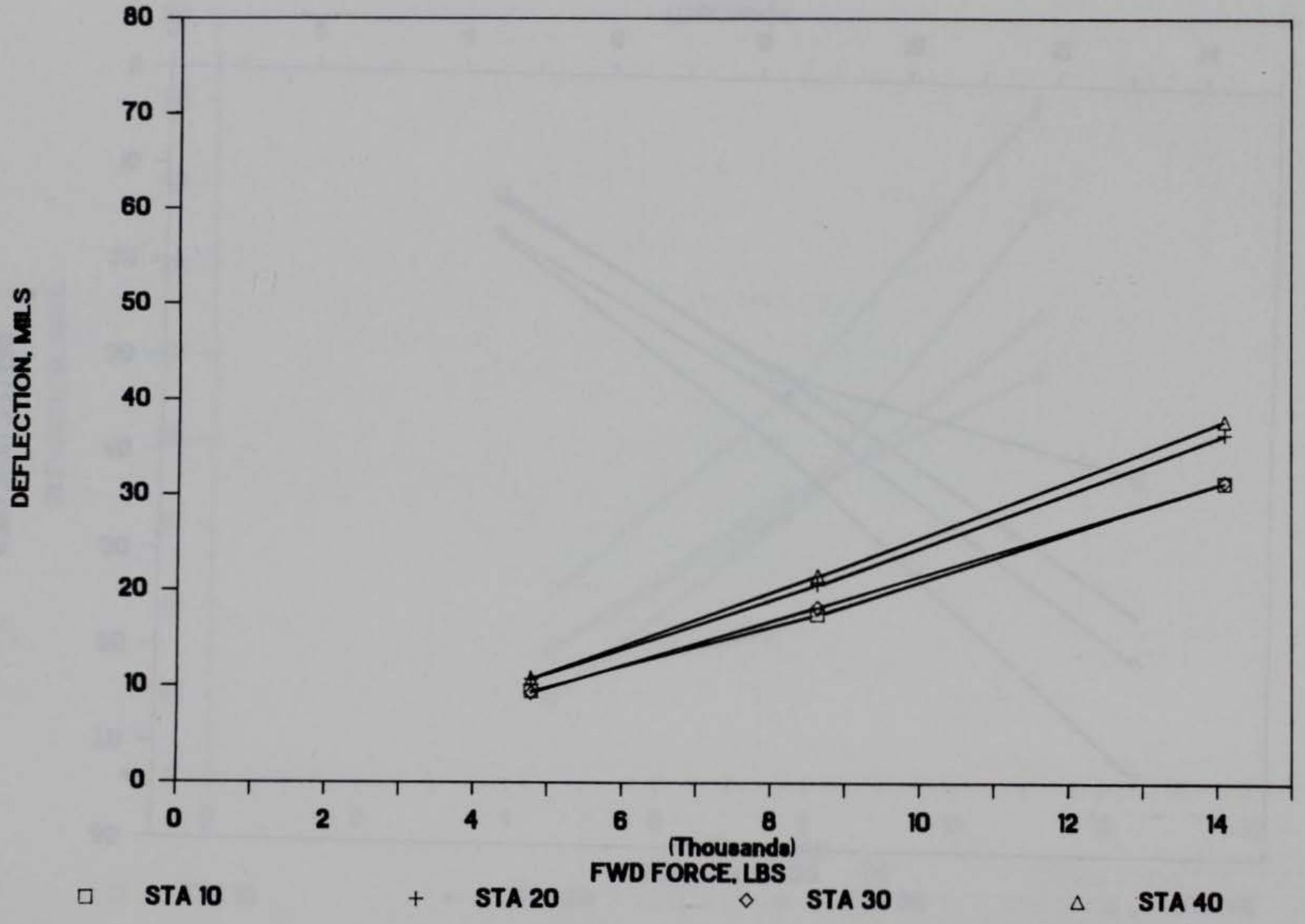


Figure IV-8. Load/Deflection Response on WES 1 Pavement.

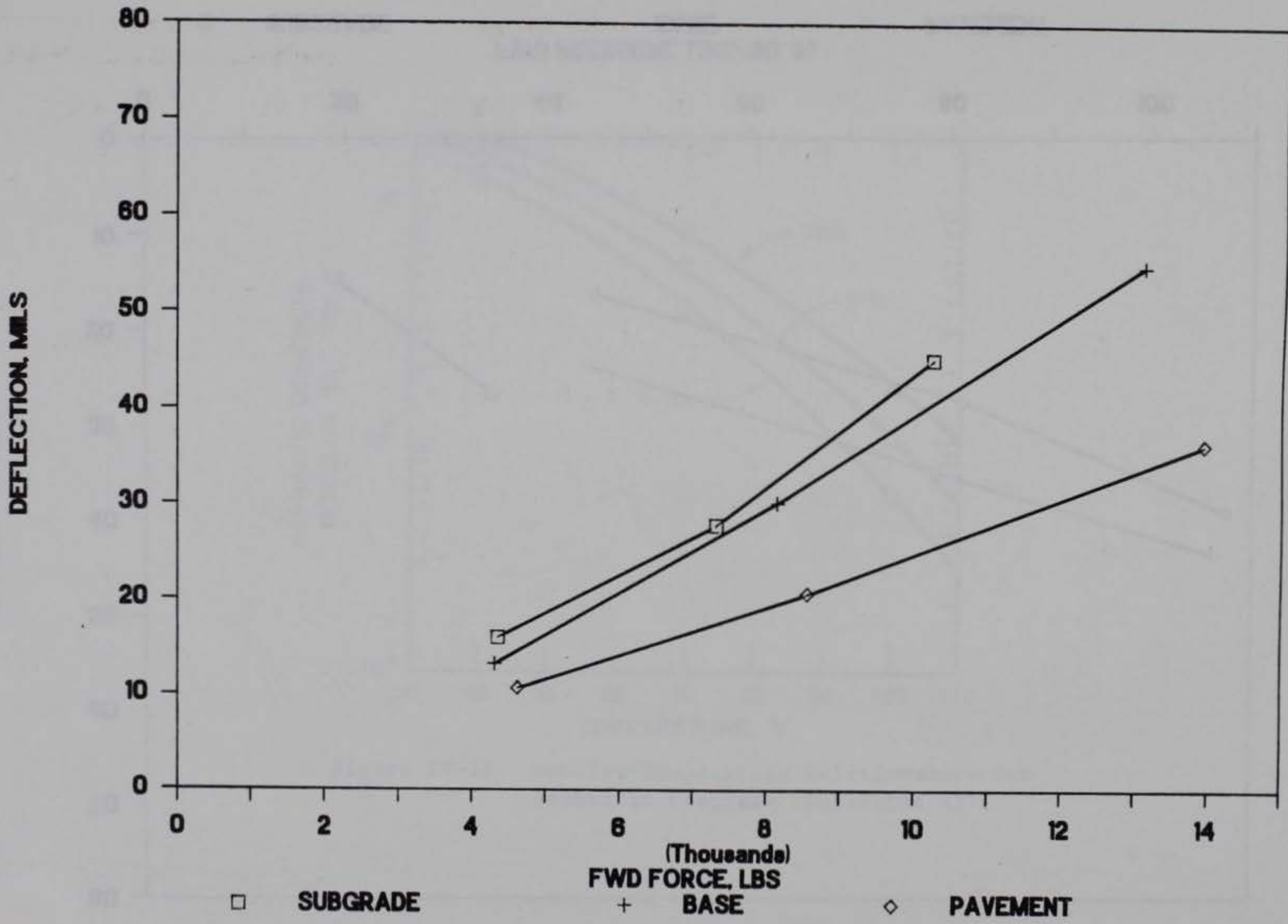


Figure IV-9. Response on WES1 from Subgrade, Base, and Pavement.

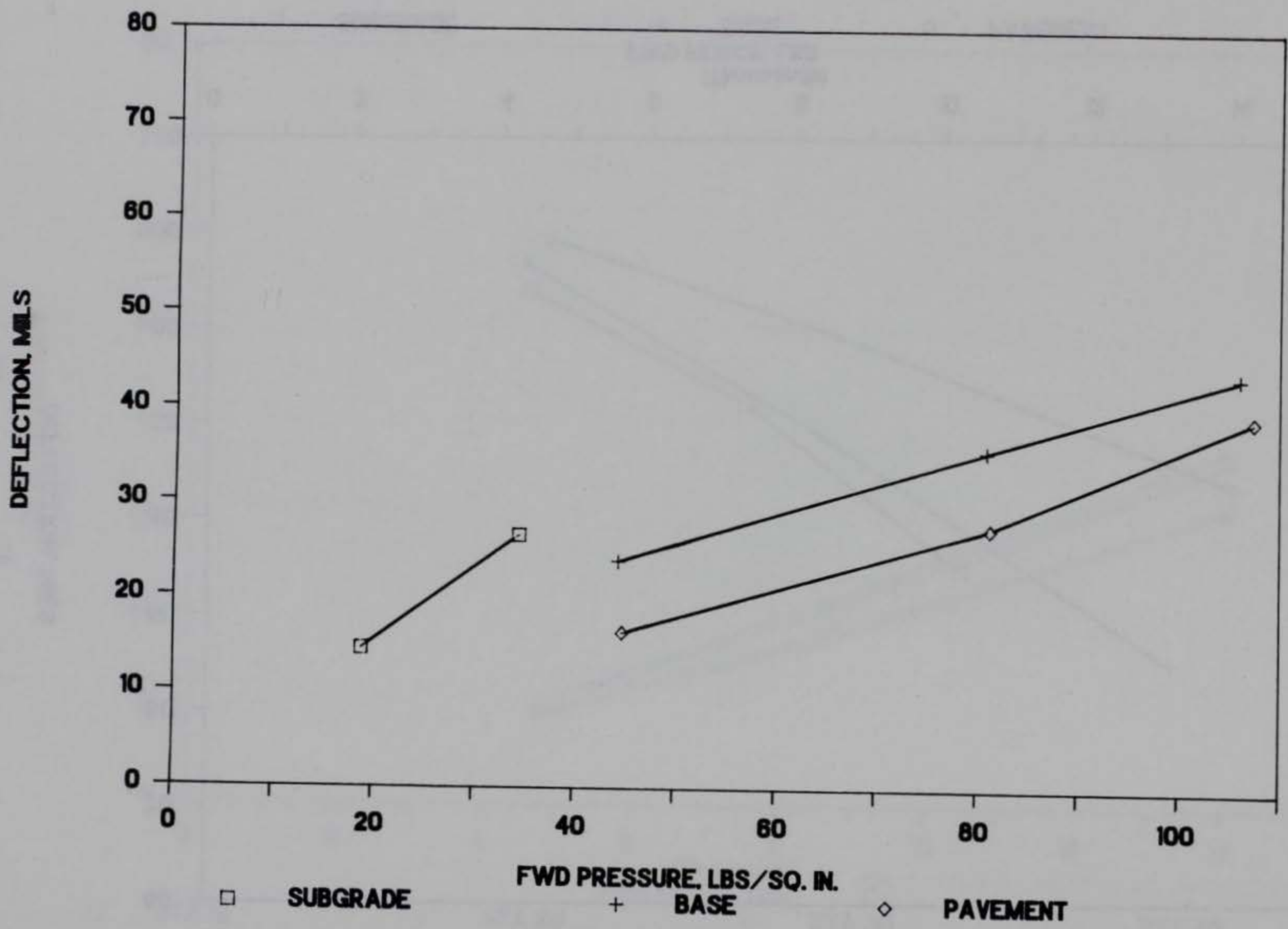


Figure IV-10. Response on NFF4 from Subgrade, Base, and Pavement.

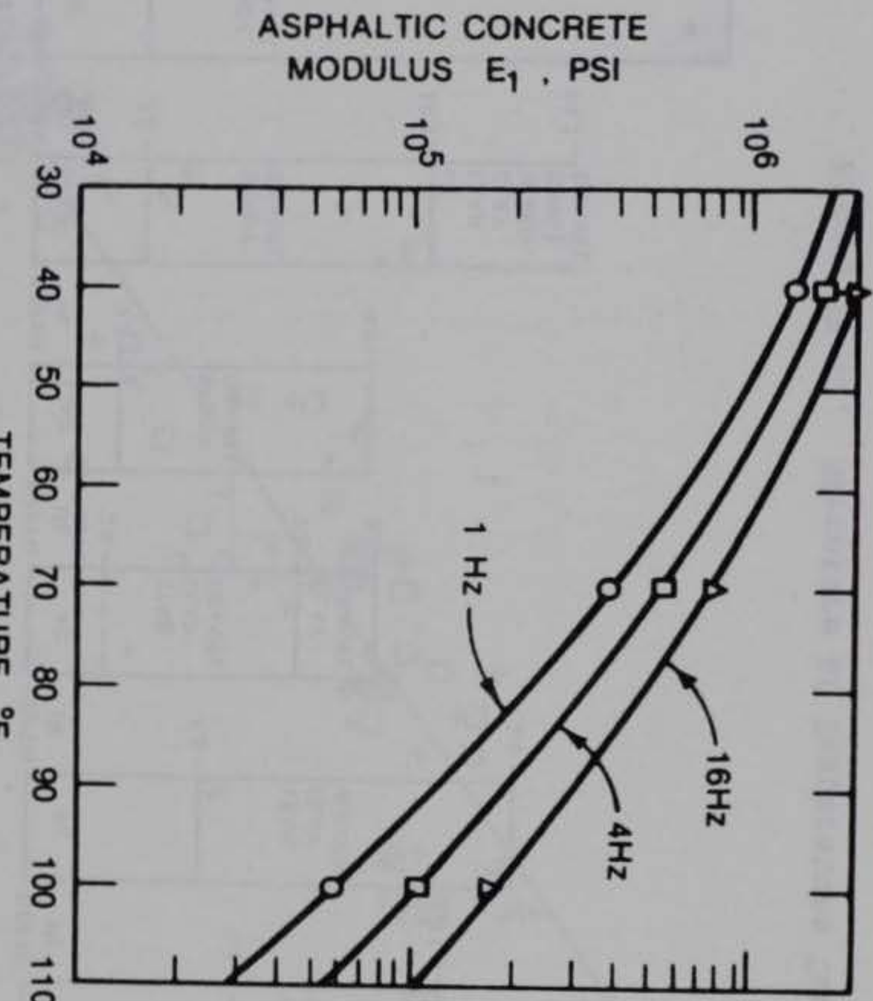


Figure IV-11. Modulus-Temperature Relationships for Asphaltic Concrete (Reference 45).

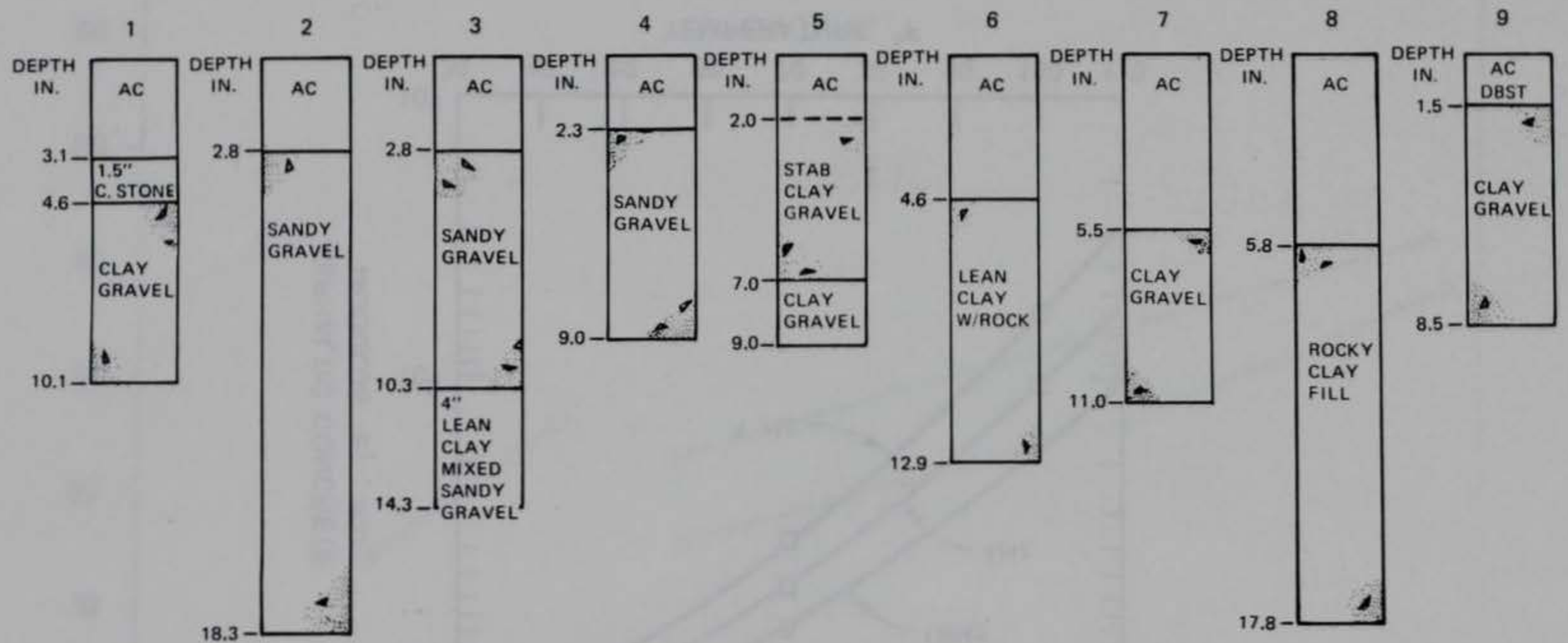


Figure IV-12. Structure of Temperature Test Site.

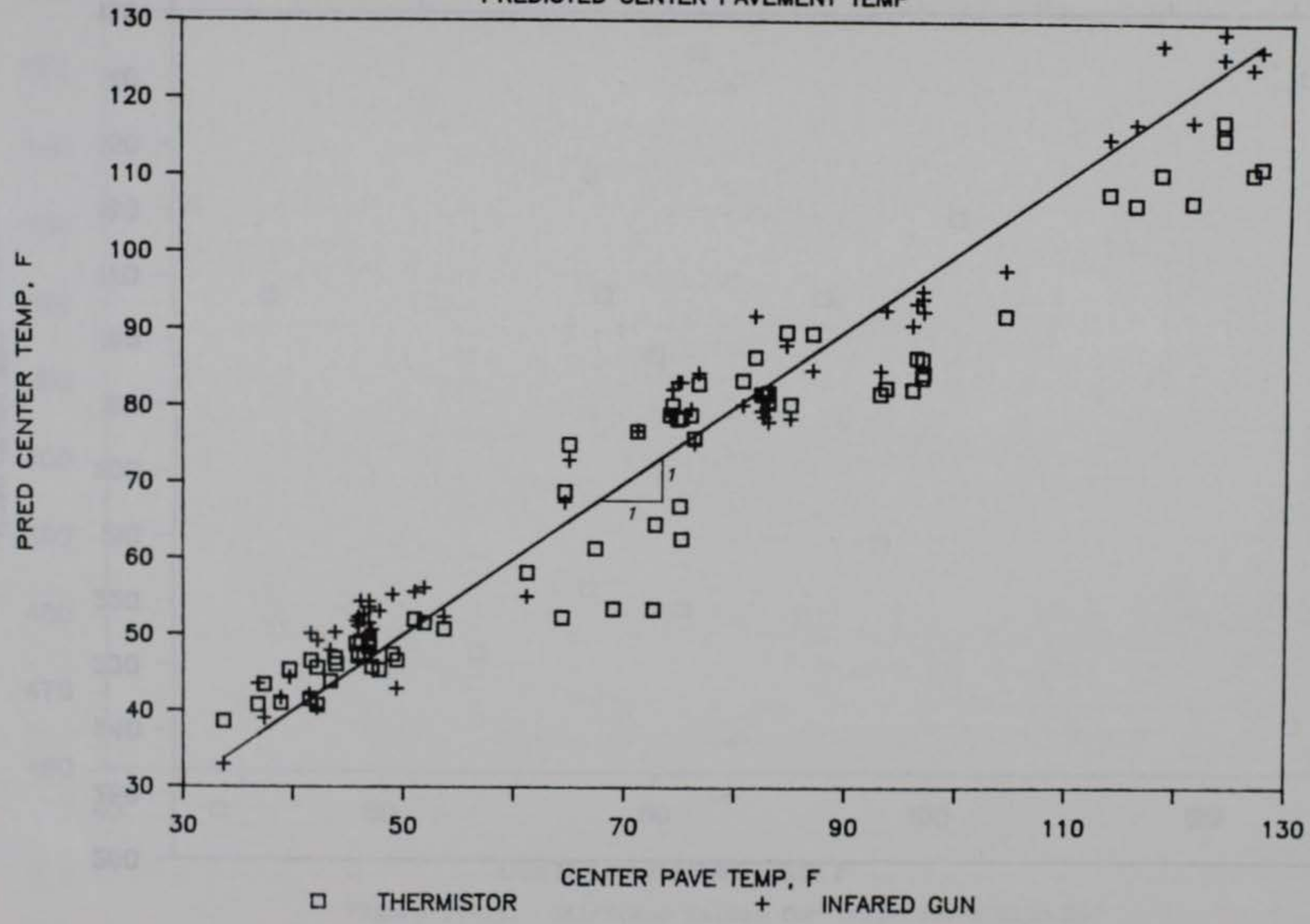


Figure IV-13. Comparison of Predicted to Measured Mean Pavement Temperature

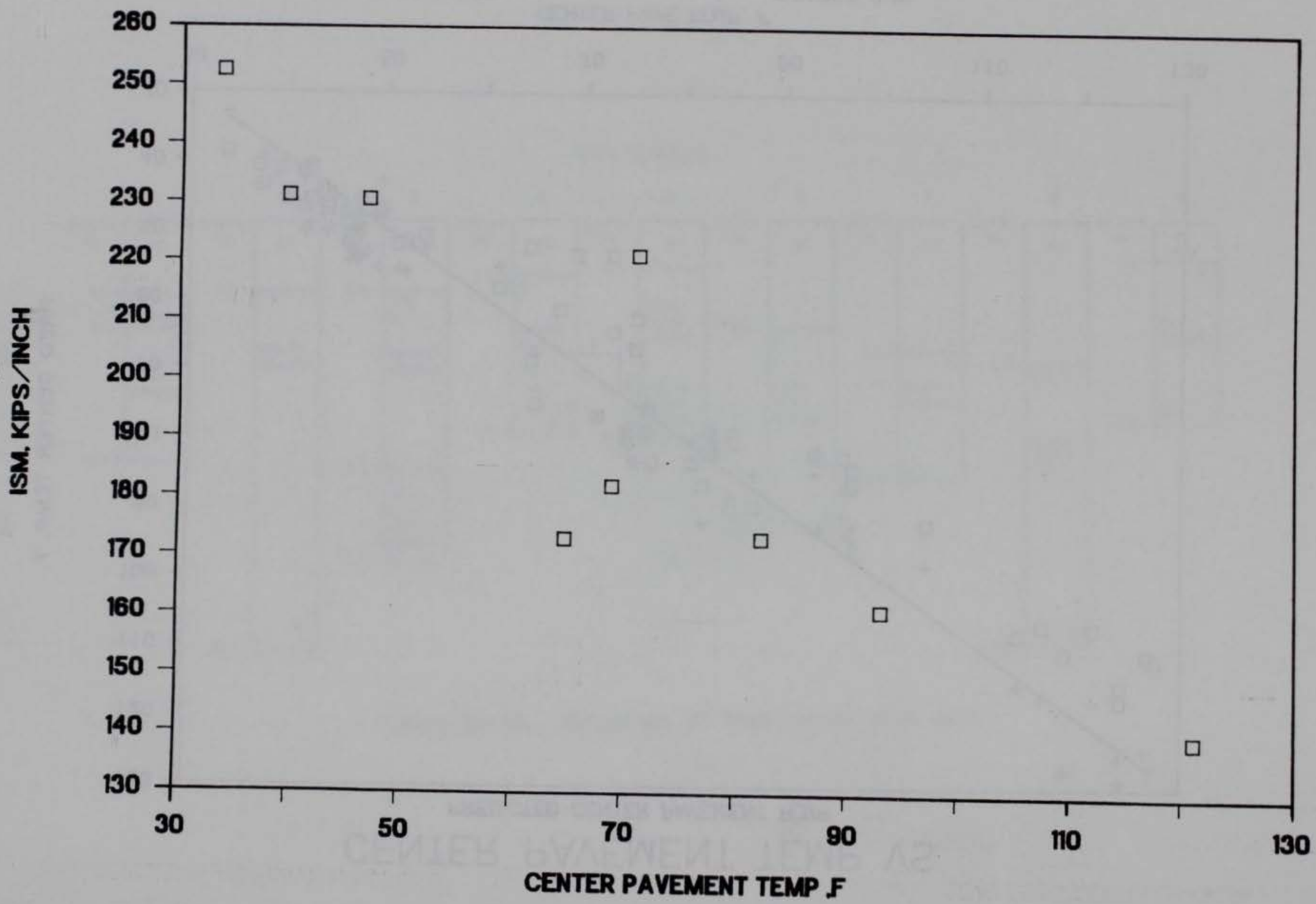


Figure IV-14. Stiffness Values for Temperature Site 1.

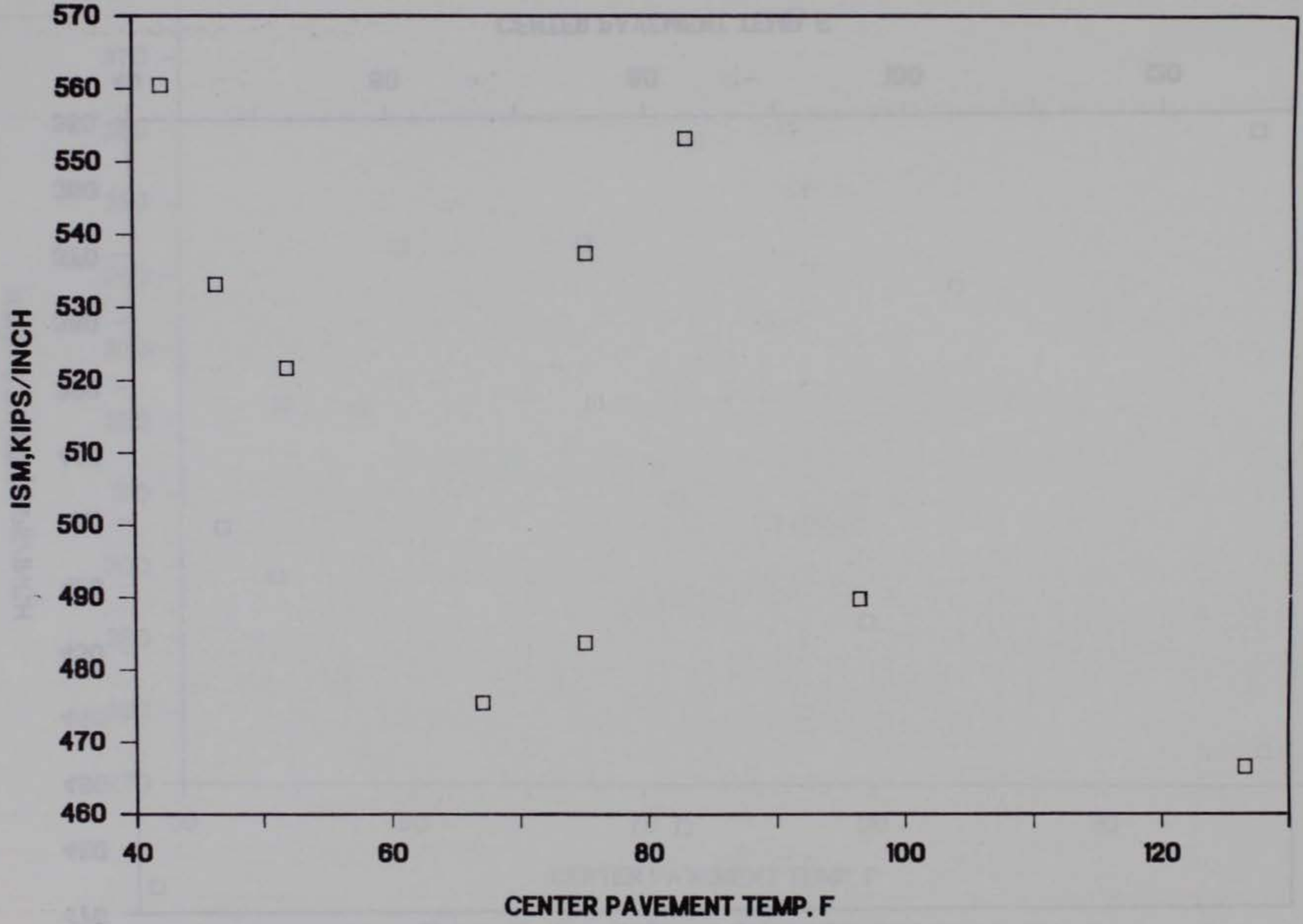


Figure IV-15. Stiffness Values for Temperature Site 2.

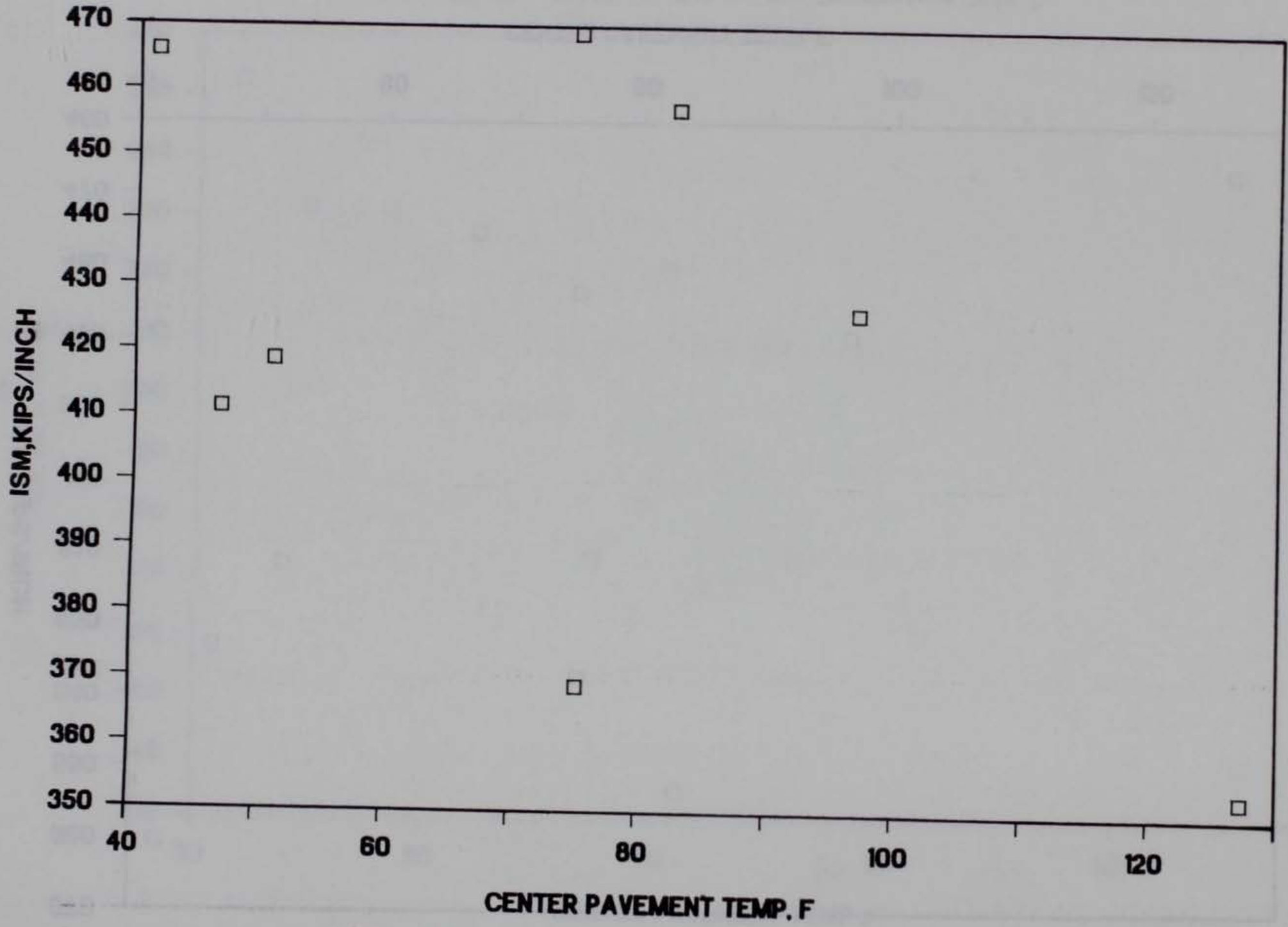


Figure IV-16. Stiffness Values for Temperature Site 3.

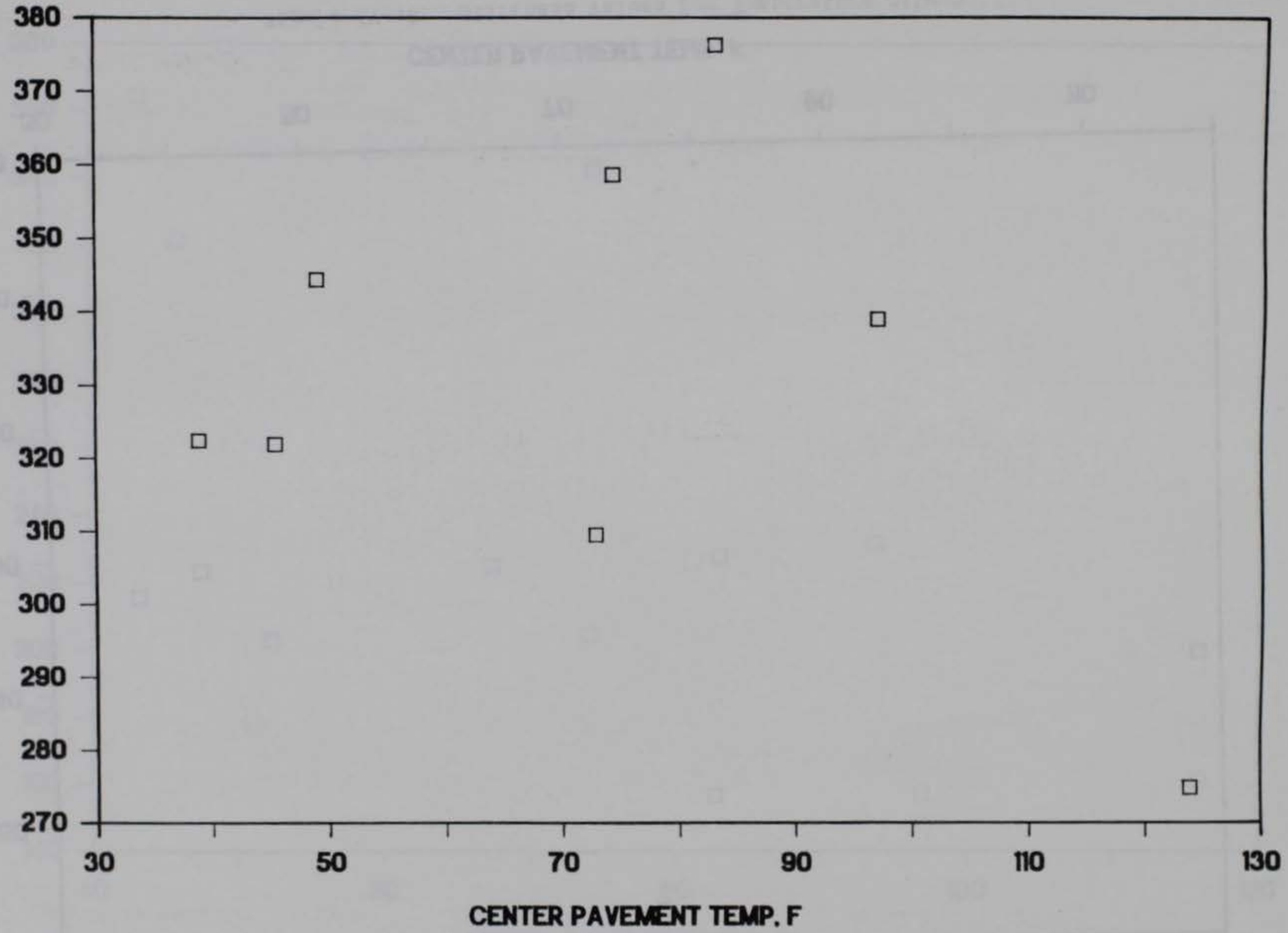


Figure IV-17. Stiffness Values for Temperature Site 4.

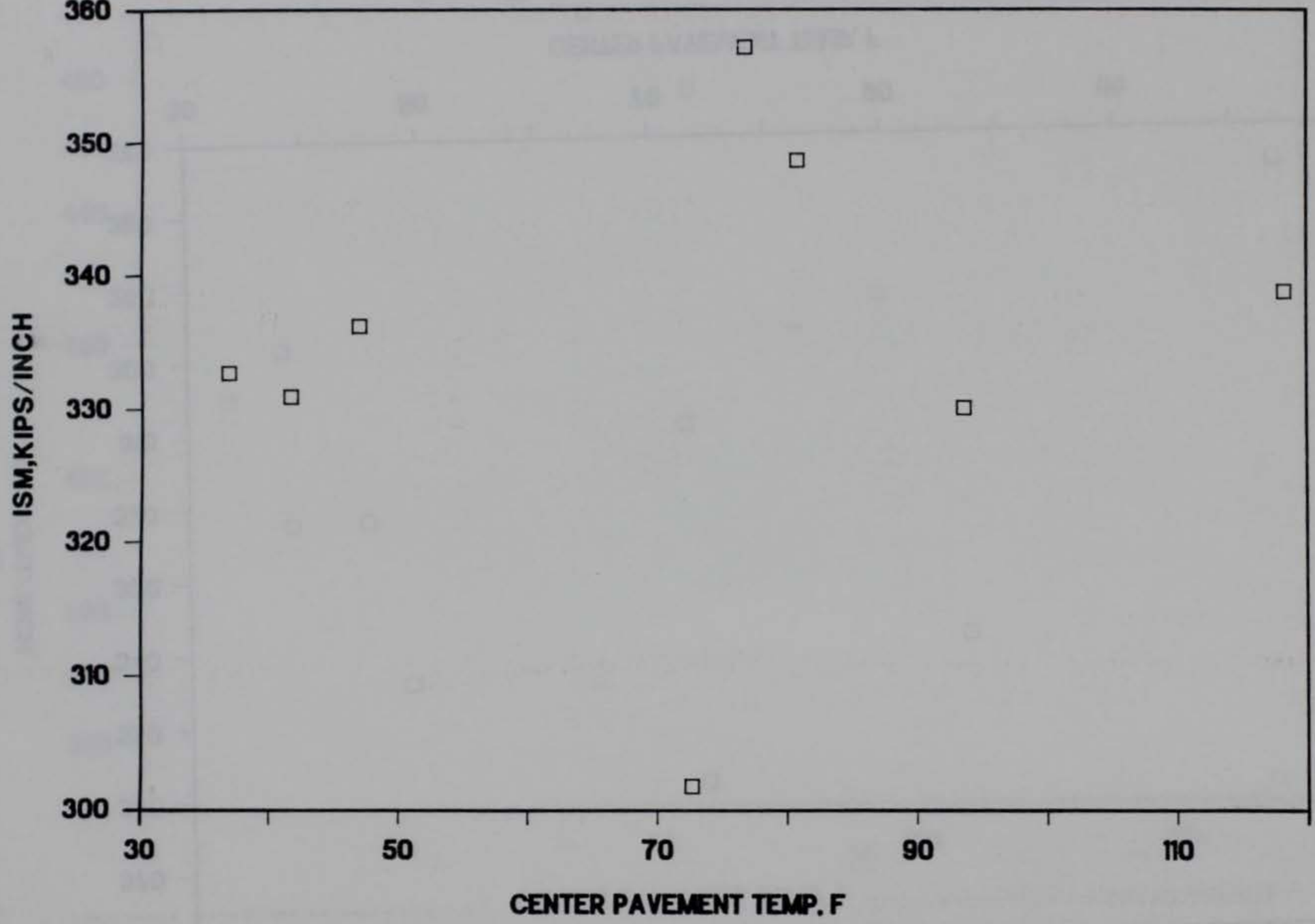


Figure IV-18. Stiffness Values for Temperature Site 5.

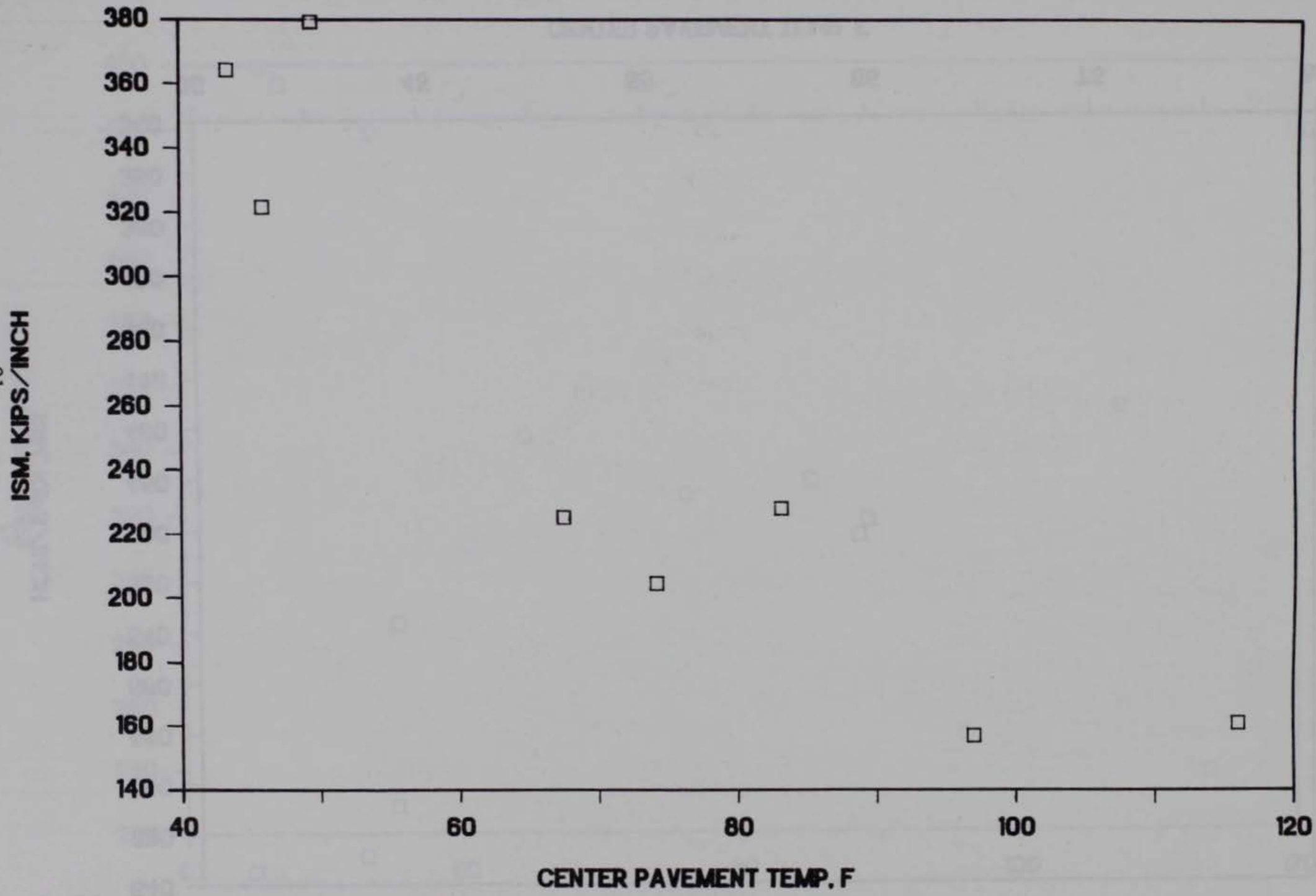


Figure IV-19. Stiffness Values for Temperature Site 6.

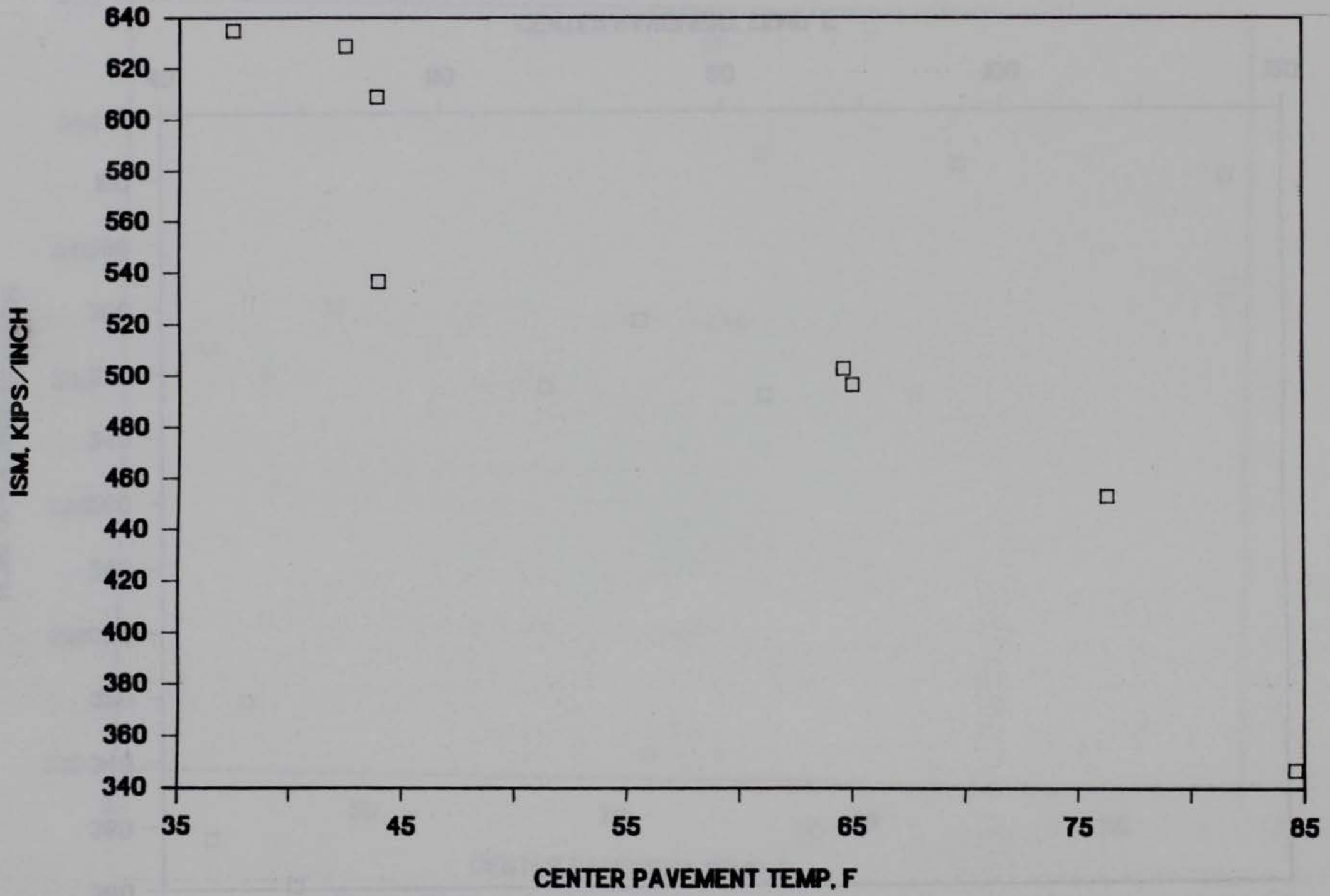


Figure IV-20. Stiffness Values for Temperature Site 7.

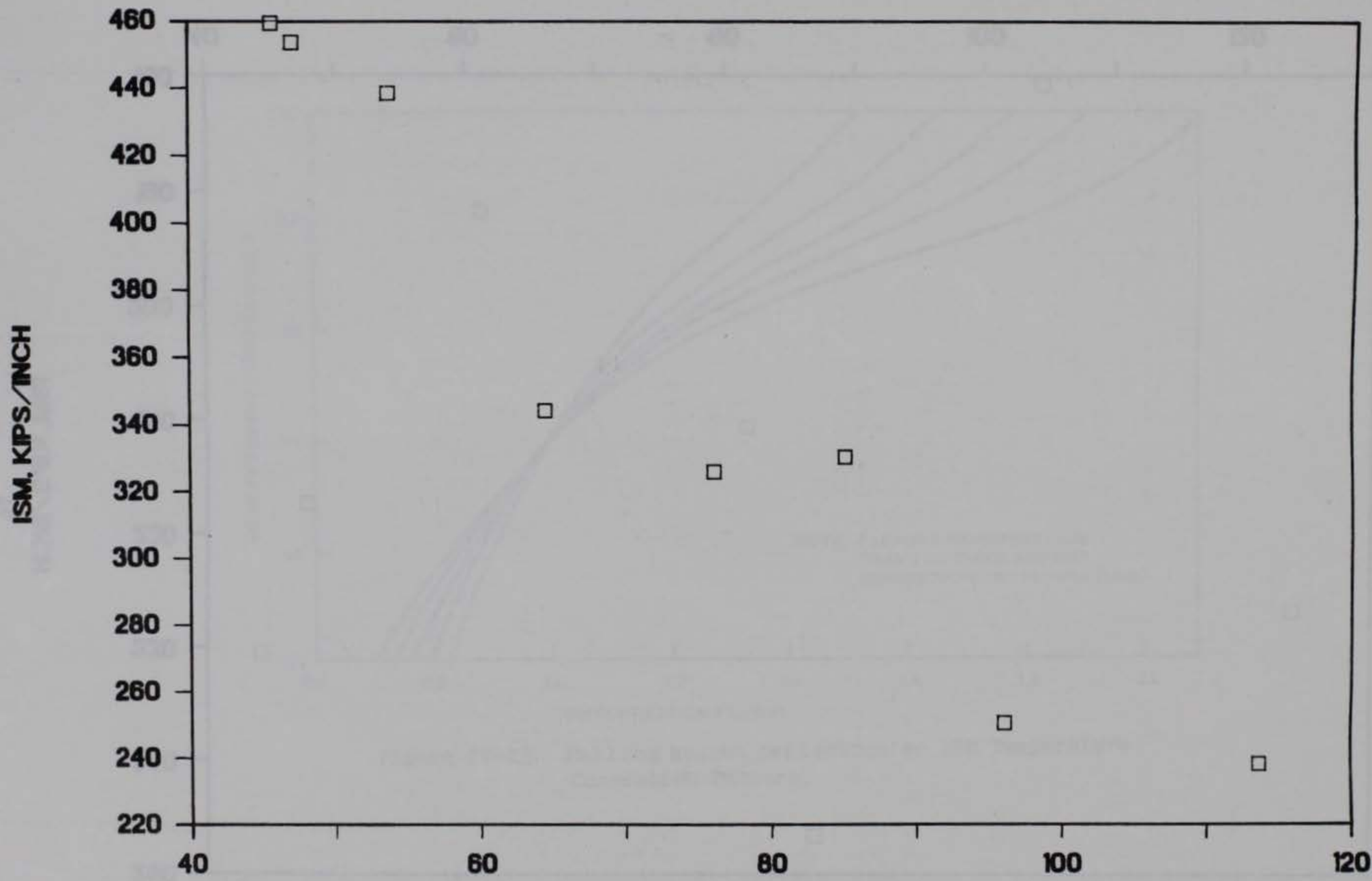


Figure IV-21. Stiffness Values for Temperature Site 8.

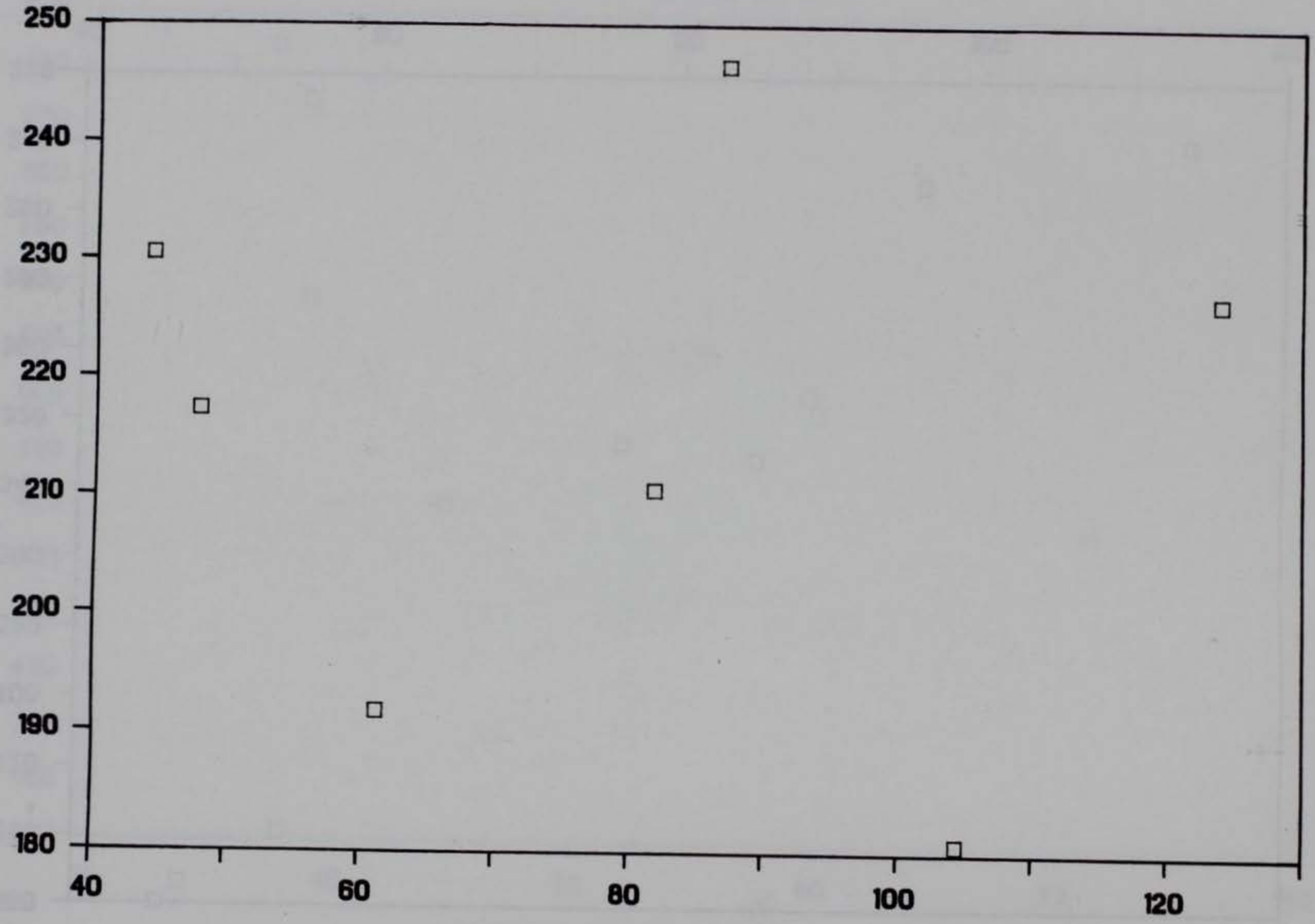


Figure IV-22. Stiffness Values for Temperature Site 9.

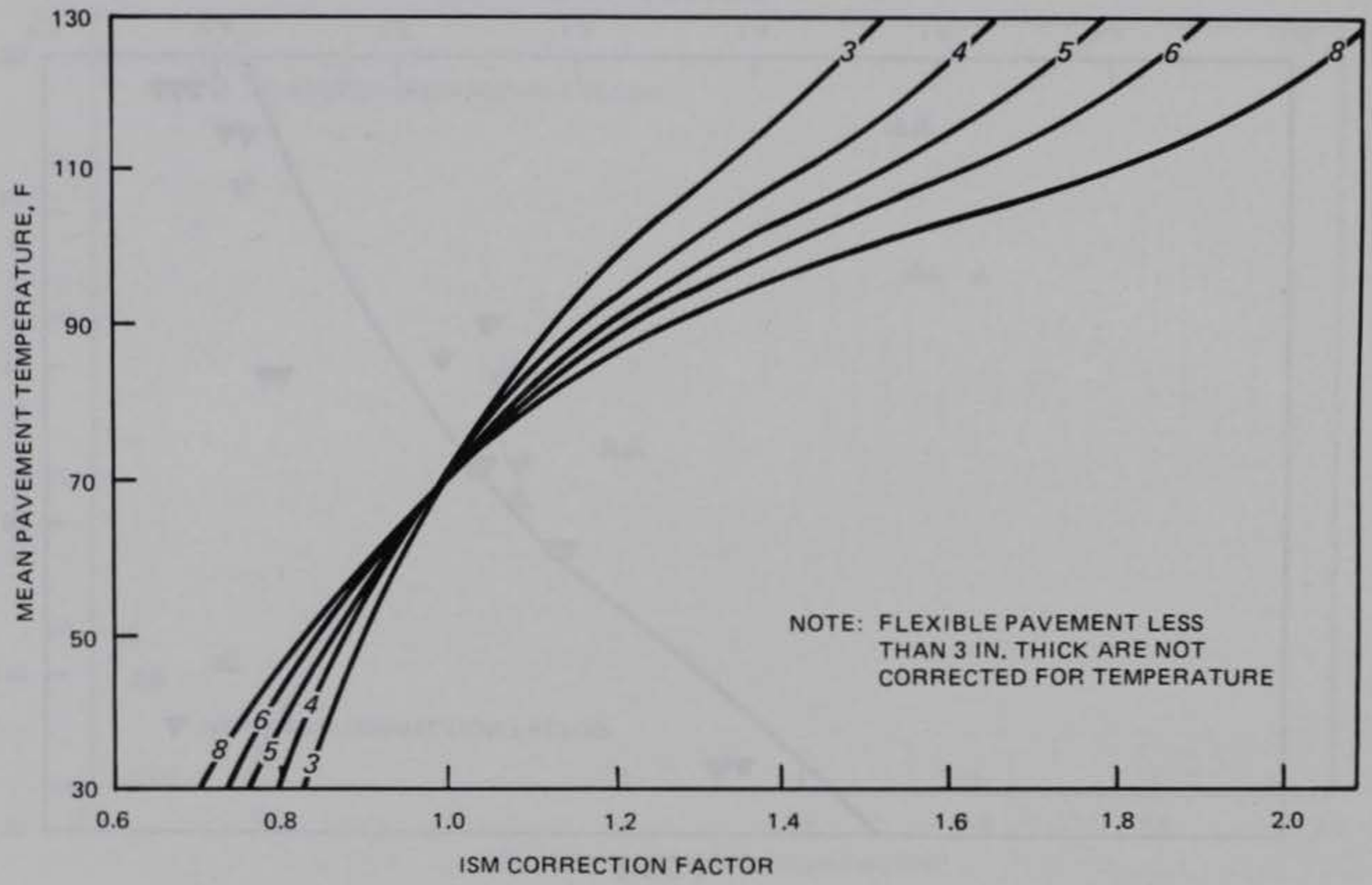


Figure IV-23. Falling Weight Deflectometer ISM Temperature Correction Factors.

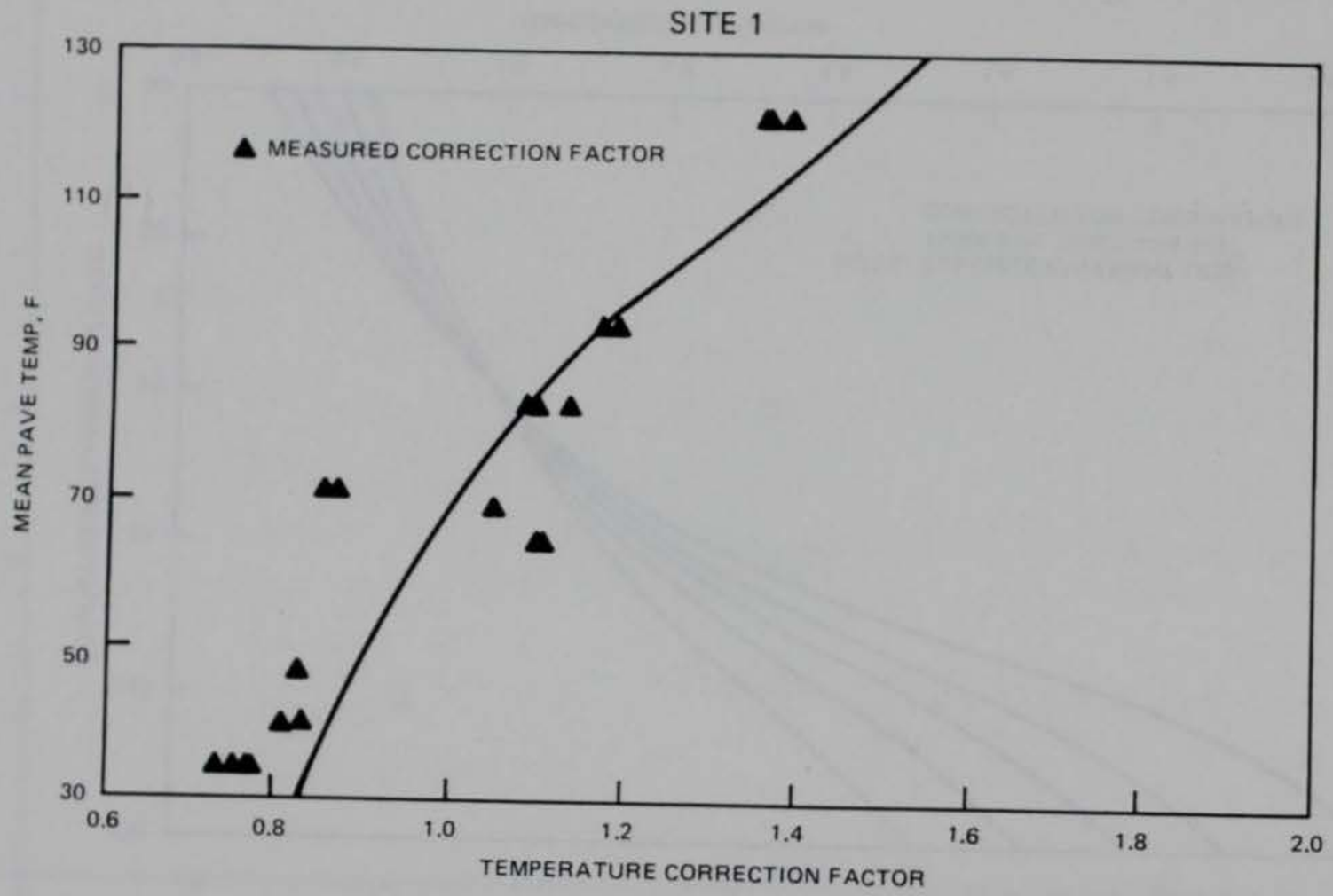


Figure IV-24. Temperature Factors for Site 1.

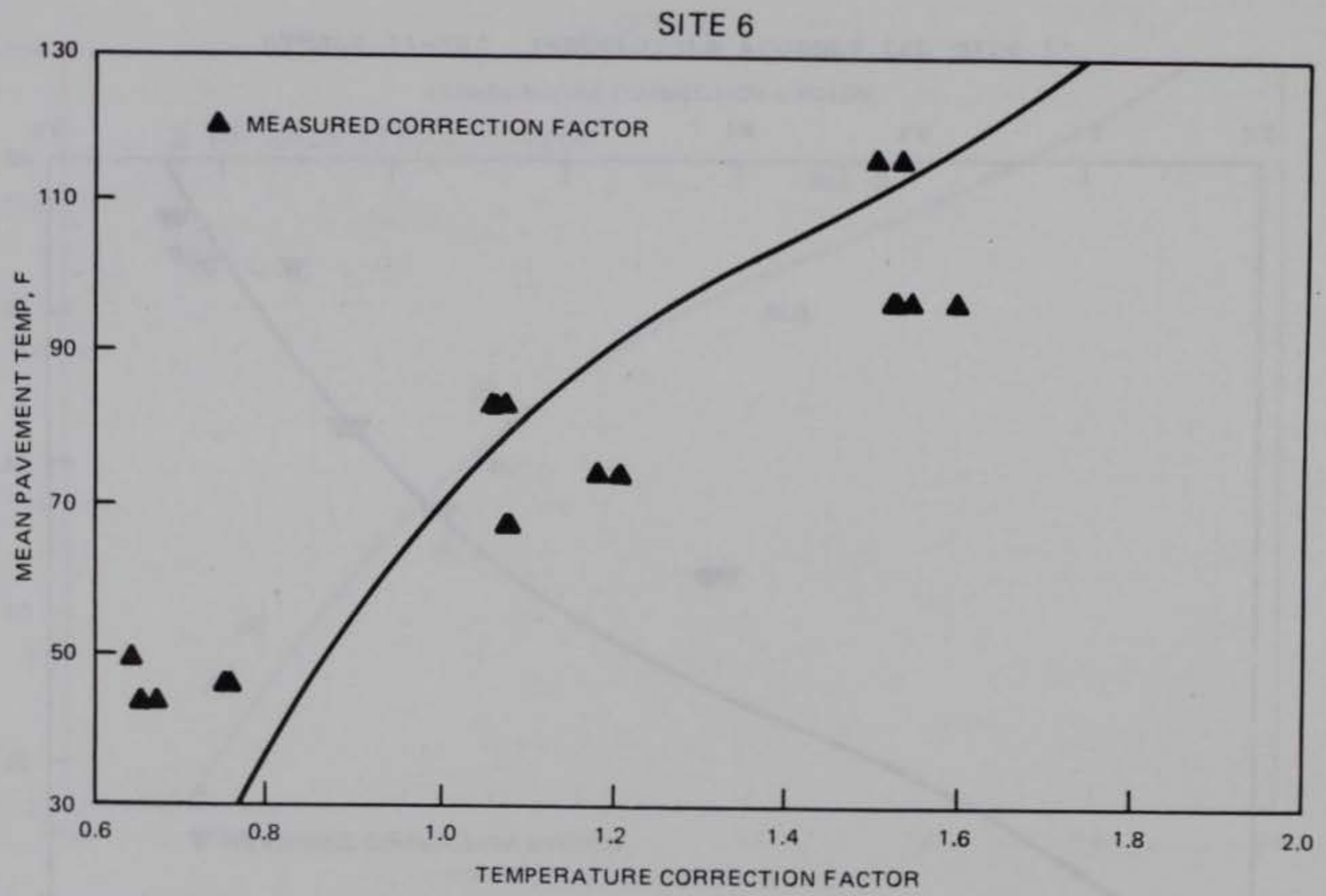


Figure IV-25. Temperature Factors for Site 6.

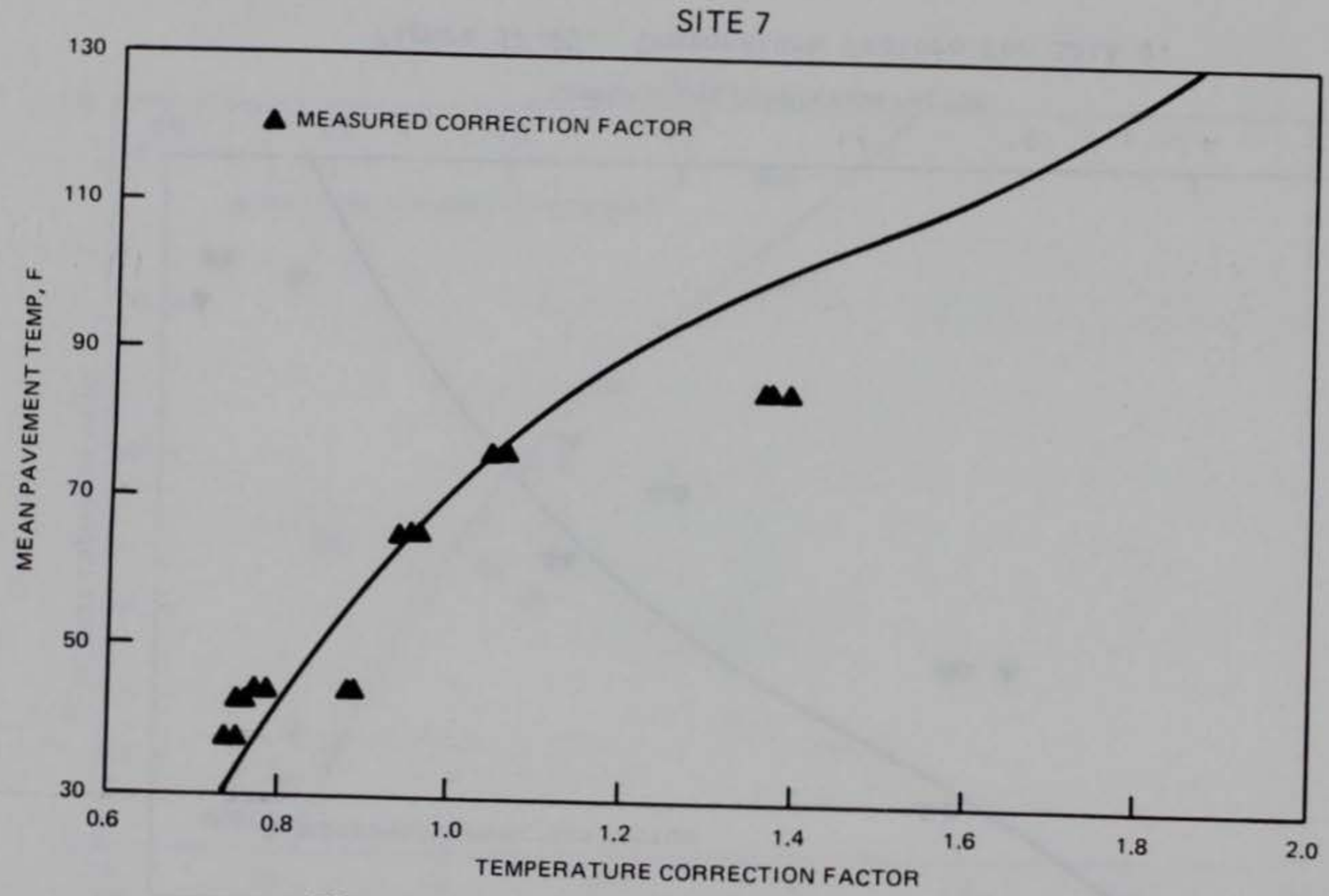


Figure IV-26. Temperature Factors for Site 7.

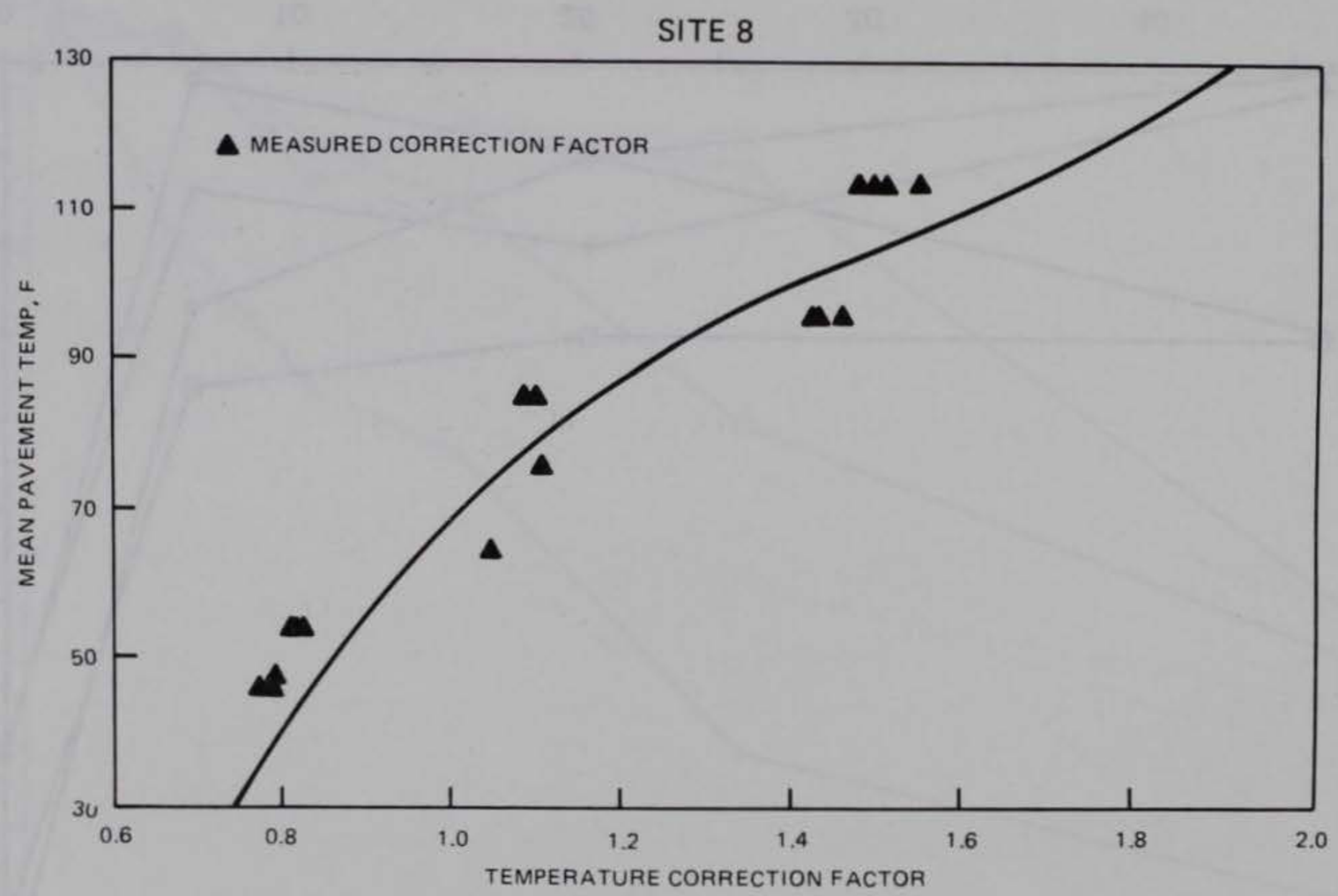


Figure IV-27. Temperature Factors for Site 8.

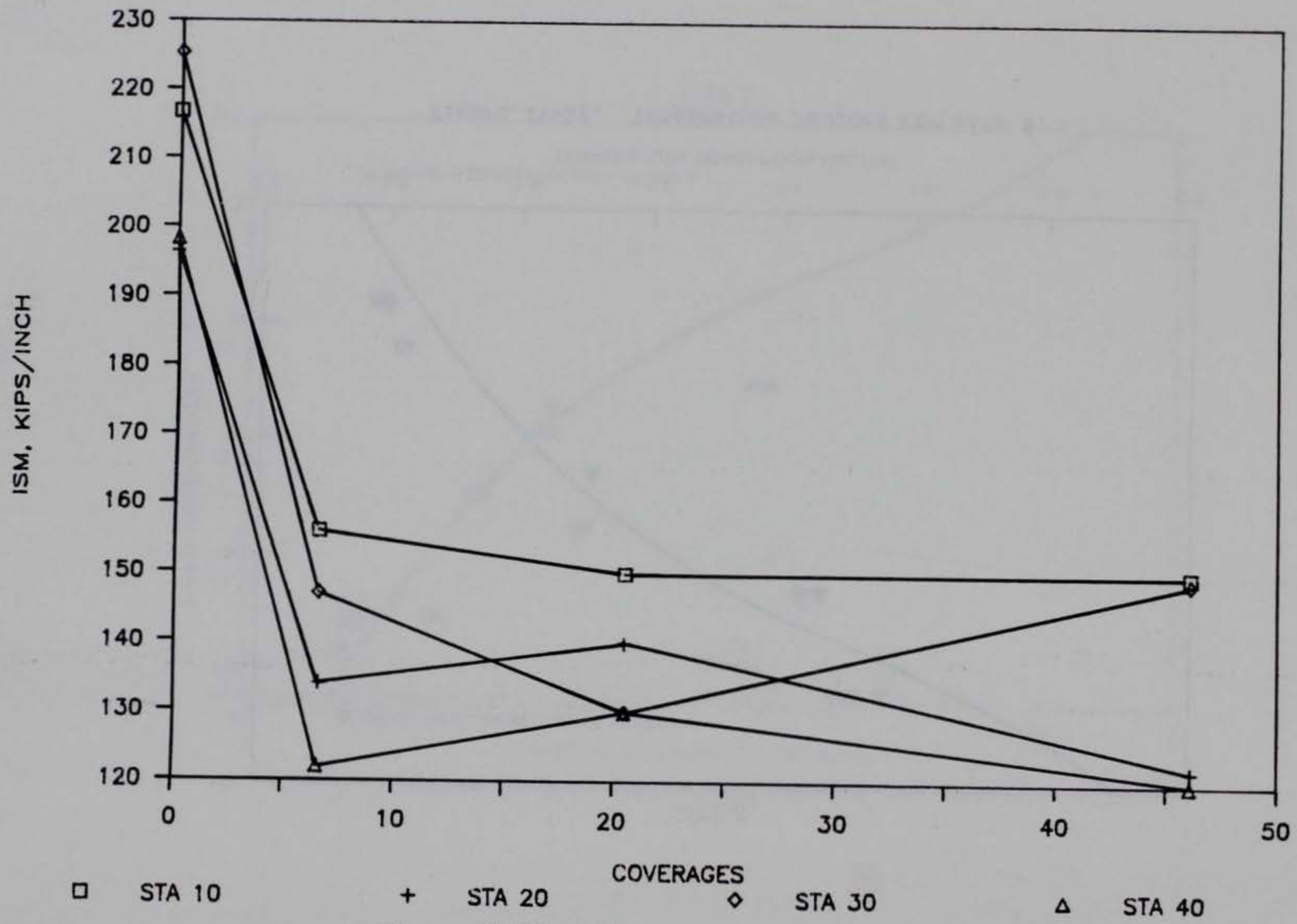


Figure IV-28. ISM versus Coverages for WES1 Items.

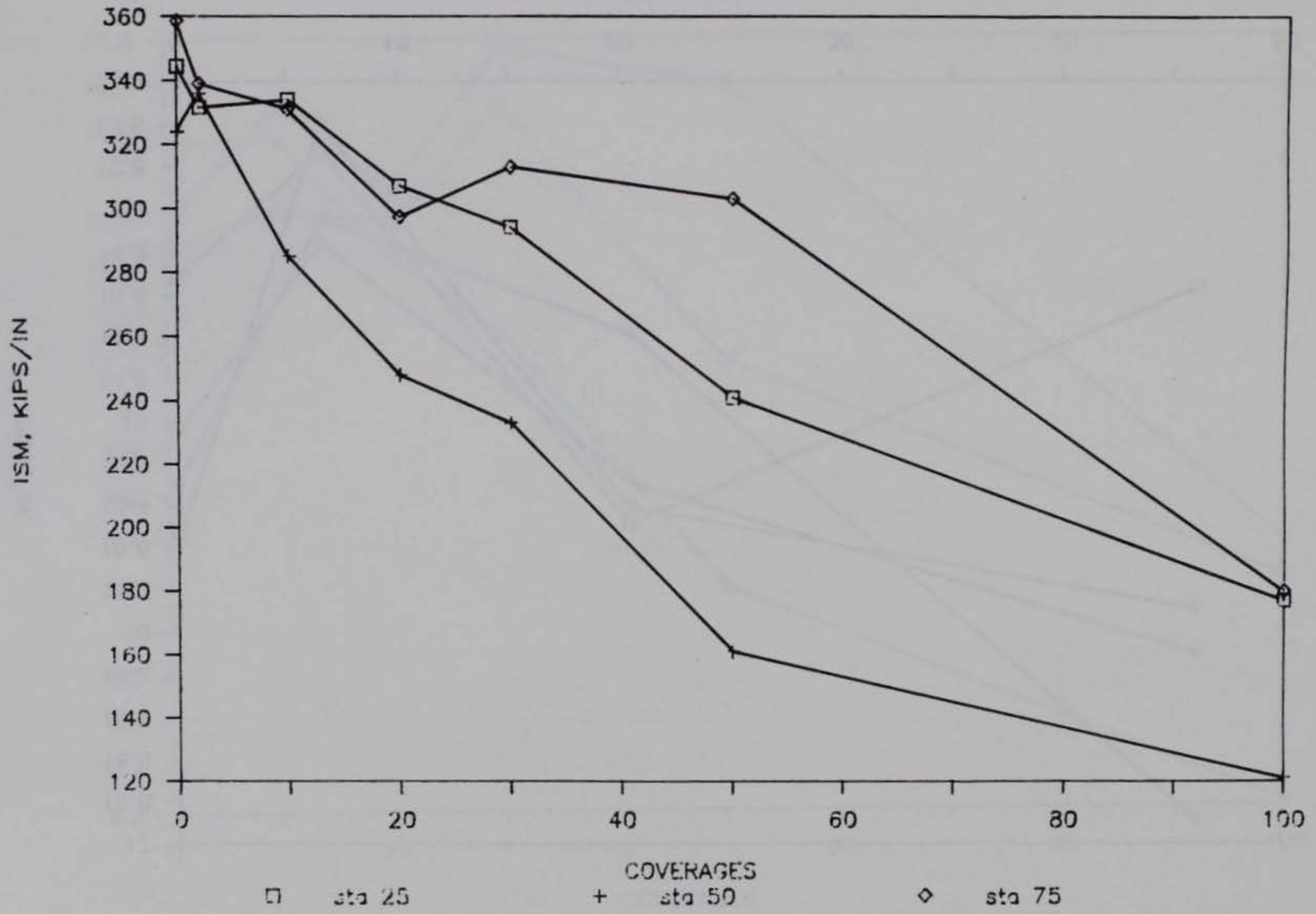


**Figure IV-29. ISM versus Coverages for NFF4 Item.**

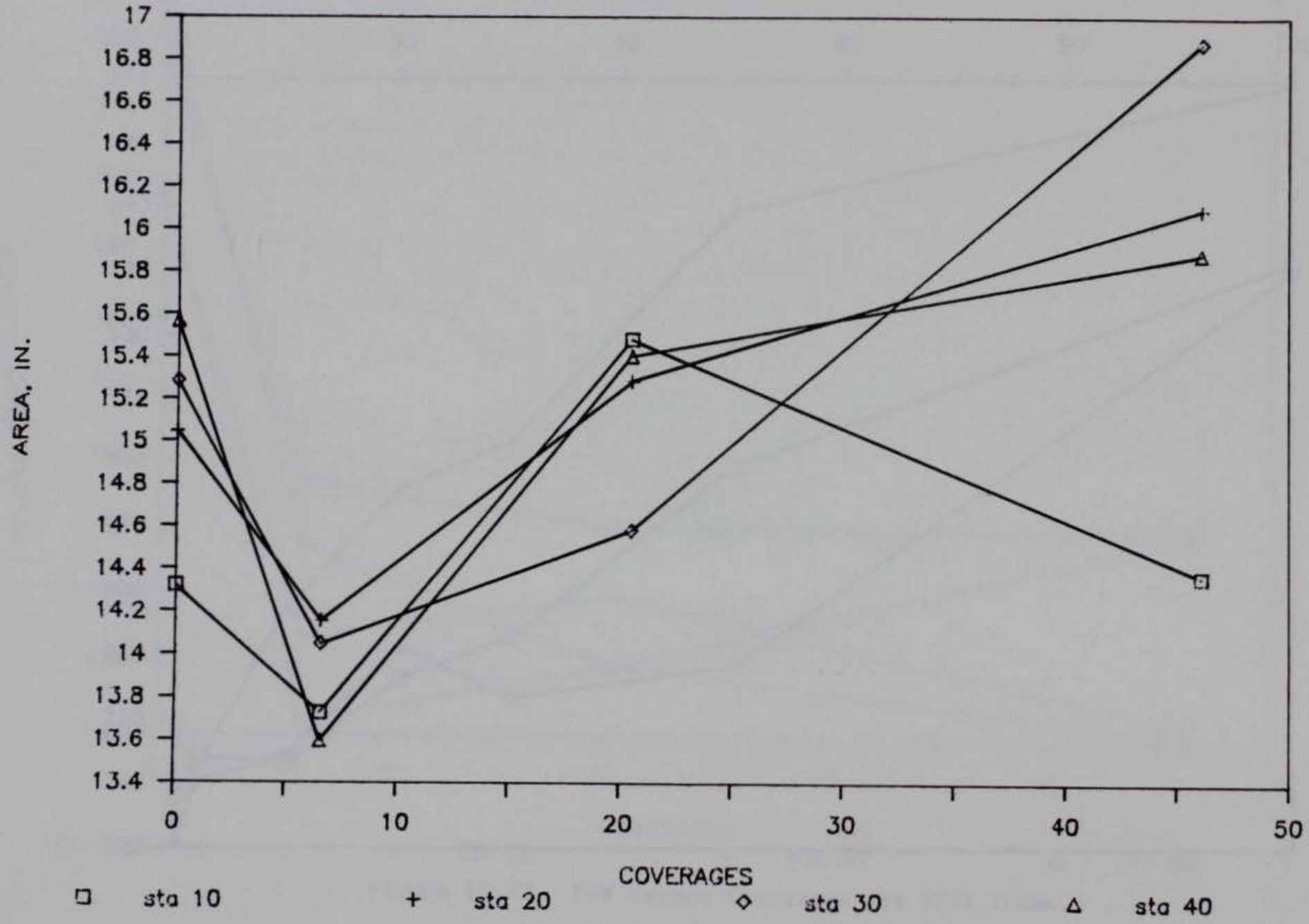


Figure IV-30. Area versus Coverages for WES1 Item.

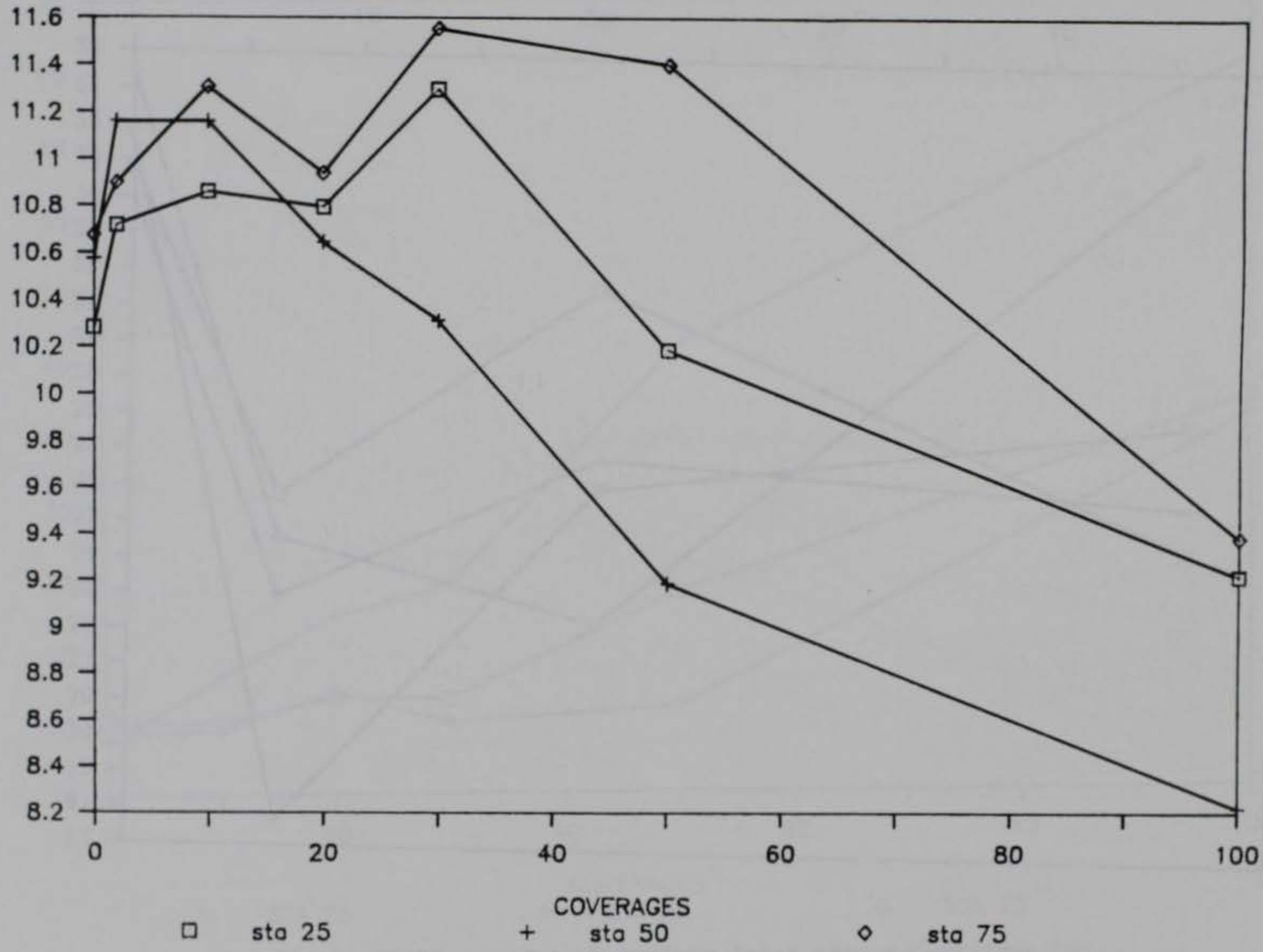


Figure IV-31. Area versus Coverages for NFF4 Item.

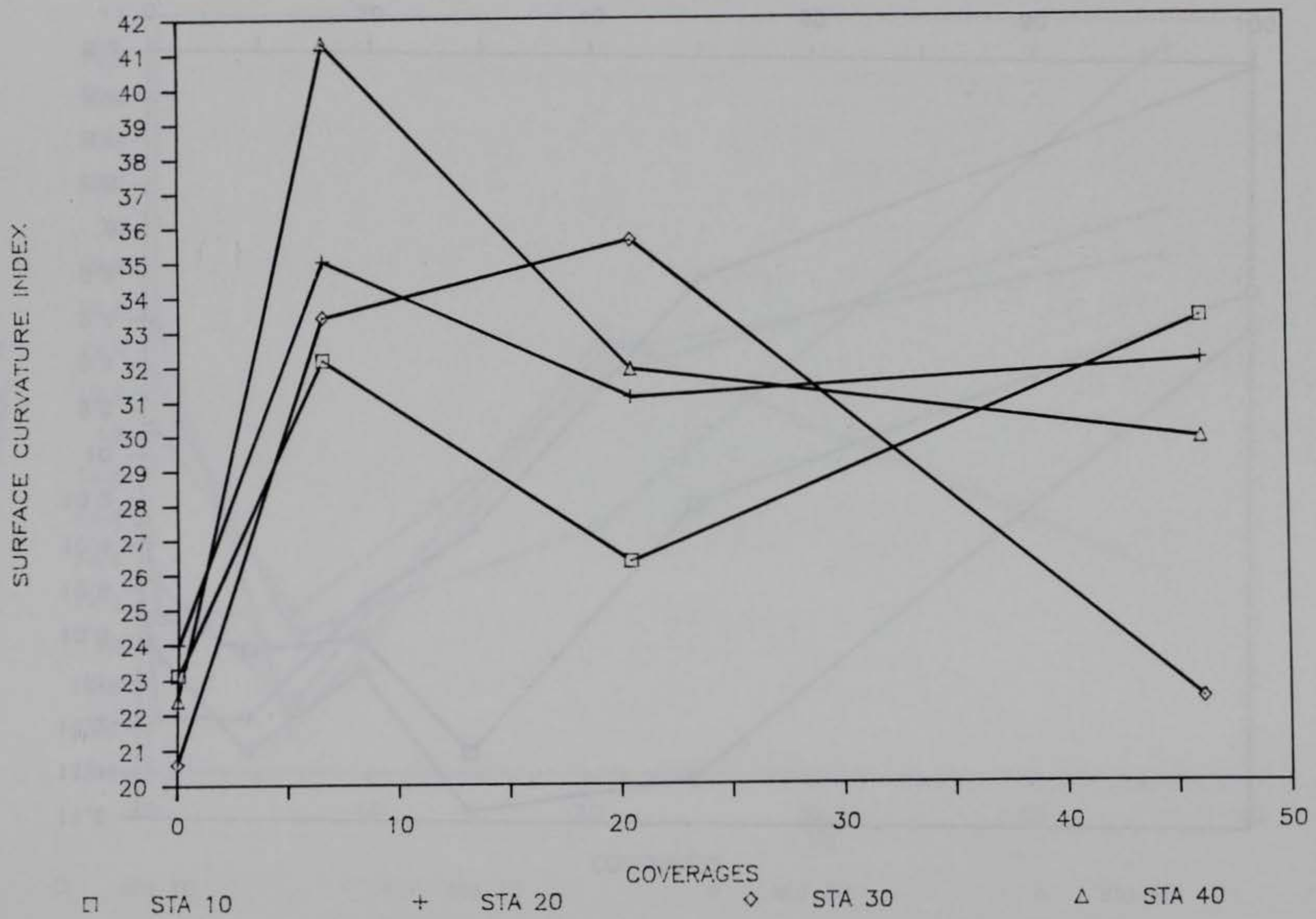


**Figure IV-32. Surface Curvature Index versus Coverages for WES1 Item.**

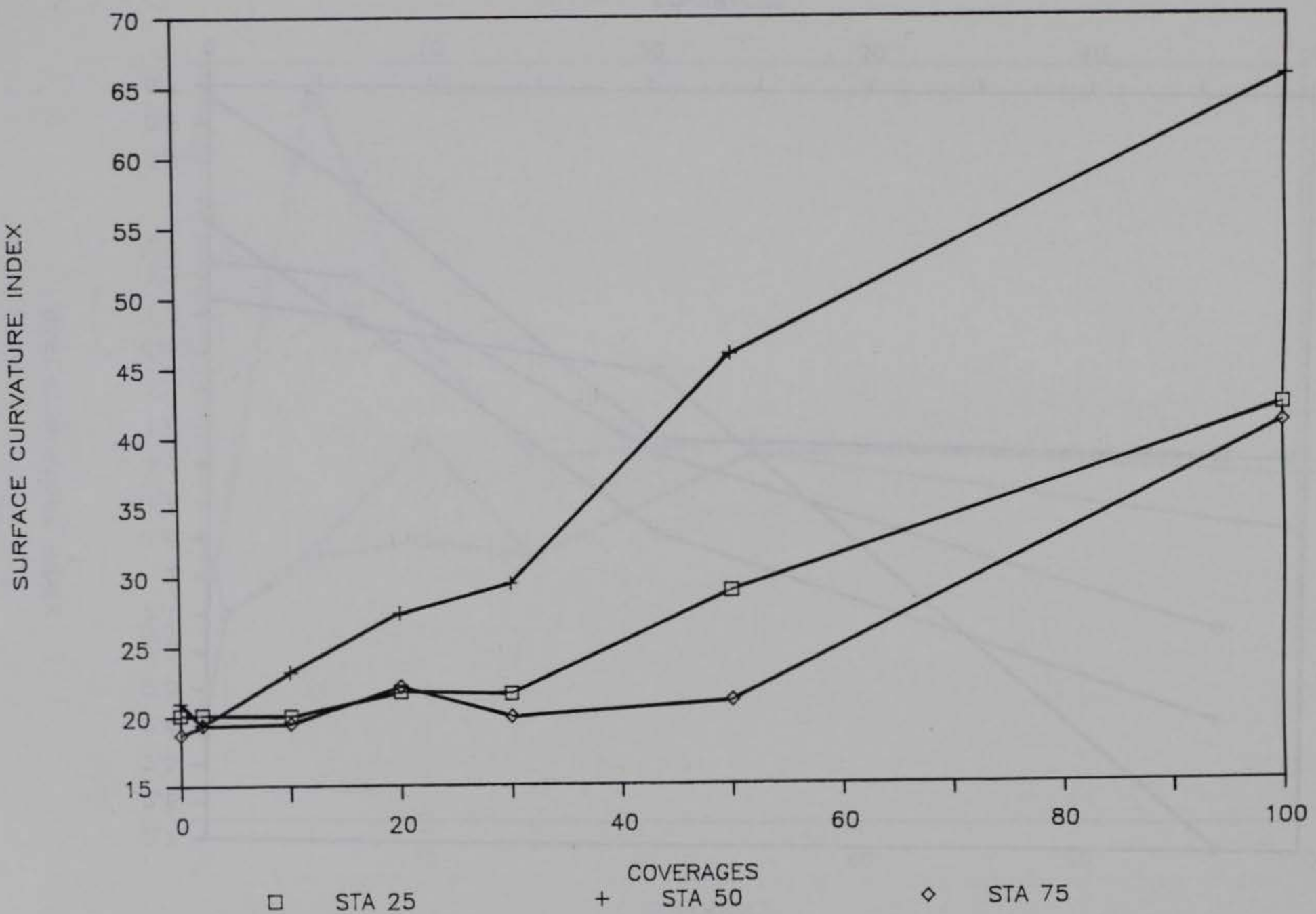


**Figure IV-33. Surface Curvature Index versus Coverages for NFF4 Item.**

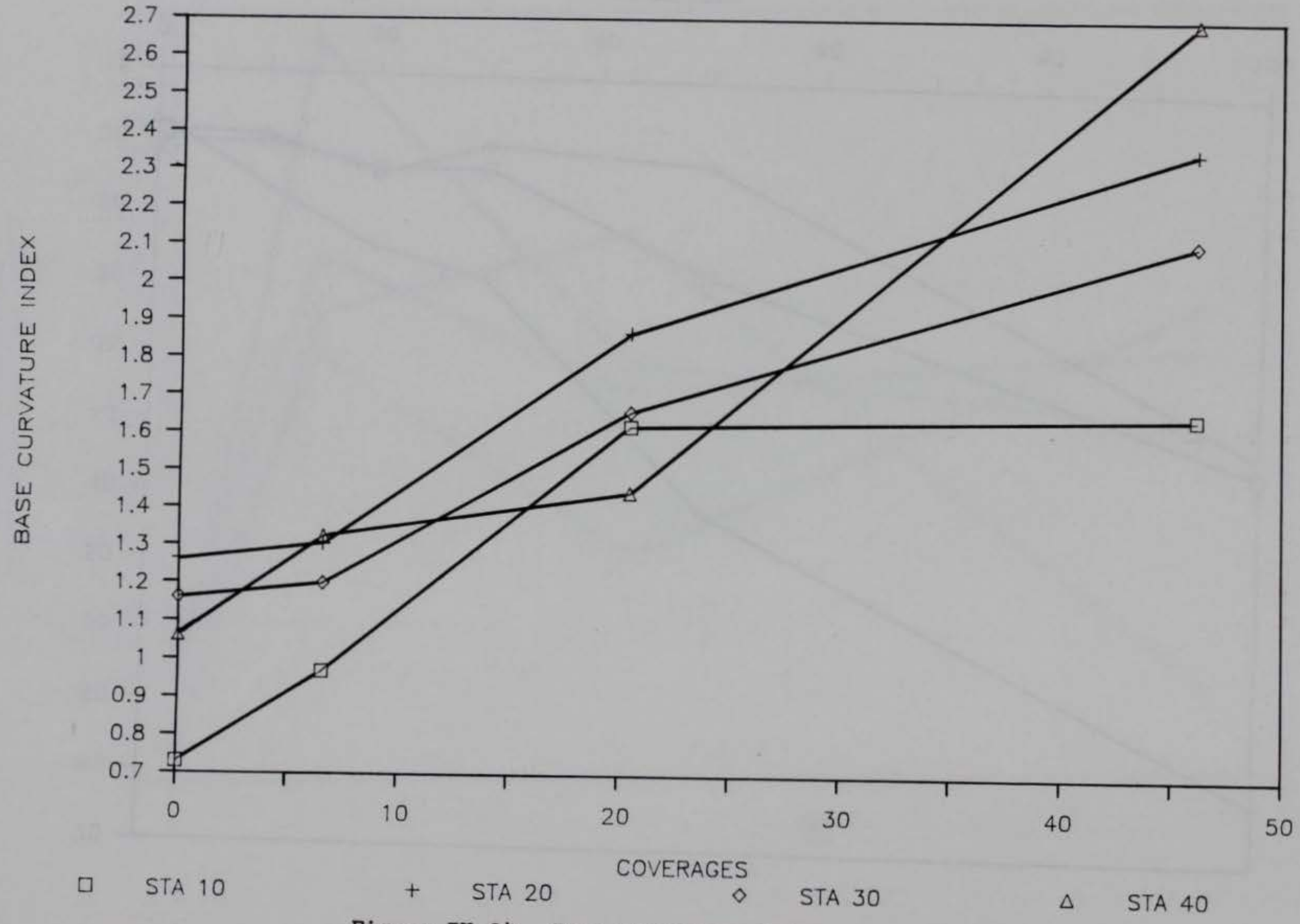


**Figure IV-34. Base Curvature Index versus Coverages for WES1 Item.**

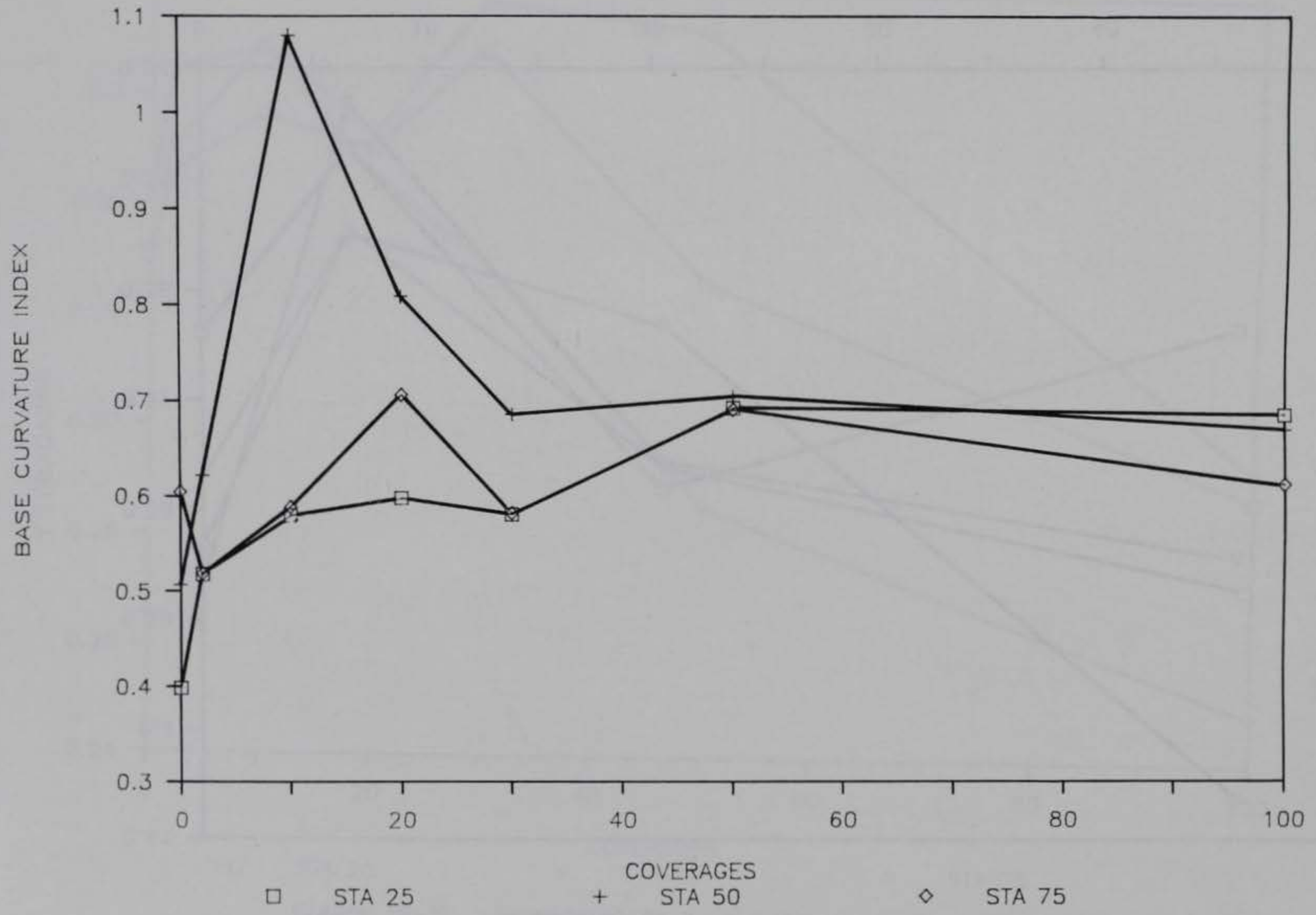


**Figure IV-35. Base Curvature Index versus Coverages for NFF4 Item.**

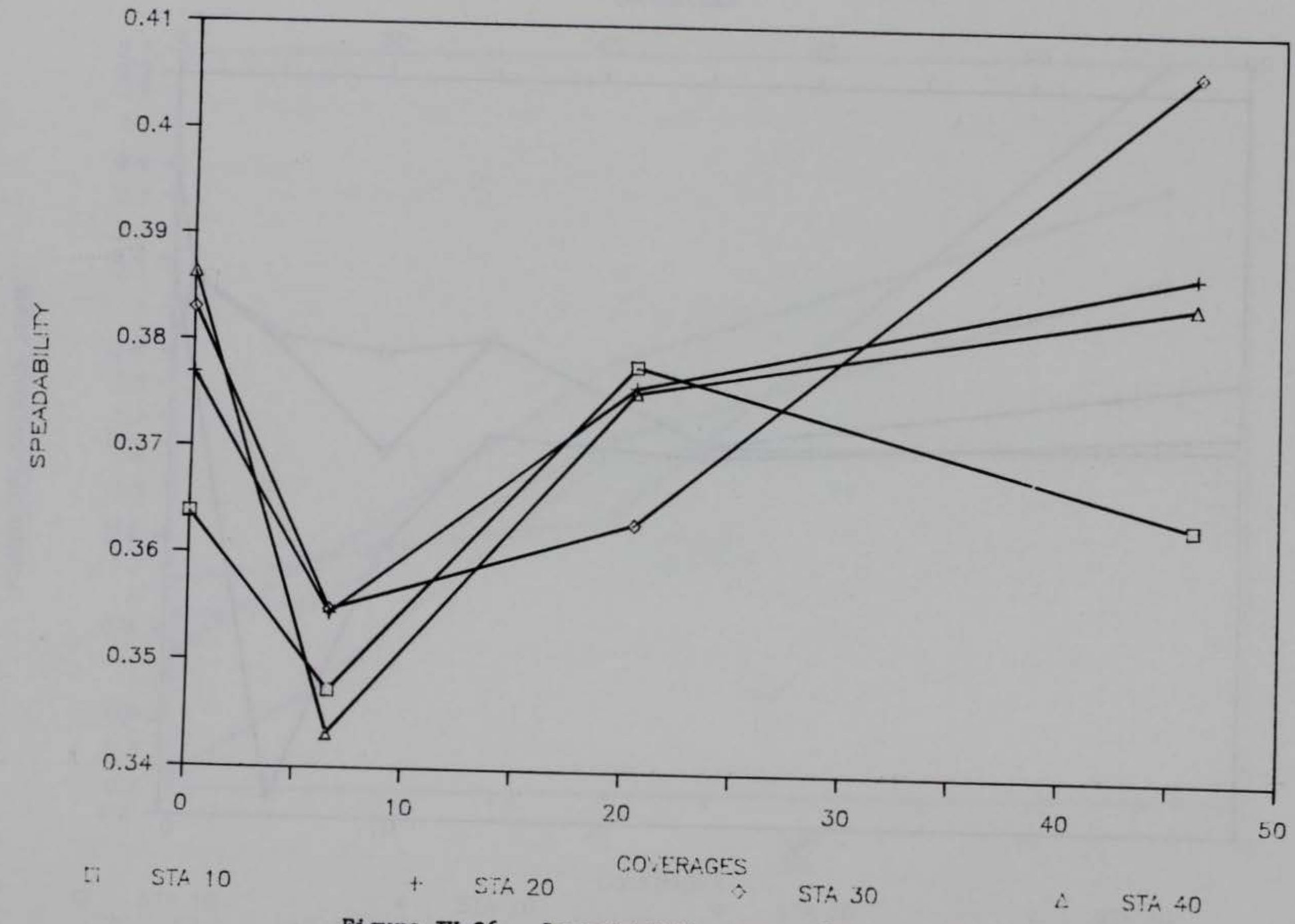


**Figure IV-36. Spreadability versus Coverages for WES1 Item.**

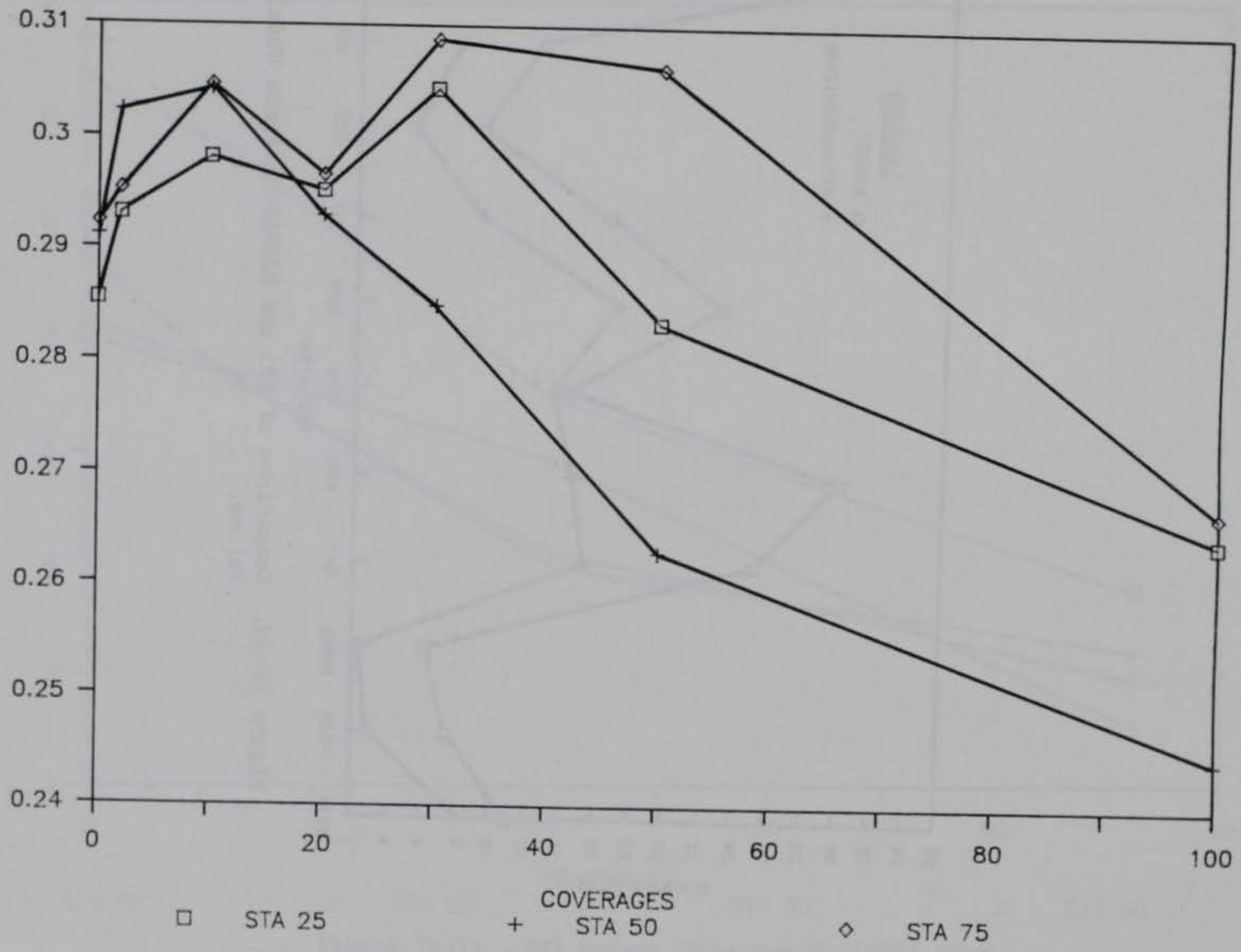


**Figure IV-37. Spreadability versus Coverages for NFF4 Item.**

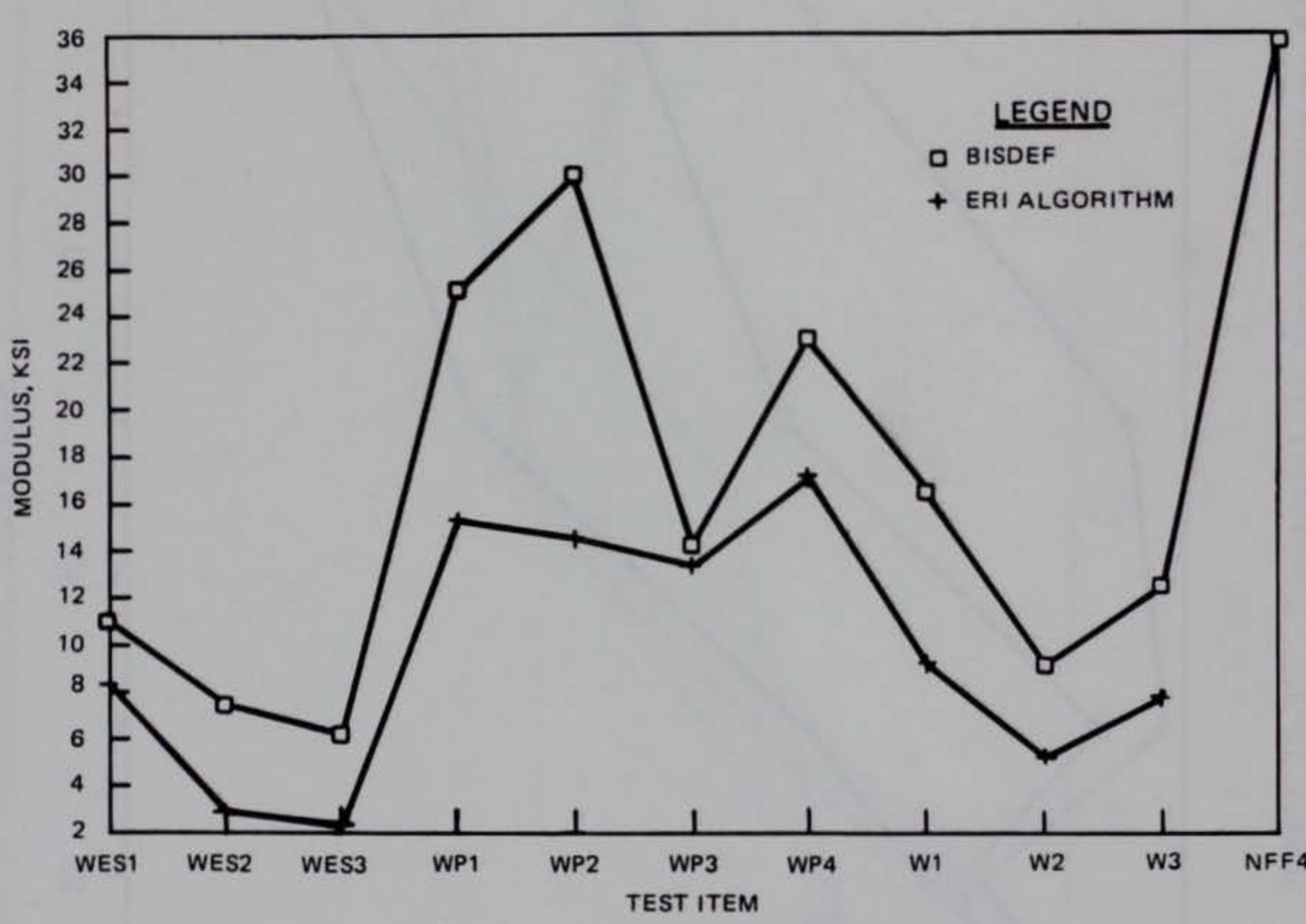


Figure IV-38. Comparison of ERI and BISDEF Subgrade Modulus Values.

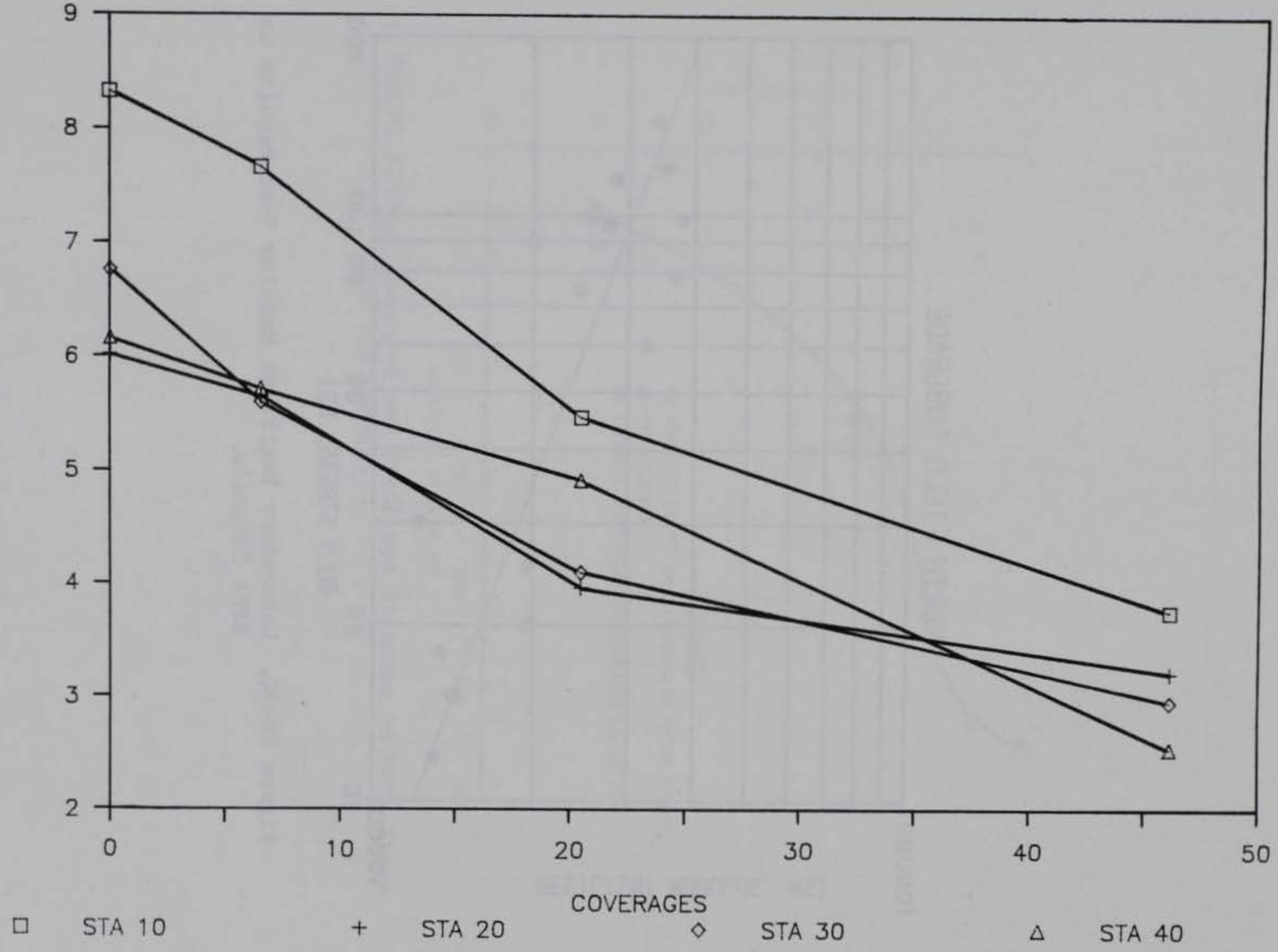


**Figure IV-39. ERI versus Coverages for WES1 Item.**

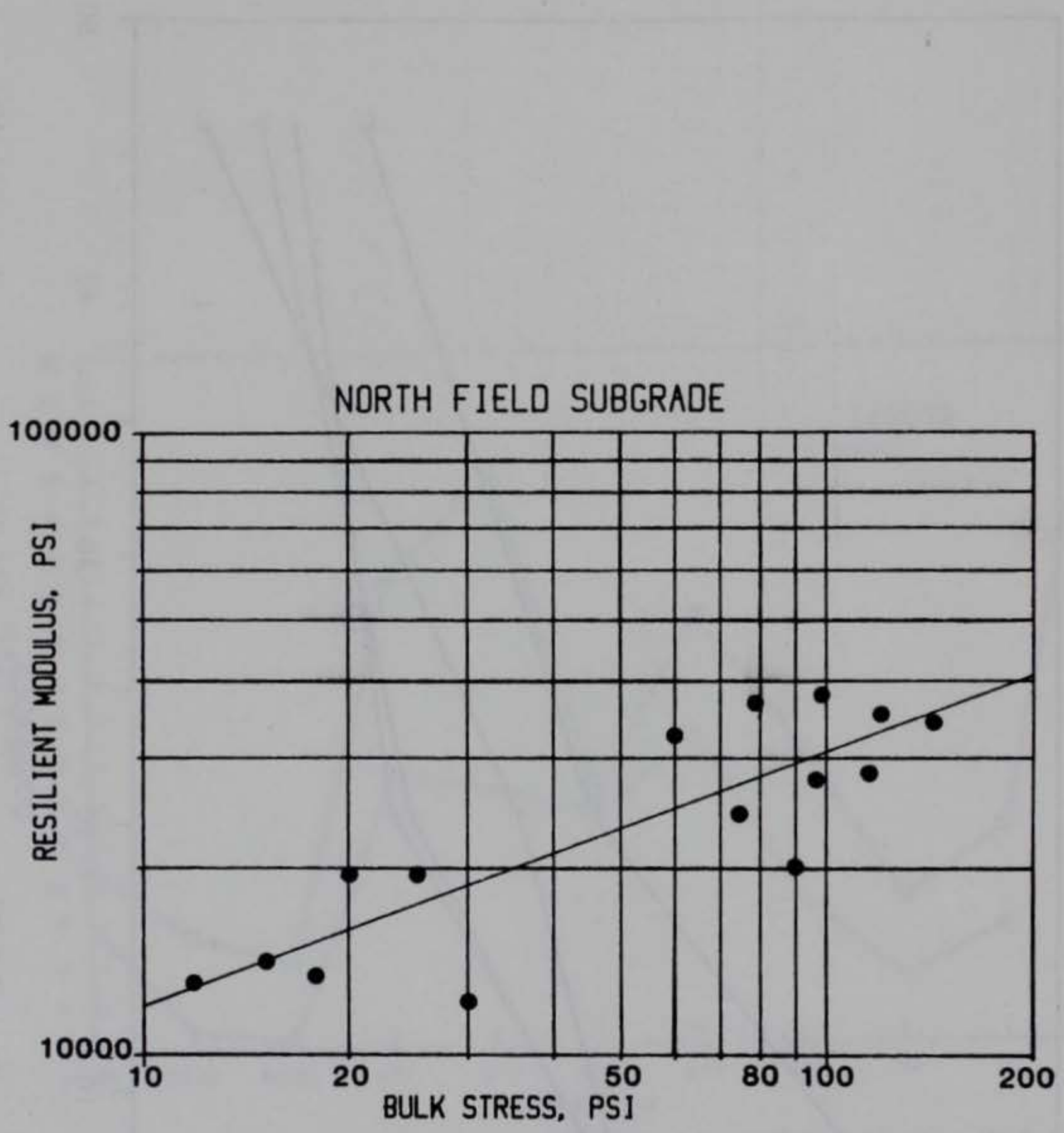


Figure IV-40. Laboratory Resilient Modulus Test Results on NFF4 Subgrade.

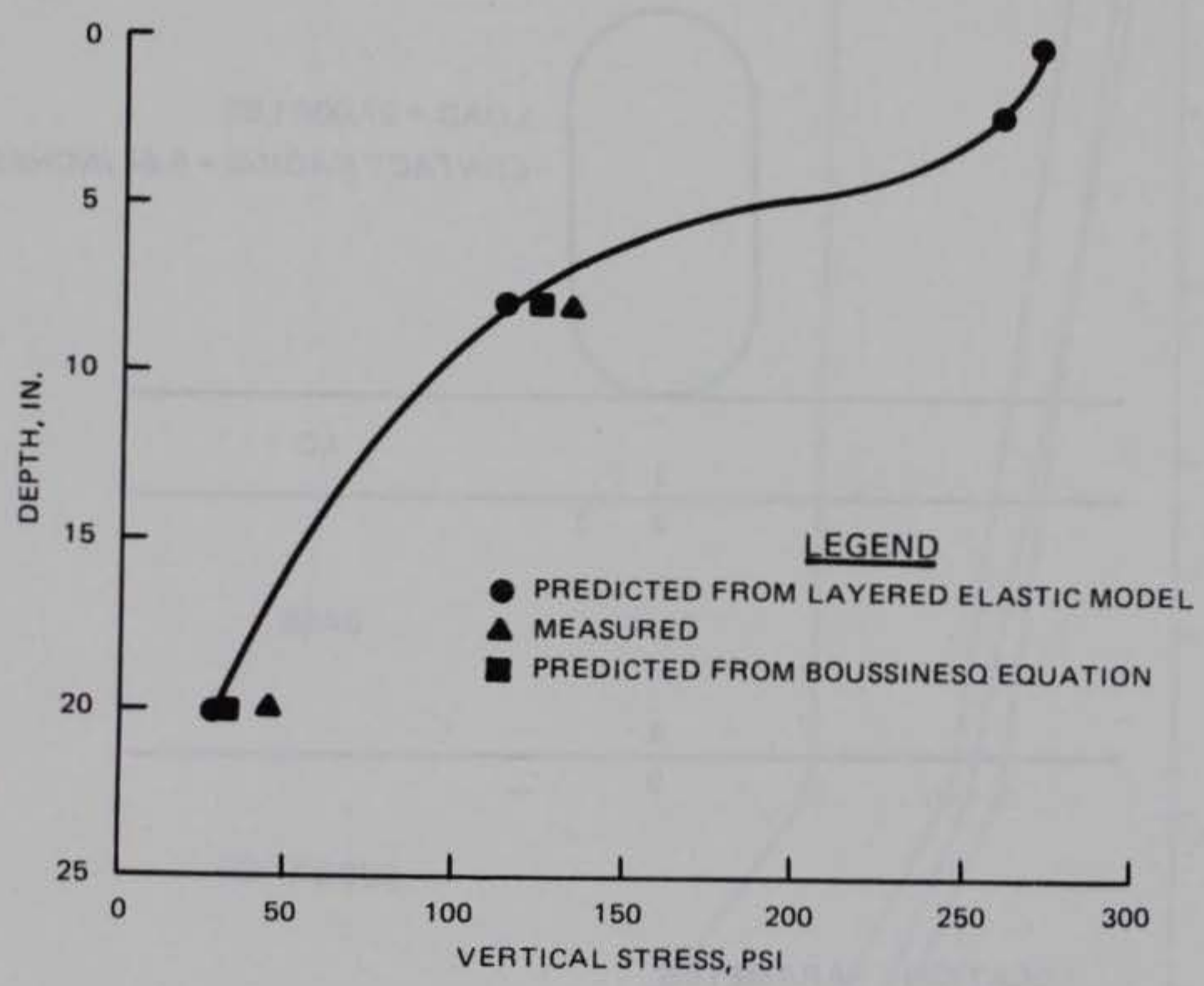


Figure IV-41. Measured and Predicted Stresses on NFF4 Items for F-4 Loading.

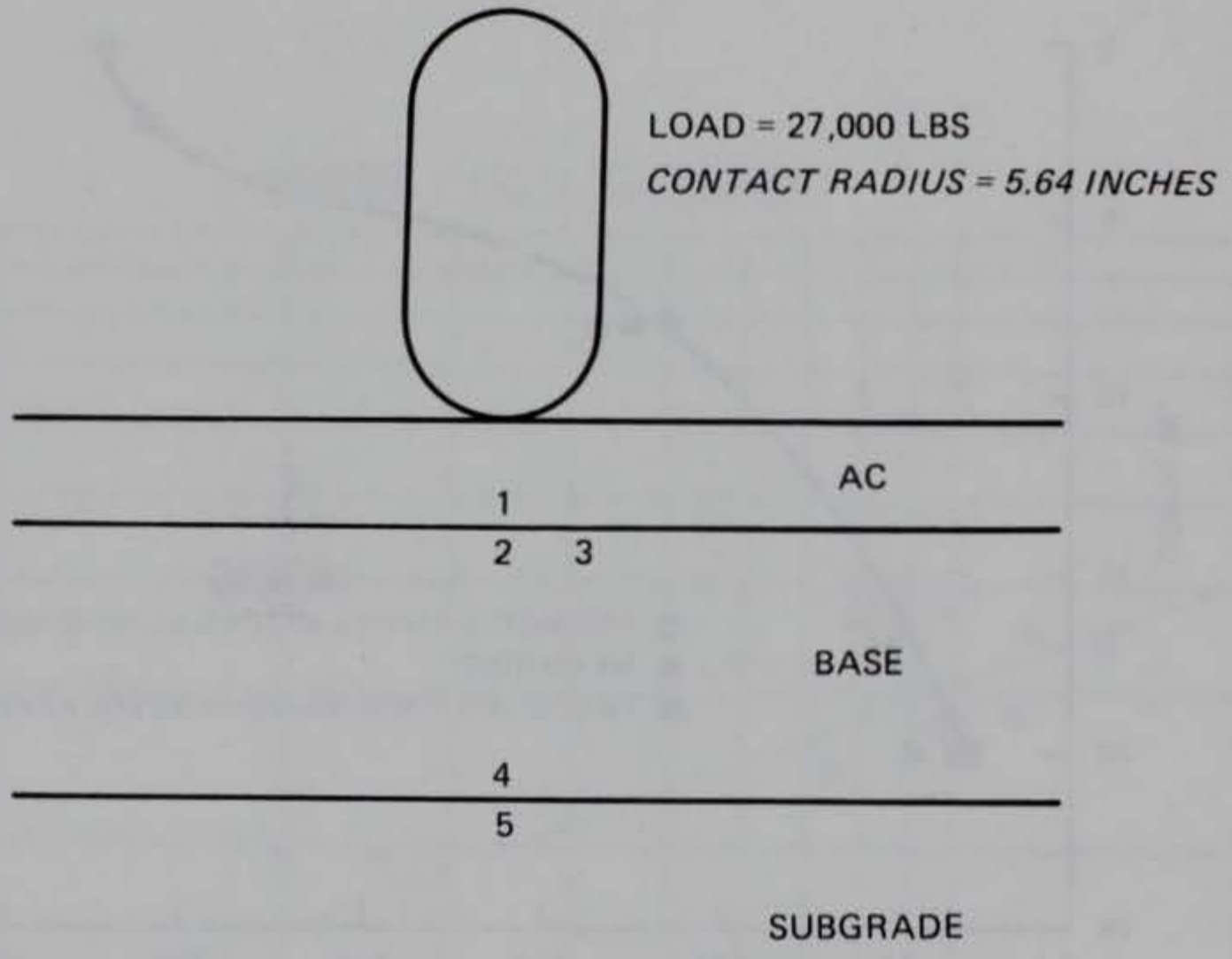


LOCATION PARAMETER

1 TENSILE STRAIN IN AC
2 VERTICAL STRESS AND STRAIN IN BASE
3 SHEAR STRESS IN BASE
4 TENSILES STRAIN IN BASE
5 VERTICAL STRESS AND STRAIN IN SUBGRADE

**Figure IV-42. Location of Stress and Strain Calculation Points.**

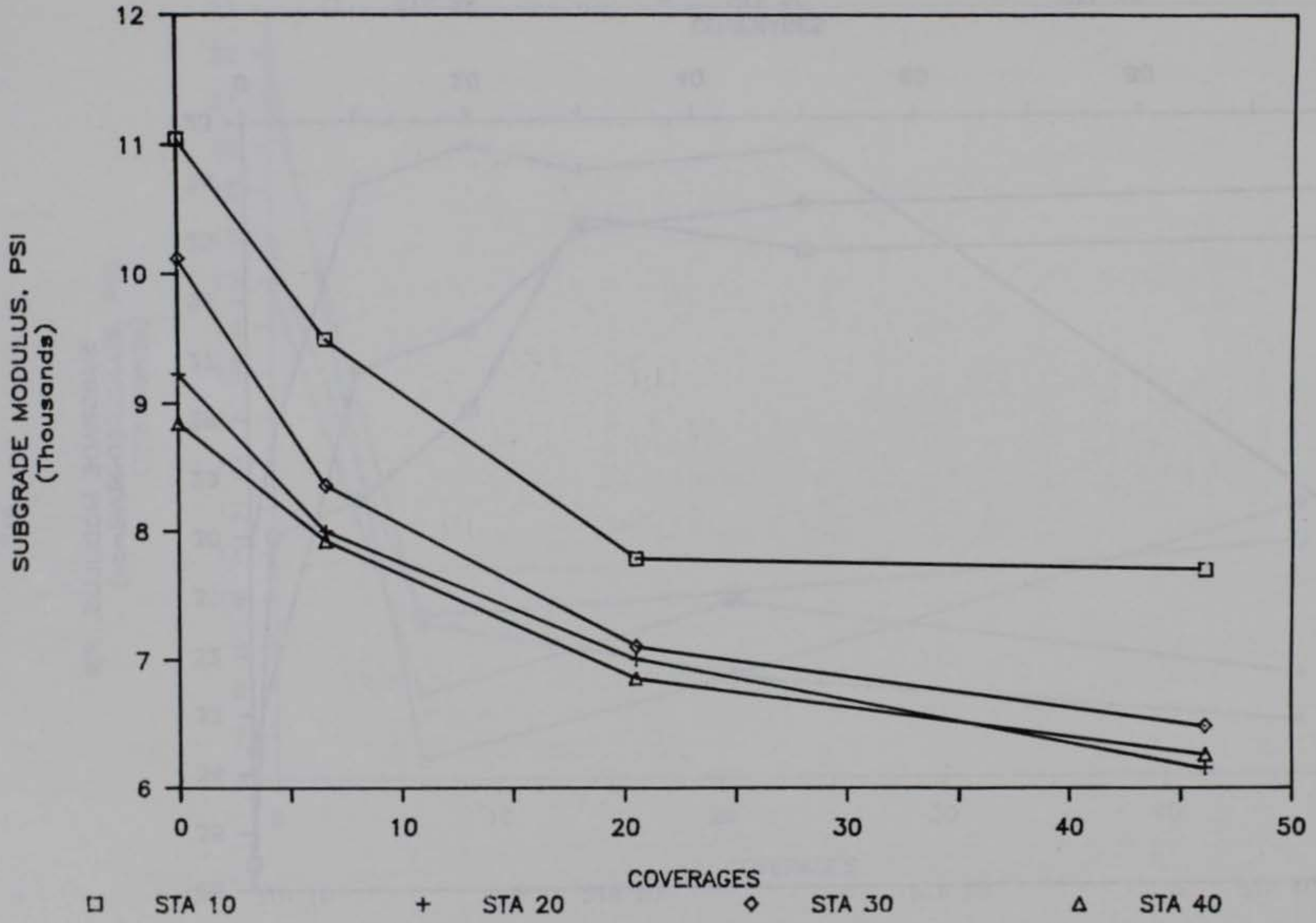


Figure IV-43. Subgrade Modulus versus Coverages for WES1 Item.

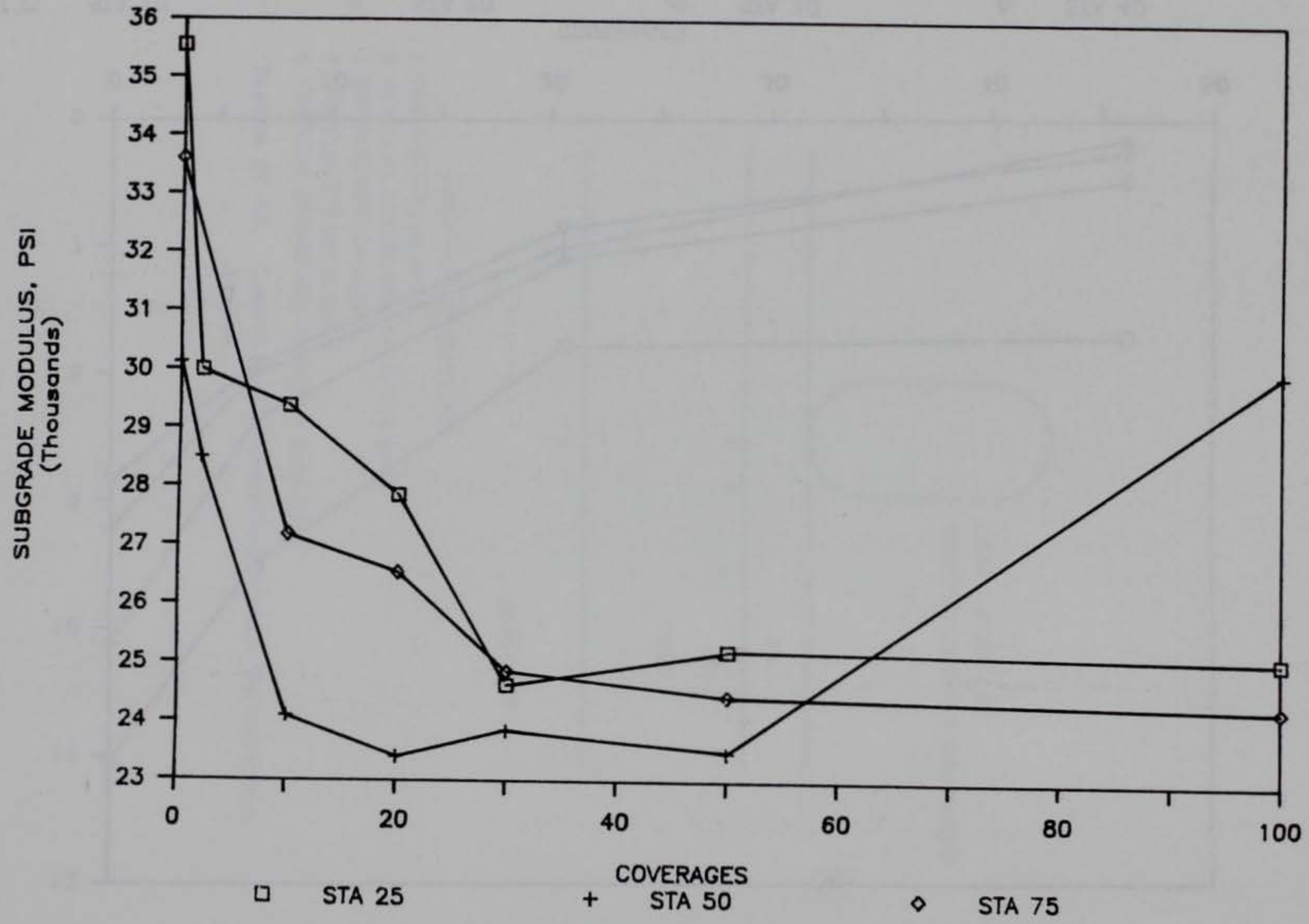


Figure IV-44. Subgrade Modulus versus Coverages for NFF4 Item.

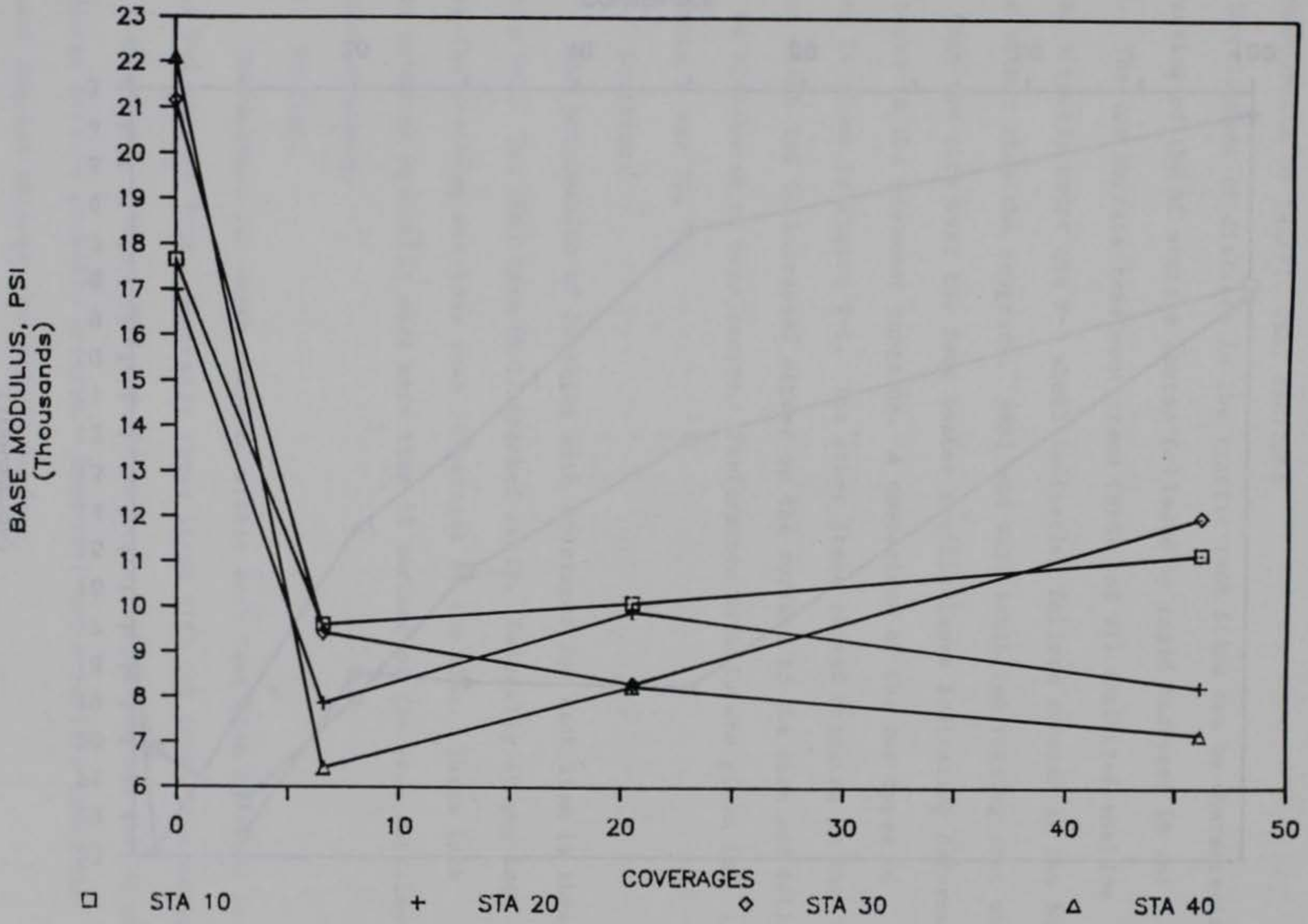


Figure IV-45. Base Modulus versus Coverages for WES1 Item.

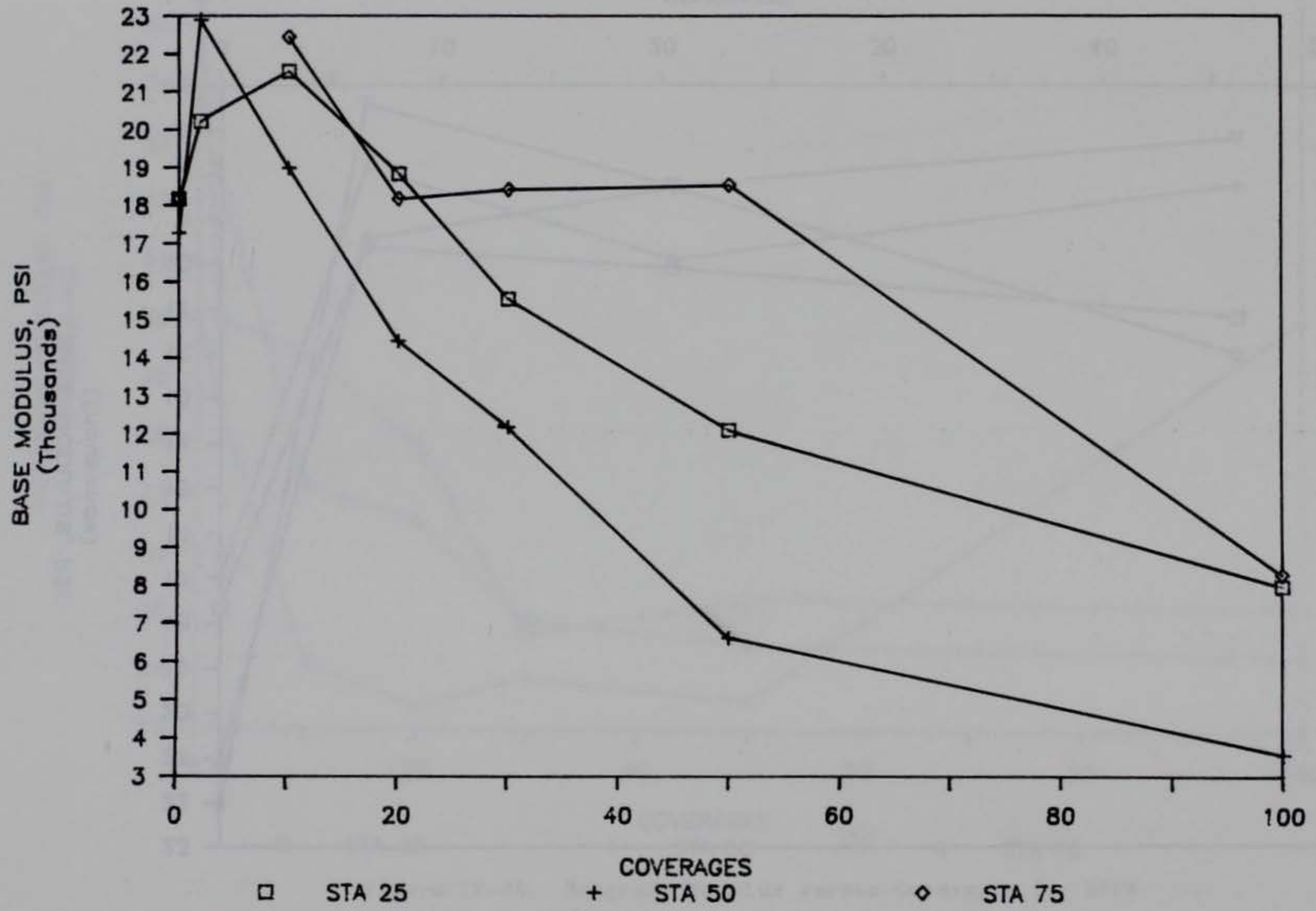


Figure IV-46. Base Modulus versus Coverages for NFF4 Item.

## SECTION V

## ANALYSIS OF PERFORMANCE OF TRAFFIC TEST ITEMS

### A. PERFORMANCE OF TRAFFIC TEST SECTIONS

Development of distress in the traffic test items can be characterized by cracking of the AC surface course followed by rapid increase in rut depth. The two surface treatment items (WES3 and W1) exhibited shallow rutting directly under the F-4 wheel indicating failure occured in the base course rather than the subgrade. WES1 and WES2 exhibited rutting that was wider than the tire over the four center traffic lanes indicating deformation lower in the pavement subgrade. A comparison of the two types of rutting is shown in Figure V-1. The other items showed cracking in the surface which led to increased stress on the surface of the base and failure could be attributed to base course. Performance details are given in References 6 and 10.

1. Cracking.

The progression of cracking with coverages for each item is shown in Table V-1. The DBST item (W-1) cracked early. Generally at one inch rutting the cracking was less than 10 percent of the area. Three inch rutting occurred generally when more than 50 percent of the area contained alligator cracking.

2. Rutting.

The maximum rut depth measured within each test item is shown in Figures V-2 through V-11. Generally those items with rut depth/time curves which flatten out, such as NFF4 and WP2 indicate the surface had failed and base course failure probably occured. Item WP-1 had a failure where the load cart punched through the asphalt surface.

B. ESTIMATE OF PERFORMANCE USING CBR PROCEDURE

The CBR procedure is the most extensively used procedure for the design and evaluation of airfield pavements, an assessment of its efficiency in predicting the performance of low volume pavements will be presented. Coverages to a one inch rut depth will be used for comparison.

The base course strengths of the Wright-Patterson and Whiteman pavements were under 80 CBR. Data on the test items are summarized in Table V-2. Gradation curves (Figures III-8 and III-9) for these base courses and densities measured in place indicate that the design specifications were probably met. Therefore, if the measured CBR of the subgrade is used for the evaluation regardless of the measured base course CBR, expected coverages to failure are as shown in Figure V-12. Also presented are the predicted coverages from the evaluation where the base course CBR was considered (i.e., the minimum coverages were selected based on the thickness above each measured CBR). These compare to the actual coverages to failure much closer than the designer would estimate based on subgrade CBR's only. The constructed test sections (NFF4, WES1, WES2, and WES3) also compared to the actual coverages to failure.

From the compaction results, (Figures III-10 through III-16) one concludes the strengths of these base course materials are highly susceptible to moisture content.

C. LAYERED ELASTIC ESTIMATE OF PERFORMANCE

1. Subgrade Vertical Strain

The most common parameter used in design and evaluation of pavements with layered elastic and finite element methods is vertical strain in

the subgrade. Many of the test items failed due to low base course strength as indicated in the CBR procedure analysis.

Chou, et al (Reference 47) presented relationships between vertical strain at the subgrade surface and coverges to failure for single wheel aircraft (Figure V-13). It should be noted that all failures that occurred before 100 coverages were classified as "subgrade not critical before initial failure."

Vertical subgrade strain for the test items as calculated from F-4 loading and modulus values (Table IV-1) backcalculated from FWD results, are presented for comparison in Figure V-14. Subgrade strain is not a good predictor for the test items evaluated in this study since base course failure occurred in most cases. The recommended relationship indicated was selected for analysis. The relationship fits the data better than the Chou, et al relationship and allows some conservatism. The relationship is for extension of the Barker criteria (Reference 35) for the subgrade modulus of 4600 psi. The variation in the data indicates that other criteria must be evaluated for the final estimate of coverages to failure for low volume pavements.

2. Base Course Vertical Strain

Base Course Vertical Strain was investigated as a possible parameter for prediction since the failures for most of these pavements occurred in the base course. A relationship is shown in Figure V-15. The equation for the relationship is as follows.

$$\epsilon_{base} = \frac{15.46}{COV^{0.14458}} \qquad (11)$$

This relationship is a better predictor of performance than subgrade strain for low volume pavements.

D. RUT DEPTH PREDICTIONS

Using the pavement thickness data and CBR data presented in Table V-2 and the Barber equations presented in Section II-B-2 an attempt was made to evaluate the rut depth prediction model. Results are presented in Figure V-16. The model consistantly predicted smaller rut depths than were measured and with a large amount of scatter. An attempt was made to use the form of the equation to develop new coefficients for low volume pavements.

Results of the analysis is as follows:

Dependent variable - Log (Rut Depth)

| Variable | Coefficient |
|---|---|
| Log COV | 0.73058 |
| Log $C_2$ | -0.81735 |
| Log[Log(1.25 Tac + Tbase)] | -3.15362 |
| Log $C_1$ | -0.57708 |

$R^2 = 0.49$

Standard Error = 0.2567

No. of cases = 47

The form as presented in Reference 28 is:

$$RD = 0.151 \left\{ \frac{P_k^{1.3127} \; t_p^{0.0499} \; COV^{0.731}}{\left[\log(1.25\ Tac + Tbase)\right]^{3.15} \; C_1^{0.577} \; C_2^{0.817}} \right\} \quad (12)$$

Standard Error = 0.91; $R^2 = 0.38$; No. of Cases = 47

where

RD = Rut Depth in inches

$P_k$ = Single wheel load, kips

$t_p$ = Tire pressure, PSI

COV = Coverages

Tac = Thickness of asphalt surface, in.

Tbase = Thickness of base course, in.

$C_1$ = CBR of base course

$C_2$ = CBR of subgrade

This model was dismissed because of the low $R^2$(0.38) and high standard error (0.91 inches).

TABLE V-1. RUTTING AND CRACKING PROGRESSION OF TEST ITEMS

| ITEM | COV | MAXIMUM RUT DEPTH, IN. | % OF AREA CRACKING |
|---|---|---|---|
| WES1 | 13.1 | 0.50 | -- |
| | 16.4 | 0.75 | 5.0 |
| | 18.6 | 1.00 | 21.0 |
| | 20.5 | 1.25 | 28.0 |
| | 22.9 | 1.50 | 48.0 |
| | 26.2 | 1.75 | 72.0 |
| | 29.5 | 2.00 | 80.0 |
| | 32.7 | 2.00 | 95.0 |
| | 36.0 | 2.25 | 95.0 |
| | 39.3 | 2.25 | 95.0 |
| | 42.6 | 2.50 | 95.0 |
| | 45.8 | 2.50 | 95.0 |
| | 46.1 | 3.75 | 95.0 |
| WES2 | 6.6 | 0.25 | -- |
| | 13.1 | 0.50 | 7.0 |
| | 16.4 | 2.00 | 14.0 |
| | 18.6 | 2.00 | 57.0 |
| | 19.7 | 2.25 | 57.0 |
| | 20.5 | 3.00 | -- |
| WES3 | 6.5 | 3.00 | 100.0 |
| WP1 | -- | -- | -- |
| | 6.0 | -- | 6.0 |

TABLE V-1. RUTTING AND CRACKING PROGRESSION OF TEST ITEMS (CONTINUED)

| ITEM | COV | MAXIMUM RUT DEPTH, IN. | % OF AREA CRACKING |
|---|---|---|---|
| WP2 | -- | -- | -- |
| | 7.0 | 0.25 | 0.6 |
| | 33.0 | 0.50 | 4.0 |
| | 46.0 | 1.50 | 15.0 |
| | 66.0 | 2.00 | 17.8 |
| | 72.0 | 2.75 | -- |
| | 88.0 | 3.50 | 51.0 |
| WP3 | 0.0 | -- | -- |
| | 7.0 | 1.125 | -- |
| | 8.0 | 1.25 | 0.6 |
| | 12.0 | 3.50 | 52.0 |
| WP4 | 7.0 | -- | 3.3 |
| | 16.0 | -- | 19.5 |
| | 20.0 | 2.25 | -- |
| | 22.0 | 3.50 | 65.0 |
| W1 | 7.0 | -- | 4.5 |
| | 14.0 | 1.75 | 100.0 |
| | 17.0 | 2.00 | -- |
| | 20.0 | -- | -- |
| | 30.0 | 2.50 | -- |
| | 34.0 | 2.75 | -- |
| | 38.0 | 3.00 | -- |

TABLE V-1. RUTTING AND CRACKING PROGRESSION OF TEST ITEMS (CONTINUED)

| ITEM | COV | MAXIMUM RUT DEPTH, IN. | % OF AREA CRACKING |
|---|---|---|---|
| W2 | 7.0 | -- | 3.0 |
| | 14.0 | 1.75 | 27.0 |
| | 18.0 | 3.75 | 100.0 |
| W3 | 0.0 | -- | -- |
| | 7.0 | 2.25 | 70.0 |
| | 12.0 | 3.50 | 75.0 |
| NFF4 | 10.0 | 0.75 | 2.8 |
| | 20.0 | 0.75 | 6.0 |
| | 30.0 | 1.00 | 6.9 |
| | 40.0 | 1.25 | 7.0 |
| | 50.0 | 2.25 | 16.4 |
| | 60.0 | 2.50 | 36.0 |
| | 80.0 | 2.75 | -- |
| | 90.0 | 2.937 | 69.0 |
| | 100.0 | 4.00 | 78.0 |

TABLE V-2. SUMMARY OF CHARACTERISTICS OF TRAFFIC TEST ITEMS

| Item | Surface | | Base | | | Subgrade | | Total Thickness inches | Maximum 1-inch rut | | Maximum 3-inch rut | |
|---|---|---|---|---|---|---|---|---|---|---|---|---|
| | Type[a] | Thickness inches | Type[b] | Thickness inches | CBR | Type[b] | CBR | | Passes | Coverages | Passes | Coverages |
| WES-1 | AC | 1.7 | GW | 8.2 | 100 | CH | 6.6 | 9.9 | 150 | 20.5 | 338 | 46.1 |
| WES-2 | AC | 1.4 | GW | 9.0 | 100 | CH | 6.3 | 10.4 | 120 | 16.3 | 150 | 20.5 |
| WES-3 | DBST | 0.5 | GW | 9.4 | 100 | CH | 6.0 | 9.9 | 12 | 1.6 | 48 | 6.5 |
| WP-1 | AC | 3.0 | GW | 6.0 | 12 | -- | --- | 3.0 | 39 | 5.3 | 44 | 6.0 |
| WP-2 | AC | 3.0 | GP-GC | 47.0 | 33 | -- | --- | 3.0 | 400 | 54.5 | 643 | 87.7 |
| WP-3 | AC | 2.0 | GP | 12.0 | 33 | SC | 7.0 | 2.0 | 60 | 8.2 | 90 | 12.3 |
| WP-4 | AC | 2.0 | GW-GM | 12.0 | 72 | SC | 8.0 | 2.0 | 100 | 13.6 | 162 | 22.1 |
| W-1 | DBST | 1.0 | GC | 29.0 | 33 | -- | --- | 1.0 | 105 | 14.3 | 280 | 38.2 |
| W-2 | AC | 2.5 | GC | 12.0 | 102 | CH | 4.2 | 14.5 | 25 | 3.4 | 132 | 18.0 |
| W-3 | AC | 2.5 | GC | 16.0 | 37 | CL | 4.2 | 2.5 | 33 | 4.5 | 86 | 11.7 |
| NFACF4 | AC | 2.1 | GM | 6.3 | 100 | AP-AM | 20.0 | 8.4 | 220 | 30.0 | 682 | 93.0 |

[a]AC = asphaltic concrete; DBST = double bituminous surface treatment.
[b]Classified according to the Unified Soil Classification System.

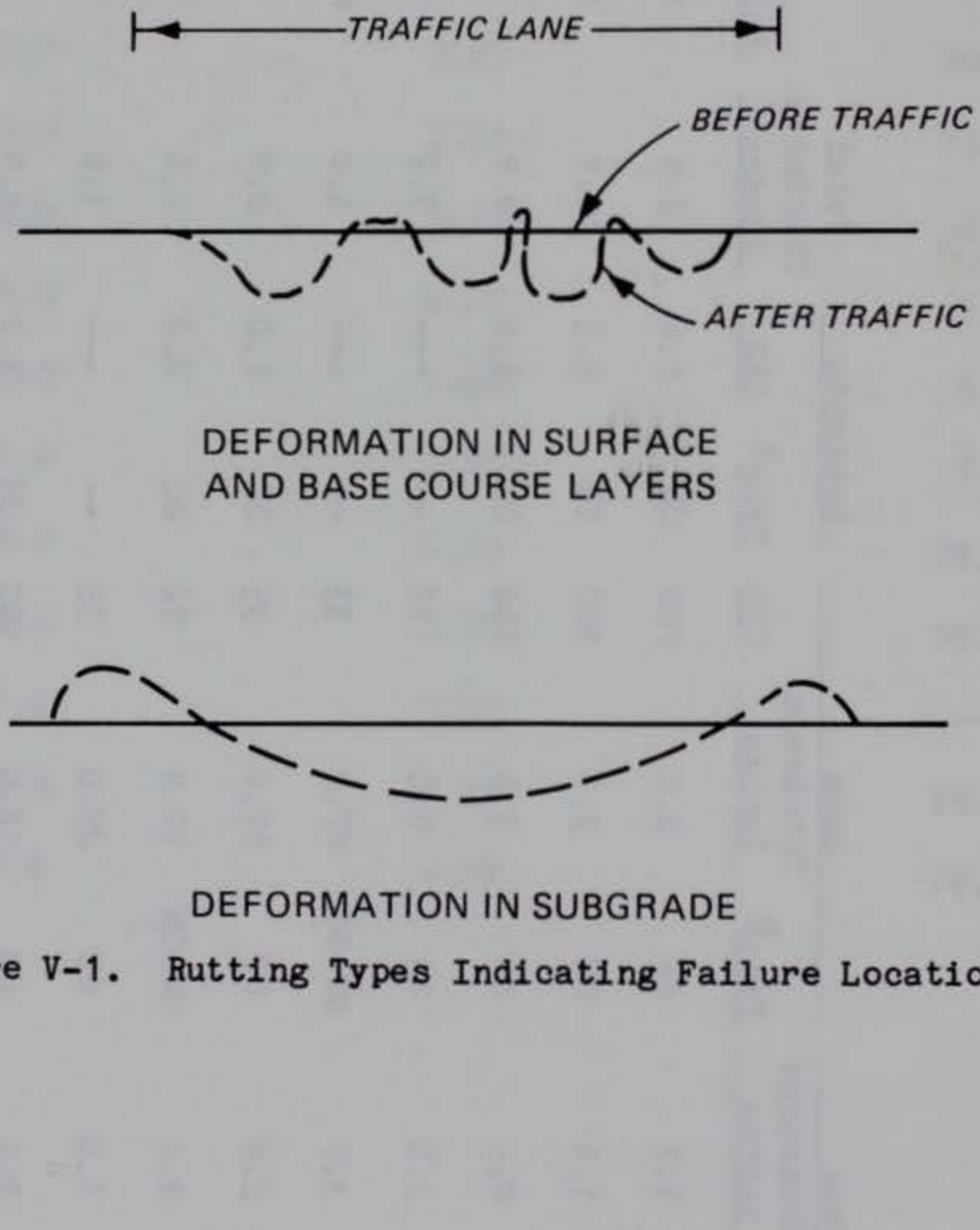


Figure V-1. Rutting Types Indicating Failure Location.

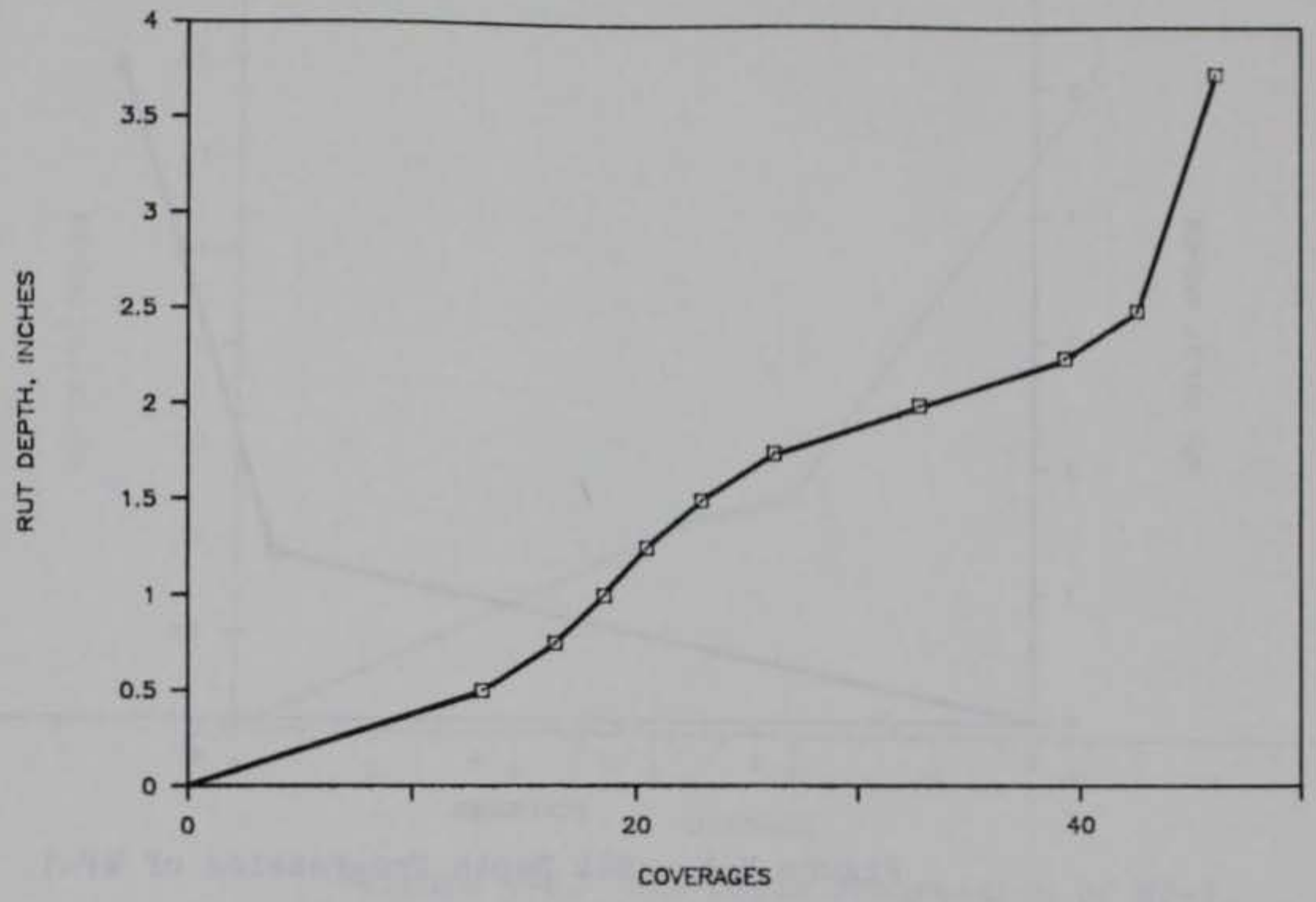


Figure V-2. Rut Depth Progression of WES1.

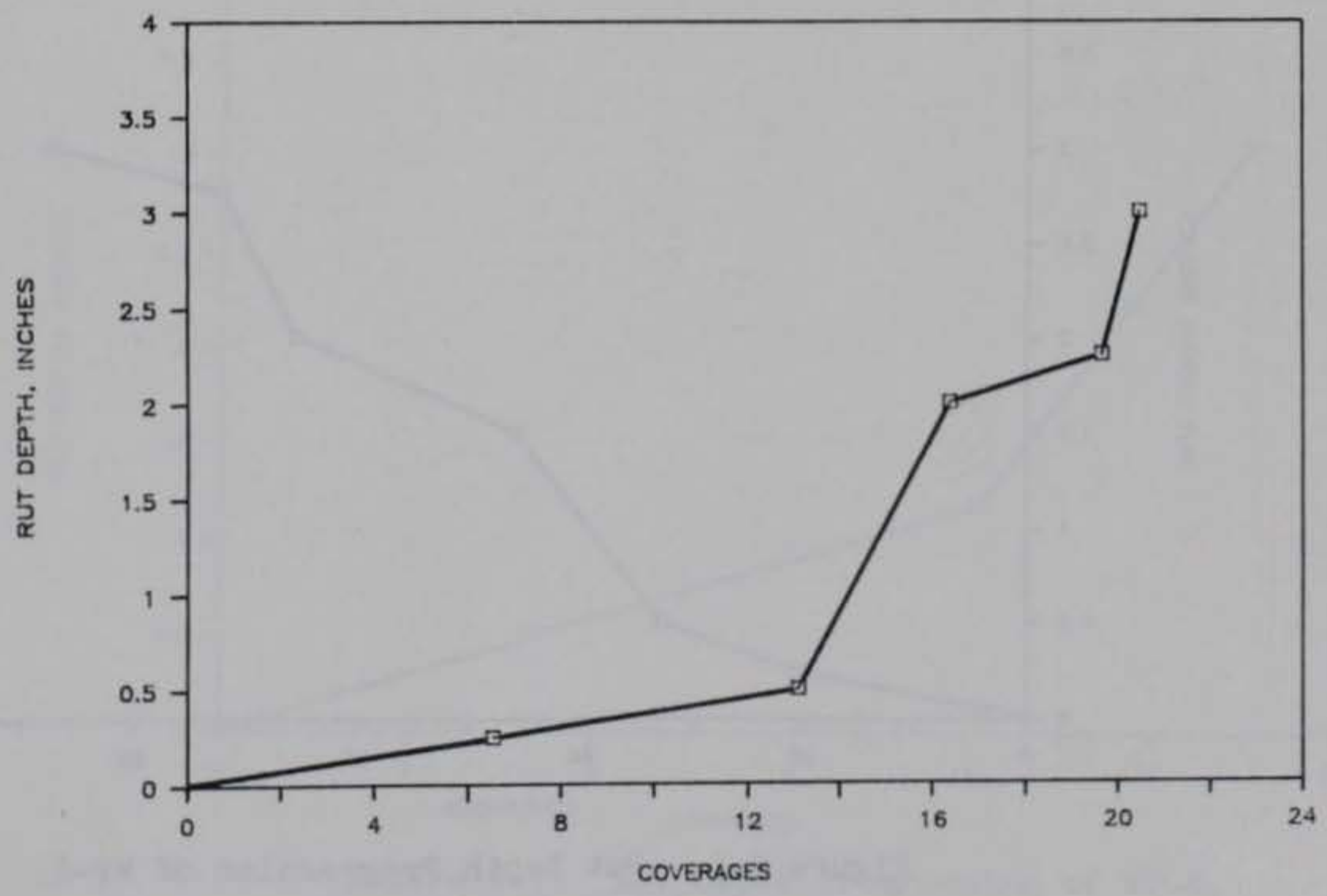


Figure V-3. Rut Depth Progression of WES2.

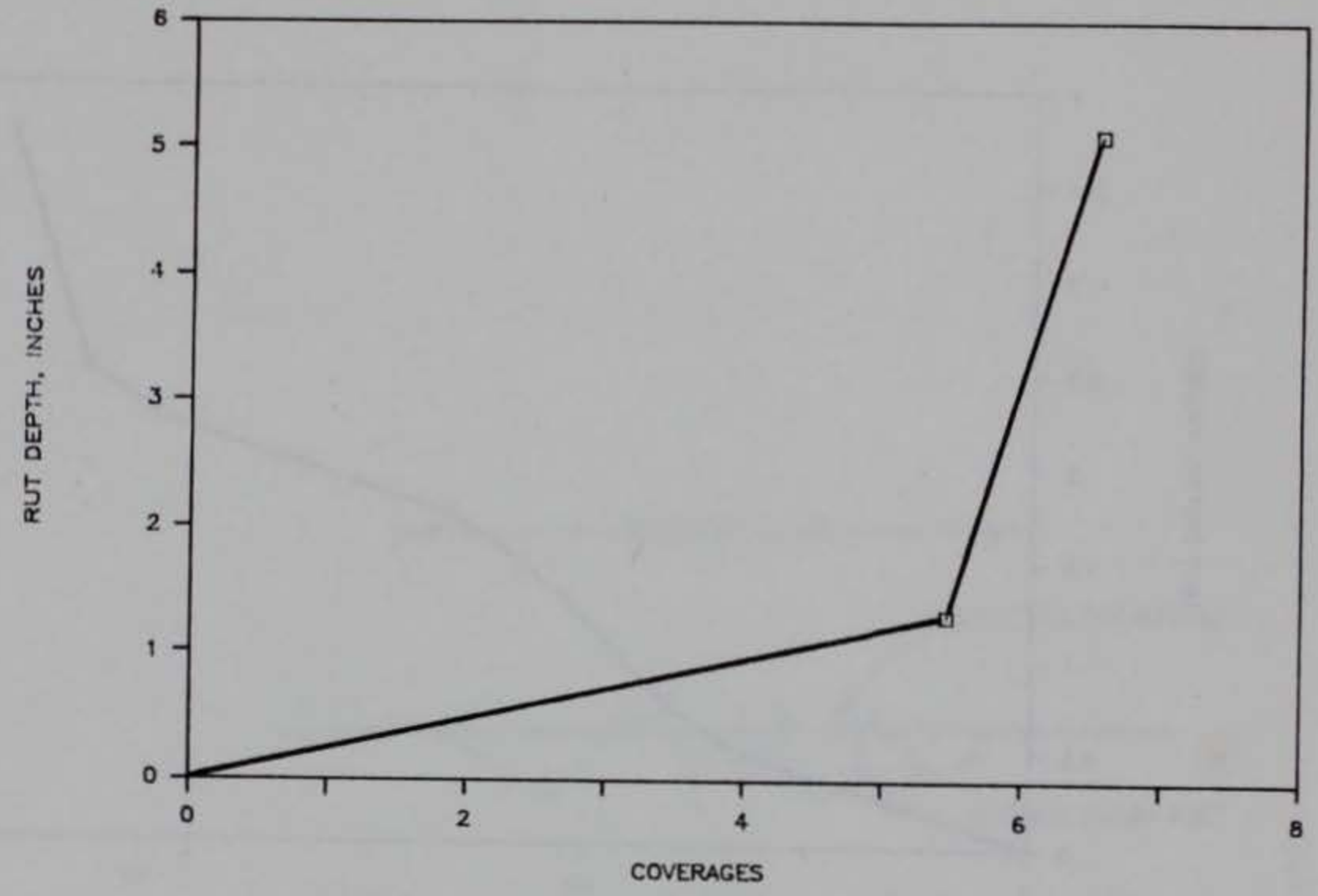


Figure V-4. Rut Depth Progression of WP-1.

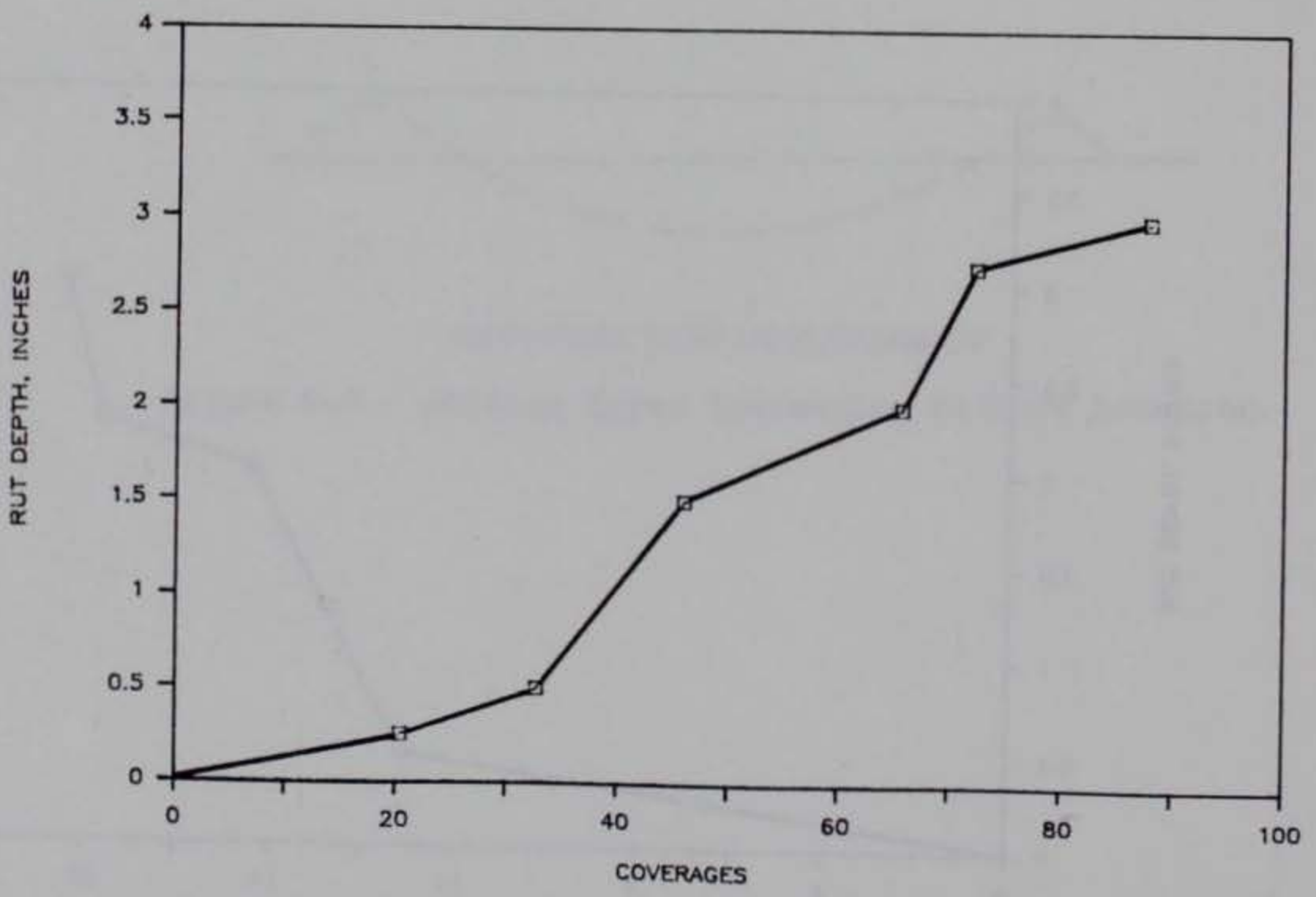


Figure V-5. Rut Depth Progression of WP-2.

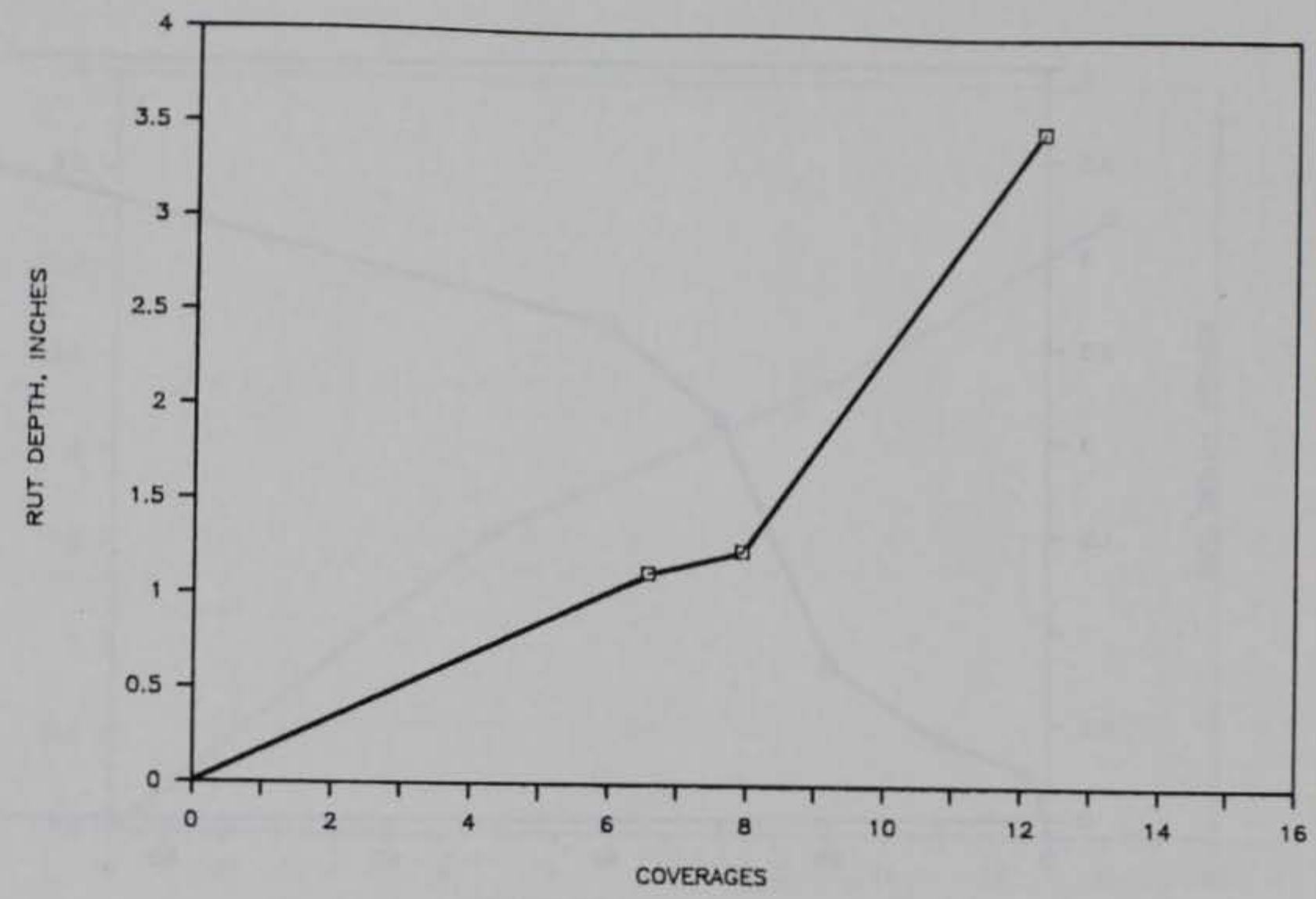


Figure V-6. Rut Depth Progression of WP-3.

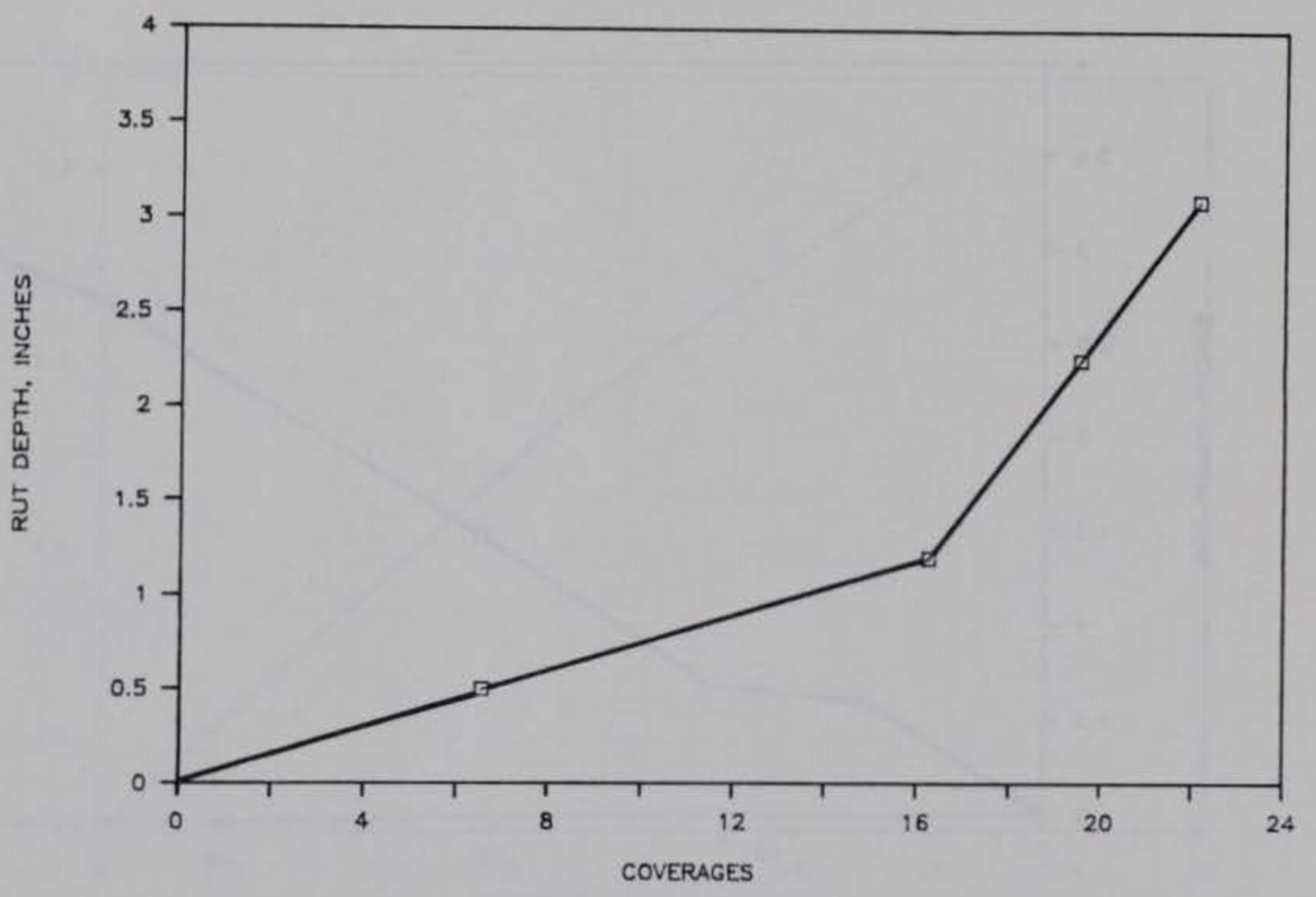


Figure V-7. Rut Depth Progression of WP-4.

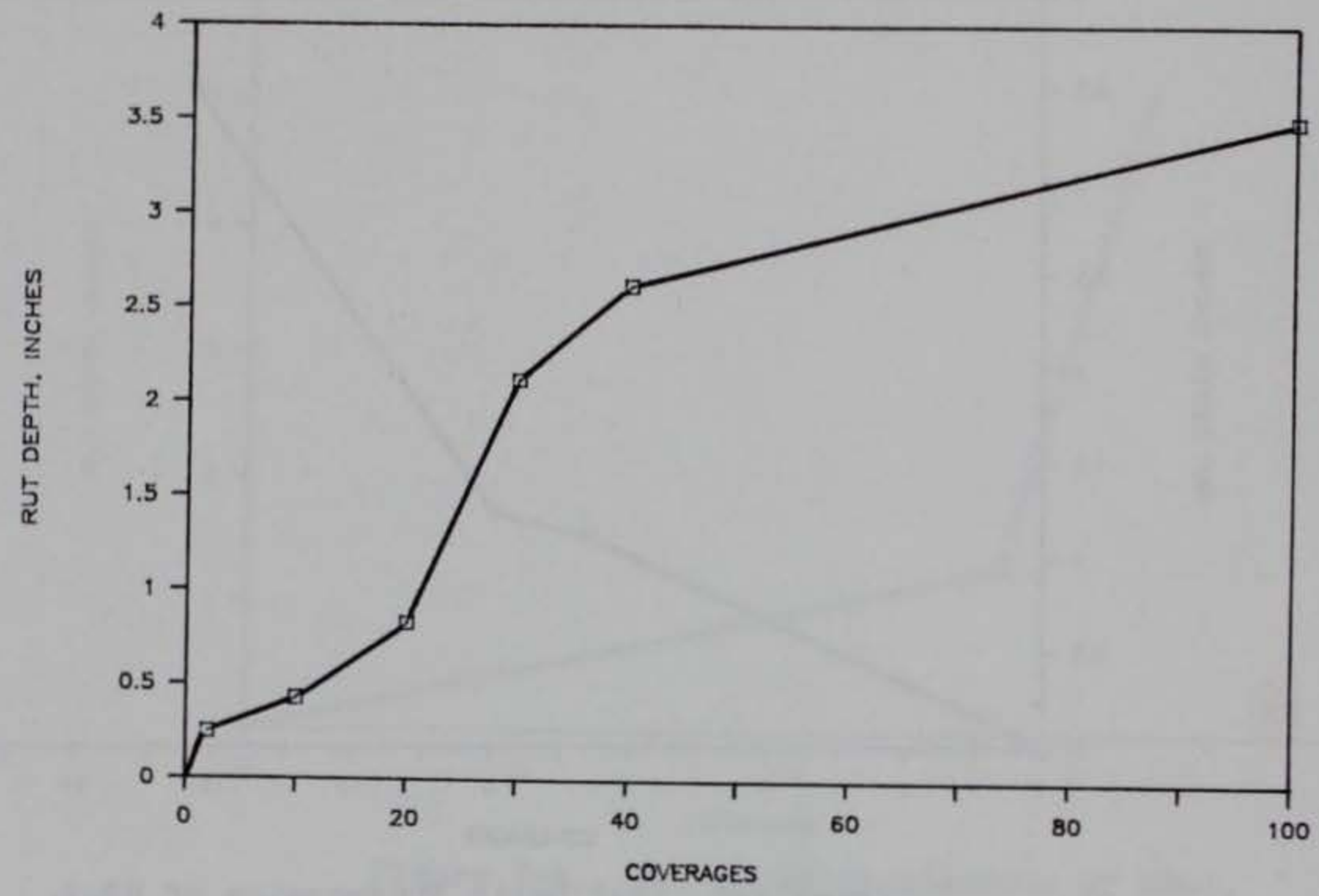


Figure V-8. Rut Depth Progression of NFF4.

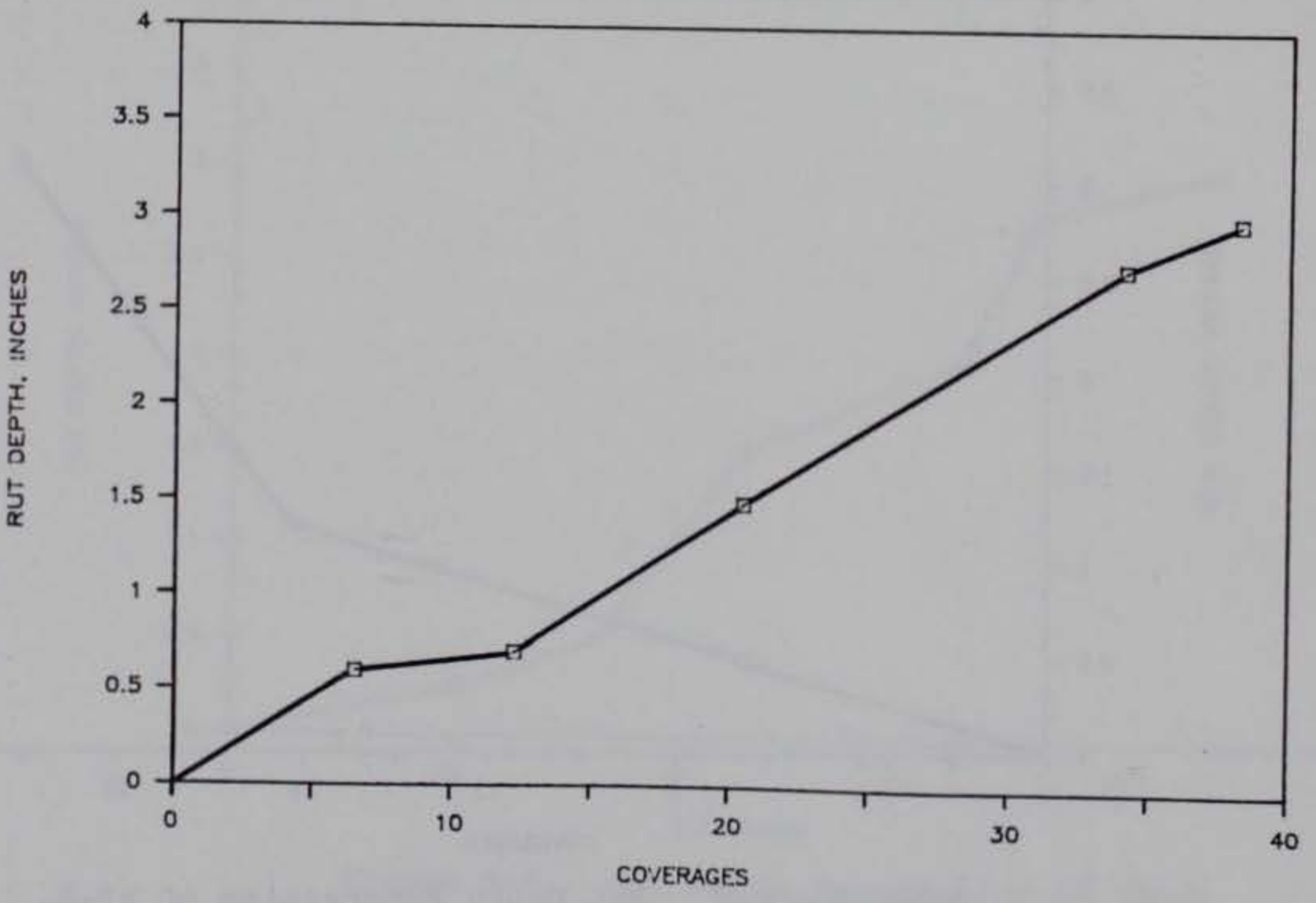


Figure V-9. Rut Depth Progression of W1.

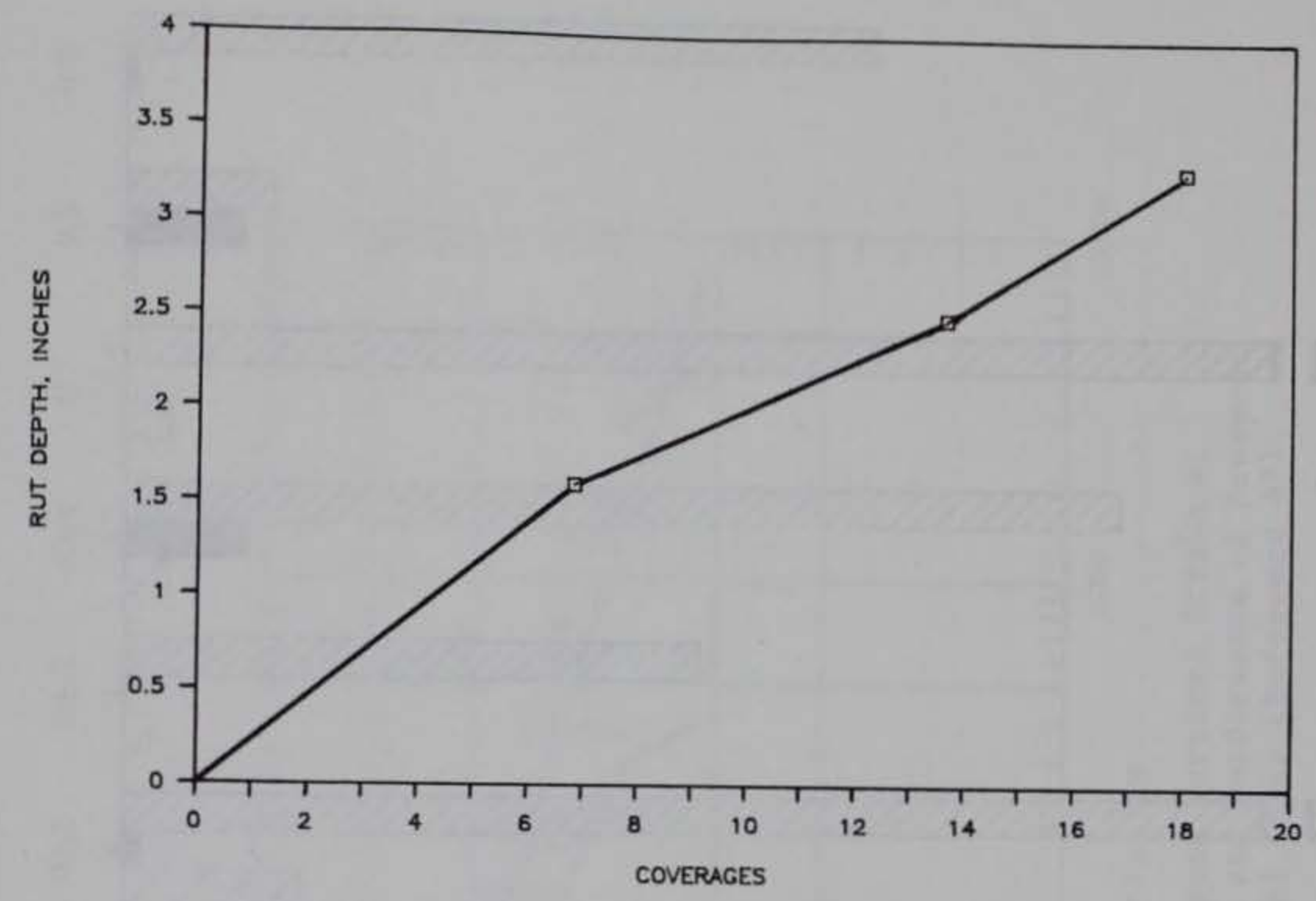


Figure V-10. Rut Depth Progression of W2.

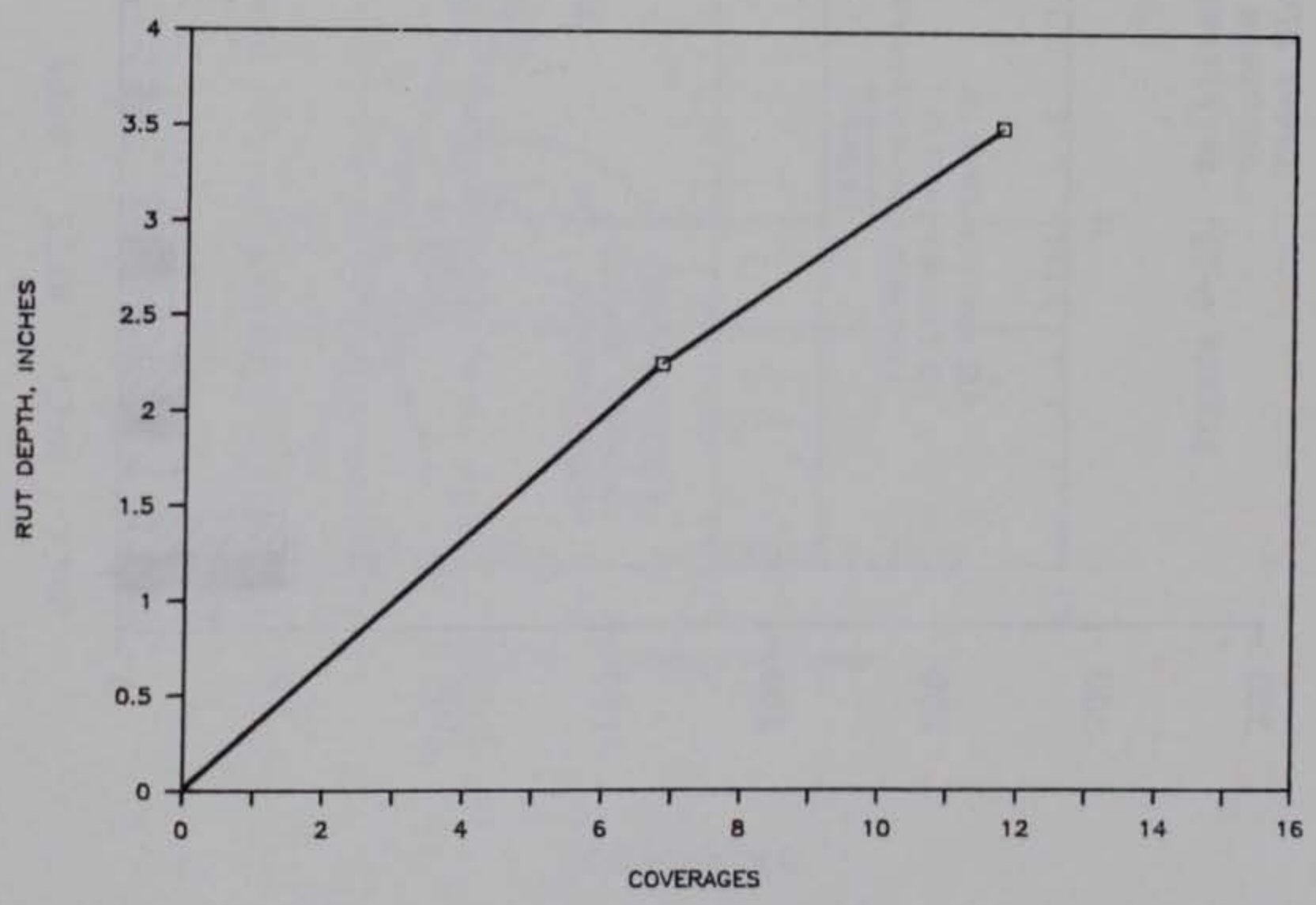


Figure V-11. Rut Depth Progression of W3.

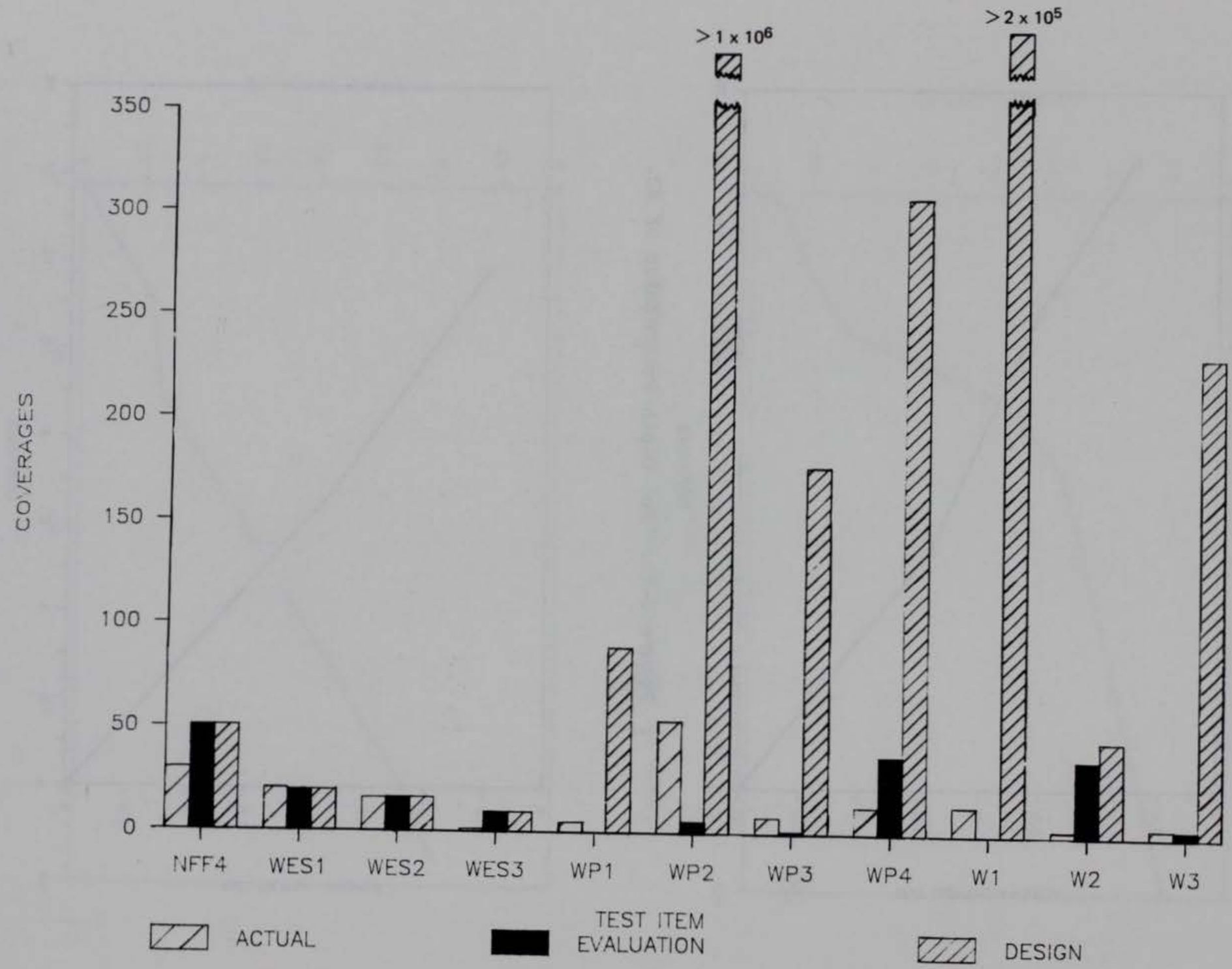


**Figure V-12. Comparison of Predictions with CBR Procedure.**

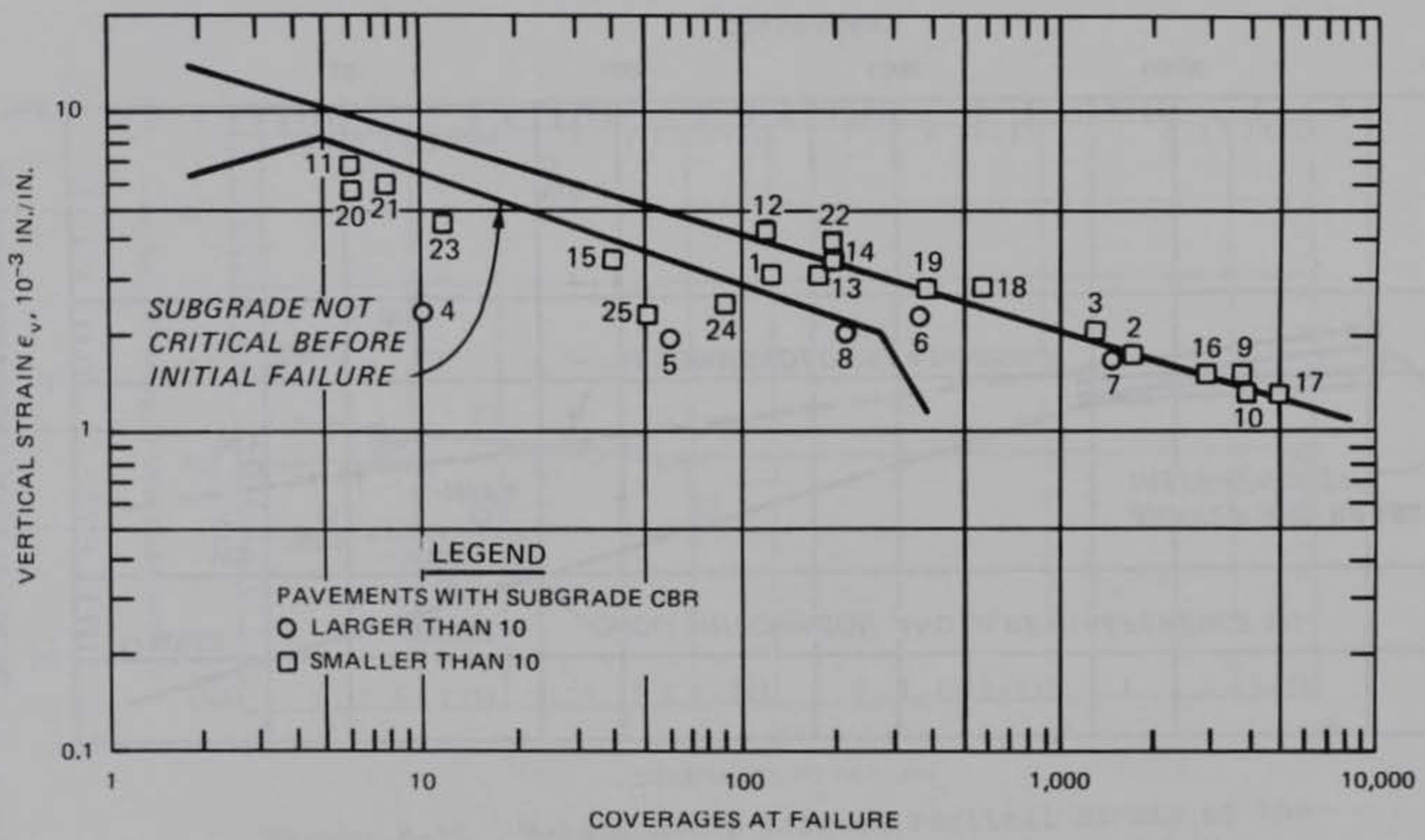


Figure V-13. Relationship Between Vertical Strain at Subgrade Surface and Performance of Pavement Under Single-Wheel Loads (Reference 47).

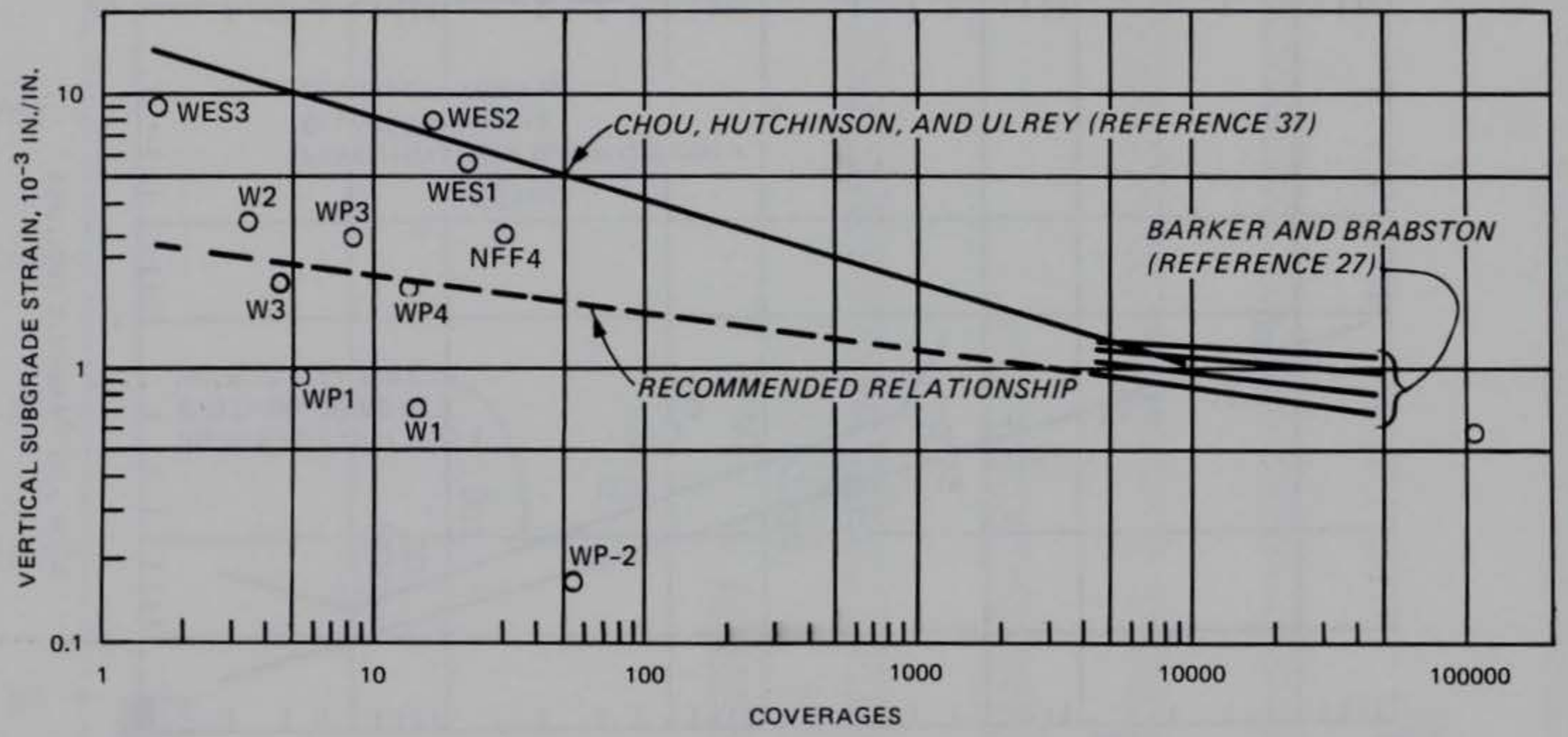


Figure V-14. Relationship Between Vertical Strain at Subgrade Surface and Performance of Pavements.

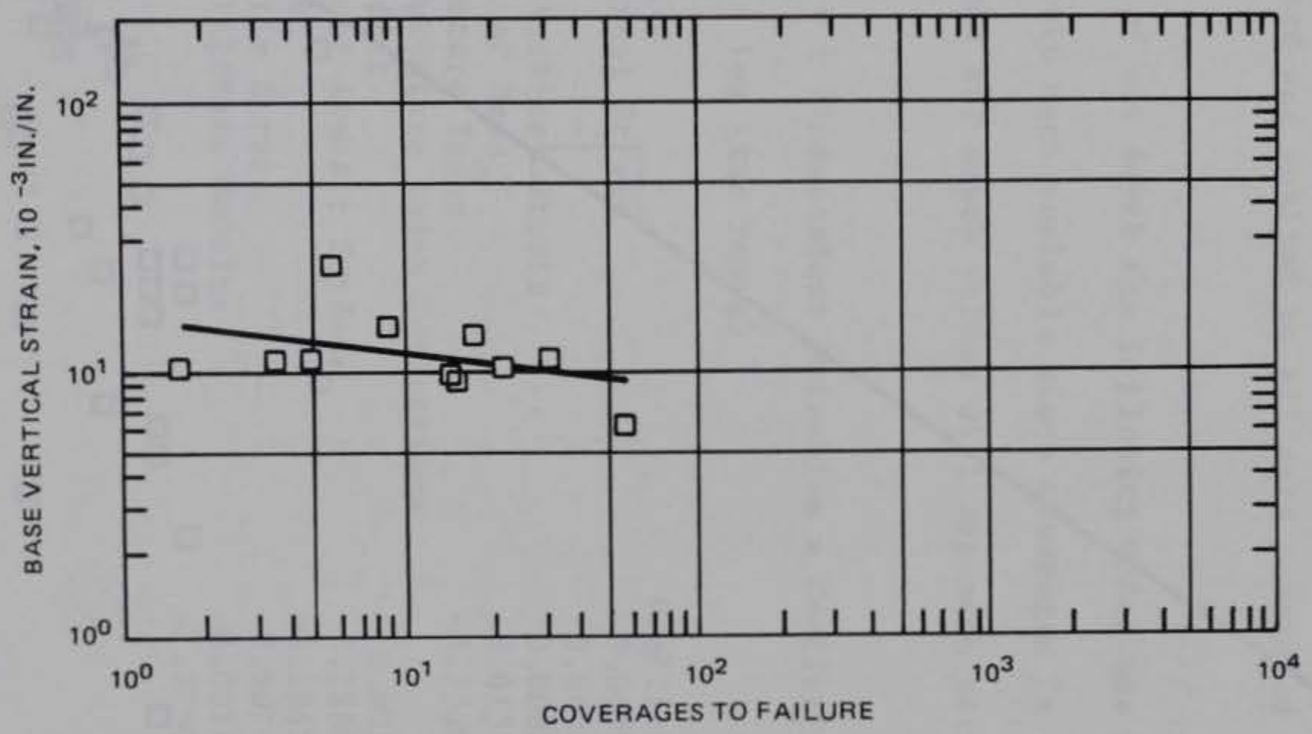


Figure V-15. Relationship Between Vertical Strain at the Base Course Surface and Performance of Pavements.

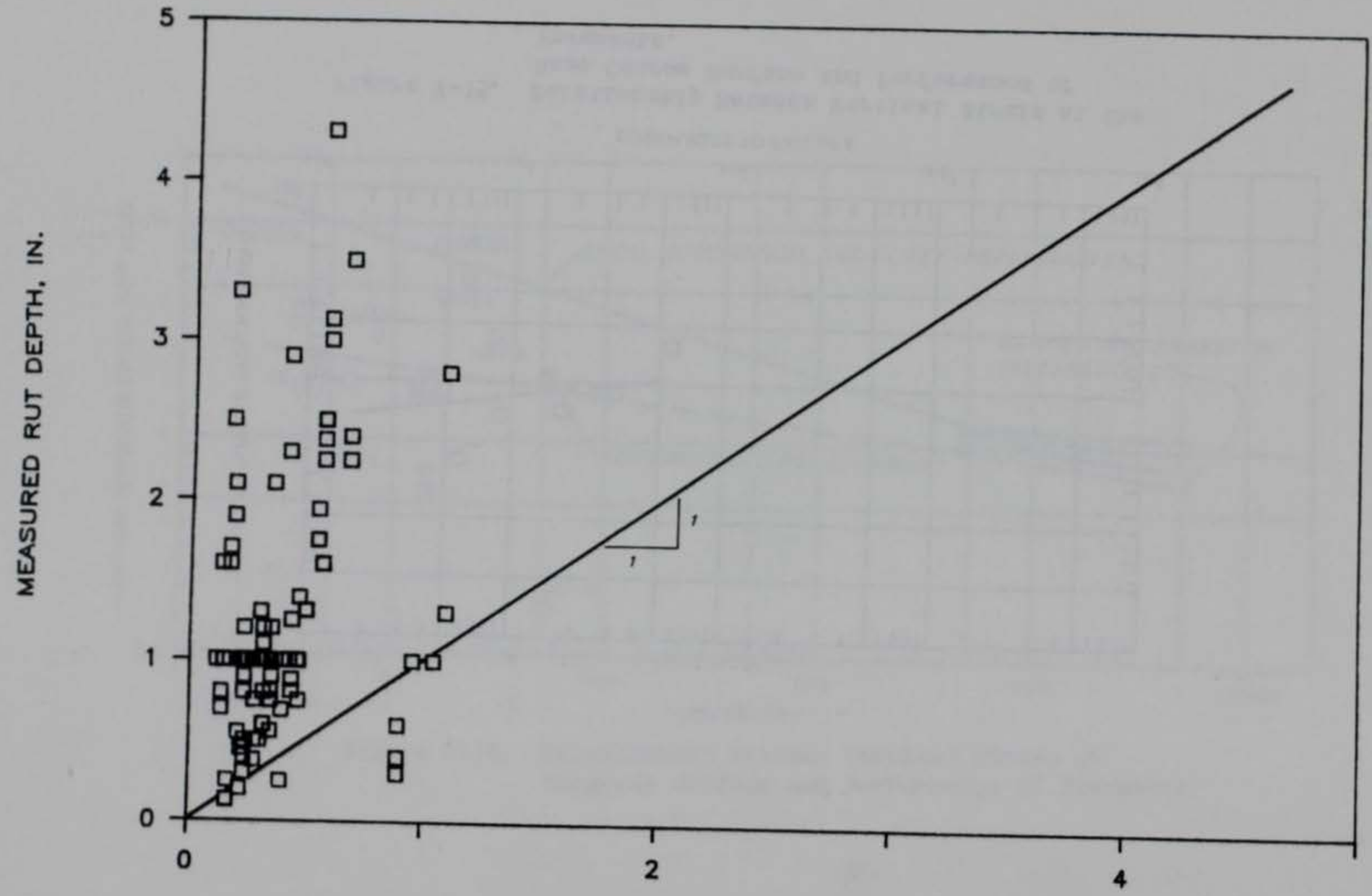


Figure V-16. Comparison of Measured Rut Depth to Predicted Rut Depth Using Barber Model.

# SECTION VI

# PREDICTION MODELS

## A. ESTIMATES OF PERFORMANCE

Prediction of rut depth and number of coverages to both one and three inch rut depths will be presented. To develop models, initially a stepwise regression method was applied to all data presented in Table VI-1.

### 1. Rut Depth

For prediction of rut depth the following model was developed. Log coverages were entered into each variable since coverages is dominant and at small coverages levels the rut depth values will approach zero as expected. where

Dependent Variable = [ (Independent Vairables x Coefficient] x Constant

Dependent Variable - Log (Rut Depth)

| Independent Variables | Coefficient |
|---|---|
| Log Cov * Base Vertical Strain | -0.00001 |
| Log Cov * AGE | 0.04586 |
| Log Cov * Subgrade Vertical Strain | 0.00029 |
| Log Cov * Thickness of Base | 0.01304 |
| Log Cov * Base Curvature Index | -0.75268 |
| Log Cov * Surface Curvature Index Deflections at "0" offset | 0.00194 |
| Log Cov * Thickness of Asphalt Surface | 0.78863 |
| Log Cov * Basin Area | -0.18625 |
| Log Cov * Base Tensile Strain | -0.00783 |
| Log Cov * Impulse Stiffness Modulus | -0.00179 |
| Constant | -1.27505 |

$R^2$ = 0.792
Standard Error = 0.177
No. of Cases = 47

The above model can be discredited since many of the variables are adding to rut depth when there should be a decrease. For example, thickness of base and thickness of AC both have positive coefficients indicating that their increase would increase rut depth. For a pavement with an AC surface

over a granular base, if the thickness of the AC was increased while the thickness and quality of the Base and the strength of the subgrade remained constant, the magnitude of the rut depth should decrease. Likewise, if the thickness of the base was increased with the other parameters remaining constant, the rut depth should decrease. Therefore, this model is not valid.

2. Coverages to a 3 inch Rut Depth.

The Impulse Stiffness Modulus proved highly significant using stepwise regression analysis in predicting both rut depth and coverages to a selected rut depth where all variables were considered. Therefore, since the data base is rather small, regression was attempted using ISM and one other variable. For predicting coverages to a 3 inch rut depth, models were developed for new pavements and aged pavements as shown in Figure VI-1. The data base for developing the coverage level models is shown in Table VI-2. Relationships are as follows:

Three Inch Rut Depth

Coverages = .530264(ISM) - 64.54 For New Pavements (13)

$R^2$= 0.99
Std Error = 0.52
No. of Cases = 4
Range of ISM = 141 to 344
Range of Coverages = 6.5 to 93

Coverages = .358388(ISM) -57.62 For Aged Pavements (14)

$R^2$= .90
Std Error = 9.65
No. of Cases = 7
Range of ISM = 187 to 382 kips per inch
Range of Coverages = 6 to 87.7

By using the variable Log (Age +1), to account for the difference in the above relationships, the following model was developed using the entire data base.

$$\text{Coverages} = -23.41(\text{Log Age}+1) + 0.4386(\text{ISM}) - 45.7 \qquad (15)$$

$R^2 = .927$
Std Error = 10.86
No. of Cases = 11
Range of Age = 0 to 30 years
Range of ISM = 141 to 382 kips per inch

Characteristics of AC that changes with age are the stiffness and ductility of the asphalt binder. Penetration of the extracted binder is an indicator of these properties. Hence, a regression model was developed for prediction of coverages to a 3 inch rut using penetration of the extracted AC binder. Results are as follows:

Dependent Variable: Cov to 3 inch rut

| Independent Variables | Coefficients |
|---|---|
| ISM | 0.4156 |
| Penetration | 0.4320 |
| Constant | -76.45 |

$R^2 = 0.907$
Standard Error = 12.3
No. of Cases = 11

This model showed no improvement over the use of ISM and Age which can be determined without destructive testing.

Another variable that is highly significant in predicting performance is the Surface Curvature Index (SCI) multiplied by the deflection measured at the center of the applied load (DO). The deflections were nomalized to 9000 lbs so that variations in the load magnitude would not affect the results.

The models developed are as follows:

Dependent Variable: Log Coverages to 3 inch rut

For new test items:

| Independent Variables | Coefficients |
|---|---|
| SCI * DO | -0.00070 |
| Constant | 2.350642 |

$R^2$ = 0.99
Standard Error = 0.055
No. of Cases = 4

For the aged test items:

Dependent Variable: Log Coverage to 3 inch rut

| Independent Variables | Coefficients |
|---|---|
| SCI * DO | -0.00099 |
| Constant | 2.128 |

$R^2$ = 0.65
Standard Error = 0.000326

By including age the results are:

Dependent Variable: Log Coverage to 3 inch rut

| Independent Variables | Coefficients |
|---|---|
| SCI * DO | -0.00077 |
| Log (Age + 1) | -0.35667 |

$R^2$ = 0.76
Standard Error = 0.22

3. Coverages to 1 inch Rut Depth.

For prediction of traffic levels to a one inch rut depth, several methods were evaluated. Prediction models using FWD data are given as follows:

One inch Rut Depth

Coverages = .164(ISM) - 22.267 (16)

$R^2$= .726
Std Error = 8.32
No. of Cases = 11
Range of ISM = 141 to 382 kips per inch
Range of Coverages = 1.6 to 54.5

Coverages = .1722(ISM) - 4.54(Log (Age + 1)) - 20.32 (17)

$R^2$= .766
Std Error = 8.17
No. of Cases = 11
Range of Age = 0 to 30 years
Range of ISM = 141 to 382 kips per inch
Range of Coverages = 1.6 to 54.5

Log Coverages = -0.344Log(Age+1) + 0.004518(ISM) + 0.00247(Penetration) (18)

$R^2$ = 0.659
Std Error = 0.307
No. of Cases = 11
Range of ISM = 141 to 382 kips per inch
Range of Age = 0 to 30 years
Range of Penetration = 10 to 85

New Pavements:
Log Coverages = -0.00072 (SCI)(DO) + 1.996 (19)

$R^2$ = 0.794
Std Error = 0.320
No. of Cases = 4

Aged Pavements:
Log Coverages = -0.00102 (SCI)(DO) + 1.839 (20)

$R^2$ = 0.598
Std Error = 0.284
No. of Cases = 7

By combining and using Age:
Log Coverages = -0.00082 (SCI)(DO) - 0.34279(Log(Age+1)) + 2.123

$R^2$ = 0.693
Std Error = 0.278 (21)
No. of Cases = 11

B. SELECTION OF BEST ESTIMATOR OF PERFORMANCE

The investigations described above were developed based on destructive test data (CBR), layered elastic methods (Base Vertical Strain) and the Impulse Stiffness Modulus (ISM). Figure VI-2 presents a comparison of the different methods.

The CBR predictions are based on the measured field CBR at the controlling layer. Hence, low base course strengths are accounted for. The base strain is based on the maximum vertical strain at the top of the base course. ISM is based on the model given as:

$$COV = 0.172\ (ISM) - 4.54\ (Log(Age + 1)) - 20.32 \qquad (22)$$

The average difference in actual and predicted for the eleven items for each method is given below:

| Prediction | Average Difference for Actual Coverages |
|---|---|
| CBR | 1.13 |
| Base Vertical Strain | 15.3 |
| ISM and Age | 0.43 |

Considering all pavement test items, ISM and age are better predictors for this data base.

C. VALIDATION OF MODEL

In addition to traffic with the F-4 load cart at the North Field test, traffic was applied with a F-15 load cart. The layer thicknesses were the same as for the F-4. The average ISM for the test item was 220 kips per inch. Using equation 22, the predicted F-4 coverages are 17.5.

Using the CBR evaluation procedure, a subgrade CBR of 9 with 2.1 inches of AC and 6.3 inches of base would produce 17.5 coverages of the F-4.

The F-15 evaluation would be as follows:

Design load - 68,000 lbs

Total Thickness - 8.4 inches

CBR - 9

Allowable passes - 112

Pass to Coverage Ratio = 9.36

Estimated Coverages = 11.9

Actual Coverages from Reference 10 - 12.1

## D. EVALUATION PROCEDURE

The evaluation procedure outlined herein is applicable only to flexible pavements containing unbound granular layers with ISM's less than 400 kips/inch. For pavements with ISM's greater than 400 kips/inch, a mechanistic procedure should be applied as described in Section V-C where the moduli are backcalculated and limited vertical subgrade strain is calculated for the design aircraft.

The evaluation procedure is outlined in Figure VI-3. A program for correcting for temperature is given in Appendix C. The model for estimating coverages of a F4 aircraft to a one inch rut is shown in Figure VI-4.

For determining the allowable passes for aircraft other than the F-4, the thickness of the layers is required. Using the allowable passes for the F-4, the load and contact area of the F-4, and the total pavement thickness above the subgrade, an "equivalent CBR" can be computed with the CBR design/evaluation procedure. With the equivalent CBR and thickness data, allowable coverages for other aircraft can be calculated.

Layer thicknesses are also required for the mechanistic analysis. Coring will be required for determining thicknesses of the pavement layers when construction data is not available.

TABLE VI-1
DATA BASE FOR RUT DEPTH PREDICTION

| ITEM | RUT DEPTH IN. | COV | ISM K/IN | AGE YRS | FORCE LBS | D0 MILS | D12 MILS | D24 MILS | D36 MILS | D48 MILS | AREA IN | AC STRAIN 10E-6 IN/IN | BASE VERT STRESS PSI | BASE VERT STRAIN 10E-6 IN/IN | BASE SHEAR STRESS PSI | BASE TENSILE STRESS PSI | SUBG VERT STRESS PSI | SUBG VERT STRAIN 10E-6 IN/IN | SURF THICK IN. | BASE THICK IN. | BASE CBR % | SUBG CBR % |
|---|---|---|---|---|---|---|---|---|---|---|---|---|---|---|---|---|---|---|---|---|---|---|
| NFF4 | 0.25 | 2.0 | 344 | 0 | 9024 | 26.2 | 6.0 | 2.6 | 1.5 | 1.1 | 10.28 | 2010 | 237 | 10300 | 54.6 | -33.6 | 115.0 | 3160 | 2.1 | 6.3 | 100 | 20 |
| NFF4 | 0.43 | 10.0 | 344 | 0 | 9024 | 26.2 | 6.0 | 2.6 | 1.5 | 1.1 | 10.28 | 2010 | 237 | 10300 | 54.6 | -33.6 | 115.0 | 3160 | 2.1 | 6.3 | 100 | 20 |
| NFF4 | 0.83 | 20.0 | 344 | 0 | 9024 | 26.2 | 6.0 | 2.6 | 1.5 | 1.1 | 10.28 | 2010 | 237 | 10300 | 54.6 | -33.6 | 115.0 | 3160 | 2.1 | 6.3 | 100 | 20 |
| NFF4 | 2.12 | 30.0 | 344 | 0 | 9024 | 26.2 | 6.0 | 2.6 | 1.5 | 1.1 | 10.28 | 2010 | 237 | 10300 | 54.6 | -33.6 | 115.0 | 3160 | 2.1 | 6.3 | 100 | 20 |
| NFF4 | 2.62 | 40.0 | 344 | 0 | 9024 | 26.2 | 6.0 | 2.6 | 1.5 | 1.1 | 10.28 | 2010 | 237 | 10300 | 54.6 | -33.6 | 115.0 | 3160 | 2.1 | 6.3 | 100 | 20 |
| NFF4 | 3.50 | 100.0 | 344 | 0 | 9024 | 26.2 | 6.0 | 2.6 | 1.5 | 1.1 | 10.28 | 2010 | 237 | 10300 | 54.6 | -33.6 | 115.0 | 3160 | 2.1 | 6.3 | 100 | 20 |
| WES1 | 0.50 | 13.1 | 217 | 0 | 8628 | 39.8 | 17.6 | 8.1 | 3.8 | 3.1 | 14.32 | 1860 | 223 | 9860 | 58.2 | 26.9 | 63.9 | 5710 | 1.7 | 8.2 | 100 | 7 |
| WES1 | 0.75 | 16.4 | 217 | 0 | 8628 | 39.8 | 17.6 | 8.1 | 3.8 | 3.1 | 14.32 | 1860 | 223 | 9860 | 58.2 | 26.9 | 63.9 | 5710 | 1.7 | 8.2 | 100 | 7 |
| WES1 | 1.00 | 18.6 | 217 | 0 | 8628 | 39.8 | 17.6 | 8.1 | 3.8 | 3.1 | 14.32 | 1860 | 223 | 9860 | 58.2 | 26.9 | 63.9 | 5710 | 1.7 | 8.2 | 100 | 7 |
| WES1 | 1.25 | 20.5 | 217 | 0 | 8628 | 39.8 | 17.6 | 8.1 | 3.8 | 3.1 | 14.32 | 1860 | 223 | 9860 | 58.2 | 26.9 | 63.9 | 5710 | 1.7 | 8.2 | 100 | 7 |
| WES1 | 1.50 | 22.9 | 217 | 0 | 8628 | 39.8 | 17.6 | 8.1 | 3.8 | 3.1 | 14.32 | 1860 | 223 | 9860 | 58.2 | 26.9 | 63.9 | 5710 | 1.7 | 8.2 | 100 | 7 |
| WES1 | 1.75 | 26.2 | 217 | 0 | 8628 | 39.8 | 17.6 | 8.1 | 3.8 | 3.1 | 14.32 | 1860 | 223 | 9860 | 58.2 | 26.9 | 63.9 | 5710 | 1.7 | 8.2 | 100 | 7 |
| WES1 | 2.00 | 32.7 | 217 | 0 | 8628 | 39.8 | 17.6 | 8.1 | 3.8 | 3.1 | 14.32 | 1860 | 223 | 9860 | 58.2 | 26.9 | 63.9 | 5710 | 1.7 | 8.2 | 100 | 7 |
| WES1 | 2.25 | 39.3 | 217 | 0 | 8628 | 39.8 | 17.6 | 8.1 | 3.8 | 3.1 | 14.32 | 1860 | 223 | 9860 | 58.2 | 26.9 | 63.9 | 5710 | 1.7 | 8.2 | 100 | 7 |
| WES1 | 2.50 | 42.6 | 217 | 0 | 8628 | 39.8 | 17.6 | 8.1 | 3.8 | 3.1 | 14.32 | 1860 | 223 | 9860 | 58.2 | 26.9 | 63.9 | 5710 | 1.7 | 8.2 | 100 | 7 |
| WES1 | 3.75 | 46.1 | 217 | 0 | 8628 | 39.8 | 17.6 | 8.1 | 3.8 | 3.1 | 14.32 | 1860 | 223 | 9860 | 58.2 | 26.9 | 63.9 | 5710 | 1.7 | 8.2 | 100 | 7 |
| WES2 | 0.25 | 6.5 | 157 | 0 | 8323 | 53.0 | 27.6 | 10.0 | 6.0 | 3.8 | 15.19 | 2150 | 238 | 13200 | 60.4 | 33.5 | 57.8 | 7730 | 1.4 | 9.0 | 100 | 6 |
| WES2 | 0.50 | 13.1 | 157 | 0 | 8323 | 53.0 | 27.6 | 10.0 | 6.0 | 3.8 | 15.19 | 2150 | 238 | 13200 | 60.4 | 33.5 | 57.8 | 7730 | 1.4 | 9.0 | 100 | 6 |
| WES2 | 2.00 | 16.4 | 157 | 0 | 8323 | 53.0 | 27.6 | 10.0 | 6.0 | 3.8 | 15.19 | 2150 | 238 | 13200 | 60.4 | 33.5 | 57.8 | 7730 | 1.4 | 9.0 | 100 | 6 |
| WES2 | 2.25 | 19.6 | 157 | 0 | 8323 | 53.0 | 27.6 | 10.0 | 6.0 | 3.8 | 15.19 | 2150 | 238 | 13200 | 60.4 | 33.5 | 57.8 | 7730 | 1.4 | 9.0 | 100 | 6 |
| WES2 | 3.00 | 20.5 | 157 | 0 | 8323 | 53.0 | 27.6 | 10.0 | 6.0 | 3.8 | 15.19 | 2150 | 238 | 13200 | 60.4 | 33.5 | 57.8 | 7730 | 1.4 | 9.0 | 100 | 6 |
| WES3 | 3.00 | 6.5 | 141 | 0 | 8164 | 57.7 | 27.2 | 12.2 | 6.3 | 4.3 | 14.85 | 354 | 270 | 9990 | 85.1 | 63.6 | 59.0 | 9560 | 0.5 | 9.4 | 100 | 6 |
| WP1 | 1.30 | 5.5 | 187 | 22 | 8851 | 47.4 | 23.5 | 3.5 | 1.9 | 1.1 | 13.08 | 2700 | 43 | 24200 | 0.6 | 24.6 | 37.3 | 932 | 3.0 | 6.0 | 12 | 6 |
| WP1 | 5.10 | 6.5 | 187 | 22 | 8851 | 47.4 | 23.5 | 3.5 | 1.9 | 1.1 | 13.08 | 2700 | 43 | 24200 | 0.6 | 24.6 | 37.3 | 932 | 3.0 | 6.0 | 12 | 6 |
| WP2 | 0.25 | 20.5 | 382 | 24 | 8867 | 23.2 | 11.3 | 3.5 | 2.1 | 1.5 | 14.20 | 1520 | 129 | 6070 | 31.0 | 1.0 | 5.1 | 169 | 3.0 | 47.0 | 33 | 6 |
| WP2 | 0.50 | 32.7 | 382 | 24 | 8867 | 23.2 | 11.3 | 3.5 | 2.1 | 1.5 | 14.20 | 1520 | 129 | 6070 | 31.0 | 1.0 | 5.1 | 169 | 3.0 | 47.0 | 33 | 6 |
| WP2 | 1.50 | 46.0 | 382 | 24 | 8867 | 23.2 | 11.3 | 3.5 | 2.1 | 1.5 | 14.20 | 1520 | 129 | 6070 | 31.0 | 1.0 | 5.1 | 169 | 3.0 | 47.0 | 33 | 6 |
| WP2 | 2.00 | 65.6 | 382 | 24 | 8867 | 23.2 | 11.3 | 3.5 | 2.1 | 1.5 | 14.20 | 1520 | 129 | 6070 | 31.0 | 1.0 | 5.1 | 169 | 3.0 | 47.0 | 33 | 6 |

TABLE VI-1 (CONCLUDED)
DATA BASE FOR RUT DEPTH PREDICTION

| ITEM | RUT DEPTH IN. | COV | ISM K/IN | AGE YRS | FORCE LBS | D0 MILS | D12 MILS | D24 MILS | D36 MILS | D48 MILS | AREA IN | AC STRAIN 10E-6 IN/IN | BASE VERT STRESS PSI | BASE VERT STRAIN 10E-6 IN/IN | BASE SHEAR STRESS PSI | BASE TENSILE STRESS PSI | SUBG VERT STRESS PSI | SUBG VERT STRAIN 10E-6 IN/IN | SURF THICK IN. | BASE THICK IN. | BASE CBR % | SUBG CBR % |
|---|---|---|---|---|---|---|---|---|---|---|---|---|---|---|---|---|---|---|---|---|---|---|
| WP2 | 2.75 | 72.2 | 382 | 24 | 8867 | 23.2 | 11.3 | 3.5 | 2.1 | 1.5 | 14.20 | 1520 | 129 | 6070 | 31.0 | 1.0 | 5.1 | 169 | 3.0 | 47.0 | 33 | 6 |
| WP2 | 3.00 | 87.7 | 382 | 24 | 8867 | 23.2 | 11.3 | 3.5 | 2.1 | 1.5 | 14.20 | 1520 | 129 | 6070 | 31.0 | 1.0 | 5.1 | 169 | 3.0 | 47.0 | 33 | 6 |
| WP3 | 1.13 | 6.5 | 201 | 9 | 9200 | 45.7 | 23.6 | 6.3 | 2.5 | 2.4 | 14.18 | 2880 | 173 | 14200 | 37.5 | 6.8 | 45.8 | 3090 | 2.0 | 12.0 | 33 | 7 |
| WP3 | 1.25 | 7.9 | 201 | 9 | 9200 | 45.7 | 23.6 | 6.3 | 2.5 | 2.4 | 14.18 | 2880 | 173 | 14200 | 37.5 | 6.8 | 45.8 | 3090 | 2.0 | 12.0 | 33 | 7 |
| WP3 | 3.50 | 12.3 | 201 | 9 | 9200 | 45.7 | 23.6 | 6.3 | 2.5 | 2.4 | 14.18 | 2880 | 173 | 14200 | 37.5 | 6.8 | 45.8 | 3090 | 2.0 | 12.0 | 33 | 7 |
| WP4 | 0.50 | 6.5 | 280 | 21 | 9057 | 32.3 | 14.3 | 3.7 | 1.5 | 1.4 | 12.97 | 1980 | 200 | 9620 | 46.6 | 5.8 | 48.2 | 2030 | 2.0 | 12.0 | 72 | 8 |
| WP4 | 1.20 | 16.2 | 280 | 21 | 9057 | 32.3 | 14.3 | 3.7 | 1.5 | 1.4 | 12.97 | 1980 | 200 | 9620 | 46.6 | 5.8 | 48.2 | 2030 | 2.0 | 12.0 | 72 | 8 |
| WP4 | 2.25 | 19.5 | 280 | 21 | 9057 | 32.3 | 14.3 | 3.7 | 1.5 | 1.4 | 12.97 | 1980 | 200 | 9620 | 46.6 | 5.8 | 48.2 | 2030 | 2.0 | 12.0 | 72 | 8 |
| WP4 | 3.10 | 22.1 | 280 | 21 | 9057 | 32.3 | 14.3 | 3.7 | 1.5 | 1.4 | 12.97 | 1980 | 200 | 9620 | 46.6 | 5.8 | 48.2 | 2030 | 2.0 | 12.0 | 72 | 8 |
| W1 | 0.60 | 6.5 | 249 | 22 | 9081 | 36.5 | 8.5 | 5.1 | 3.7 | 2.9 | 11.08 | 870 | 272 | 9370 | 68.5 | 2.7 | 11.7 | 720 | 1.0 | 29.0 | 33 | 4 |
| W1 | 0.70 | 12.3 | 249 | 22 | 9081 | 36.5 | 8.5 | 5.1 | 3.7 | 2.9 | 11.08 | 870 | 272 | 9370 | 68.5 | 2.7 | 11.7 | 720 | 1.0 | 29.0 | 33 | 4 |
| W1 | 1.50 | 20.5 | 249 | 22 | 9081 | 36.5 | 8.5 | 5.1 | 3.7 | 2.9 | 11.08 | 870 | 272 | 9370 | 68.5 | 2.7 | 11.7 | 720 | 1.0 | 29.0 | 33 | 4 |
| W1 | 2.75 | 34.1 | 249 | 22 | 9081 | 36.5 | 8.5 | 5.1 | 3.7 | 2.9 | 11.08 | 870 | 272 | 9370 | 68.5 | 2.7 | 11.7 | 720 | 1.0 | 29.0 | 33 | 4 |
| W1 | 3.00 | 38.2 | 249 | 22 | 9081 | 36.5 | 8.5 | 5.1 | 3.7 | 2.9 | 11.08 | 870 | 272 | 9370 | 68.5 | 2.7 | 11.7 | 720 | 1.0 | 29.0 | 33 | 4 |
| W2 | 1.60 | 6.8 | 203 | 30 | 9149 | 45.0 | 25.9 | 9.7 | 5.3 | 3.8 | 16.20 | 2530 | 141 | 10900 | 33.1 | 5.4 | 33.2 | 3570 | 2.5 | 12.0 | 102 | 4 |
| W2 | 2.50 | 13.6 | 203 | 30 | 9149 | 45.0 | 25.9 | 9.7 | 5.3 | 3.8 | 16.20 | 2530 | 141 | 10900 | 33.1 | 5.4 | 33.2 | 3570 | 2.5 | 12.0 | 102 | 4 |
| W2 | 3.30 | 18.0 | 203 | 30 | 9149 | 45.0 | 25.9 | 9.7 | 5.3 | 3.8 | 16.20 | 2530 | 141 | 10900 | 33.1 | 5.4 | 33.2 | 3570 | 2.5 | 12.0 | 102 | 4 |
| W3 | 2.25 | 6.8 | 210 | 24 | 8875 | 42.2 | 18.4 | 7.1 | 4.1 | 2.8 | 13.83 | 2550 | 144 | 11100 | 33.1 | -0.6 | 25.9 | 2040 | 2.5 | 16.0 | 37 | 4 |
| W3 | 3.50 | 11.7 | 210 | 24 | 8875 | 42.2 | 18.4 | 7.1 | 4.1 | 2.8 | 13.83 | 2550 | 144 | 11100 | 33.1 | -0.6 | 25.9 | 2040 | 2.5 | 16.0 | 37 | 4 |

TABLE VI-2. DATA BASE FOR PREDICTING COVERAGES

| ITEM | RUT DEPTH IN. | COVERAGES | FORCE LBS | NORMALIZED BASINS FOR 9000 LBS FORCE D0 MILS | D12 MILS | D24 MILS | D36 MILS | D48 MILS | ISM K/IN | AREA IN | D0 MILS | D12 MILS | D24 MILS | D36 MILS | D48 MILS | SCI MILS | BCI MILS | SPR | ERI KSI | SCI*D0 MILS^2 | AGE YEARS | AC BINDER PENETRATION 0.1 mm |
|---|---|---|---|---|---|---|---|---|---|---|---|---|---|---|---|---|---|---|---|---|---|---|
| NFF4 | 1 | 30.0 | 9024 | 26.2 | 6.0 | 2.6 | 1.5 | 1.1 | 344 | 10.28 | 26.1 | 6.0 | 2.6 | 1.5 | 1.1 | 20.1 | 0.399 | 0.285 | 17.1 | 526.4 | 0 | 80 |
| WES1 | 1 | 20.5 | 8628 | 39.8 | 17.6 | 8.1 | 3.8 | 3.1 | 217 | 14.32 | 41.5 | 18.4 | 8.4 | 4.0 | 3.2 | 23.2 | 0.730 | 0.364 | 8.3 | 961.4 | 0 | 80 |
| WES2 | 1 | 16.3 | 8323 | 53.0 | 27.6 | 10.0 | 6.0 | 3.8 | 157 | 15.19 | 57.3 | 29.8 | 10.8 | 6.5 | 4.1 | 27.5 | 2.379 | 0.379 | 2.9 | 1574.1 | 0 | 80 |
| WES3 | 1 | 1.6 | 8164 | 57.7 | 27.2 | 12.2 | 6.3 | 4.3 | 141 | 14.85 | 63.6 | 30.0 | 13.4 | 6.9 | 4.7 | 33.6 | 2.205 | 0.373 | 2.3 | 2138.7 | 0 | 80 |
| WP1 | 1 | 5.3 | 8851 | 47.4 | 23.5 | 3.5 | 1.9 | 1.1 | 187 | 13.08 | 48.2 | 23.9 | 3.6 | 1.9 | 1.1 | 24.3 | 0.813 | 0.327 | 15.3 | 1171.3 | 22 | 19 |
| WP2 | 1 | 54.5 | 8867 | 23.2 | 11.3 | 3.5 | 2.1 | 1.5 | 382 | 14.20 | 23.5 | 11.5 | 3.6 | 2.1 | 1.5 | 12.1 | 0.609 | 0.359 | 14.5 | 284.4 | 24 | 24 |
| WP3 | 1 | 8.2 | 9200 | 45.7 | 23.6 | 6.3 | 2.5 | 2.4 | 201 | 14.18 | 44.7 | 23.1 | 6.2 | 2.4 | 2.3 | 21.6 | 0.098 | 0.352 | 13.3 | 966.5 | 9 | 19 |
| WP4 | 1 | 13.6 | 9057 | 32.3 | 14.3 | 3.7 | 1.5 | 1.4 | 280 | 12.97 | 32.1 | 14.2 | 3.7 | 1.5 | 1.4 | 17.9 | 0.099 | 0.329 | 17.1 | 574.1 | 21 | 20 |
| W1 | 1 | 14.3 | 9081 | 36.5 | 8.5 | 5.1 | 3.7 | 2.9 | 249 | 11.08 | 36.2 | 8.4 | 5.1 | 3.7 | 2.9 | 27.8 | 0.793 | 0.311 | 9.2 | 1003.8 | 22 | 9 |
| W2 | 1 | 3.4 | 9149 | 45.0 | 25.9 | 9.7 | 5.3 | 3.8 | 203 | 16.20 | 44.3 | 25.5 | 9.5 | 5.2 | 3.7 | 18.8 | 1.476 | 0.399 | 5.2 | 831.7 | 30 | 2 |
| W3 | 1 | 4.5 | 8875 | 42.2 | 18.4 | 7.1 | 4.1 | 2.8 | 210 | 13.83 | 42.8 | 18.7 | 7.2 | 4.2 | 2.8 | 24.1 | 1.318 | 0.354 | 7.8 | 1032.9 | 24 | 5 |
| NFF4 | 3 | 93.0 | 9024 | 26.2 | 6.0 | 2.6 | 1.5 | 1.1 | 344 | 10.28 | 26.1 | 6.0 | 2.6 | 1.5 | 1.1 | 20.1 | 0.399 | 0.285 | 17.1 | 526.4 | 0 | 80 |
| WES1 | 3 | 46.1 | 8628 | 39.8 | 17.6 | 8.1 | 3.8 | 3.1 | 217 | 14.32 | 41.5 | 18.4 | 8.4 | 4.0 | 3.2 | 23.2 | 0.730 | 0.364 | 88.0 | 961.4 | 0 | 80 |
| WES2 | 3 | 20.5 | 8323 | 53.0 | 27.6 | 10.0 | 6.0 | 3.8 | 157 | 15.19 | 57.3 | 29.8 | 10.8 | 6.5 | 4.1 | 27.5 | 2.379 | 0.379 | 2.9 | 1574.1 | 0 | 80 |
| WES3 | 3 | 6.5 | 8164 | 57.7 | 27.2 | 12.2 | 6.3 | 4.3 | 141 | 14.85 | 63.6 | 30.0 | 13.4 | 6.9 | 4.7 | 33.6 | 2.205 | 0.373 | 2.3 | 2138.7 | 0 | 80 |
| WP1 | 3 | 6.0 | 8851 | 47.4 | 23.5 | 3.5 | 1.9 | 1.1 | 187 | 13.08 | 48.2 | 23.9 | 3.6 | 1.9 | 1.1 | 24.3 | 0.813 | 0.327 | 15.3 | 1171.3 | 22 | 19 |
| WP2 | 3 | 87.7 | 8867 | 23.2 | 11.3 | 3.5 | 2.1 | 1.5 | 382 | 14.20 | 23.5 | 11.5 | 3.6 | 2.1 | 1.5 | 12.1 | 0.609 | 0.359 | 14.5 | 284.4 | 24 | 24 |
| WP3 | 3 | 12.3 | 9200 | 45.7 | 23.6 | 6.3 | 2.5 | 2.4 | 201 | 14.18 | 44.7 | 23.1 | 6.2 | 2.4 | 2.3 | 21.6 | 0.098 | 0.352 | 13.3 | 966.5 | 9 | 19 |
| WP4 | 3 | 22.1 | 9057 | 32.3 | 14.3 | 3.7 | 1.5 | 1.4 | 280 | 12.97 | 32.1 | 14.2 | 3.7 | 1.5 | 1.4 | 17.9 | 0.099 | 0.329 | 17.1 | 574.1 | 21 | 20 |
| W1 | 3 | 38.2 | 9081 | 36.5 | 8.5 | 5.1 | 3.7 | 2.9 | 249 | 11.08 | 36.2 | 8.4 | 5.1 | 3.7 | 2.9 | 27.8 | 0.793 | 0.311 | 9.2 | 1003.8 | 22 | 9 |
| W2 | 3 | 18.0 | 9149 | 45.0 | 25.9 | 9.7 | 5.3 | 3.8 | 203 | 16.20 | 44.3 | 25.5 | 9.5 | 5.2 | 3.7 | 18.8 | 1.476 | 0.399 | 5.2 | 831.7 | 30 | 2 |
| W3 | 3 | 11.7 | 8875 | 42.2 | 18.4 | 7.1 | 4.1 | 2.8 | 210 | 13.83 | 42.8 | 18.7 | 7.2 | 4.2 | 2.8 | 24.1 | 1.318 | 0.354 | 7.8 | 1032.9 | 24 | 5 |

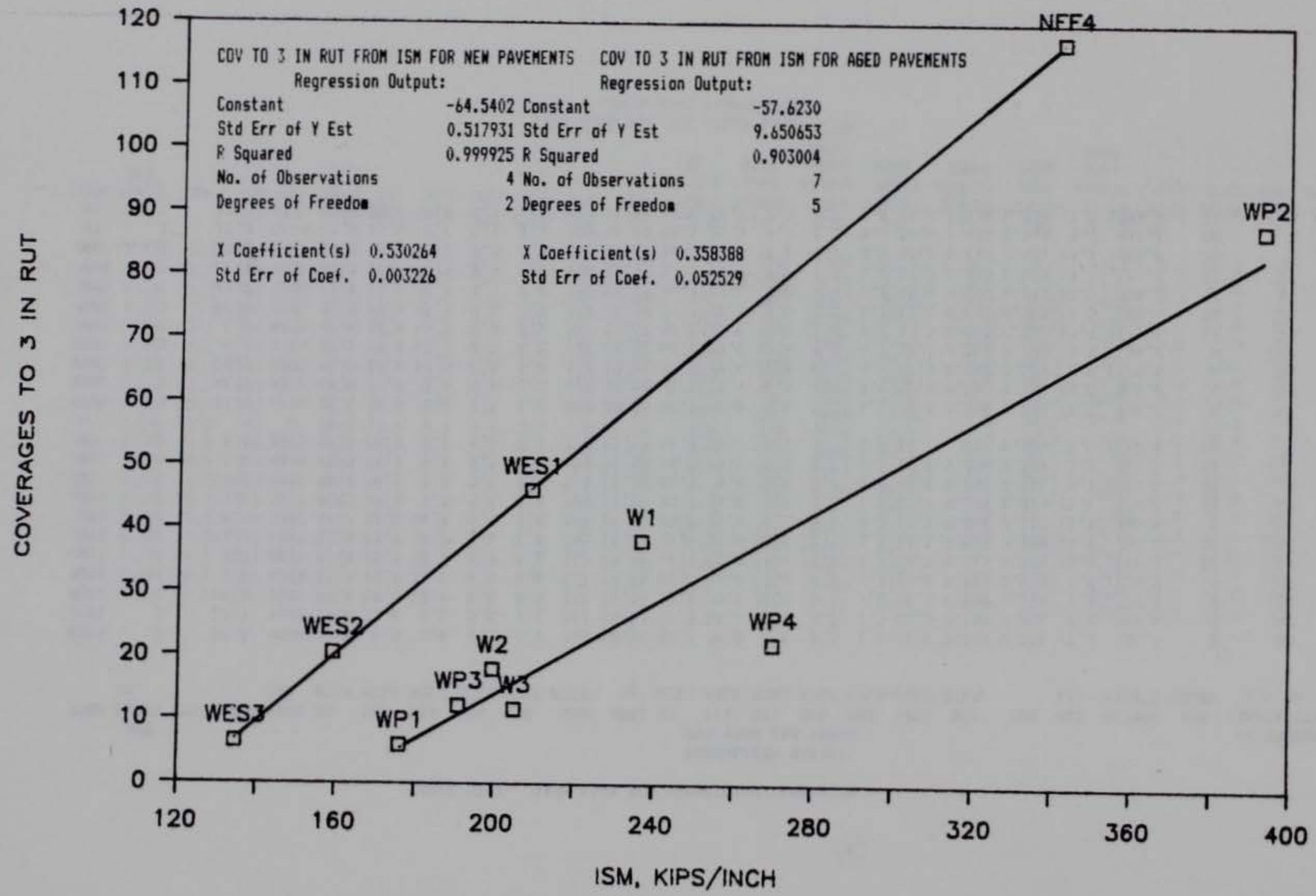


Figure VI-1. Estimates of Coverages to a 3 inch Rut Depth.

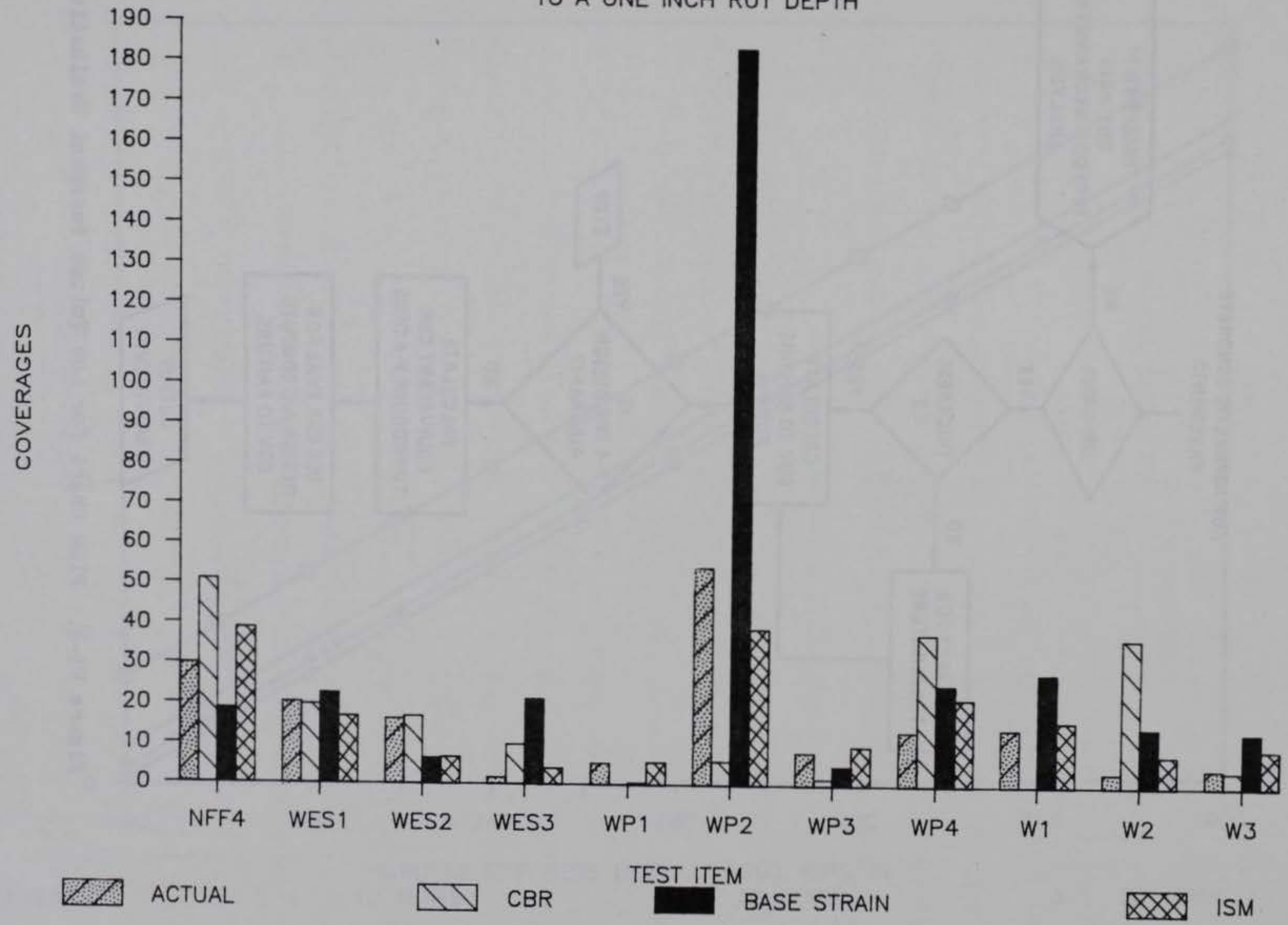


**Figure VI-2. Comparisons of Prediction Methods for Coverages to a 1 inch Rut Depth.**

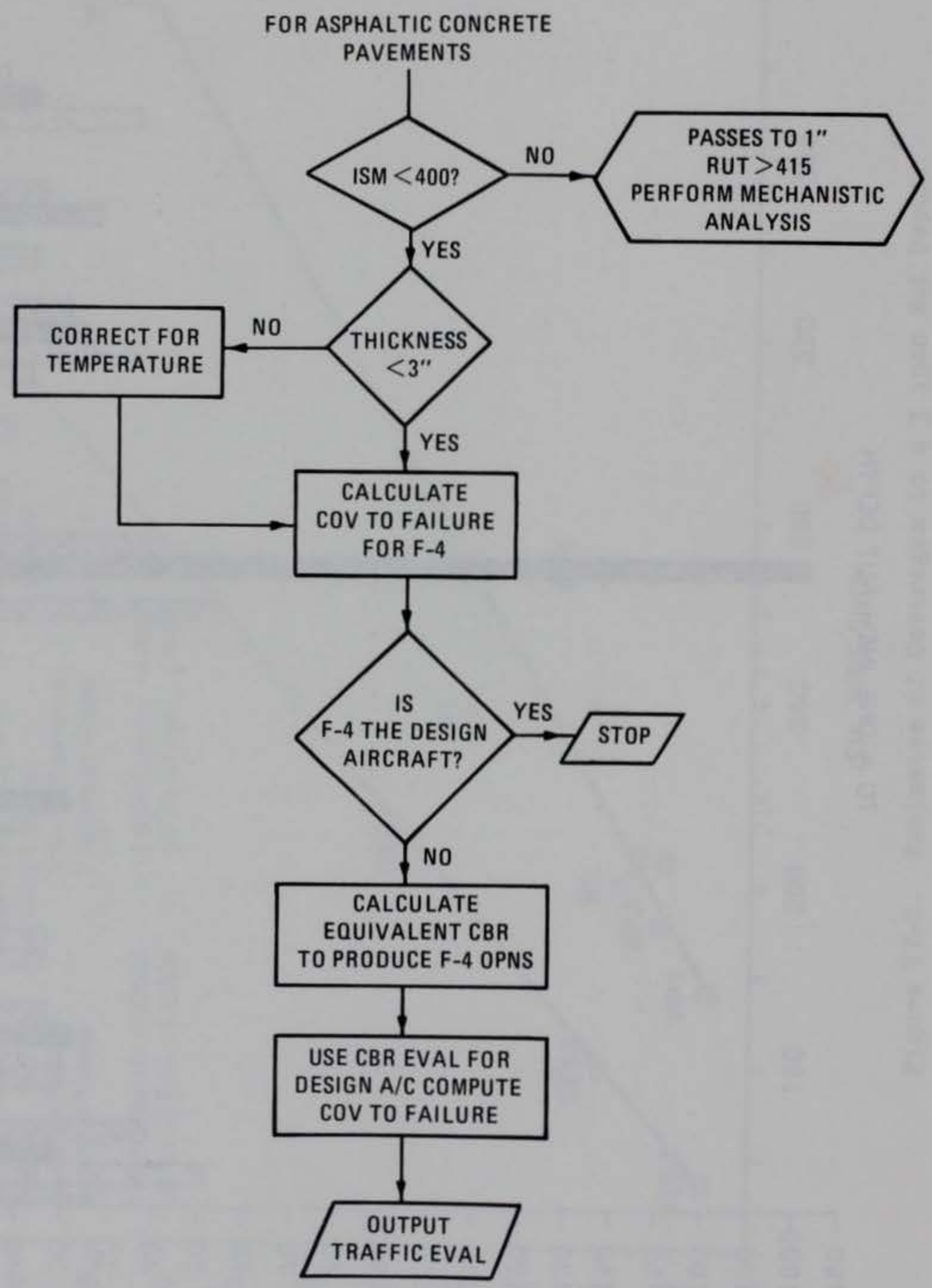


Figure VI-3. Flow Chart for Low Volume Pavement Evaluation.

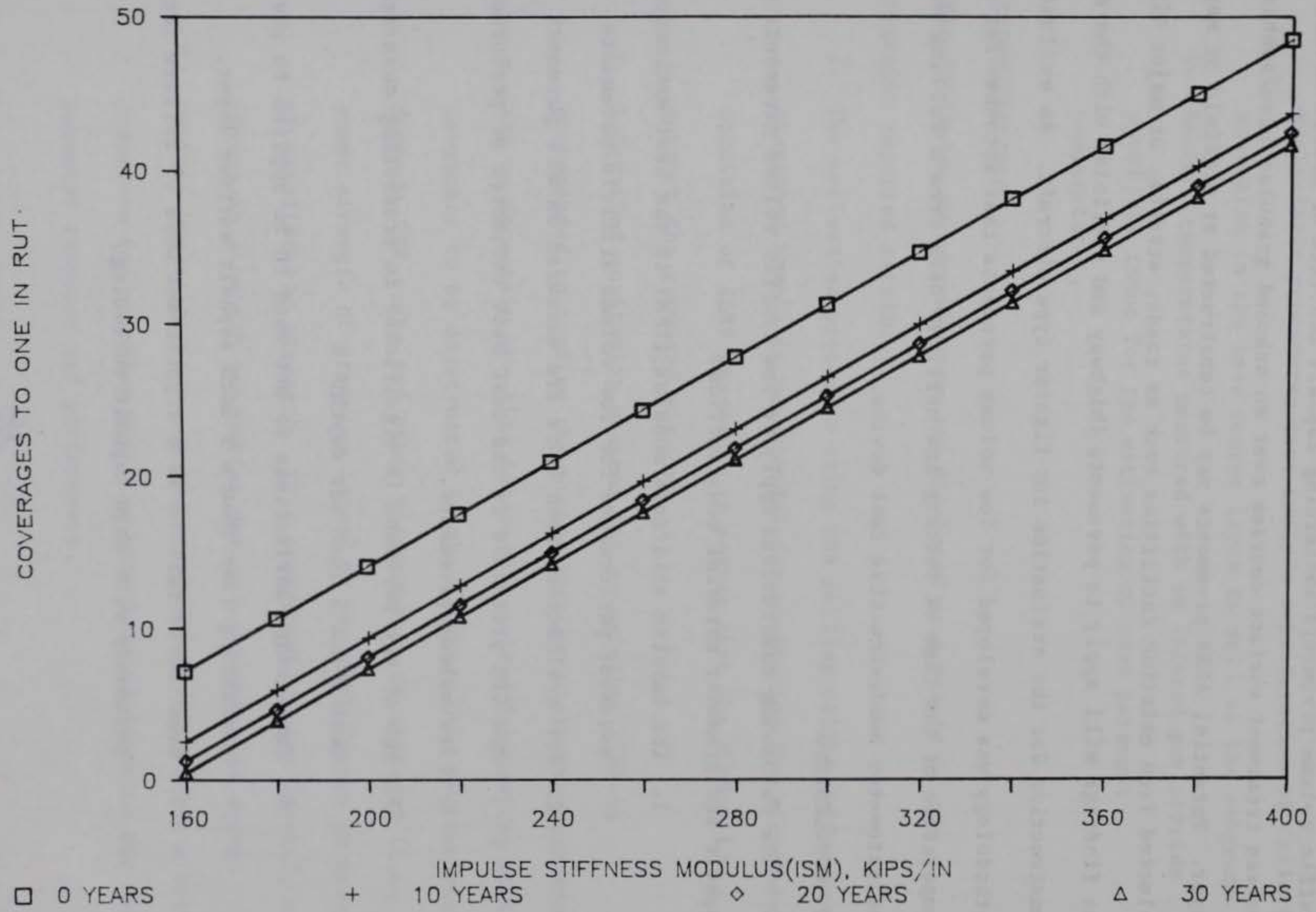


**Figure VI-4. ISM versus Allowable Coverages of an F-4 Aircraft for Low-Volume Flexible Pavements.**

## SECTION VII

## CONCLUSIONS AND RECOMMENDATIONS

The findings of this report are applicable to the evaluation of low traffic volume pavements containing asphalt concrete or double-bituminous surface treatment surface courses over an unbound granular base/subbase layer. Potential ALRS pavements may be constructed at airfield or may be selected from existing facilities such as roads, streets, or major highways. The findings will apply to pavements (highway and airfield) with the above construction for the evaluation for fighter type aircraft. An evaluation methodology was developed for low volume pavements that accounts for age and temperature of the time of testing and utilizes data from a Falling Weight Deflectometer nondestructive test device.

### A. CONCLUSIONS

The following conclusions apply to low traffic volume pavements of asphalt and granular material construction.

1. The impulse stiffness modulus (ISM) is the best estimator of pavement performance for low volume airfield pavements.
2. For evaluation, when CBR's are measured on all pavement layers, the CBR procedure is the next best estimator of performance of low volume pavements.
3. Age of the pavement is significant in predicting coverages to both 1 and 3 inch rut depth.
4. Temperature corrections do not need to be applied to pavements containing less than a 3 inch asphalt surface layer.
5. Base Course failure is a significant mode of failure for pavements with thin asphalt surfacing.

6. Base Course modulus estimated from backcalculation methods may be unreasonably low when the AC surface course contains cracks and does not perform as a continum.
7. Mechanistic procedures must include consideration of failure mechanism in the base course layer as well as the subgrade.
8. Surface temperatures measured with an Infared gun provide excellent input for the estimation of mean pavement temperatures.

## B. RECOMMENDATIONS

The following recommendations are presented as a result of the investigation reported herein.

1. The evaluation procedure using the falling weight deflectometer presented herein is recommended for monitoring the structural condition of ALRS pavements to ensure that the ALRS will support the required mission.
2. A detailed monitoring program for an existing ALRS is recommended to confirm the nondestructive evaluation procedure and to ascertain the time interval required for testing ALRS pavements to be constructed in the future. This program should include CBR tests and other measurements of strength (i.e., shear strength of granular layer) on pavement layers in areas of questionable strength. This program will also identify any change in strength properties due to environmental aging.
3. Further investigations are recommended for determining a better procedure for modeling granular materials to describe the total pavement response and performance.

4. The base course materials selected for construction of ALRS pavements should have strength properties with minimum moisture sensitivity.
5. For ALRS pavement evaluations where the FWD is not available, the CBR procedure is recommended where CBR's are obtained for all unbound pavement layers.
6. For testing pavements under simulated service traffic, a detailed laboratory investigation should be performed on the AC, base, and subgrade materials. The test program should include repeated load test to determine modulus and permanent strain for all materials and triaxial testing on unbound materials.

# APPENDIX A

## FALLING WEIGHT DEFLECTOMETER DEFLECTION BASIN DATA

TABLE A-1. FALLING WEIGHT DEFLECTOMETER DEFLECTION BASIN DATA

| Station No. | Force lbs. | Deflections 0-in. mils | 12-in. mils | 24-in. mils | 36-in. mils | 48-in. mils |
|---|---|---|---|---|---|---|
| | | WES 1 (Clay Subgrade)[a] | | | | |
| 0+10 | 4,560 | * | 9.9 | 4.4 | 2.9 | 3.4 |
| | 7,749 | * | 20.8 | 7.2 | 10.0 | 3.3 |
| | 11,102 | * | 39.0 | 10.0 | 6.5 | 4.8 |
| 0+20 | 4,350 | * | 16.1 | 5.5 | 2.8 | 1.9 |
| | 7,309 | * | 27.9 | 9.6 | 4.8 | 3.0 |
| | 10,233 | * | 45.3 | 12.2 | 6.6 | 4.3 |
| 0+30 | 4,420 | * | 12.8 | 4.1 | 2.4 | 1.8 |
| | 7,325 | * | 21.0 | 6.8 | 4.0 | 2.9 |
| | 10,226 | * | 32.5 | 8.9 | 5.5 | 4.3 |
| 0+40 | 4,358 | * | 13.0 | 5.4 | 2.8 | 1.7 |
| | 7,266 | * | 22.0 | 9.8 | 4.4 | 2.6 |
| | 10,129 | * | 29.2 | 12.2 | 5.8 | 5.0 |
| | | WES 2 (Clay Subgrade) | | | | |
| 0+10 | 4,258 | * | 18.8 | 6.8 | 18.1 | 18.1 |
| | 7,107 | * | 32.9 | 10.8 | 5.6 | 3.7 |
| | 9,902 | * | 45.7 | 14.0 | 6.4 | 4.2 |
| 0+20 | 4,001 | * | 17.5 | 7.4 | 3.5 | 1.8 |
| | 6,781 | * | 36.8 | 12.2 | 5.3 | 3.8 |
| | 9,403 | * | 51.1 | 15.4 | 7.0 | 5.3 |
| 0+30 | 4,172 | * | 17.2 | 6.3 | 3.1 | 2.0 |
| | 7,007 | * | 31.4 | 10.7 | 5.1 | 3.4 |
| | 9,721 | * | 7.5 | 14.7 | 7.3 | 4.8 |
| 0+40 | 4,366 | * | 15.2 | 5.9 | 3.0 | 2.0 |
| | 7,312 | * | 29.6 | 10.6 | 5.0 | 3.4 |
| | 10,115 | * | 45.6 | 14.8 | 7.7 | 4.8 |

a 11.8-in. diameter plate

TABLE A-1. FALLING WEIGHT DEFLECTOMETER DEFLECTION BASIN DATA (CONTINUED)

| Station No. | Force lbs. | Deflections 0-in. mils | 12-in. mils | 24-in. mils | 36-in. mils | 48-in. mils |
|---|---|---|---|---|---|---|
| | | WES 3 (Clay Subgrade) | | | | |
| 0+10 | 4,190 | * | 16.2 | 6.6 | 3.5 | 2.1 |
| | 7,091 | * | 30.5 | 11.4 | 5.3 | 3.3 |
| | 9,772 | * | 66.1 | 15.9 | 7.5 | 4.8 |
| 0+20 | 4,258 | * | 17.7 | 6.9 | 4.4 | 2.2 |
| | 7,147 | * | 33.0 | 12.8 | 6.4 | 3.8 |
| | 9,939 | * | 52.2 | 17.3 | 8.4 | 5.7 |
| 0+30 | 3,707 | * | 16.7 | 8.3 | 4.0 | 2.3 |
| | 6,225 | * | 36.4 | 13.6 | 6.5 | 4.0 |
| | 8,906 | * | 51.0 | 19.3 | 9.7 | 5.6 |
| 0+40 | 4,295 | * | 14.4 | 6.0 | 3.2 | 2.1 |
| | 7,334 | * | 30.5 | 10.5 | 5.5 | 3.5 |
| | 10,265 | * | 46.7 | 25.6 | 7.9 | 5.2 |
| | | WES South Overrun (Silt Subgrade) | | | | |
| | 4,457 | 28.5 | 6.0 | 3.3 | 1.8 | 1.3 |
| | 8,485 | 49.1 | 12.2 | 5.3 | 3.4 | 2.6 |
| | 14,092 | 77.9 | 19.5 | 9.0 | 5.4 | 3.9 |
| | | WES-North Overrun (Silt Subgrade) | | | | |
| | 4,488 | 32.3 | 6.9 | 4.7 | 1.8 | 1.1 |
| | 8,485 | 51.3 | 12.0 | 4.8 | 2.9 | 2.4 |
| | 14,067 | * | 20.7 | 7.3 | 4.7 | 3.5 |
| | | WES 1 (Base Course) | | | | |
| 0+10 | 4,510 | 40.6 | 12.6 | 5.0 | 2.7 | 1.8 |
| | 8,279 | 76.6 | 30.8 | 9.4 | 4.8 | 3.6 |
| | 13,201 | * | 40.6 | 14.6 | 7.2 | 3.6 |
| 0+20 | 4,303 | 38.1 | 13.3 | 5.3 | 3.1 | 2.0 |
| | 8,136 | 72.8 | 30.3 | 10.6 | 5.4 | 3.7 |
| | 13,085 | * | 55.1 | 17.7 | 9.1 | 5.7 |

TABLE A-1. FALLING WEIGHT DEFLECTOMETER DEFLECTION BASIN DATA (CONTINUED)

| Station No. | Force lbs. | Deflections 0-in. mils | 12-in. mils | 24-in. mils | 36-in. mils | 48-in. mils |
|---|---|---|---|---|---|---|
| | | WES 1 (Base Course) Continued | | | | |
| 0+30 | 4,338 | 42.4 | 16.5 | 6.3 | 3.5 | 2.4 |
| | 8,088 | * | 32.9 | 11.6 | 6.2 | 3.9 |
| | 12,982 | * | 60.0 | 18.9 | 9.4 | 6.2 |
| 0+40 | 4,288 | 46.1 | 17.0 | 6.0 | 3.1 | 2.0 |
| | 8,021 | * | 38.1 | 11.4 | 5.4 | 3.4 |
| | 12,796 | * | 71.9 | 19.7 | 8.7 | 5.6 |
| | | WES 2 (Base Course) | | | | |
| 0+10 | 4,327 | 54.1 | 22.8 | 8.1 | 3.8 | 2.4 |
| | 7,870 | * | 47.6 | 14.6 | 6.6 | 4.3 |
| | 12,450 | * | * | 24.0 | 9.7 | 6.8 |
| 0+20 | 4,160 | 53.5 | 22.3 | 8.7 | 4.3 | 2.5 |
| | 7,818 | * | 46.5 | 16.1 | 7.4 | 4.7 |
| | 12,466 | * | * | 26.2 | 11.5 | 7.2 |
| 0+30 | 4,227 | 46.1 | 19.5 | - | 3.5 | - |
| | 7,894 | * | 42.1 | 12.8 | 6.3 | 3.8 |
| | 12,644 | * | 76.0 | 21.9 | 9.8 | 6.4 |
| 0+40 | 4,168 | 46.5 | 19.5 | 7.5 | 3.7 | 1.9 |
| | 7,894 | * | 39.4 | 13.4 | 6.5 | 4.3 |
| | 12,718 | * | 69.7 | 23.5 | 10.4 | 6.5 |
| | | WES 3 (Base Course) | | | | |
| 0+10 | 4,259 | 41.1 | 19.5 | 7.5 | 3.9 | 2.4 |
| | 7,905 | 77.6 | 40.4 | 15.0 | 7.0 | 4.0 |
| | 12,788 | * | 73.8 | 25.2 | 11.4 | 6.5 |
| 0+20 | 4,096 | 37.5 | 17.5 | 7.1 | 3.6 | 1.9 |
| | 7,918 | 77.3 | 38.4 | 13.8 | 6.9 | 4.2 |
| | 12,812 | * | 73.0 | 23.6 | 11.3 | 6.9 |

* Overranged

TABLE A-1. FALLING WEIGHT DEFLECTOMETER DEFLECTION BASIN DATA (CONTINUED)

| Station No. | Force lbs. | Deflections 0-in. mils | 12-in. mils | 24-in. mils | 36-in. mils | 48-in. mils |
|---|---|---|---|---|---|---|
| | | WES 3 (Base Course) Continued | | | | |
| 0+30 | 4,136 | 35.4 | 16.1 | 6.9 | 3.9 | 2.3 |
| | 7,926 | 69.1 | 35.4 | 13.8 | 7.1 | 4.2 |
| | 12,895 | * | 66.9 | 24.8 | 11.2 | 7.3 |
| 0+40 | 4,009 | 32.4 | 13.8 | 5.9 | 3.0 | 2.0 |
| | 7,910 | 64.0 | 30.3 | 11.8 | 6.3 | 3.8 |
| | 12,987 | * | 59.1 | 21.3 | 10.7 | 6.7 |
| | | WES 1 (0 Coverages) | | | | |
| 0+10 | 8,628 | 39.8 | 17.6 | 8.1 | 3.8 | 3.1 |
| | 14,099 | 65.0 | 31.4 | 14.3 | 6.5 | 5.2 |
| 0+20 | 8,546 | 43.5 | 20.7 | 9.8 | 4.6 | 3.4 |
| | 13,952 | 72.6 | 36.5 | 17.3 | 7.7 | 5.6 |
| 0+30 | 8,517 | 37.8 | 18.3 | 8.8 | 4.3 | 3.2 |
| | 13,999 | 62.2 | 31.5 | 18.5 | 7.4 | 5.9 |
| 0+40 | 8,466 | 42.7 | 21.6 | 10.2 | 4.5 | 3.5 |
| | 13,840 | 70.1 | 37.9 | | 8.1 | |
| | | WES 1 (6.5 Coverages) | | | | |
| 0+10 | 8,358 | 53.5 | 23.6 | 8.9 | 3.9 | 3.0 |
| | 13,546 | * | 44.1 | 14.6 | 6.5 | 5.1 |
| 0+20 | 8,271 | 61.5 | 29.3 | 10.2 | 4.6 | 3.4 |
| | 13,305 | * | 45.1 | 17.7 | 7.3 | 5.6 |
| 0+30 | 8,239 | 56.2 | 25.6 | 9.8 | 4.6 | 3.5 |
| | 13,435 | * | 45.3 | 17.1 | 7.9 | 5.8 |
| 0+40 | 8,144 | 66.9 | 29.5 | 10.6 | 4.5 | 3.3 |
| | 13,197 | * | 51.0 | 18.9 | 7.8 | 5.7 |

*Deflection exceeded range of velocity transducer.

TABLE A-1. FALLING WEIGHT DEFLECTOMETER DEFLECTION BASIN DATA (CONTINUED)

| Station No. | Force lbs. | Deflections 0-in. mils | 12-in. mils | 24-in. mils | 36-in. mils | 48-in. mils |
|---|---|---|---|---|---|---|
| | | WES 1 (20.5 Coverages) | | | | |
| 0+10 | 8,326 | 55.5 | 31.1 | 10.4 | 4.7 | 3.2 |
| | 13,479 | * | 45.5 | 18.1 | 7.5 | 5.4 |
| 0+20 | 8,188 | 58.6 | 30.3 | 12.4 | 5.3 | 3.6 |
| | 13,273 | * | 51.4 | 21.9 | 8.8 | 6.1 |
| 0+30 | 8,136 | 62.5 | 30.3 | 11.8 | 5.2 | 3.7 |
| | 13,217 | * | 50.6 | 21.7 | 9.0 | 6.5 |
| 0+40 | 8,093 | 62.4 | 33.7 | 12.8 | 4.8 | 3.5 |
| | 13,141 | * | 56.9 | 22.8 | 8.7 | 5.8 |
| | | WES 1 (46.1 Coverages) | | | | |
| 0+10 | 8,180 | 54.5 | 24.2 | 11.1 | 5.4 | 3.9 |
| | 13,344 | * | 42.5 | 20.5 | 9.7 | 7.0 |
| 0+20 | 8,040 | 66.1 | 37.4 | 15.4 | 5.6 | 3.5 |
| | 13,077 | * | 74.6 | 26.6 | 11.6 | 5.8 |
| 0+30 | 8,112 | 54.5 | 34.3 | 12.2 | 5.8 | 3.9 |
| | 13,260 | * | 62.2 | 20.9 | 10.6 | 6.5 |
| 0+40 | 8,021 | 67.0 | 40.4 | 11.8 | 6.0 | 3.6 |
| | 13,046 | * | 63.2 | 22.0 | 10.0 | 6.2 |
| | | WES 2 (0 Coverages) | | | | |
| 0+10 | 8,342 | 56.1 | 28.0 | 10.6 | 5.5 | 3.9 |
| | 13,543 | * | 54.3 | 18.5 | 9.6 | 6.1 |
| 0+20 | 8,323 | 53.0 | 27.6 | 10.0 | 6.0 | 3.8 |
| | 13,575 | * | 51.0 | 19.3 | 10.4 | 6.7 |
| 0+30 | 8,252 | 55.6 | 31.5 | 10.6 | 5.8 | 3.6 |
| | 13,464 | * | 58.7 | 20.5 | 9.8 | 6.4 |

* Deflection exceeded range of velocity transducer.

TABLE A-1. FALLING WEIGHT DEFLECTOMETER DEFLECTION BASIN DATA
(CONTINUED)

| Station No. | Force lbs. | Deflections 0-in. mils | 12-in. mils | 24-in. mils | 36-in. mils | 48-in. mils |
|---|---|---|---|---|---|---|
| | | WES 2 (0 Coverages) Continued | | | | |
| 0+40 | 8,339 | 45.7 | 26.4 | 10.0 | 5.6 | 3.7 |
| | 13,734 | 75.9 | 45.9 | 18.3 | 9.5 | 6.2 |
| | | WES 2 (6.5 Coverages) | | | | |
| 0+10 | 8,048 | * | 30.1 | 10.4 | 4.8 | 3.6 |
| | 12,887 | * | 53.5 | 17.9 | 7.8 | 6.0 |
| 0+20 | 8,056 | * | 33.1 | 11.6 | 5.3 | 3.7 |
| | 12,915 | * | 55.3 | 19.7 | 8.7 | 6.2 |
| 0+30 | 8,053 | * | 33.5 | 11.8 | 5.3 | 3.9 |
| | 12,966 | * | 56.7 | 20.7 | 9.0 | 6.5 |
| 0+40 | 8,109 | 66.5 | 31.3 | 12.0 | 5.8 | 4.1 |
| | 13,213 | * | 53.3 | 22.8 | 9.8 | 7.0 |
| | | WES 2 (20.5 Coverages) | | | | |
| 0+10 | 8,017 | 73.8 | 32.3 | 13.0 | 5.6 | 4.1 |
| | 12,958 | * | 55.9 | 22.6 | 9.5 | 6.7 |
| 0+20 | 8,085 | 66.9 | 32.7 | 12.4 | 5.9 | 4.1 |
| | 13,058 | * | 53.5 | 22.2 | 10.0 | 7.0 |
| 0+30 | 8,088 | 60.6 | 34.4 | 13.0 | 6.4 | 4.1 |
| | 13,146 | * | 54.1 | 24.4 | 10.4 | 7.2 |
| 0+40 | 8,077 | 60.8 | 30.4 | 13.0 | 6.3 | 4.2 |
| | 13,213 | * | 53.1 | 23.6 | 10.7 | 7.3 |
| | | WES 3 (0 Coverages) | | | | |
| 0+10 | 8,167 | 65.7 | 30.3 | 13.0 | 6.7 | 4.1 |
| | 13,241 | * | 56.1 | 20.5 | 11.8 | 6.5 |

TABLE A-1. FALLING WEIGHT DEFLECTOMETER DEFLECTION BASIN DATA (CONTINUED)

| Station No. | Force lbs. | Deflections 0-in. mils | 12-in. mils | 24-in. mils | 36-in. mils | 48-in. mils |
|---|---|---|---|---|---|---|
| | | WES 3 (0 Coverages) Continued | | | | |
| 0+20 | 8,180 | 64.3 | 35.4 | 13.4 | 7.3 | 4.6 |
| | 13,340 | * | 51.8 | 23.2 | 11.8 | 7.7 |
| 0+30 | 8,164 | 57.7 | 27.2 | 12.2 | 6.3 | 4.3 |
| | 13,472 | * | 52.2 | 21.2 | 11.9 | 7.0 |
| 0+40 | 8,204 | 56.3 | 23.2 | 10.2 | 5.7 | 3.9 |
| | 13,638 | * | 45.2 | 18.1 | 10.4 | 6.3 |
| | | WES 3 (6.5 Coverages) | | | | |
| 0+10 | 7,902 | * | 29.1 | 13.8 | 5.5 | 3.8 |
| | 12,431 | * | 53.9 | 22.8 | 9.1 | 6.2 |
| 0+20 | 7,842 | * | 23.6 | 13.2 | 5.4 | 4.2 |
| | 12,224 | * | 41.3 | 19.1 | 8.0 | 6.3 |
| 0+30 | 6,141 | * | 22.0 | 11.4 | 5.4 | 3.8 |
| | 9,610 | * | 37.8 | 20.1 | 8.5 | 6.1 |
| 0+40 | 8,005 | * | 23.4 | 11.0 | 5.6 | 4.1 |
| | 12,756 | * | 43.1 | 19.9 | 9.0 | 6.3 |
| | | WP-1 (0 Coverages) | | | | |
| 0+05 | 8,803 | 62.8 | 18.9 | 3.9 | 1.3 | 2.3 |
| | 13,205 | * | 29.9 | 2.4 | 1.4 | 2.8 |
| 0+15 | 8,819 | 43.7 | 17.7 | 3.2 | 1.6 | 1.2 |
| | 13,236 | 60.4 | 28.0 | 5.0 | 1.7 | 2.4 |
| 0+25 | 8,851 | 47.4 | 23.5 | 3.5 | 1.9 | 1.1 |
| | 13,352 | 66.3 | 34.8 | 5.3 | 3.0 | 1.7 |

TABLE A-1. FALLING WEIGHT DEFLECTOMETER DEFLECTION BASIN DATA
(CONTINUED)

| Station No. | Force lbs. | Deflections 0-in. mils | 12-in. mils | 24-in. mils | 36-in. mils | 48-in. mils |
|---|---|---|---|---|---|---|
| | | WP-2 (0 Coverages) | | | | |
| 0+05 | 8,994 | 20.9 | 9.4 | 3.2 | 1.5 | 1.5 |
| | 13,538 | 27.8 | 13.5 | 4.3 | 2.3 | 1.8 |
| 0+15 | 8,898 | 24.2 | 12.2 | 3.4 | 1.9 | 1.5 |
| | 13,538 | 31.3 | 17.6 | 4.7 | 2.7 | 2.1 |
| 0+25 | 8,867 | 23.2 | 11.3 | 3.5 | 2.1 | 1.5 |
| | 13,522 | 31.5 | 16.1 | 4.8 | 3.0 | 2.3 |
| | | WP-2 (46 Coverages) | | | | |
| 0+05 | 8,612 | * | 42.9 | 10.6 | 1.5 | 1.7 |
| 0+15 | 8,596 | * | 62.6 | 9.1 | 1.0 | 1.8 |
| | 13,093 | * | 65.7 | 10.6 | 1.5 | 2.7 |
| 0+25 | 8,724 | * | 51.2 | 5.9 | 1.5 | 1.6 |
| | 13,363 | * | 50.4 | 7.9 | 2.2 | 2.5 |
| | | WP-2 (65.6 Coverages) | | | | |
| 0+05 | 9,375 | * | 49.2 | 12.6 | 3.6 | 2.2 |
| | 13,888 | * | 52.4 | 14.6 | 3.5 | 2.5 |
| 0+15 | 9,296 | * | 58.7 | 11.4 | 2.4 | 2.0 |
| | 13,761 | * | 63.4 | 12.6 | 3.0 | 2.9 |
| 0+25 | 9,200 | * | 41.7 | 5.5 | 2.2 | 3.4 |
| | 13,650 | * | 46.9 | 7.1 | 3.2 | 3.3 |
| | | WP-2 (87.7 Coverages) | | | | |
| 0+05 | 8,787 | 67.7 | 35.4 | 9.8 | 2.4 | 1.6 |
| | 13,379 | * | 42.1 | 11.0 | 2.8 | 2.8 |

* Deflection exceeded range of velocity transducer.

TABLE A-1. FALLING WEIGHT DEFLECTOMETER DEFLECTION BASIN DATA (CONTINUED)

| Station No. | Force lbs. | Deflections 0-in. mils | 12-in. mils | 24-in. mils | 36-in. mils | 48-in. mils |
|---|---|---|---|---|---|---|
| | | WP-2 (87.7 Coverages) Continued | | | | |
| 0+15 | 8,771 | * | 46.9 | 6.3 | 1.2 | 1.6 |
| | 13,284 | * | 49.2 | 8.7 | 2.0 | 2.4 |
| 0+25 | 8,708 | * | 31.1 | 4.7 | 1.6 | 2.8 |
| | 13,205 | * | 38.2 | 5.1 | 3.5 | 2.8 |
| | | WP-3 (0 Coverages) | | | | |
| 0+05 | 9,200 | 45.7 | 23.6 | 6.3 | 2.5 | 2.4 |
| | 13,618 | 66.3 | 36.2 | 8.3 | 3.1 | 2.7 |
| 0+15 | 9,200 | 44.5 | 21.6 | 4.9 | 2.2 | 2.0 |
| | 13,665 | 63.3 | 33.9 | 7.7 | 2.7 | 2.5 |
| 0+25 | 9,184 | 55.7 | 28.0 | 4.3 | 2.6 | 2.6 |
| | 13,602 | 77.2 | 40.6 | 6.7 | 3.3 | 2.7 |
| | | WP-3 (12.3 Coverages) | | | | |
| 0+05 | 8,464 | * | 62.6 | 16.1 | 2.4 | 1.6 |
| | 12,172 | * | 97.6 | 24.8 | 2.3 | 1.0 |
| 0+15 | 8,168 | * | 77.2 | 21.7 | 4.4 | 2.4 |
| | 11,854 | * | * | 31.5 | 5.6 | 3.0 |
| 0+25 | 7,786 | * | * | 21.7 | 7.0 | 2.6 |
| | 11,314 | * | * | 31.5 | 12.2 | 3.0 |
| | | WP-4 (0 Coverages) | | | | |
| 0+05 | 9,137 | 37.2 | 19.3 | 5.4 | 1.9 | 1.2 |
| | 13,427 | 52.4 | 28.8 | 8.5 | 2.6 | 1.8 |
| 0+15 | 9,121 | 32.1 | 14.3 | 3.9 | 1.5 | 1.3 |
| | 13,570 | 44.3 | 22.5 | 6.2 | 2.1 | 2.2 |

TABLE A-1. FALLING WEIGHT DEFLECTOMETER DEFLECTION BASIN DATA (CONTINUED)

| Station No. | Force lbs. | Deflections 0-in. mils | 12-in. mils | 24-in. mils | 36-in. mils | 48-in. mils |
|---|---|---|---|---|---|---|
| | | WP-4 (0 Coverages) Continued | | | | |
| 0+25 | 9,057 | 32.3 | 14.3 | 3.7 | 1.5 | 1.4 |
| | 13,475 | 44.5 | 22.6 | 5.9 | 2.0 | 1.3 |
| | | WP-4 (22.1 Coverages) | | | | |
| 0+05 | 8,295 | * | * | 13.0 | 2.6 | 1.7 |
| | 11,965 | * | * | 20.0 | 4.5 | 2.8 |
| 0+15 | 8,692 | * | 58.0 | 7.9 | 3.1 | 1.3 |
| | 12,648 | * | * | 13.4 | 4.1 | 3.4 |
| 0+25 | 8,279 | * | * | 7.5 | 2.3 | 1.3 |
| | 11,886 | * | * | 11.0 | 4.8 | 2.3 |
| | | W-1 (0 Coverages) | | | | |
| 0+05 | 9,081 | 36.5 | 8.5 | 5.1 | 3.7 | 2.9 |
| | 14,063 | 53.4 | 11.6 | 7.8 | 5.5 | 4.3 |
| 0+15 | 9,049 | 43.1 | 9.9 | 4.9 | 3.7 | 2.9 |
| | 13,955 | 59.7 | 15.6 | 7.5 | 5.6 | 4.3 |
| 0+25 | 9,033 | 35.8 | 7.1 | 5.2 | 3.8 | 2.8 |
| | 14,019 | 51.3 | 11.5 | 7.8 | 5.9 | 4.4 |
| | | W-1 (6.8 Coverages) | | | | |
| 0+05 | 9,101 | 48.9 | 22.1 | 8.8 | 5.0 | 3.6 |
| | 13.982 | 69.5 | 32.6 | 13.5 | 7.5 | 5.4 |
| 0+15 | 8,930 | 62.1 | 25.2 | 8.2 | 5.4 | 3.5 |
| | 13,781 | * | 37.8 | 13.0 | 7.7 | 5.4 |
| 0+25 | 8,890 | 60.3 | 23.6 | 8.1 | 5.1 | 3.6 |
| | 13,721 | * | 35.2 | 13.0 | 8.1 | 5.4 |

TABLE A-1. FALLING WEIGHT DEFLECTOMETER DEFLECTION BASIN DATA
(CONTINUED)

| Station No. | Force lbs. | Deflections 0-in. mils | 12-in. mils | 24-in. mils | 36-in. mils | 48-in. mils |
|---|---|---|---|---|---|---|
| | | W-1 (13.6 Coverages) | | | | |
| 0+05 | 8,941 | 76.5 | 33.4 | 11.5 | 6.7 | 3.6 |
| | 13,693 | * | 49.2 | 19.0 | 9.0 | 5.6 |
| 0+15 | 8,771 | * | 44.9 | 5.9 | 5.6 | 3.8 |
| | 13,518 | * | 55.3 | 9.5 | 9.1 | 6.0 |
| 0+25 | 8,815 | * | 36.4 | 11.5 | 5.9 | 3.8 |
| | 13,448 | * | 52.0 | 18.5 | 9.5 | 6.1 |
| | | W-1 (20.5 Coverages) | | | | |
| 0+05 | 8,644 | 67.1 | 33.4 | 11.4 | 5.3 | 3.7 |
| | 13,371 | * | 49.4 | 19.7 | 8.8 | 5.7 |
| 0+15 | 6,491 | * | 33.5 | 11.6 | 5.7 | 3.2 |
| | 10,333 | * | 53.0 | 18.9 | 9.1 | 5.3 |
| 0+25 | 8,263 | * | 36.2 | 15.0 | 7.1 | 3.9 |
| | 13,066 | * | 56.3 | 20.2 | 11.7 | 6.3 |
| | | W-1 (27.3 Coverages) | | | | |
| 0+05 | 9,200 | * | 48.2 | 17.9 | 6.5 | 3.7 |
| | 13,999 | * | 68.5 | 26.0 | 9.4 | 5.9 |
| 0+15 | 8,871 | * | 60.6 | 17.9 | 7.3 | 3.7 |
| | 13,594 | * | * | 26.8 | 9.7 | 5.7 |
| 0+25 | 8,673 | * | 70.1 | 28.4 | 11.8 | 4.1 |
| | 13,400 | * | * | 42.3 | 18.4 | 5.9 |
| | | W-1 (38.2 Coverages) | | | | |
| 0+05 | 4,151 | 71.3 | 26.4 | 8.3 | 2.8 | 2.2 |
| | 9,176 | * | 50.6 | 16.6 | 6.9 | 5.0 |

TABLE A-1. FALLING WEIGHT DEFLECTOMETER DEFLECTION BASIN DATA (CONTINUED)

| Station No. | Force lbs. | Deflections 0-in. mils | 12-in. mils | 24-in. mils | 36-in. mils | 48-in. mils |
|---|---|---|---|---|---|---|
| | | W-1 (38.2 Coverages) Continued | | | | |
| 0+15 | 3,432 | * | 37.1 | 8.7 | 2.6 | 1.5 |
| | 7,624 | * | 68.5 | 19.8 | 6.7 | 3.9 |
| 0+25 | 4,020 | * | 38.3 | 11.3 | 4.8 | 3.0 |
| | 8,673 | * | * | 26.3 | 11.2 | 6.0 |
| | | W-2 (0 Coverages) | | | | |
| 0+05 | 9,160 | 48.2 | 28.4 | 11.0 | 5.9 | 4.6 |
| | 14,173 | 67.0 | 41.9 | 17.2 | 9.7 | 7.3 |
| 0+15 | 9,137 | 44.5 | 27.5 | 11.3 | 5.9 | 4.5 |
| | 14,106 | 62.8 | 41.3 | 17.5 | 9.8 | 7.2 |
| 0+25 | 9,149 | 45.0 | 25.9 | 9.7 | 5.3 | 3.8 |
| | 14,118 | 62.8 | 39.2 | 15.7 | 8.7 | 6.4 |
| | | W-2 (6.8 Coverages) | | | | |
| 0+05 | 4,080 | 61.2 | 35.4 | 10.4 | 4.4 | 2.8 |
| | 8,390 | * | 76.4 | 20.9 | 9.9 | 7.2 |
| 0+15 | 4,028 | 52.7 | 31.9 | 9.3 | 5.0 | 2.5 |
| | 8,446 | * | 72.6 | 19.1 | 10.1 | 6.1 |
| 0+25 | 4,000 | 54.8 | 32.5 | 8.6 | 5.6 | 2.3 |
| | 8,390 | * | 70.3 | 33.5 | 9.6 | 5.7 |
| | | W-2 (13.6 Coverages) | | | | |
| 0+05 | 3,583 | * | 58.7 | 12.3 | 4.6 | 3.3 |
| 0+15 | 3,899 | 68.0 | 30.5 | 11.6 | 5.1 | 3.0 |
| 0+25 | 3,822 | 60.3 | 32.9 | 9.7 | 4.2 | 2.4 |

TABLE A-1. FALLING WEIGHT DEFLECTOMETER DEFLECTION BASIN DATA
(CONCLUDED)

| Station No. | Force lbs. | Deflections 0-in. mils | 12-in. mils | 24-in. mils | 36-in. mils | 48-in. mils |
|---|---|---|---|---|---|---|
| | | W-3 (0 Coverages) | | | | |
| 0+05 | 8,827 | 46.1 | 17.0 | 7.8 | 4.2 | 3.2 |
| | 13,844 | 68.9 | 27.2 | 12.2 | 6.5 | 4.9 |
| 0+15 | 8,934 | 41.8 | 20.1 | 7.9 | 4.4 | 3.0 |
| | 13,884 | 60.9 | 30.9 | 12.2 | 6.8 | 4.9 |
| 0+25 | 8,875 | 42.2 | 18.4 | 7.1 | 4.1 | 2.8 |
| | 13,848 | 61.4 | 28.6 | 10.9 | 6.4 | 4.7 |
| | | W-3 (6.8 Coverages) | | | | |
| 0+05 | 4,044 | * | 41.9 | 10.0 | 3.3 | 2.2 |
| 0+15 | 4,020 | 66.0 | 41.9 | 10.9 | 3.6 | 2.2 |
| | 8,267 | * | * | 24.2 | 6.4 | 4.2 |
| 0+25 | 3,958 | * | 51.2 | 10.7 | 3.0 | 1.8 |
| | 8,064 | * | * | 20.0 | 4.5 | 2.2 |
| | | W-3 (11.7 Coverages) | | | | |
| 0+05 | (Unable to use Station 0+05) | | | | | |
| 0+15 | 4,004 | * | 47.2 | 10.1 | 2.6 | 2.0 |
| 0+25 | 2,300 | * | 45.1 | 8.2 | 2.3 | 2.2 |

TABLE A-2. FALLING WEIGHT DEFLECTOMETER DEFLECTION BASIN DATA
NORTH FIELD

| Station No. | Force lbs. | Deflections 0-in. mils | 12-in. mils | 18-in. mils | 24-in. mils | 36-in. mils | 48-in. mils | 60-in. mils |
|---|---|---|---|---|---|---|---|---|
| | | | | NFF4 (Subgrade)[a] | | | | |
| 1+25 | 4,846 | 11.7 | 6.3 | 2.9 | 1.8 | 0.9 | 0.5 | 0.4 |
| 1+50 | 4,728 | 14.5 | 8.7 | 3.8 | 2.3 | 1.1 | 0.6 | 0.5 |
| 1+75 | 4,848 | 14.5 | 6.0 | 2.8 | 1.7 | 0.7 | 0.5 | 0.3 |
| 1+25 | 8,664 | 22.6 | 11.5 | 5.2 | 3.4 | 1.7 | 1.1 | 0.8 |
| 1+50 | 8,648 | 26.5 | 16.5 | 6.4 | 4.2 | 2.0 | 1.2 | 0.8 |
| 1+75 | 8,784 | 25.9 | 10.8 | 4.9 | 2.8 | 1.3 | 0.9 | 0.7 |
| | | | | NFF4 (Base Course)[b] | | | | |
| 1+25 | 5,160 | 19.9 | 6.2 | 3.2 | 2.1 | 1.6 | 1.0 | 0.7 |
| 1+50 | 4,840 | 23.8 | 7.3 | 3.4 | 2.0 | 1.3 | 1.0 | 0.7 |
| 1+75 | 4,816 | 23.3 | 6.8 | 3.8 | 2.5 | 1.7 | 1.1 | 0.7 |
| 1+25 | 9,080 | 27.5 | 12.6 | 6.3 | 4.0 | 2.7 | 1.9 | 1.3 |
| 1+50 | 8,832 | 35.6 | 12.9 | 6.2 | 3.9 | 2.6 | 1.8 | 1.3 |
| 1+75 | 8,872 | 34.7 | 12.4 | 7.1 | 4.2 | 2.8 | 1.9 | 1.3 |
| 1+25 | 11,720 | 32.0 | 16.9 | 8.8 | 5.5 | 3.9 | 2.6 | 1.8 |
| 1+50 | 11,584 | 43.6 | 16.3 | 7.7 | 4.3 | 3.1 | 2.2 | 1.5 |
| 1+75 | 11,720 | 42.2 | 16.3 | 8.5 | 4.7 | 3.2 | 2.1 | 1.5 |
| | | | | NFF4 (Before Traffic) | | | | |
| 1+25 | 4,960 | 15.6 | 6.6 | 3.1 | 1.9 | 1.7 | 0.8 | 0.5 |
| 1+50 | 4,888 | 16.3 | 7.6 | 3.6 | 2.3 | 1.6 | 0.9 | 0.6 |
| 1+75 | 4,976 | 14.8 | 6.8 | 3.4 | 2.0 | 1.4 | 0.8 | 0.5 |
| 1+25 | 9,024 | 26.2 | 12.0 | 6.0 | 3.6 | 2.6 | 1.5 | 1.1 |
| 1+50 | 8,880 | 27.4 | 13.3 | 6.7 | 4.2 | 2.9 | 1.7 | 1.2 |
| 1+75 | 8,928 | 24.9 | 12.2 | 6.3 | 3.7 | 2.6 | 1.6 | 1.0 |
| 1+25 | 11,904 | 37.4 | 16.1 | 7.3 | 4.3 | 3.1 | 1.9 | 1.3 |
| 1+50 | 11,736 | 39.1 | 18.1 | 8.2 | 5.1 | 3.5 | 2.0 | 1.4 |
| 1+75 | 11,760 | 34.7 | 16.1 | 7.5 | 4.3 | 3.1 | 1.9 | 1.2 |

[a]17.7-in.-diameter plate.
[b]11.8-in.-diameter plate.

TABLE A-2. FALLING WEIGHT DEFLECTOMETER DEFLECTION BASIN DATA
NORTH FIELD (CONTINUED)

| Station No. | Force lbs. | Deflections 0-in. mils | 12-in. mils | 18-in. mils | 24-in. mils | 36-in. mils | 48-in. mils | 60-in. mils |
|---|---|---|---|---|---|---|---|---|
| | | NFF4 (After Proof Testing - 2 Coverages, F-4) | | | | | | |
| 1+25 | 8,688 | 26.2 | 11.7 | 6.7 | 4.2 | 2.8 | 1.6 | 1.1 |
| 1+50 | 8,680 | 25.8 | 11.5 | 7.0 | 4.5 | 3.2 | 1.8 | 1.2 |
| 1+75 | 8,672 | 25.6 | 12.0 | 6.9 | 4.1 | 2.8 | 1.5 | 1.0 |
| 1+25 | 13,976 | 43.8 | 19.1 | 10.6 | 6.5 | 3.6 | 2.4 | 1.6 |
| 1+50 | 13,992 | 43.2 | 18.9 | 11.1 | 6.9 | 4.7 | 2.7 | 1.8 |
| 1+75 | 14,016 | 42.9 | 19.5 | 10.9 | 6.4 | 2.8 | 2.3 | 1.5 |
| | | NFF4 (After F-4 Aircraft) | | | | | | |
| 1+25 | 8,992 | 25.1 | 13.0 | 7.0 | 4.3 | 3.1 | 1.8 | 1.2 |
| 1+50 | 8,848 | 30.2 | 12.5 | 7.2 | 4.8 | 3.4 | 1.9 | 1.3 |
| 1+75 | 8,896 | 23.5 | 12.5 | 6.9 | 4.3 | 3.1 | 1.7 | 1.1 |
| 1+25 | 14,408 | 41.0 | 20.9 | 11.0 | 6.7 | 4.6 | 2.7 | 1.9 |
| 1+50 | 14,200 | 46.3 | 21.7 | 12.3 | 7.4 | 4.8 | 2.8 | 1.9 |
| 1+75 | 14,272 | 39.3 | 20.1 | 10.8 | 6.6 | 5.0 | 2.5 | 1.6 |
| | | NFF4 (10 Coverages) | | | | | | |
| 1+25 | 9,312 | 27.9 | 12.2 | 7.1 | 4.6 | 3.2 | 2.0 | 1.4 |
| 1+50 | 9,168 | 32.2 | 14.2 | 8.5 | 5.5 | 4.0 | 2.7 | 1.6 |
| 1+75 | 9,168 | 27.7 | 13.0 | 7.8 | 5.0 | 3.5 | 1.9 | 1.3 |
| 1+25 | 14,576 | 47.0 | 19.9 | 10.9 | 6.9 | 4.9 | 2.8 | 1.9 |
| 1+50 | 14,352 | 54.0 | 22.7 | 12.7 | 7.9 | 5.4 | 3.5 | 2.1 |
| 1+75 | 14,672 | 46.7 | 20.9 | 12.0 | 7.4 | 4.9 | 2.7 | 1.7 |
| | | NFF4 (20 Coverages) | | | | | | |
| 1+25 | 9,032 | 29.4 | 13.3 | 7.5 | 4.7 | 3.3 | 1.9 | 1.3 |
| 1+50 | 8,904 | 35.9 | 15.1 | 8.7 | 5.5 | 4.0 | 2.4 | 1.6 |
| 1+75 | 8,920 | 30.0 | 13.7 | 8.0 | 5.0 | 3.4 | 1.9 | 1.2 |
| 1+25 | 14,528 | 44.8 | 20.9 | 11.8 | 7.2 | 5.0 | 2.8 | 1.9 |
| 1+50 | 14,136 | 60.9 | 25.1 | 13.7 | 8.0 | 5.4 | 3.1 | 2.2 |
| 1+75 | 14,424 | 50.9 | 22.3 | 12.5 | 7.4 | 5.0 | 2.6 | 1.7 |

TABLE A-2. FALLING WEIGHT DEFLECTOMETER DEFLECTION BASIN DATA
NORTH FIELD (CONCLUDED)

| Station No. | Force lbs. | Deflections 0-in. mils | 12-in. mils | 18-in. mils | 24-in. mils | 36-in. mils | 48-in. mils | 60-in. mils |
|---|---|---|---|---|---|---|---|---|
| | | | NFF4 (30 Coverages) | | | | | |
| 1+25 | 9,296 | 31.6 | 16.1 | 9.2 | 5.3 | 3.7 | 2.1 | 1.5 |
| 1+50 | 9,184 | 39.5 | 17.1 | 9.3 | 5.5 | 3.8 | 2.2 | 1.5 |
| 1+75 | 9,272 | 29.6 | 15.0 | 9.0 | 5.4 | 3.7 | 2.0 | 1.4 |
| 1+25 | 14,600 | 57.8 | 28.2 | 15.0 | 8.2 | 5.4 | 3.0 | 2.0 |
| 1+50 | 14,720 | 68.6 | 28.7 | 14.5 | 7.9 | 5.4 | 3.0 | 2.0 |
| 1+75 | 14,800 | 54.6 | 25.7 | 14.4 | 8.1 | 5.3 | 2.8 | 1.8 |
| | | | NFF4 (50 Coverages) | | | | | |
| 1+25 | 9,096 | 37.8 | 16.7 | 8.5 | 5.0 | 3.6 | 2.2 | 1.5 |
| 1+50 | 8,936 | 55.5 | 21.2 | 9.8 | 5.3 | 3.8 | 2.3 | 1.6 |
| 1+75 | 9,120 | 30.1 | 15.0 | 8.7 | 5.3 | 3.8 | 2.1 | 1.4 |
| 1+25 | 14,120 | 62.8 | 27.5 | 13.3 | 7.5 | 5.2 | 3.1 | 2.2 |
| 1+50 | 11,720 | 68.8 | 26.9 | 12.5 | 6.7 | 4.7 | 2.8 | 2.0 |
| 1+75 | 14,424 | 51.8 | 25.0 | 13.7 | 8.0 | 5.4 | 2.9 | 2.0 |
| | | | NFF4 (100 Coverages) | | | | | |
| 1+25 | 9,200 | 52.0 | 18.5 | 8.8 | 5.4 | 4.0 | 2.3 | 1.6 |
| 1+50 | 9,416 | 77.9 | 24.9 | 9.1 | 5.6 | 4.1 | 2.4 | 1.7 |
| 1+75 | 8,832 | 49.1 | 17.8 | 8.9 | 5.5 | 3.9 | 2.1 | 1.5 |
| 1+25 | 11,672 | 73.6 | 27.6 | 11.2 | 6.8 | 5.0 | 2.8 | 2.0 |
| 1+50 | Overranged 12,000 and 15,000 | | | | | | | |
| 1+75 | 11,728 | 68.6 | 24.6 | 11.4 | 6.8 | 4.7 | 2.5 | 1.7 |

# APPENDIX B

# BISDEF PROGRAM

## INTRODUCTION

The BISDEF program takes measured deflections from a deflection basin with critical estimates and ranges of layer modulus and computes the modulus values that best describe the airport deflection basin. A linearly layered elastic computer program developed by the Shell Oil Corporation is used as a subroutine to calculate the deflections. The program has been adapted to operate on a personal computer. The information provided herein is as follows:

a. Flowchart

b. Input guide

c. Example input

d. Example output

## FLOWCHART

A flowchart describing the logic of the program is presented on the following page.

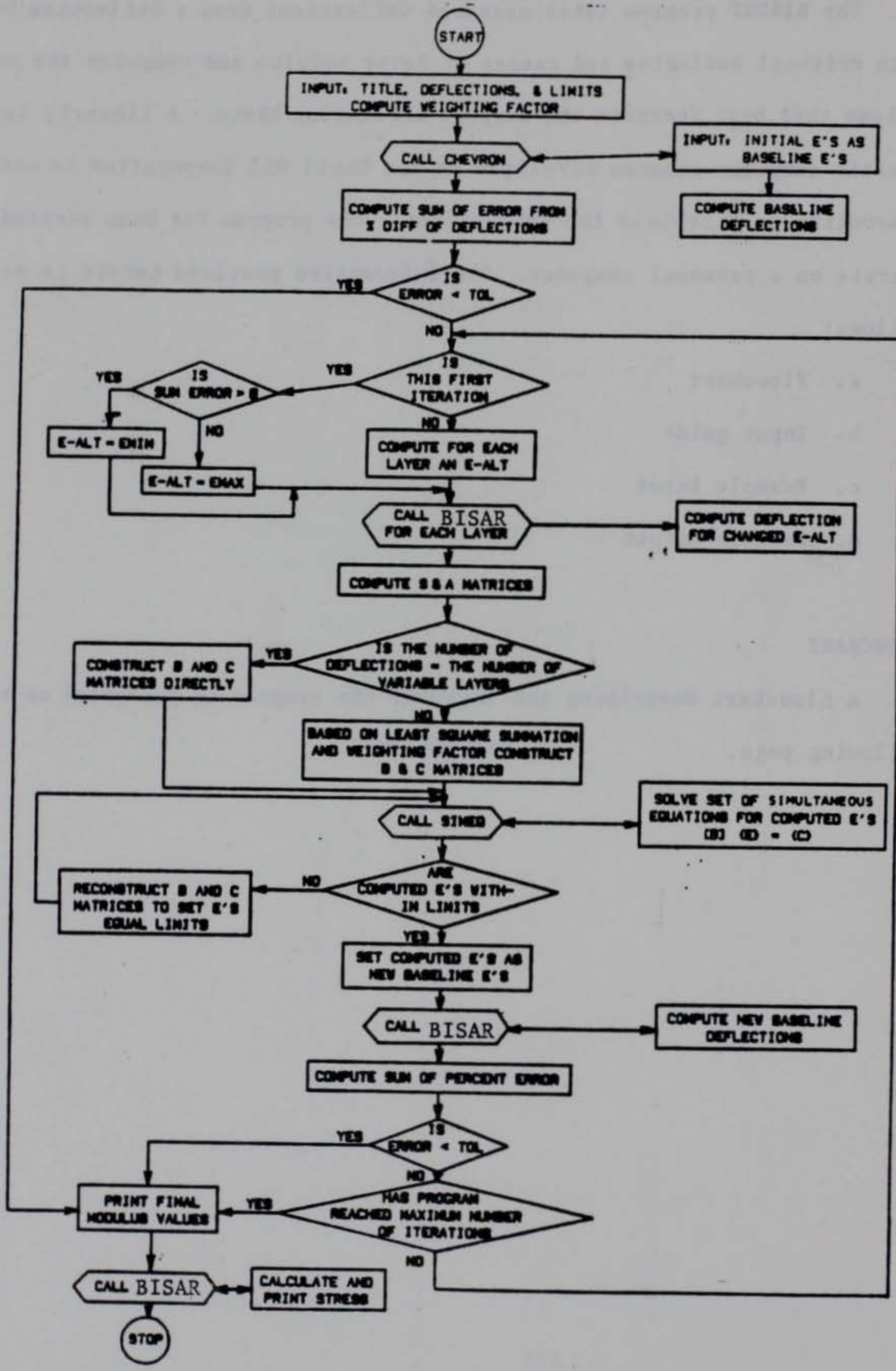
START
INPUT: TITLE, DEFLECTIONS, & LIMITS
COMPUTE WEIGHTING FACTOR
CALL CHEVRON
INPUT: INITIAL E'S AS BASELINE E'S
COMPUTE BASELINE DEFLECTIONS
COMPUTE SUM OF ERROR FROM % DIFF OF DEFLECTIONS
IS ERROR < TOL
YES
NO
IS THIS FIRST ITERATION
YES
NO
IS SUM ERROR > E
YES
NO
E-ALT = EMIN
E-ALT = EMAX
COMPUTE FOR EACH LAYER AN E-ALT
CALL BISAR FOR EACH LAYER
COMPUTE DEFLECTION FOR CHANGED E-ALT
COMPUTE S & A MATRICES
IS THE NUMBER OF DEFLECTIONS = THE NUMBER OF VARIABLE LAYERS
YES
NO
CONSTRUCT B AND C MATRICES DIRECTLY
BASED ON LEAST SQUARE SUMMATION AND WEIGHTING FACTOR CONSTRUCT B & C MATRICES
CALL SIMEQ
SOLVE SET OF SIMULTANEOUS EQUATIONS FOR COMPUTED E'S [B] {E} = {C}
ARE COMPUTED E'S WITHIN LIMITS
NO
YES
RECONSTRUCT B AND C MATRICES TO SET E'S EQUAL LIMITS
SET COMPUTED E'S AS NEW BASELINE E'S
CALL BISAR
COMPUTE NEW BASELINE DEFLECTIONS
COMPUTE SUM OF PERCENT ERROR
IS ERROR < TOL
YES
NO
HAS PROGRAM REACHED MAXIMUM NUMBER OF ITERATIONS
YES
NO
PRINT FINAL MODULUS VALUES
CALL BISAR
CALCULATE AND PRINT STRESS
STOP

## EXAMPLE INPUT

```
THIS PROGRAM CREATES A DATA FILE FOR THE PAVEMENT
    MODULUS BACK-CALCULATION PROGRAM "BISDEF"

ENTER A NAME FOR YOUR DATA FILE (10 CHARACTERS OR LESS)
=NFF4

INPUT: NUMBER OF PROBLEMS= 1


 INPUT TITLE FOR PROBLEM NO.  1

==> NFF4 0 CDV F4 STA 1+25

INPUT THE NUMBER OF SURFACE DEFLECTIONS FROM NDT
(MAXIMUM OF SEVEN READINGS).....==> 7

ARE SENSORS SPACED AT 1-FT INTERVALS?
   (Y=YES, N=NO) ==> Y

****MAGNITUDE AND LOCATION OF DEFLECTION READINGS****

        GAGE NUMBER 1 :

             DEFLECTION (MILS) ==> 26.2

      DISTANCE FROM CENTER OF LOADED AREA, (IN.) ==> 3


        GAGE NUMBER 2 :

             DEFLECTION (MILS) ==> 12.0


        GAGE NUMBER 3 :

             DEFLECTION (MILS) ==> 6.0


        GAGE NUMBER 4 :

             DEFLECTION (MILS) ==> 3.6

        GAGE NUMBER 5 :

             DEFLECTION (MILS) ==> 2.6

        GAGE NUMBER 6 :

             DEFLECTION (MILS) ==> 1.5

        GAGE NUMBER 7 :

             DEFLECTION (MILS) ==> 1.1
```

```
*******ENTER LOAD INFORMATION******

NUMBER OF LOADED AREAS..............==> 1

 LOAD NUMBER  1 :

      VERTICAL LOAD (LB).......==> 9024

      RADIUS OF LOADED AREA (IN)......==> 5.9


ENTER NUMBER OF LAYERS IN PAVEMENT SYSTEM ==> 3

************PAVEMENT INFORMATION***********
****ENTER THE FOLLOWING FOR EACH SYSTEM LAYER****

 LAYER NUMBER  1 :

IS MODULUS (E) TO BE :   1) FIXED
                         2) COMPUTED
          ENTER 1 OR 2 ==> 2

TO COMPUTE THE LAYER MODULUS, BISDEF REQUIRES AN INITIAL MODULUS VALUE
AND A RANGE (MINIMUM AND MAXIMUM MODULUS VALUES)!!!
    WOULD YOU LIKE TO:    1)  USE COMPUTER DEFAULT VALUES
                                    OR
                          2)  INPUT INITIAL E AND RANGE
          ENTER  1  OR  2  ==> 1

ENTER MATERIAL TYPE:  1) ASPHALTIC CONCRETE
                      2) PORTLAND CEMENT CONCRETE
                      3) HIGH-QUALITY STABILIZED BASE
                      4) BASE - SUBBASE, STABILIZED
                      5) BASE - SUBBASE, UNSTABILIZED
                      6) SUBGRADE

      ENTER SELECTION (1-6) ==> 1

        LAYER THICKNESS (IN)..... ==> 2.1

ENTER LAYER INTERFACE CONDITION RANGING FROM
 0 (COMPLETE ADHESION) TO 1000 (FRICTIONLESS SLIP) ......==> 0

 LAYER NUMBER  2 :

IS MODULUS (E) TO BE :   1) FIXED
                         2) COMPUTED
          ENTER 1 OR 2 ==> 2
```

```
TO COMPUTE THE LAYER MODULUS, BISDEF REQUIRES AN INITIAL MODULUS VALUE
AND A RANGE (MINIMUM AND MAXIMUM MODULUS VALUES)!!!
    WOULD YOU LIKE TO:    1)  USE COMPUTER DEFAULT VALUES
                                      OR
                          2)  INPUT INITIAL E AND RANGE
            ENTER  1  OR  2  ==> 1

ENTER MATERIAL TYPE:  1) ASPHALTIC CONCRETE
                      2) PORTLAND CEMENT CONCRETE
                      3) HIGH-QUALITY STABILIZED BASE
                      4) BASE - SUBBASE, STABILIZED
                      5) BASE - SUBBASE, UNSTABILIZED
                      6) SUBGRADE

      ENTER SELECTION (1-6) ==> 5

        LAYER THICKNESS (IN)..... ==> 6.2

   ENTER LAYER INTERFACE CONDITION RANGING FROM
    0 (COMPLETE ADHESION) TO 1000 (FRICTIONLESS SLIP) .....==> 0


 LAYER NUMBER  3 :


IS MODULUS (E) TO BE :   1) FIXED
                         2) COMPUTED
            ENTER 1 OR 2 ==> 2


TO COMPUTE THE LAYER MODULUS, BISDEF REQUIRES AN INITIAL MODULUS VALUE
AND A RANGE (MINIMUM AND MAXIMUM MODULUS VALUES)!!!
    WOULD YOU LIKE TO:    1)  USE COMPUTER DEFAULT VALUES
                                      OR
                          2)  INPUT INITIAL E AND RANGE
            ENTER  1  OR  2  ==> 1

ENTER MATERIAL TYPE:  1) ASPHALTIC CONCRETE
                      2) PORTLAND CEMENT CONCRETE
                      3) HIGH-QUALITY STABILIZED BASE
                      4) BASE - SUBBASE, STABILIZED
                      5) BASE - SUBBASE, UNSTABILIZED
                      6) SUBGRADE

      ENTER SELECTION (1-6) ==> 6

BISDEF AUTOMATICALLY PUTS IN A STIFF LAYER BELOW
THIS FINAL (SUBGRADE) LAYER.  BEST RESULTS ARE USUALLY
OBTAINED BY HAVING THIS STIFF LAYER AT A DEPTH OF 20-FT (240 IN.).
PLEASE ENTER A THICKNESS FOR THE SUBGRADE LAYER
REMEMBERING THAT THIS WILL SET THE LOCATION OF A RIGID
BOUNDARY IN BISDEF!!!

        LAYER THICKNESS (IN)..... ==> 231.7

ENTER LAYER INTERFACE CONDITION RANGING FROM
 0 (COMPLETE ADHESION) TO 1000 (FRICTIONLESS SLIP) .....==> 0
```

EXAMPLE INPUT FILE

```
                1
NFF4 0 COV F4 STA 1+25
                7
   26.20   12.00    6.00    3.60    2.60    1.50    1.10
    3.00   12.00   24.00   36.00   48.00   60.00   72.00
 1
 9024.00    5.900     0.00     0.00
 3
COMPUTE E
DEFAULT VALUES FOR INITIAL E AND RANGE
1    2.10     0.
COMPUTE E
DEFAULT VALUES FOR INITIAL E AND RANGE
5    6.20     0.
COMPUTE E
DEFAULT VALUES FOR INITIAL E AND RANGE
6  231.70     0.
```

```
* # ** # ** # *VERSION  DRA-7.86.02* # ** # ** # *
          P R O B L E M   N U M B E R  =   1
* # ** # ** # ** # ** # ** # ** # ** # ** # ** # *
```

NFF4 0 COV F4 STA 1+25

NUMBER OF VARIABLE LAYERS AND TARGET DEFLECTIONS = 3

| VARIABLE LAYER NO. | SYSTEM LAYER NO. | ESTIMATED INITIAL MODULUS PSI | ASSIGNED RANGE FOR LAYER MODULUS MINIMUM MODULUS PSI | MAXIMUM MODULUS PSI |
|---|---|---|---|---|
| 1 | 1 | 350000. | 200000. | 1000000. |
| 2 | 2 | 30000. | 5000. | 150000. |
| 3 | 3 | 19736. | 14736. | 24736. |

INITIAL PAVEMENT PARAMETERS

| LAYER NO. | MATERIAL TYPE | MODULUS PSI | POISSON'S RATIO | THICK. IN. | INTERFACE VALUE |
|---|---|---|---|---|---|
| 1 | AC | 350000. | 0.35 | 2.10 | 0. |
| 2 | BASE OR SUBBASE | 30000. | 0.35 | 6.20 | 0. |
| 3 | SUBGRADE | 19736. | 0.40 | 231.70 | 0. |
| 4 | RIGID BOUNDARY | 1000000. | 0.50 | SEMI-INF | |

LOAD INFORMATION

| LOAD NUMBER | LOAD POUNDS | RADIUS OF LOADED AREA, IN. | LOAD CO-ORDINATES X, IN. | Y, IN. |
|---|---|---|---|---|
| 1 | 9024. | 5.90 | 0.00 | 0.00 |

**********BISDEF OUTPUT SUMMARY**********

NUMBER OF ITERATIONS PERFORMED: 3

PREDICTED E DISREGARDING BOUNDRY CONDITIONS

| LAYER NO. | MODULUS |
|---|---|
| 1 | 1568. |
| 2 | 143365. |
| 3 | 15979. |

PREDICTED E WITH BOUNDARY CONDITIONS CONSIDERED

| LAYER NO. | MODULUS |
|---|---|
| 1 | 200000. |
| 2 | 42270. |
| 3 | 15689. |

DEFLECTIONS COMPUTED FOR FINAL MODULUS VALUES

| POSITION | SENSOR OFFSET IN. | MEASURED DEFLECTION MILS | COMPUTED DEFLECTION MILS | DIFFERENCE | % DIFF. |
|---|---|---|---|---|---|
| 1 | 3.0 | 26.2 | 25.8 | 0.4 | 1.6 |
| 2 | 12.0 | 12.0 | 12.1 | -0.1 | -0.4 |
| 3 | 24.0 | 6.0 | 5.8 | 0.2 | 2.6 |
| 4 | 36.0 | 3.6 | 3.5 | 0.1 | 4.1 |
| 5 | 48.0 | 2.6 | 2.3 | 0.3 | 11.4 |
| 6 | 60.0 | 1.5 | 1.6 | -0.1 | -9.8 |
| 7 | 72.0 | 1.1 | 1.2 | -0.1 | -11.4 |
| | | | ABSOLUTE SUM: | 1.4 | 41.4 |
| | | | ARITHMETIC SUM: | | -1.8 |
| | | | AVERAGE: | 0.2 | 5.9 |

FINAL MODULUS VALUES

| LAYER NO. | MATERIAL TYPE | MODULUS PSI | POISSON'S RATIO | THICK. IN. | INTERFACE VALUE |
|---|---|---|---|---|---|
| 1 | AC | 200000. | 0.35 | 2.10 | 0. |
| 2 | BASE OR SUBBASE | 42270. | 0.35 | 6.20 | 0. |
| 3 | SUBGRADE | 15689. | 0.40 | 231.70 | 0. |
| 4 | RIGID BOUNDARY | 1000000. | 0.50 | SEMI-INF | |

REACHED MAX NO OF ITERATIONS
ABSOLUTE SUM OF % DIFF. NOT WITHIN TOLERANCE
CHANGE IN MODULUS VALUES WITHIN TOLERANCE

# APPENDIX C

## PROGRAM FOR CORRECTING FWD ISM DATA FOR TEMPERATURE

```
      DATA A0/6.4832942E-01/,A1/-5.1830783E-02/,A2/4.9277325E-03/
      DATA A3/-.00021081954/,A4/3.2681272E-06/
      DATA B0/-9.6757755/,B1/3.6665256/,B2/-3.5506826E-01/
      DATA B3/1.8453128E-02/, B4/-4.4352426E-04/
      DATA D0/9.896776E-01/,D1/-5.820991E-02/
      DATA D2/-1.692166E-03/
      DATA E0/1.854619E-04/,E1/-9.401799E-04/
      DATA E2/3.268749E-04/
      DATA F0/-2.872853E-06/,F1/3.093604E-05/
      DATA F2/-6.76536E-06/
      DATA G0/3.461658E-08/,G1/-8.454449E-08/
      DATA G2/3.507406E-08/
10    CONTINUE
      WRITE (*,100)
 100  FORMAT(/,1X,'INPUT-PAVEMENT THICKNESS,SURF.+5DAY MEAN',/,'= ')
      READ(*,*) HI,S5
      IF(HI.LT.1.0E-06)GO TO 140
C     IF(HI.LT.3.) GO TO 151
      H=HI/2
      SL=A0+A1*H+A2*H**2.+A3*H**3.+A4*H**4.
      CP=B0+B1*H+B2*H**2.+B3*H**3.+B4*H**4.
      TD=SL*S5+CP
C     IF(TD.LT.30.OR.TD.GT.110) GO TO 131
      IF(TD.LT.30.OR.TD.GT.150) GO TO 131
      C0=D0+D1*HI+D2*HI**2.
      C1=E0+E1*HI+E2*HI**2.
      C2=F0+F1*HI+F2*HI**2.
      C3=G0+G1*HI+G2*HI**2.
      CF=C0+C1*TD+C2*TD**2.+C3*TD**3.
      CFD=1./CF
      WRITE (*,110)
 110  FORMAT(/,1X,'PAV.THICK.',2X,'SURF.+5 DAY MEAN',2X,'MPTEMP',2X,
     1'DSM CF',2X,'DEFL CF')
      WRITE(*,120)HI,S5,TD,CF,CFD
 120  FORMAT(3X,F4.1,11X,F5.1,8X,F5.1,4X,F4.2,4X,F4.2)
      GO TO 10
 131  WRITE (*,130)
 130  FORMAT(/,1X,'TEMP IS OUT OF RANGE OF CURVES')
      GO TO 10
 151  WRITE (*,150)
 150  FORMAT(/,' THICKNESS OF LESS THAN 3 IN IS NOT CORRECTED FOR TEMP')
      GO TO 10
 140  STOP
      END
```

## REFERENCES


1. Rone, C. L., et al., Membrane Encapsulated Soil Layer (MESL) for Contingencies Surfaces, Technical Report No. TR 77-21, US Army Engineer Waterways Experiment Station, Vicksburg, Mississippi, April 1977.

2. Rone, C. L., et al., Evaluation of Material for Contingency Runways, Technical Report No. TR 78-46, US Army Engineer Waterways Experiment Station, Vicksburg, Mississippi, July 1979.

3. Beatty, D. N., et al., Preliminary Feasibility Study of Concepts of Contingency Surface Materials for Alternate Launch and Recovery Systems, Report No. ESL-TR-81-24, Air Force Engineering and Services Center, Tyndall Air Force Base, Florida, April 1981.

4. Baird, G. T., et al., Interim Crater Repair Test - North Field, Report No. ESL-TR-82-03, Air Force Engineering and Services Center, Tyndall Air Force Base, Florida, August 1982.

5. Rone, C. L., et al., Alternate Launch and Recovery Surfaces - State-of-the-Art Study, Report No. ESL-TR-83-13, Air Force Engineering and Services Center, Tyndall Air Force Base, Florida, February 1984.

6. Bush, A. J., et al., Design of Alternate Launch and Recovery Surfaces for Environmental Effects, Report No. ESL-TR-83-64, Air Force Engineering and Services Center, Tyndall Air Force Base, Florida, July 1984.

7. Styron, C. R., Performance Data for F-4 Operations on Alternate Launch and Recovery Surfaces, Report No. ESL-TR-83-96, Air Force Engineering and Services Center, Tyndall Air Force Base, Florida, July 1984.

8. Thompson, M. R., et al., Development of a Preliminary ALRS Stabilizer Material Pavement Analysis System, Report No. ESL-TR-83-34, Air Force Engineering and Services Center, Tyndall Air Force Base, Florida, March 1984.

9. Costigan, R. R., and Thompson, M. R., Response and Performance of Alternate Launch and Recovery Surfaces Containing Stabilized-Material Layers, Report No. ESL-TR-84-25, Air Force Engineering and Services Center, Tyndall Air Force Base, Florida, January, 1985.

10. Bush, A. J., and Alford, S. J., Alternate Launch and Recovery Surface Test Section Design, Construction, and Evaluation, North Field, South Carolina, Air Force Engineering and Services Center, Tyndall Air Force Base, Florida, To be Published.

11. Alexander, D. R., Bush, A. J., and McCaffrey, P. S., Jr., Spangdahlem ALRS Pavement Evaluation Support To Salty Demo 85, Phase I, Air Force Engineering and Services Center, Tyndall Air Force Base, Florida, To be published.

12. Hoffman, M. S., and Thompson, M. R., Mechanistic Interpretation of Nondestructive Pavement Testing Deflections, Report No. UILU-ENG-91-2010, University of Illinois, Urbana, Illinois, June 1981.

13. Green, J. L., and Hall, J. W., Nondestructive Vibratory Testing of Airport Pavements, Volume 1, Experimental Test Results and Development of Evaluation Methodology and Procedure, Report No. TR-S-75_14, U. S. Army Engineer Waterways Experiment Station, Vicksburg, Mississippi, September, 1975.

14. Bush, Albert J., Nondestructive Testing for Light Aircraft Pavements, Phase II, Development of the Nondestructive Evaluation Procedure, Report No. FAA-RD-9-II, U. S. Department of Transportation, Federal Aviation Administration, Washington, D. C., November, 1980.

15. Hall, J. W., Jr., Comparative Study of Nondestructive Pavement Testing -Macdill Air Force Base, Air Force Engineering and Services Center, Tyndall Air Force Base, Florida, September, 1983.

16. Smith, Roger E., and Lytton, Robert L., Synthesis Study of Nondestructive Testing Devices for Use in Overlay Thickness Design of Flexible Pavements, FHWA Report RD/83/097, Federal Highway Administration, Washington, D. C., November, 1983.

17. Bush, A. J., and Alexander D. R., Pavement Evaluation Using Deflection Basin Measurements and Layered Theory, Transportation Research Board, Washington, D. C., January, 1985.

18. Lytton, R. L., et al, Determination of Asphaltic Concrete Pavement Structural Properties By Nondestructive Testing, NCHRP Project 10-27, Washington, D. C., April, 1986.

19. Thompson, M. R., "Important Properties of Base and Subgrade Materials," unpublished paper presented to Conference on Crushed Stone for Road and Street Construction and Reconstruction, Arlington, Virginia, June, 1984.

20. Barksdale, Richard D., "Laboratory Evaluation of Rutting in Base Course Materials," Proceedings Third International Conference on the Structural Design of Asphalt Pavements, Vol 1, University of Michigan, Ann Arbor, Michigan, 1972.

21. Kondner, R. L., "Hyperbolic Stress-Strain Response: Cohesive Soils," Journal, Soils Mechanics and Foundations Division, American Society of Civil Engineers, Vol. 89, No. SM1, January 1963.

22. Duncan, J. M. and Chong, C. Y., "Non-Linear Analysis of Stress and Strain in Soils," Journal, Soil Mechanics and Foundations Division, American Society of Civil Engineers, Vol. 96, No. SM5, September 1970.

23. Brabston, W. N., Deformation Characteristics of Compacted Subgrade Soils and Their Influence in Flexible Pavement Structures, PhD. Thesis, Texas A and M university, College Station, Texas, August, 1982.

24. Departments of the Navy, the Army, and the Air Force, Flexible Pavement Design for Airfields, Navy DM21.3, Army TM5-825.2, Air Force AFM 88-6 Chapter 2, August, 1978.

25. U. S. Department of Transportation, Airport Pavement Design and Evaluation, AC 150/5320-6C, Federal Avaiation Administration, Washington, D. C., December, 1978.

26. International Civil Aviation Organization, Aerodrome Design Manual, Part 3, Pavements, Montreal, Quebec, Canada, 1983.

27. Pereira, A. T., Procedures for Development of CBR Design Curves, IR-S-77-1, U. S. Army Engineer Waterways Experiment Station, Vicksburg, Mississippi, June, 1977.

28. Barber, V. C., et. al., The Deterioration and Reliability of Pavements, TR-S-78-8, U. S. Army Engineer Waterways Experiment Station, Vicksburg, Mississippi, July 1978.

29. Barker, W. R., Prediction of Pavement Roughness, MP GL-82-11, U. S. Army Engineer Waterways Experiment Station, Vicksburg, Mississippi, September 1982.

30. Baird, G. T., and Kirst, J. A., Nondestructive Pavement Testing System: Theory and Operation, ESL-TR-83-28, Air Force Engineering and Services Center, Tyndall Air Force Base, Florida, January, 1983.

31. Nazarian, S., and Stokoe, K. H., II, "Nondestructive Testing of Pavements using Surface Waves," unpublished paper presented at Transportation Research Board, Washington, D. C., January, 1984.

32. Peterson, D. F., et al., Asphalt Overlays and Pavement Rehabilitation - Evaluating Structural Adequacy for Flexible Pavement Overlays, Report No. 8-996, Utah Department of Transportation, January, 1976.

33. ILLI-PAVE Users Manual, Civil Engineering Department, University of Illinois, Urbana-Champaign, May 1982.

34. Koninilijke/Shell Laboratorium, BISAR Users Manual; Layered Systems Under Normal and Tangential Loads, Amsterdam, Holland, 1972.

35. Barker, W. R., and Brabston, W. N., Development of a Structural Design Procedure for Flexible Airport Pavements, FAA-RD-74-199, Department of Transportation, Federal Aviation Administration, Washington D. C., September, 1975.

36. American Sociey for Testing and Materials, Standard Test Method for Density of Soil and Soil-Aggregate in Place by Nuclear Methods (Shallow Depth), ASTM D 2922-81, Philadelphia, Pennsylvania, 1982.

37. _____, Standard Test Method for Density of Soil in Place by the Rubber-Balloon Method, ASTM D 2167, Philadelphia, Pennsylvania, 1982.

38. Department of Defense, Military Standard Test Method for Pavement, Subgrade, Subbase, and Base Course Materials, MILSTD-621A, Washington, D. C., December 1964.

39. Horn, W. J., and Ledbetter, R. H., Pavement Response to Aircraft Dynamic Loads, Vol. 1, Instrumentation Systems and Testing Program. Report No. TR-S-75-11, U. S. Army Waterways Experiment Station, Vicksburg, Mississippi, June, 1975.

40. Woodman, E. H., Pressure Cells for Field Use, Bullentin No. 40, U. S. Army Engineer Waterways Experiment Station, CE, Vicksburg, Mississippi, January, 1955.

41. U. S. Army Engineer Waterways Experiment Station, CE, Soil Pressure Cell Investigation, Technical Memorandum No. 210-1, Vicksburg, Mississippi, July, 1944.

42. Ahlvin, R. G., et al, Multiple-Wheel Heavy Gear Load Pavement Tests, Volume 1, Basic Report, TR-S-71-17, U. S. Army Engineer Waterways Experiment Station, Vicksburg, Mississippi, November, 1971.

43. Foxworthy, P. T., Concepts for the Development of a Nondestructive Testing and Evaluation System for Rigid Airfield Pavements, Ph.D. Thesis, University of Illinois, Ureana - Champaign, June, 1985.

44. Bush, A. J. III, unpublished Memorandum For Record, Subject: Correction Factors for Deflections Measured on Pavements Containing Asphaltic Concrete Layers, U. S. Army Engineer Waterways Experiment Station, November, 1979.

45. Kingham, R. I., and Kallas, B. F., "Laboratory Fatigue and Its Relationship to Pavement Performance," Proceedings, Third International Conference on the Structural Design of Asphalt Pavements, Vol. 1, University of Michigan, Ann Arbor, Mich., 1972.

46. Asphalt Institute, "Asphalt Overlays and Pavement Rehabilitation", Manual Series No. 17, College Park, MD, 1969.

47. Chou, Y. T., Hutchinson, R. L., and Ulery, H. H. Jr., "Design Method For Flexible Airfield Pavement", Asphalt Concrete Pavement Design and Evaluation, Transportation Research Record 521, Transportation Research Board, Washington, D. C., January, 1974.